ENERGY MANAGEMENT STRATEGIES FOR SMART GRIDS WITH RENEWABLES

by

Uzma Amin

Dissertation submitted in fulfilment of the requirements

for the degree of

DOCTOR OF PHILOSOPHY

School of Engineering
Faculty of Science and Engineering
Macquarie University
Sydney, Australia

October 2019

STATEMENT OF CANDIDATE

I certify that the work in this thesis entitled "Energy Management Strategies for Smart Grids with Renewables" has not previously been submitted for a degree nor has it been submitted as part of the requirements for a degree to any other university or institution other than Macquarie University.

I also certify that this thesis is an original piece of research and it has been written by me.

In addition, I certify that all information sources and literature used are indicated in the thesis.

……

Uzma Amin

Dedicated to my lovely parents, beloved sister

&

best husband Atif Chaudary.

ACKNOWLEDGMENTS

"All praise and thanks to almighty ALLAH"

I would like to express my deepest gratitude to my principal supervisor Prof. Jahangir Hossain for his extensive guidance and continuous support throughout this tenure of Ph.D. Without his unconditional dedication and productive reproach, it would not have been possible for me to complete this dissertation. I am also grateful to my associate supervisors Professor Graham Town & Professor Junwei Lu for their kind support and inspiring words.

My sincere thanks to fellow colleague Mr. Edstan Fernandez for his ideas and valuable suggestions in challenging problems. I am also thankful to Macquarie University for providing me the opportunity of pursuing a Ph.D. in the field of power engineering with scholarships and supporting my domestic and international research visits. I am heartily grateful to Dr. Keith Imrie, Ex-Honorary Associate at Macquarie University, for proofreading my publications within a very short period.

I would like to show deepest appreciation and respect to my family, especially my father, the one to whom I owe all the success in my life. No words can express my gratitude to him, but I pray ALLAH to bless and reward him. A final word to my beloved husband Atif Chaudary and sister Maria Amin. Their support and love made my Ph.D. study a happy journey

ABSTRACT

With increasing environmental concerns raised from fossil fuel sources, the prominent feature of next-generation smart grids is to supply power from clean/renewable energy sources (i.e., solar, wind and fuel cell, etc) in order to provide economic, environmental, reliability and security benefits. To achieve these goals, future smart grids will work in highly complex and dynamic environments and will have small-capacity distributed renewable energy generators (DREGs) with non-dispatchable and intermittent characteristics. Moreover, the utilization of DREGs on a large-scale helps to flatten peak demand to avoid substantial overcapacity in the size of a power system due to high aggregated peak demand. However, DREGs need to manage, and they required interaction with each other, with storage systems and an energy provider for improved asset utilization and energy efficiency. In this context, an efficient demand-side management system (DSMS) is essential for coordinate control of DREGs and responsive loads to maximize the system's utilization and reliability in a smart grid. Fundamentally, demand-side management (DSM) is a process of shifting/reshaping electrical loads and utilizing new technologies to reduce power bills, overall operational costs and increase energy efficiency. This thesis addresses the challenges of developing a framework for optimal DSMS by modeling the energy usage behavior of self-interested distributed entities through studying the propriety DREGs and consumers in a smart grid. The major contributions of this research are given below.

The first contribution of this research is to develop an algorithm for analyzing the performance of an experimental smart building through real-time data analysis, and then recommend possible measures to improve its energy efficiency. It focusses on the performance gap in terms of energy efficiency and the criticalities related to the characteristics of chosen devices and demand management strategies adopted. In addition, new technologies (to enhance DREGs production), coordinated measures (to improve building energy management system) and transactive control (to control the building's responsive load) are proposed. The scientific analysis of proposed recommendations for an intelligent energy management system demonstrates significant energy and cost savings for smart buildings.

The second contribution of this research is to present a three-level hierarchical energy-trading framework for encouraging the owners of DREGs to voluntarily take part in an energy trading process. The developed strategy captures the complex interactions between the owners of geographically DREGs and the aggregator in the smart grid using a non-cooperative contract theoretic approach. Moreover, a dynamic pricing scheme is developed that the aggregator can utilize to incentivize the owners of DREGs and a distributed algorithm is proposed to enable the energy-trading process. Various categories, types, and constraints of DREGs, different trading scenarios and wholesale price impact on trading are considered in the analysis for practical applications. The solution of the developed scheme shows that socially optimal energy management for both trading partners can be achieved.

The third contribution of this research is to develop an occupant's comfort aware energy imbalance management scheme for efficiently curtailing responsive loads of commercial buildings with the market price. The aim is to reduce the aggregated and peak demand to deal with energy imbalance problem in case of DREGs intermittency and/or power shortage from the grid while providing

the desired quality of service. To achieve this goal, an intelligent and new price-based demand response (PBDR) control strategy is proposed to optimize the responsive load scheduling. Occupants' varying thermal preferences in the response of price signals are considered and modeled using the artificial neural network (ANN) to integrate into the optimal scheduling problem.

The performance of the proposed management techniques is tested in real Australian power distribution networks under real load, weather conditions, and electricity tariff structure. The developed models, algorithms, and techniques can capture the different cost-benefit trade-offs that exist for efficiently managing buildings energy in a smart grid. These strategies have shown significant performance improvement when compared with existing solutions. The work in this thesis demonstrates that modeling power usage behavior of distributed entities in a smart grid for robust DSMS is both possible and beneficial for increasing the energy efficiency of smart buildings in a smart grid.

Table of Contents

List of Figures

List of Tables

List of Acronyms

AC	Alternating Current
ACs	Air Conditioners
AEMO	Australian Energy Market Operator
AHU	Air-Handling Unit
AMI	Advanced Metering Infrastructure
ANN	Artificial Neural Network
ASHRAE	American Society of Heating Refrigeration and Air-Conditioning Engineers
BAS	Building Automation System
BMS	Building Management System
CC	Conventional Control
CCA	Central Control Agent
CL	Cooling Load
CLTD	Cooling Load Temperature Difference
CO_2	Carbon Dioxide
DC	Direct Current
DERs	Distributed Energy Resources
DG	Distributed-Generation
DMPP	Demand Management and Planning Project
DR	Demand Response
DREGs	Distributed Renewable Energy Generators
DSM	Demand-Side Management
DSMS	Demand-Side Management System
EMS	Energy Management Systems
ES	Electricity Supplier
ESs	Electricity Suppliers
BESS	Battery Energy Storage Systems

EVs	Electric Vehicles
HL	Heating Load
HVAC	Heating Ventilation and Air-Conditioning
IC	Incentive Compatibility
IoT	Internet of Things
IR	Individual Rationality
MCP	Market-Clearing Price
MOSFET	Metal Oxide Semiconductor Field-Effect Transistor
MPC	Model Predictive Control
NIST	National Institute of Standards and Technology
PBDR	Price-Based Demand Response
PCC	Point of Common Coupling
PMV	Predicted Mean Vote
PV	Photovoltaic
RERs	Renewable Energy Resources
RTP	Real-Time Pricing
SRC	Soft Robotic Actuator
SSGC	Sir Samuel Griffith Centre
TC	Transactive Control
T&D	Transmission and Distribution
TOU	Time-of-Use
US-DOE	United States Department of Energy
VAV	Variable-Air-Volume
ZCA	Zero Carbon Australia

Symbols

The symbols used in this thesis have different meanings in different chapters, thus, the global definition is not provided here. All symbols will be defined in the context of each chapter in which they appear.

List of Publications

Refereed Journal Papers

1. **Uzma Amin**, J. Hossain, J. Lu, "Performance Analysis of Experimental Smart Building: Expectations and Outcomes", Elsevier Energy Journal, Vol. 135, pp. 740-753, September 2017. [Chapter 3]

2. **Uzma Amin**, W. Tushar, J. Hossain, and K. Mahmud, "Energy Trading in Local Electricity Market with Renewables- A Contract Theoretic Approach", Manuscript No. TII-19-3109, IEEE Transaction on Industrial Informatics, Submitted on 10th July 2019, Impact Factor: 7.337 [Chapter 4]

3. **Uzma Amin**, J. Hossain, E. Fernandez "Optimal Price Based Control of HVAC Systems in Multizone Office Buildings for Demand Response", Manuscript No. JCLEPRO-D-19-09999, Journal of Clean Production, Submitted on 8th June 2019, Impact Factor: 6.395 [Chapter 5]

Refereed Conference Papers

4. **Uzma Amin**, J. Hossain, J. Lu, A. Mahmud, "Cost-Benefit Analysis for Proactive Consumer in a Microgrid for Transactive Energy Management", AUPEC-2016, 25-28 September 2016, Brisbane. [Chapter 3]

5. **Uzma Amin**, M. J. Hossain, J. Lu, E. Fernandez, "Optimal Utilization of Renewable Power Production by Sharing Power among Commercial Buildings: Case Study of Griffith University", AUPEC- 2018, 27-30 November 2018, Auckland.

6. **Uzma Amin**, E. Fernandez, K. Mahmud, M. J. Hossain, J. Lu, "Categorizing Electricity Suppliers in Smart Grid: A Contract Theory Approach", under review. [Chapter 4]

Other Co-authored Publications during Ph.D. Candidature

7. E. Fernandez, P. Jamborslamati, M. J. Hossain, **Uzma Amin**, "A Communication-enhanced Price-based Control Scheme for HVAC Systems", IEEE Innovative Smart Grid Technologies (ISGT) Conference, 4-7 December 2017, Auckland.

8. K. Mahmud, **Uzma Amin**, M. J. Hossain, J. Ravishankar, "Computational tools for design, analysis, and management of residential energy systems", Elsevier Applied Energy, Vol. 221, pp. 535-556, July 2018.

Chapter 1

Introduction

The awareness for efficient usage and conservation of energy in various sectors, specifically in the power sector, grew tremendously in the twenty-first century. The reasons behind this consciousness are 1) increasing fuel prices, 2) environmental issues, and 3) carbonization of the energy system. These reasons drive an energy transition from fossil fuels to distributed renewable energy generators (DREGs) to meet the growing electricity demand and to provide clean energy. The smart grid with its flexible and bidirectional power and information flow strategy is capable of integrating a large percentage of renewable energy resources (RERs) to form an advanced energy delivery network at a distribution level. One prominent feature of a smart grid is to facilitate the on-site deployment of RERs due to their proven technical, economical, environmental and peak load management feasibility. However, the smart grid power management and control infrastructure will indeed face a number of challenges due to the large-scale deployment of RERs. For example, enabling services, products, and techniques for energy efficiency, increasing consumer's choices in new emerging markets such as microgrids, and

facilitating two-way delivery of energy information at the device level. This thesis addresses the challenges of developing mechanisms for the optimal demand-side management system (DSMS) by modeling the energy usage behavior of rational distributed entities in a smart grid. The focus is on the optimal utilization and management of DREGs to develop a techno-economic DSMS for smart grids, and further, to increase the building's energy efficiency and reducing the energy consumption in the energy-constrained smart network.

1.1. Background and Motivation

1.1.1 The Future Electric Power System

The existing power system infrastructure, or as it is universally called, the 'Power Grid' is an interconnected network for delivering electricity from power plants to remotely located electricity consumers. It consists of generating stations, high voltage transmission lines, and distribution systems designed in a vertical fashion. Each subsystem of the power grid is supported by controllers and associated devices to ensure unidirectional reliable and efficient operation [1]. However, due to increased environmental concern, high penetration of RERs into the traditional system, and growing user prospects are compelling utilities to redesign an electricity generation and distribution system. Consequently, the transition of the conventional 'power grid' towards a modernized system is required. This modernized system needs advanced monitoring, information-gathering, communication, control, management, and decision-making capabilities. Driven by the dynamics of a new energy environment including low-cost telecommunication technologies, new generation options, and advanced automation systems, different organizations have envisioned a future energy delivery network known as 'The Smart Grid' [2]. The Australian standards for Smart Grids [3], defines the smart grid as:

"A smart grid is an electricity system incorporating electricity and communications networks that can intelligently integrate the actions of parties connected to it".

According to the International Energy Agency and the United States Department of Energy (US-DOE) [4, 5], the smart grid has to be:

Intelligent: capable of sensing and monitoring for rapid diagnosis and solutions to power outage events, and aligns the utilities, regulatory authorities, and consumers goals;

Efficient: capable to apply the latest technologies to manage the increased load demand without adding surplus expenditures;

Accommodating: competent in accepting not only large power plants but also the consumer-sited distributed energy resources (DERs). These resources include any type of renewable e.g. mini-hydropower plant, combined heat and power plant and energy storage technologies;

Motivating: facilitate real-time communication among consumers and associated utilities so consumers help balance supply and demand by modifying their energy consumption considering electricity pricing and incentives;

Opportunistic: capable of creating new opportunities in the market to exploit plug-and-play facilities irrespective of place and time. It provides flexibility to energy operators, regulators, and users to change the procedures of business to suit market/operating conditions;

Quality-focused: capable of delivering the essential quality of power that is free from interruptions and disturbances to increase the digital economy;

Resilient: resistant to natural disasters and cyber-attacks with a self-healing ability using smart grid security protocols. This feature helps service providers better manage the delivery infrastructure.

Green: enable the slow growth of global climate change by offering the transition towards clean energy sources to significantly reduce environmental problems.

The smart grid must offer the above-mentioned features in order to function efficiently, deliver the level of service consumers are expecting e.g. affordable electricity system, and offer a sustainable environment. However, the development of essential characteristics of the smart grid faces a number of challenges including power management with large scale deployment of RERs, enabling valuable technologies for energy efficiency, and increasing consumer's choices with aid of bidirectional communication infrastructure. The aim of this research is to overcome these challenges by developing mechanisms for an efficient energy management system. The developed system is capable of optimally utilize and manage RERs, enable consumers' participation, increase the building's energy efficiency and cut electricity cost and consumption.

1.1.2 Green Energy Technologies

Owing to increasing fuel costs and global concern regarding environmental issues, green energy technologies including solar, wind, mini-hydropower plants and storage technologies, are gaining market demand. These clean energy sources offer substantial advantages over fossil fuel sources such as coal, diesel and natural gas [6]. Taking advantage of the smart grid feature of facilitating the on-site deployment of RERs, a number of countries around the world developed the policies and regulations to promote green energy technologies. For instance, Sweden, Denmark, Vietnam, Cambodia, Australia, Japan, China, and the USA aim at 100% renewable electricity by 2040, and have established targets, policies and plans to succeed in deploying RERs in both residential and commercial sectors [7, 8].

A thorough and state-of-the-art condition regarding policies and targets with planned or installed projects regarding renewable energy throughout the world can be extracted from [8]. The large-scale deployment of DERs will indeed present a number of challenges for the smart grid power management and control infrastructure, grid stability, and energy exchange[9]. An uncoordinated and inefficient distributed resources management system could add considerably to electricity costs. For instance, Energy Networks Australia determines that over $16 billion in network expenses could be avoided through proper management of DERs [10].

Moreover, the increased deployment of intermittent renewable sources escalates the challenging 'ramping' and voltage management issues. The renewable generation increases in the middle of the day due to the high penetration of residential PV panels. Meanwhile, electricity demand from the grid decreases as solar is generating enough energy. As a result, export to the grid at midday and electricity demand in the evening time rapidly increases, which causes a voltage rise at the grid side [11]. A small-scale power system with efficient demand-side management (DSM) programs can add value to renewable energy by reducing electricity costs, avoiding exports to the grid and enabling consumers to participate in emerging energy markets.

1.1.3 Microgrid/Active Distribution System

Successful integration of DERs in the presence of dynamic loads and storage has yet to overcome abundant technical challenges to ensure reliability and efficiency. These challenges include optimum DSM, proper scheduling, and dispatch of RERs, uncertain distributed-generation (DG) unit dynamics, load forecasting, voltage and frequency control using a power electronics interface and the unified plug-and-play features of DG units. The concept of microgrids could be an appealing solution to confronting these challenges.

The term “microgrid" actually refers to a localized and miniature version of the existing grid that can support particular electrical vicinity during an outage. The US-DOE has adopted the following definition of microgrid [5]: “A microgrid is a group of interconnected loads and distributed energy resources within clearly defined electrical boundaries that act as a single controllable entity with respect to the grid and that connects and disconnects from such grid to enable it to operate in both grid-connected and islanded mode".

These miniature and smart versions of the existing grid can support a self-sustaining military base, hospitals, industrial plants, data centers or any institutions that cannot afford a power outage for even a minuscule period of time. Both utilities and customers are looking beyond the capability of microgrids used just as support, but rather as distributed generators that can generate power and contribute to overall demand management. A self-sustaining microgrid cannot only help its corresponding neighborhood riding through disruptions but can also support the grid during that time by exporting extra power. These microgrids, used as active distribution systems, could be unavoidable building blocks for the next generation smart grid if they can be properly planned and coordinated. They will also need to be able to operate the microgrid in grid-tied or islanded modes. Smart energy management and/or a DSMS is required for the successful operation of a microgrid in different operating modes with the following technical challenges [12].

- Optimum power flow control within and outside of the microgrid
- Dynamic load management by balancing generation-load-storage-loss balance
- Reserve margin by introducing battery energy storage systems (BESS)
- Adequate installed DG units within islanded microgrids to serve loads

This thesis is an effort to address the microgrid technical challenges by exploiting the customer's capacity to develop load flexibility with renewable energy, storage systems, and demand controls by developing robust DSMS. The proposed demand management system includes novel distributed models and algorithms to facilitate interactions among distributed entities, power flow control within and outside of the microgrid with economic analysis, and supply-demand balance with demand response (DR).

1.1.4 Smart Energy Management System

Modern residential/commercial buildings are equipped with renewable and sustainable technologies such as efficient inverters, smart thermostats and meters, storage technologies, and building automation systems. These buildings can contribute to both the electricity market and the electric power grid by managing their demand by utilizing these technologies [13]. Particularly, smart energy management systems (EMS) incorporation with DG units and storage systems can ensure flexible, reliable, secure and profitable power delivery. Keeping track of the global trends, the number of green star rated buildings is rapidly increasing in Australia, which shows a tendency toward a sustainable and clean environment [14].

By proper utilization of available technologies, smart buildings can operate as self-sufficient electrical entities or microgrids. Nevertheless, the coordination and control of multiple internal loads, storage, and generation in these vicinities is a difficult task, specifically with an emphasis to enable informed participation by customers. Considering the prospects of smart autonomous buildings, research interest in the applications of DERs in microgrids for energy management are increasing. In [15, 16], EMS that consists of ultra-capacitors and flywheel storage systems respectively, are presented for active power balancing and voltage regulation in microgrids when the wind turbine is the

primary supply source. An intelligent building often employs a building automation system to monitor and optimally control the various building loads, such as lighting [17, 18], air conditioning [19-21], thermal and comfort control [22-24] to better manage the energy demand and to increase the building's energy efficiency. Incentive driven energy trading schemes are developed in [25, 26] to trade power between electricity suppliers and consumers. These energy management strategies model the electricity market mechanisms to maximize trading partners' utilities with a truthful bidding auction. Real-time peak shaving models based on predictive and fuzzy control are presented in [27, 28] respectively to curtail peak load using DR and thermostatic load scheduling techniques.

However, in most of the above-mentioned studies, the scale of the demand management systems is limited to the domestic level, not large-scale. This may be due to the inadequate engagement of commercial consumers. Moreover, in previous studies, the evaluation of the environmental and economic impacts of energy-saving measures is based on assumed and/or market average data. Thus, these models are unable to provide an insight into real cost and benefit analysis required to improve the smart buildings' energy efficiency. This research focuses on optimal DSM strategies by modeling the energy usage behavior of distributed entities in a smart grid, which are often self-centered in nature. The aim of this thesis has been to find the optimal techno-economic solution vectors for consumer-centric DSM schemes in smart grids and to conduct real cost and benefit analysis to support energy-saving measures in a smart building.

1.2. Research Challenges and Objectives

While the importance of RERs and numerous policies and regulations, such as financial incentives and feed-in-tariffs, has been addressed in the literature [29] to support the investment on DREGs, there is a need to address DREGs power management issues to achieve the full benefits of the smart grid. These challenges include exploiting the customer's capacity to develop load flexibility with RERs and integrating renewable energy, storage systems, energy efficiency, and demand controls to develop an economical demand management system. In this context, energy analysis of a building integrating RERs that includes the economics of two-way power flow, islanded operation, and an evaluation of technological advancements and energy management strategies to improve the buildings' energy efficiency are worth investigating. There is a need to develop distributed models and algorithms to maximize the use of available renewable power with the support of accurate cost-benefit analyses of two-way power flow between buildings with RERs building, a battery storage system and/or the utility grid. These analyses and models can help to achieve a power profile of buildings integrating RERs that is socially optimal for both the utility grid and the users.

It is worth mentioning that to improve the smart buildings' energy efficiency monitoring and performance analyses are crucial to gain insight into built-environment projects in order to pave the path towards a rapid energy transition from fossil fuels to RERs. This transition helps to reduce energy consumption and carbon footprints from the commercial sector, which could lead to developed countries to achieve zero carbon-building targets. In the literature, various approaches such as empirical research [30-32], simulation research [33-36] and mathematical modeling for cost-benefit analysis [37-39] have been proposed to evaluate the environmental and economic impacts of energy-saving measures in a smart building. Although the existing studies have provided useful

methodological and theoretical insights, the main challenges are limited evidence of real cost and benefits involved and the use of assumed and/or market-average data to conduct a cost-benefit analysis to support the implementation of energy-saving measures. Considering these challenges, a thorough, practical methodology is needed to assess the performance of experimental green buildings where a range of energy conservation measures has already been implemented. Performance analysis could include islanded operation, coordinated measures, energy management strategies and technologies adopted to provide more positive development solutions for the building industry.

Renewable energy trading is an important aspect of energy management in smart grids with an increasing share of electricity supply from DREGs. This energy trade is created by the deliberate involvement of the geographically DERs and energy users of the network. This participation could improve grid reliability and provide social benefits for the entire network. Therefore, economic consideration of energy management of geographically DERs for energy trading at a large scale is important and is mutually beneficial for both the aggregator and prosumer. However, the participation of prosumer in voluntary energy management programs is necessary to exploit the benefits of the smart grid. Therefore, to encourage the prosumer's participation it is necessary to design an incentive-driven energy-trading scheme.

In addition to energy trading schemes, the voluntary participation of consumers is desired in energy imbalance management strategies at times of power supply shortage in a smart grid. As DREGs are owned by self-seeking individual personnel [1], it is a challenging task to provoke the energy consumers to effectively manage their energy usage, while achieving the desired quality of service. While most of the research in this area has been devoted to incentive-based DR programs such as direct load control and peak time rebates, the method of energy reduction in

response to real-time pricing (RTP) during the supply shortage has seemed to receive less attention. Managing an energy imbalance and reducing peak demand is crucial to decreasing the impact of growing demand on network infrastructure. For example, in 2012, the annual expense of energy imbalance in Australia was assessed to be approximately $11 billion [40, 41]. Hence, energy imbalance management in the smart grid in the event of supply shortage is worth investigating to reduce the considerable stress on the entire grid system. Motivated by the issues related to the DSM in a smart grid considering high penetration of RERs the objectives of the current research are defined as follows:

- Developing a profound understanding of the characteristics of RERs which involve uncertainty, privacy and intermittency, and their applicability to the microgrid paradigm.
- Proposing new technologies and coordinated measures to improve real-world smart buildings' energy efficiency, and to gain insight into built environment projects.
- Developing communication-assisted distributed control techniques to facilitate interactions among distributed entities in a smart grid.
- Designing a novel energy-imbalance management strategy for efficiently curtailing responsive loads of commercial buildings with the market price.
- Building a platform for consumers to take part in evolving energy market opportunities such as energy trading, DR, and network provision.
- Providing cost-effective socially optimal solutions for efficiently managing a building's energy in a smart grid as compared to existing solutions.

1.3. Contribution

To develop an efficient DSMS framework by modeling the energy usage behavior of self-interested distributed entities in a smart grid, the questions that must be asked are:

1) Which strategies/techniques should be adopted to improve the smart buildings' energy efficiency for an islanded operation?

2) How to design the incentives for distributed entities so as to motivate them to optimally utilize their resources as well as come to an energy trading agreements, which are socially optimal for all the energy users of the network?

3) What are the most applicable strategies for energy consumers to reduce the energy demand to not only decrease the burden on network infrastructure but that also lead to the energy consumers accomplishing the required quality of service?

The main contributions of this thesis are to provide answers to the above-mentioned questions by exploring the new research possibilities as discussed in Section 1.2. To that end, the aim of my research has been to develop the optimal techno-economic solution vectors for DREGs in a smart grid, and to determine the energy reduction potential for energy users to reduce the aggregated and peak load demand stress on the power system while providing them the desired quality of service by making the following contributions:

1. To assess the effectiveness of the energy efficiency measures and technical solutions incorporated in a net-zero energy building for an islanded operation in a smart grid, the performance of an experimental smart building is studied systematically:
   - A comprehensive energy analysis of an experimental green building is presented by monitoring energy conservation measures through real-time data analysis. It focuses on the

performance gap in terms of energy efficiency, possible explanations, the criticalities related to the characteristics of the chosen devices and demand management strategies adopted.

- Since the monitoring and data analysis results show significant differences from the estimated and real-time energy-saving results, solutions are recommended for optimal performance of the green building. The solution set comprises new technologies, coordinated measures, and control strategies for a robust demand management system. These solutions are proposed to enhance the DREGs generation capacity, improve building energy management system and efficient control of responsive loads in a smart building.
- Several scientific analyses of the proposed recommendations are conducted using Solar Pro and a MATLAB/Simulink tool. The results show a significant improvement in the DREGs generation capacity, the building's energy efficiency and a reduction in energy consumption and cost with the proposed intelligent/advanced energy management system.

2. Taking advantage of the bidirectional communication structure of smart grids, the economics of hierarchical energy trading framework in a smart grid is analytically evaluated by
   - Providing a comprehensive framework based on a non-cooperative contract theoretic approach by encouraging the prosumers to voluntarily take part in an energy trading process. The developed strategy captures the complex interactions between trading partners such as energy retailers known as aggregators and prosumers in an asymmetrical information environment.
   - Presenting a novel dynamic pricing mechanism and a distributed algorithm to incentivize the consumers and

enable the energy trading process respectively. Moreover, various categories, types, and constraints of DREGs, different trading scenarios and wholesale price impact on trading are considered in the analysis for practical applications.

- Evaluating the simulation results of the developed scheme shows that by adopting the contract theoretic approach the aggregator can maximize its profit while stimulating the prosumers to satisfy the load demand with positive utility.

3. To minimize the commercial aggregated and peak load demand in the event of a power shortage, an occupant's comfort-aware energy imbalance management scheme is proposed. In developing the energy curtailment scheme:
   - A commercial building heating, ventilation, and air-conditioning (HVAC) system with multiple zones is considered, where occupants of each zone have different thermal comfort preferences. In the proposed scheme, occupants in various zones decide on an amount of energy curtailed in a zone considering their thermal requirements in the co-efficient of bidding price. These preferences are modeled using an artificial neural network, which is trained using a machine learning algorithm.
   - A novel price-based demand response (PBDR) control algorithm is developed to control the HVAC thermostat setting in various zones in response to RTP signals. Occupant's preferences are directly integrated into the objective function for the optimal scheduling of the HVAC system.

     In the numerical analysis various case studies are conducted, in which the effects of properties such as the occupants bidding price and the set-point interval's effect on energy consumption and thermal comfort are considered.

The results indicate substantial peak and off-peak load curtailment in various zones according to the chosen bidding price. They also reveal that energy savings at a low-set point interval are more significant than at a high set-point interval. With the proposed strategy, the total energy cost of the HVAC system reduces and energy users achieve the quality of service they are expecting.

1.4. Thesis Outline

Subject to the above research objectives and targeted contributions this dissertation is outlined as follows:

Chapter 1 provides the motivation and scope of the current research including the inadequacies of the previous studies, research gaps, and the main contributions of the research. Later, the thesis outline is presented at the end of this chapter.

Chapter 2 focuses on a contemporary literature survey in smart grid DSM including an overview of the smart grid, DERs, microgrid, and DSM techniques. It discusses the existing research trends, research methodologies, and research progress in the selected research area.

Chapter 3 begins by providing an overview of a real smart building considered for energy analysis with monitoring and data analysis results. It describes the possible explanations of the performance gap, criticalities related to the chosen devices, and energy management strategies adopted. It then proposes new techniques, coordinated measures, and control strategies to improve building energy efficiency. It also includes several scientific analyses to show the effectiveness of proposed recommendations.

Chapter 4 provides the mathematical modeling of an aggregator and the consumers that capture the complex interactions between trading partners using a non-cooperative contract theoretic approach. It then proposes a novel dynamic pricing mechanism to incentivize consumers under different trading scenarios. Further, a distributed algorithm is presented for a socially optimal solution for both trading partners. Finally, it describes case studies to analyze the proposed energy trading scheme.

Chapter 5 concentrates on a comfort-aware energy-imbalance management scheme, in the event of a supply shortage in an energy-constrained environment. It provides a model of a multi-zone office building's HVAC system and formulation of the control problem with constraints. The next occupant's thermal preference is modeled using an artificial neural network that is trained using a machine learning algorithm. Thereafter, a PBDR control strategy is developed for optimal scheduling of the HVAC system. Finally, this chapter concludes with numerical simulations and discussion of the proposed strategy.

Chapter 6 provides the concluding remarks by signifying the importance of contributions for a smart grid energy management system. The chapter conclusion shows that the development of a robust DSMS with advanced techniques and algorithms is both feasible and valuable for the whole power system. Future directives for this research are also described in this chapter.

Chapter 2

Literature Review

This chapter highlights the different aspects of the background literature regarding energy management in the smart grid, which covers an introduction to the smart grid, the integration of renewable energy resources (RERs) and various DSM programs in order to promote more efficient energy consumption in the smart grid.

2.1. Introduction to Smart Grid

The next-generation electric power system known as the "Smart Grid" is a considerable improvement to the standard twentieth-century traditional electric grid [42]. The Smart Grid can be described as an electrical system that incorporates information, digital communication technology, and computational methodologies into every aspect of electricity generation, delivery and consumption for improving system reliability and efficiency, reducing environmental impacts and costs, and providing energy markets and services [1, 43]. Moreover, it facilitates the deployment of small-scale distributed renewable energy generators (DREGs), such as solar, wind, and fuel cells, which can be

dispersed around the load centers to reduce the transmission losses and enhance the system's reliability and to add flexibility to the current power system, while also increasing the system complexity [9]. To manage the DREGs, the Smart Grid introduces the idea of demand-control systems, advanced metering infrastructure (AMI), and monitoring and control of power system components for enhancing energy efficiency and grid reliability against malevolent damages [44]. However, its initial scope is widening with the emergence of new markets, and the growing desires of consumers to achieve the specified quality of service. There are different definitions and descriptions of Smart Grid that are available in the literature, as it is envisioned by different organizations, and each has many technology options and functionalities [45]. Considering standard concepts of Smart Grid, which are integrated communications, power system automation and smart power generation different organizations have anticipated the benefits and requirements of future Smart Grid systems as follows:

1. Improving electricity system flexibility, security, and reliability, and optimizing facility utilization using communications, sensors, and automation to avoid construction of backup power plants [46, 47].
2. Efficiently supporting a failure protection mechanism with self-healing retaliation to system disruptions [47].
3. Accommodating various distributed energy resources (DERs) with storage technologies and electric vehicles (EVs) charging support to reduce reliance on fossil fuels for a clean environment [46].
4. Enhancing capacity and efficiency of existing electric power networks by bringing all components of the electric power system generation, distribution, and consumption near each other for the benefit of consumers and the environment [46, 47].

5. Enabling device level near-instantaneous balance of supply and demand by delivering real-time information with the aid of distributed computing and advanced communication infrastructure [5].
6. Ability to monitor the whole power system including power plants, individual appliances and consumer requirements with an automated widely distributed energy delivery network [5].
7. Integrating the actions and behavior of all connected devices using advanced communication infrastructure to provide economical, sustainable, and secure power supply systems [45].
8. Enable new technologies, facilities, and markets, and increase consumer's selections and connections[47].
9. Facilitate opportunities for consumers to respond to dynamic electricity pricing by controlling their electricity use, specifically during peak usage periods [46].

In order to support the planning and organization of the several power supplying and power absorbing distributed entities, which are connected through a communication network in the Smart Grid, the National Institute of Standards and Technology (NIST) provides a framework that divides the Smart Grid into seven domains [47] as shown in Fig. 2.1. Each domain and its subdomain consists of Smart Grid actors and applications. Actors are responsible for making decisions, performing application-specific roles by exchanging information, and include devices, systems or programs. Contrariwise, applications are functions executed by single or several actors within a realm. For instance, applications can be renewable power production, storage system, home automation, and power control and management.

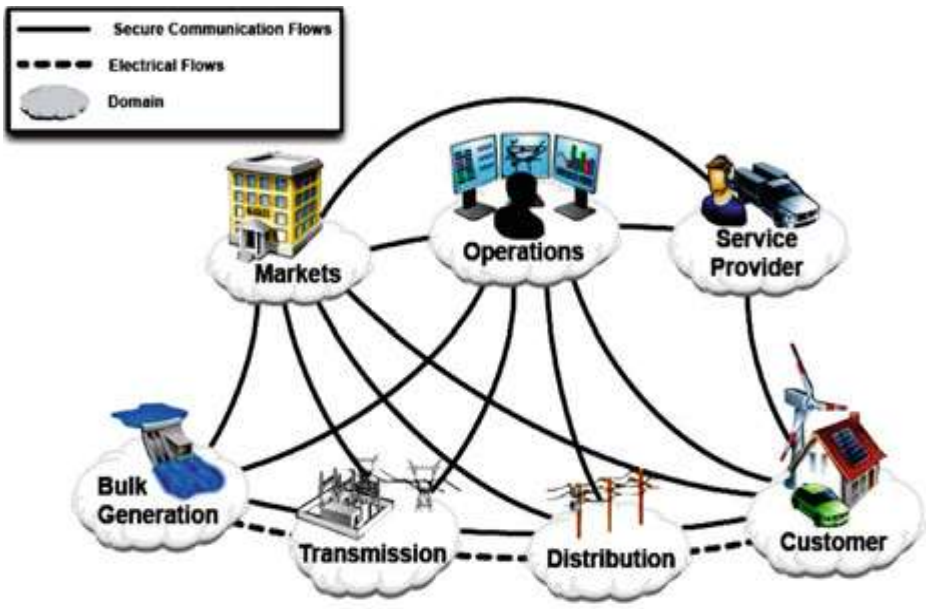

Figure 2.1. NIST smart grid framework [47].

Seven domains with the actors' definition in each domain are: 1) Customers: they are electricity consumers that may produce, store, and control the energy within their premises; 2) Markets: electricity market operators and participants; 3) Service providers: these are organizations delivering facilities to utilities and electricity consumers; 4) Operations: they are managers to ensure the flow of power and information; 5) Bulk generation: the power plants responsible for producing electricity in bulk and may later distribute this energy with the aid of storage technologies; 6) Transmission: the transporters of bulk electricity from a generation site to a distribution site, usually located at long distances from the site of generation, and possibly will produce and store energy; 7) Distribution: the traders of electricity responsible for two-way power flow between the utility and customers. They will possibly produce and store energy. To enable Smart Grid functionality, a specific domain of actors needs to communicate with other domain actors, as illustrated in Fig 2.1. Although actors in one domain have comparable goals, they may have different communications requirements within the same domain.

The detailed description of each domain with the actors' role can be found in [47].

To successfully deploy the Smart Grid technologies and services in the near future, NIST prioritizes six key functional areas that are critical for the development of the Smart Grid [47]. The six key priority areas were recommended by the Federal Energy Regulatory Commission and include wide-area situational awareness, demand-side management, consumer energy efficiency, energy storage, electric transportation, advanced metering infrastructure, and distributed grid management with the aid of cybersecurity and network communications [47, 48]. The six key functionalities are described below:

1. **Wide-area Situational Awareness**

Monitoring critical infrastructures such as transformers, generators, data acquisition and control systems, and utility control centers. The objectives of situational awareness are to detect and prevent malicious threats occurring within critical infrastructure by generating an efficient response to disruptions, as well as optimizing the performance of power system components.

2. **Demand Response and Consumer Energy Efficiency**

Technology-enabled strategies and incentive payments for electric power supply users such as residential and commercial consumers to reduce their energy consumption at times of peak demand or when power reliability is jeopardized. Demand response (DR) is essential for matching the demand for power with the supply.

3. **Energy Storage**

Collection of methods to store energy on a small and large scale within an electric grid. A wide variety of energy storage technologies are now commercially available e.g. pumped-storage hydroelectricity, electrochemical, and electromagnetic storage.

The grid-connected energy storage system is a valuable tool for improving system resiliency by providing emergency backup power.

4. Electric Transportation

This refers to the use of electric motor technology to facilitate large-scale integration of plug-in hybrid electric vehicles, plug-in fuel cell vehicles, and electric batteries. Electrifying transportation could bring significant benefits by reducing diesel consumption and carbon footprints and enhancing the use of renewable resources and their integration.

5. Advanced Metering Infrastructure

To implement a dynamic pricing mechanism for demand management programs, utilities are concentrating on developing AMI. It is composed of several systems including consumer energy controllers, meter data management software, hardware, communications, and consumer-related systems. These systems enable bi-directional communications between energy providers and smart meters, and collect, analyze, and distribute information to energy-users and other parties involved. AMI enables consumers to make informed consumption decisions and facilitate the integrated operation of DR for utilities.

6. Distribution grid management

Utilities are investing in updated advanced distribution management systems to meet customers' anticipations of power quality, reliability, and security by optimizing the performance of distribution systems components. The development of advanced metering and data management strategies and the deployment of DERs and hybrid EVs on a large scale, pave the path towards automation of distribution systems to achieve reliable system operation. The prospective advantages of distribution grid management with next-generation control capabilities include the management of DERs,

interactions with building energy management systems (EMS), and automated billing.

For the development of Smart Grid, governments with a focus on the above-mentioned six key functionalities, universities, businesses, and research institutions have attempted several experimental projects, field trials, and demand management programs. Meanwhile, the key challenges, as elaborated in [1], for realizing the vision of the Smart Grid can be described as follows:

- Accurate modeling of RERs due to the stochastic nature of renewable resources e.g. solar, wind and hydro generation. To overcome this challenge efficient, reliable, and high-quality forecasting and scheduling models are required. Various forecasting models including extreme weather forecasting, short term, long term, and variations in resource levels should be.
- With large scale deployment of EVs, the electric grid certainly has to overcome two main challenges: 1) EVs charging will present a considerable new load on current distribution networks where several grid circuits do not have any extra capacity; 2) As EVs can only deliver power when they are parked and connected to the grid, there is uncertainty in how much power EVs can deliver if a vehicle to grid system is implemented.
- A large amount of data/information is available in a smart grid that is collected from smart meters, phase measurement units, and sensors. Constructing a meaningful database or history from abundant data and deciding which data ought to be stored in a smart grid control system is another challenging task.

- Effective communication between smart grid nodes depends on the interoperability of communication protocols. Since in a smart grid, a wide range of communication technologies, functions and protocols will be utilized, where each technology most probably relies on its own protocol and/or algorithm [1], the interoperability of communication protocols is a challenging task.
- The development of new markets, products, and services enable customers to participate in the energy market by utilizing energy bidding strategies. However, the design of a truthful bidding strategy while protecting the user's privacy is a highly challenging task. It is because certain consumers may make untruthful bids to swindle the seller to acquire benefits they cannot get with truthful bidding.
- Efficient management of energy is a difficult task in the presence of renewable resources e.g. wind and solar due to their stochastic and fluctuating characteristics. Therefore, the design and development of a robust energy management system are crucial to maintain the supply-demand balance and enhance system reliability, while considering the uncertainty associated with renewable resources and forecast values.
- The smart grid vision from various perspectives relies on some basic characteristics e.g. protection and resilience to failures, reliable system operation, and active participation of consumers. However, the realization of these aims presents several challenges such as the effect of growing energy demand, complex decision-making processes, availability of information under users' privacy constraints, cryptographic systems interpretability issues, and analyzing system complexity.

The most of the technologies that are needed to achieve services and standards for future deployment of the Smart Grid are known [49], and the critical issue is the incorporation of these technologies and services under the common Smart Grid structure. The aim of this research is to contribute to two key functional areas of the Smart Grid e.g. DR and consumer's energy efficiency, and distribution grid management as discussed above. The contribution in these two areas is done by developing new techniques and algorithms for energy management in an Smart Grid. These techniques are capable to incorporate voluntary participation of consumers in DR programs, and energy trading schemes to optimally utilize renewable resources, and to enhance the building's energy efficiency.

As previously mentioned the one important aspect of the Smart Grid is to facilitate the deployment of DREGs that create a new market mechanism known as a smart microgrid distribution network. A microgrid is a building block of future Smart Grid which is capable to coordinate various types of DERs utilizing dynamic energy management strategies. A brief introduction of DERs and a microgrid are provided in the subsequent sections.

2.2. Distributed Energy Resources

Around the globe, continuing exhaustion of fossil fuels, environmental issues, and inefficiency in energy systems divert the world's attention towards new ways of power generation at the distribution level from clean energy resources. These resources include a variety of technologies such as biogas, fuel cells, mini-hydropower plants, wind power, and solar photovoltaic cells and their integration into the distribution system. These types of power generators are known as DREGs and the energy resources are labeled as DERs. The DERs are capable of providing a local supply of electricity because they could be placed at utility amenities or at consumers' buildings due to their small size. DERs could

possibly bring about a noteworthy change in conventional approaches to power production, where energy is produced by large generators and is then transmitted using high voltage transmission lines over long distances to load centers. DERs technology can further offer electricity to distant places where the necessary Transmission and Distribution (T&D) services are not obtainable or are too expensive to construct. In addition, DERs offer economical construction charges and low deployment time compared to large centralized power plants and T&D services [50].

Among available renewable technologies, commonly and widely used DERs are wind power, solar cells, and battery energy storage systems (BESS). Due to the clean and sustainable nature of such DERs, government organizations have ordered the wide-scale deployment of DREGs and imposed environmental policies to alleviate the greenhouse gas effect created by the fatigue of petroleum products. Moreover, the struggle against global warming is also an influencing factor in increasing the DREGs proliferation. DREGs suggest a range of advantages such as abundant natural resources, fewer harmful emissions, a sustainable environment, and lower operating costs [51, 52]. There are numerous rules and strategies proposed and implemented by several world economies to encourage speculation on RERs including output-based environmental regulations, interconnection standards, state-based feed-in-tariff schemes, renewable energy certificates, financial incentives, production tax credit, buildings, and vehicle clean energy standards as described in [29, 53-55].

2.2.1 Challenges

With a massive growth in the deployment of DREGs and the broad diversity of related technologies, a number of challenges arise out of increased decentralization. The conventional power network is not intended to integrate electricity production and storage at a low voltage level for distribution. It is also not capable of

supporting the system with a vision to directly supply power to consumers [55]. Therefore, interconnection and integration of DERs to the existing power system is a critical issue and involve significant and critical technical issues as described below [56-58]:

i. Voltage Fluctuations

The existing power system and its associated distribution feeders are designed for unidirectional power flow that avoids voltage sags and swells for end consumers. However, the introduction of DREGs in low voltage networks will require bidirectional power flow where consumers will act as prosumers. They export power to the grid at a higher voltage than their local supply and as a result, the traditional grid may suffer significant overvoltage events, specifically during midday when PV generation is the highest and renewable power is available for export. Complexities related to bidirectional power flow such as unbalanced voltage levels, reverse power flow and unexpected power flow patterns may arise if existing feeder systems persist in the presence of distributed-generation (DG) units in low voltage networks.

ii. Uncertainty

RERs generation capacity normally relies on climatic aspects, which make these resources intermittent and stochastic in nature with a high probability of uncertainty in their power generation. Due to the intermittent nature of DREGs, the balance between supply and demand is difficult to obtain, as sometimes the energy supply is lower than the demand and on other occasions, there is an abundance of supply. For instance, the power output of intermittent energy sources is determined by the diurnal cycle such as the wind turbine’s power output being influenced by air density and wind speed. Likewise, solar generation is affected by the position of

the sun, the amount of cloudiness and solar irradiance at a given time. Thus, intermittent resource variability is one of the challenges that need to be addressed to integrate renewable energy at a broader level.

iii. Distributed Network Protection

With the integration of DREGs, the traditional network protection philosophy that assumes single-source in-feed and radial current flow no longer apply. The traditional strategy uses time and current graded protection, where the coordination of overcurrent devices is employed to clear all types of faults. Principally, DREGs utilize dynamic mechanisms to transform the low voltage distribution system into a multisource energy system with a bidirectional flow of power, which may cause a possible loss of coordination because of unpredictable operating times of the existing protection devices. The reliability of the distribution system is affected adversely due to this loss of protection coordination. Thus, an appropriate protection mechanism is required to maintain coordination between devices under two-way and inconstant power flow conditions with the integration of DREGs.

iv. Privacy and Security

DREGs with their associated controllers are capable of communicating with a number of dispersed consumers, DG units, and the power grid through distributed computing schemes and communication network infrastructure. However, cyber network computing schemes are vulnerable to malware and data infringement, resulting in infrastructure disaster, violation of consumer privacy agreements, theft of energy, and jeopardizing the security of operating personnel. Therefore, with the growing number of consumers and DG units, cyber-physical security and customers' privacy are important issues, which need to be tackled to prevent possible threats and failures.

The proposed work overcome the voltage fluctuations, RERs uncertainty and consumer privacy challenges through a robust demand-side management system. With developed demand management schemes the voltage fluctuations at the grid level can be overcome by avoiding the power export to grid at midday by efficiently managing the demand at the local level. Moreover, with proposed strategies supply and demand balance is achieved while taking into account RERs uncertainty and consumer privacy challenges.

To implement the energy management schemes, a small-scale power system known as microgrid is required with islanding and self-support capability in order to deliver electricity to local consumers. The following section provides a brief overview of microgrid, expected features of the microgrid system and the applications of DREGs in microgrids.

2.3. Microgrid: A Future for Distribution Systems

Considering the significant growth in DREGs in recent years, the microgrid concept is being introduced to facilitate local-scale power generation and consumption systems. There are different definitions of microgrid available in the literature.

1. A controlled system with a cluster of distributed micro-energy sources and loads, which is known as a microgrid, and is capable of delivering electricity to its neighbor communities [59].
2. The United States Department of Energy defines a microgrid as "a group of interconnected loads and distributed energy resources within clearly defined electrical boundaries that acts as a single controllable entity with respect to the grid (and can) connect and disconnect from the grid to enable it to operate in both grid-connected and islanded-mode."

3. A microgrid is viewed as an evolutionary concept of future smart grids with the integration of distributed small-scale renewable energy resources [1].

Figure 2.2 shows a conceptual framework of a microgrid in the context of a smart grid. A microgrid typically consists of a wide variety of small-scale power generating and storage units e.g. rechargeable batteries, capacitors, and phase-change materials to generate power at a distribution level. It usually includes a variety of small power generating sources, as well as storage units such as batteries, flywheels, and super-capacitors [55, 60]. The DG units that are ordinarily found near or at customer premises may include clean energy sources such as solar panels and wind turbines [60]. The point of common coupling (PCC) is a single connection used to connect the electric grid with a microgrid. Depending on the energy supply and demand in a microgrid, the electric power can flow in either direction through this coupling. The scenario in which a microgrid is disconnected from the power grid has termed as microgrid operating in islanded mode. In an islanded mode, DREGs maintain the supply of power to consumers without obtaining the power from the electric grid [1, 61]. The PCC defines the connect and disconnect procedures in a microgrid.

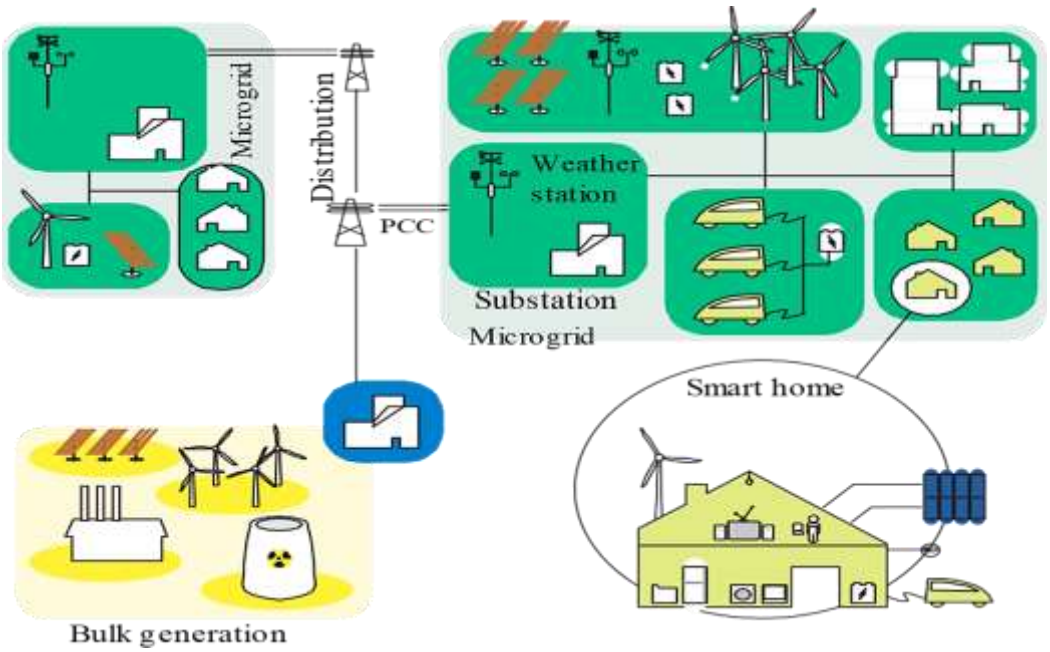

Figure 2.2. A conceptual illustration of a microgrid [4].

The application of DERs in microgrids is extensively studied in the literature with the aim to overcome the challenges arising out of increased DG. In [62] to compensate for the fluctuating demand and output of renewable energy, a microgrid utilizes controllable prime movers, such as the gas engine. An aggregate wind generation system is developed in [63] using a sequential Monte Carlo algorithm to mitigate the effects of the high variability in the output of the wind turbines. In [64] and [65] a 'perturb and observe' technique and a neural network system are proposed for maximum power point tracking of PV systems respectively. These studies show that efficient stable operation can be accomplished without any fluctuations around the maximum power point and the quantity of achievable power from solar panels in a microgrid can be estimated. The work in [66] exhibits that energy balance fluctuations in a microgrid can be reduced by including various technologies of sustainable power generation and optimizing asset utilization.

Another group of researchers supports the installations of BESS to compensate for the variable nature of DREGs and for smooth islanding events in microgrids. With this technology, DREGs can continue to meet load demand even in the absence of power generation sources such as sunlight and wind, which means having the ability to achieve a sustainable energy solution with reduced grid dependency. Moreover, BESS benefits can be seen in terms of extra profits, avoided costs, and reducing electricity bills for the operator, owner and electricity end-users respectively [67]. One of the benefits of avoided costs with a BESS is that the operators can avoid the cost of generation equipment because there is no need to install it. The extra profit would be related to the profit earned by selling stored energy and other facilities obtained by the BESS owner. From a consumer point of view, the benefits of a storage system would be a reduction in their

electricity bill, which means a lower cost of electricity [68, 69].

In literature, studies have been proposed to overcome the microgrids' voltage regulation, security, and privacy challenges. In [70], the intermittent energy source consists of a wind turbine that is considered and its operational challenges in capacity-limited microgrids are presented. In this study, the researchers proposed to utilize static synchronous compensator to reduce the microgrid voltage fluctuations in case of short circuit faults. In [15], a composite storage system that consists of ultra-capacitors and batteries with high power and high energy density respectively is presented for active power balancing and voltage regulation in microgrids. The developed system ensures load leveling and lessening the power trade with the grid for more efficient and flexible system operation. In addition to the above-mentioned technologies, power electronics can likewise assume a significant role in microgrid integration. Electronically coupled units that utilize power electronics converters acting as voltage sources in AC/DC microgrids can interface DERs with a microgrid. Therefore, power converters are required with an unregulated output voltage to integrate the power sources to the electric grid [71, 72]. A three-phase voltage source converter system is investigated in [72] by developing a control system framework to perform stability analysis. The simulation results indicate that the proposed control strategy is effective to regulate the real and reactive power production and alleviates the grid voltage distortion online currents influence.

Dispersed generating units are capable of interacting with each other and/or the energy providers by using the enhanced communication infrastructure in a microgrid. These interactions happening on a large scale has raised an energy security concern with energy being a premium resource. Adequate cybersecurity measures against fraudulent acts, breach of consumer’s privacy,

and loss of data and information related to energy consumption are important to ensure the stability of the microgrid [73]. There are three main objectives of cyber-secure systems:

1) integrity,

2) confidentiality, and

3) availability.

Integrity is the protection of the system against unauthorized modifications or destruction of information. Confidentiality ensures the user's privacy and proprietary over information through authorized access to data and control over disclosure. Availability means to provide well-timed and trustworthy access to data, information, and amenities. Previously from a system reliability perspective, integrity and availability are considered the most important security objective in a microgrid. Now, the importance of confidentiality has significantly grown as users' interactions with the system increased. This interaction involves a bidirectional communication system that interconnects various components of the power system, such as smart meters, AMI systems, data centers, and communication interfaces. A specific point of vulnerability for cyber-attack starts from a consumer's smart meter and goes to the AMI collector system, where customers may utilize a wireless communication interface that provides an opportunity of attack to hacker [74]. In literature, several security mechanisms such as public key infrastructure [75], anonymization [76], privacy-preserving smart meters [77], aggregated data strategy for bill calculation [78] and cooperative methodology for resource utilization [79] have been proposed to handle the security issues in a microgrid system.

Overall, microgrids can incorporate RERs to alleviate environmental concerns [1]. It could offer a reliable power system by limiting line losses, improving power quality, and enhancing

system resiliency and flexibility [80]. However, microgrid reliability depends on the dynamic control of power supply sources and controllable loads. This research work proposes an appropriate energy management system to make sure system efficiency, reliability, and stability with various DERs, storage systems, and internal loads integration. The section below discusses the various demand-side management (DSM) techniques to improve energy consumption, energy efficiency and optimal economic dispatch in smart grid systems.

2.4. Demand Side Management

At the end of the 1970s, the term DSM was introduced which aimed to make aware and encourage the customer to participate in energy management programs. In the middle of the 1980s, DSM programs came into practice and at the end of this decade, these programs were familiar with everyone. There are different definitions of DSM in the literature.

1. DSM programs encourage customers to be more energy efficient by using energy management algorithms and building control strategies [81].

2. DSM has a set of rules or planning to monitor and implement the customer awareness programs used to manage the energy efficiency along with peak shaving [82].

In traditional energy supply systems, energy demand is fulfilled by turning on peak power plants. On the other hand, DSM uses different strategies or developed incentives for smart grid customers to change their energy consumption patterns to reduce the peak load demand on the electric grid or simply shutting off the undesired load. Thus, the DSM strategies help to stabilize the smart grid by providing a balance between energy demand and supply. Moreover, DSM facilitates the consumers to act as a virtual power plant by lowering their energy demand, which ultimately lowers the risk factors on the grid side.

DSM is a collective term used to describe distributed or non-generation demand-side resources. Based on this definition, the concept of DSM includes energy efficiency and DR programs where the DR objective is to support the peak reduction while energy efficiency focus is on energy-saving measures [83]. DSM programs in order to promote more efficient energy consumption in the smart grid include:

1) Promoting high-efficiency buildings, which include a focus on the design of 100% renewable energy systems at consumer premises and utilizing high-efficiency equipment and technologies including energy-efficient lighting, appliances, and heating, ventilation, and air-conditioning (HVAC) units.
2) Facilitating consumers' participation in energy trading schemes with consumer-centric energy management schemes.
3) Encouraging customers to reduce their energy consumption demand at different time slots in response to electricity price variations or based on incentives offered by utilities or control of responsive thermostatic loads for DR to contribute to the efficient operation of the grid.

In the above-mentioned DSM programs, customers could be viewed as flexible power consumers because they play a significant role in power system stability. They allow the utility to monitor and control their appliances or lower, shift and change their consumption patterns in return for incentive payments [84]. Thus, it is important to make the consumers an integral part of energy management schemes to encourage voluntary participation in the DSM programs. The concept of DSM is utilized to facilitate the consumer's participation in order to exploit the complete benefits of the smart grid, which facilitates the customer's interaction with the utility through two-way communication technology [85]. Thus to implement the vision of Smart Grid, it is imperative to

focus on the DSM models and their associated challenges. The following section elaborates on the DSM programs in detail discussed above.

2.4.1 Energy Efficient Buildings

Energy efficiency is a way of managing and limiting the incredible growth in energy consumption. In other words, energy-efficiency means using less energy to achieve the same outcomes or doing more using the same energy [86, 87]. Energy efficiency includes using RERs, installation of efficient appliances and energy monitoring and control using advanced techniques [88]. The notion of power generation from DERs facilities the smooth transition from conventional buildings to energy-efficient buildings.

There are numerous studies [89-91] showing the practicability of a variety of technologies related to renewable energy for both existing and newly constructed buildings including potential advantages and the estimated cost of installation, financial incentives, CO_2 savings over time, and improvements to building energy efficiency. For instance, the study results reported in [89] show that in Australia within 10 years solar and wind technologies including concentrated solar thermal power could meet over 90% of energy demands with a minor extra cost to households. The full-scale residential building retrofit analysis located in north China indicates that a retrofit of both buildings envelop and the space heating system with temperature control of the space can reduce the space heating load up to 65% and the retrofit building can achieve a good improvement of the indoor thermal environment with an acceptable payback period [91]. Moreover, the importance of energy-saving measures including building refurbishment, investment in energy-efficient appliances, and energy monitoring and control using advanced tools have gained researchers' attention for DSM.

The refurbishment of existing buildings is required to achieve energy-saving goals because these buildings, unlike new buildings, are unable to satisfy current building energy codes. In [92], a refurbished university building's energy performance, daylighting features, and the facilities' thermal behavior are studied. The researchers utilized real-time operating schedules and mechanical data of the test building and completed an investigation using both numerical and experimental techniques. In the refurbishment procedure, the single-glazed aluminum framed windows are replaced with double glazed polyvinyl chloride framed windows. The results demonstrate that the yearly cooling and heating demand for energy is reduced by 9.7% and 5.3% respectively, which corresponds to a 4.3% reduction in annual building energy consumption. A life cycle assessment at the material level is used in [93] to show the energy savings in the refurbishment of the buildings. This study compared the environmental sustainability and thermal performance of three different insulation materials. The study recommended expanded polystyrene and extruded polystyrene for the facade, terraces, foundations, basement walls, and floor insulation over polyurethane. The analysis of the results indicates that there is a 55% reduction in operational energy usage of the refurbished building compared to the building with old insulation technology.

Along with the refurbishment of existing buildings, many research studies [94-97] stimulate energy conservation behaviors and supplanting of traditional appliances with energy-efficient equipment. For example, in [94] resident's actions and behaviors related to the utilization of household machines and equipment were evaluated for energy performance. The simulation results demonstrate that the most compelling energy conservation actions to reduce energy consumption in Thai style homes include turning on electric fans rather than using air-conditioners when comfort requirements are satisfactory at room temperature, replacing cathode ray tube TV technology with light-emitting diode

technology, and upgrading incandescent lamps to LED lighting. These measures have the potential to save 978.06, 369.36 and 245.04 kWh/year respectively. The work in [96] reported the survey results of 215 commercial buildings located in an Indian state. The study was conducted to gain insight into commercial consumer's activities and their energy usage patterns. The results show that both small and large scale buildings can achieve an 11% to 26% reduction in energy consumption by replacing non-star rated Air Conditioners (ACs) and conventional lighting with star-rated ACs and LED lighting.

Furthermore, improving building EMS using optimization strategies and robust control can help to increase the energy efficiency of the building [98, 99][13][14]. A smart building usually utilized a building automation system to monitor and optimally control the various building loads, such as lighting [17, 18], air conditioning [19-21], thermal and comfort control [22-24] for dynamic control of load and to enhance the energy efficiency of the building. In [17], consumer-centric software is developed to monitor, control and manage the power demand in public buildings that are operational at the current time. The designed system monitors and controls the lighting of various office places with the support of hardware-independent interoperability and the integration of heterogeneous technologies. The monitoring data shows that the standby power consumed by luminaires and sensor noise contributed to parasitic power consumption. In [21], a model predictive control mechanism is designed for the building to decide HVAC system variability for an upcoming operating schedule in order to maximize the profit. The simulation results indicate that the variable frequency drive fans' energy demand could fluctuate up to 25% in a short span of time around its minimal energy demand without creating a significant impact on the temperature of the building. A hierarchical multi-agent control system with an intelligent optimizer using a particle swarm optimization

technique is developed in [23]. The proposed system control goals are to coordinate the multiple agents and the optimizer to optimize the overall system and enhance the intelligence of the integrated building.

2.4.2 Consumer-Centric Energy Trading Schemes

Energy trading refers to the transfer of energy from a player that produces more energy than it needs to a player with a deficit within a certain time interval in an energy market [100]. Energy trading/energy exchange is an effective way of energy management with the development of DREGs to satisfy the growing demand for electricity. The renewable growth rate has increased the number of participants/players in the energy market including consumers and end-users [101]. These players have created positive competition and investment in the area of energy trading, and an opportunity to develop trading frameworks. There are many factors that need to be considered for efficient energy trading schemes such as players' rationality and privacy, trading volume, number of buyers/sellers and fair pricing between supply and demand prices [102].

The Internet of Things (IoT) incorporates the energy-trading framework with an ability to distribute energy and transmit information. All consumers and end-users are connected through the IoT to communicate in real-time and regulate supply and demand imbalance [103]. With the development of IoT technologies and DREGs, the energy market relies more and more on new players with renewable energies to relieve the power generation pressure of energy suppliers in utility grids. An efficient energy trading framework is required to assess the behavior of all trading partners and includes their personal requirements [100]. In the literature, game-theoretic and contract-theoretic approaches are adopted to tackle the energy-trading problem.

i. Game Theory

To implement an energy management scheme efficiently, the participation of both supply and demand sides is required and they are assumed selfish and self-centered in nature. In an energy management mechanism, suppliers are required to modify their generation, transmit their techniques and energy rates considering various operating conditions. While end-users answer the suppliers' strategies by purchasing more cost-effective electricity than on the traditional market to capitalize on their profit. As both suppliers and end-users are part of the energy market for an electricity trading mechanism, the decision making strategies of one side can influence the other. In such a situation, game theory is an excellent option that provides an opportunity to design a framework to analyze the decisions and techniques of rational players [100, 104].

There are three main components of the model based on game theory such as the set of players symbolized as N, the action set A_i belongs to the ith player, and utility function U_i that corresponds to the ith player, where $i \in \mathrm{N}$. The game mechanism is that each player i selects an action $a_i \in A_i$ to maximize its utility function $u_i(a_i, a_{i-1})$. The ith player's action is not only contingent on its own action a_i but also on the actions chosen by the players other than ith player, symbolized as $\{a_{i-1}\}$.

The aim of the players is to maximize their revenues by changing their techniques. A significant aspect of game-theoretic approaches is the Nash equilibrium, which is a particular condition where no player can enhance its revenue by adjusting its action individually with respect to the actions of the other players. The Nash equilibrium with unaltered techniques could be defined in a mathematical term as a vector of actions $a^* \in A$, provided $u_i(a_i^*, a_{i-1}^*) \geq u_i(a_i, a_{i-1}^*)$ holds, $\forall\ a_i \in A_i$, $i \in \mathrm{N}$, for a static game [105].

The game-theoretic approaches can be categorized into two main types: cooperative and non-cooperative games depending on whether players achieve the Nash equilibrium state by doing competition or cooperation with each other [100, 106]. In a smart grid framework, the non-cooperative game-theoretic approach can be utilized to analyze the energy trading decisions of competitive suppliers and customers. On the other hand, cooperative game-theoretic schemes are appropriate when energy-trading partners cooperate with each other by utilizing communication infrastructure to obtain a socially optimal solution or enhance the efficiency of the traders.

ii. Contract Theory

The energy trading players may have different characteristics according to their power generation and consumption priorities. Innately, different incentives must be offered to these players based on their characteristics. Some players may mislead the utility about their type in order to obtain more revenue owing to their rationality. In addition, in the real-world energy market information asymmetry is present where energy suppliers have no knowledge about the actual types of players. These two challenges make the trading scheme designing tasks very challenging [106-109].

To design an effective trading scheme that overcomes the above-mentioned challenges, the contract-theoretic approach is suitable which categorizes the players into various types depending on their trading features under an asymmetric information environment.

Contract theory which is categorized within an economics field is a powerful mechanism that can be utilized to incentivize the trading players according to their actual types in the presence of asymmetric information [110]. Taking into account N types of players, the trading contract for each type can be written as (a_i, q_i), where $i \in \mathrm{N}$, $\mathrm{N} = \{1, 2, \ldots, N\}$. Here q_i is the quantity

of traded electricity and a_i is the ith player's reward to provide that electricity.

For a realistic contract theoretic approach, the designed contracts must meet the Individual Rationality (IR) and the Incentive Compatibility (IC) constraints. These constraints can be described as follows

- **IR constraint**

Definition: A designed contract meets the individual rationality constraint if the utility of each type of players is assured to be non-negative or positive, i.e.,

$$U_i(a_i, q_i) \geq 0, i \in \mathrm{N} \tag{2.1}$$

Where U_i is the ith player's utility.

The IR constraint stimulates the rational trading players to take part in a trading process with a guarantee of positive revenue.

- **IC constraint**

Definition: A designed contract meets the incentive compatibility constraint if the contract (a_i, q_i) selected by the ith player obtains the maximum utility they can achieve, i.e.,

$$U_i(a_i, q_i) \geq U_i(a_j, q_j) 0,\ i, j \in \mathrm{N},\ i \neq j \tag{2.2}$$

The IC constraint encourages the ith player to choose the (a_i, q_i) contract from all available contracts.

In the energy trading mechanism, primarily, an aggregator or retailer designs and offers the contracts to consumers and/or producers. Therefore, the aggregator can use a well-designed contract scheme to achieve the highest revenue by stimulating other players to act in a required manner.

2.4.3 Demand Response via Control of Thermostatic Loads

The DR definition as provided in [111, 112] is "changes in electric usage by end-use customers from their normal consumption patterns in response to changes in the price of electricity over time, or to incentive payments designed to induce lower electricity use at times of high wholesale market prices or when system reliability is jeopardized". Based on this definition most of the DR programs are designed with an objective to alleviate the power system's burden during peak demand periods or during emergencies. The utility incentivizes customers to modify, shift, and control their appliances consumption through DR programs [113]. They are attracting public attention in contemporary power systems due to their added advantages [114-117].

The highest percentage of electricity in a building is consumed by responsive/thermostatic loads such as air conditioners, refrigerators, and heaters [118]. For instance, HVAC systems in Australia are responsible for nearly half (45%) of the commercial peak demand [119][9]. There are various benefits of controlling thermostatic loads including peak demand reduction, voltage regulation, frequency stability, and supply and demand balance to the microgrid with renewable sources [120]. The control mechanism of these loads is to utilize the small variations in temperature around the temperature band while maintaining the desired temperature for most of the occupied hours. This characteristic amounts to the possibility of shifting demand from one moment in time to another in response to the network's needs, without noticeably affecting the quality of service [121]. Control of thermostatic loads for DR can be generally classified as:

2.4.3.1 Price Based

Price-based demand response depends on consumers modifying their consumption patterns while responding to time-varying electricity

pricing e.g. time-of-use (TOU), critical peak, and real-time pricing (RTP).

i. Time-of-Use Pricing

In the TOU model, the entire day is partitioned into various time periods and electricity pricing is known ahead of time and is usually monthly or seasonal based. The price of energy changes and depends on the time periods of usage such as the off-peak, the shoulder, and the peak period. In this pricing mechanism, the customers can cut electricity costs by scheduling their appliance usage in the cost-effective shoulder and off-peak period instead of the costly peak period. Prices are cheaper in off-peak and shoulder periods and more expensive during peak periods. For instance, energy prices are usually high from 2 pm to 8 pm during the summer months, thus, consumers can save money by turning on the least appliances during this time. The spirit of the DR program relies on the electricity market principle that is energy prices cannot be kept constant for a long-time period and differ along with supply and demand fluctuations. Therefore, to take advantage of TOU mechanisms, customers are required to do rescheduling in order to operate their appliances in the lower-priced period as prices stay constant for a month or a season [122].

ii. Critical Peak Pricing

This pricing model utilizes predetermined pricing values and is normally implemented in combination with other pricing models e.g. TOU or RTP. In the event that consumers exceed the energy consumption limit specified by the energy providers, utilities substantially raise energy prices to limit energy consumption. However, the utility notifies the consumers before preceding to execute a critical peak-pricing scheme. The prominent feature of this plan is to restrict consumers to use minimum power during peak demand periods to obtain supply-demand balance. An investigation directed in California state reveals that the power

consumed by a heater can be decreased by 41% when utility imposes two hours threshold limit to hot water usage with a consumer control [123]. However, without consumer control with a five-hour threshold limit about 13% power is conserved.

iii. Real-Time Pricing

Unlike TOU which doesn't change frequently, the RTP fluctuates as the load conditions vary [106]. RTP is known as electricity retail charges and wholesale electricity prices as determined by the retail market prices. These are the charges to provide the electric power that varies each hour depending on the current load demand [124]. In other words, the RTP scheme provides accurate information about electricity charges at any given time as determined by overall demand. RTP allows end-users to modify their energy usage according to the actual cost of electricity. For instance, adjusting the usage of thermostatic loads when load demand and prices are low because they consume a large amount of electricity [125]. To implement the RTP mechanism, smart metering technologies are essential for a two-way flow of information between the smart meter and consumers [122].

2.4.3.2 Transaction-Based Control

Transaction-based control, a market-based control technique, is a distributed control scheme. It stimulates self-centered thermostatic loads to utilize market mechanisms in order to provide amenities to the electric grid. One important aspect of this control scheme is that it represents consumers' privacy, preferences, and free will because it only requires the electricity price and the amount of desired power information from end-users for implementation. In transaction-based schemes, responsive loads offer their bidding price which is an amount of money they are willing to pay for a specific quantity of power. The bidding price

is submitted to the aggregator, also known as a market operator. The end-user bidding price is calculated considering three main factors: 1) current load condition; 2) customer comfort requirement; 3) anticipated market price and its instability. The aggregator accumulates buy and sell bids from end-users and energy suppliers respectively and clears a double auction market at a clearing price. If the consumer bidding price is higher than the clearing price then the end-user allows using the power at the clearing price. Otherwise, the consumer will wait for the upcoming market-clearing and defer consumption. Afterward, it broadcasts the clearing price and schedules future operations according to the amount of cleared power.

Since the transaction-based approach is like an indirect control operation that does not limit consumers' independence or attack their privacy, it is more popular among users than direct control techniques [126]. The previous studies [127, 128] demonstrate that transaction-based control can be easily implemented by modernizing current thermostatic loads using bidding operation. Another way of implementation is to develop a novel thermostatic controller that is only responsive to market-clearing price and does not operate based on a set temperature dead band. The benefit of this scheme is that the amount of electricity available for consumption corresponds to the clearing price thus provides better tracking for DR [129].

The above literature review reveals that researches have done a lot of work in the area of energy management in smart grids, however, for smart grid realization, there are several prospects in the area of energy management where novel contributions are required. This thesis makes various novel contributions in the area of energy management by modeling the energy usage behavior of distributed entities in a smart grid and making the consumers an integral part of smart grid demand management schemes.

2.5. Chapter Summary

A thorough literature survey on smart grid technology including key functionalities and challenges, DERs potential and challenges, microgrid technologies and DERs application in microgrids and DSM techniques are presented in this Chapter. Based on the analysis presented in this chapter, an energy management system in smart grids with DERs has been designed by utilizing various approaches shown to be effective for DSM in smart grids. Albeit the above literature review shows that researchers have proposed various energy management approaches within the context of the smart grid, still there is sufficient room to do novel contributions in the area of energy management in the smart grid. This thesis proposes various significant novel contributions in this area, beginning with a comprehensive energy analysis of experimental smart building by monitoring energy conservation measures through real-time data analysis as presented in Chapter 3. The next Chapter provides the design and modeling of energy trading schemes in a smart grid for energy management with large penetration of DERs to attain social benefits for trading partners. In Chapter 5, an optimal energy imbalance management strategy is developed for efficiently curtailing responsive loads of commercial buildings with the market price when the energy at the grid and/or from DREGs is limited.

Chapter 3
Performance Analysis of an Experimental Smart Building

This chapter investigates the performance of an experimental green building funded by the Australian Research Council, Australia, as a part of a Zero Carbon Australia (ZCA) building plan to reduce energy consumption and carbon footprints. Beyond Zero Emissions (an Australian research and education organization) draws up a ZCA building plan to avoid average global warming of greater than 2°C and achieve zero carbon emissions from the commercial sector in a decade. In order to implement this plan, the Australian Government and other non-profit organizations offer a large number of grants, subsidies, and incentives to commercial building owners for an energy transition from fossil fuels to renewable energy resources (RERs). In this chapter, the energy analysis of an experimental (6-star rated) green building where a range of energy conservation measures was undertaken is presented. The objective of developing this green building is to reduce emissions and energy consumption from the built environment.

The outcome obtained from the monitored data has shown some significant differences from the expected and previously estimated energy-saving results. This chapter focuses on some possible explanations and criticalities related to the characteristics of the chosen devices and to the strategies adopted. In addition, some coordinated measures, strategies and new technologies to mitigate the highlighted problems are recommended. Furthermore, it includes several analyses to show the effectiveness of proposed recommendations. Through this case study, building designers and operators can gain insights into built-environment projects to provide more positive development solutions for the building industry in Australia and other countries.

3.1. Introduction

In Australia, the majority of the energy used (72%) in the building sector is from electricity and the energy consumption in the commercial sector contributes approximately 26% of Australia's carbon emissions [130, 131]. These figures indicate that participation of the building sector in climate solutions is crucial to make Australia a carbon-neutral country. Australia's emission output, which is high, compared to any other developed economy, indicates that more effort is needed to reduce the average global warming. Research indicates that a 2-degree increase in average global warming will have very significant and adverse effects on human health, species extinction, weather, and sea levels. Therefore, it is extremely important to make an energy transition from fossil fuels to clean renewable sources [98, 132-134]. Australia's net zero-carbon emissions plan is a guideline to achieve a zero-carbon emission goal from the commercial sector within a decade [135]. Research from the Green Building Council of Australia has found that energy-efficient and green star-rated buildings produce 62% fewer greenhouse gas emissions and use 66% less electricity than the average Australian building [136, 137].

However, a good understanding of wide-ranging and coordinated measures is required to make a move towards a zero-carbon future for Australia.

ZCA building plan strategies include reducing electricity demand, enhancing energy efficiency, and improving building energy management and occupant interaction. Electricity demand can be reduced via distributed energy generation at individual building sites, and by sourcing electricity from RERs such as solar, wind and fuel cells [89, 138, 139]. A range of measures can be taken to improve energy efficiency, such as the installation of efficient appliances, lighting and mechanical systems and the passive design of a building to work with the climatic conditions of the site. Advanced control and optimization techniques can be applied to improve the building energy management system [98, 140]. Above all, customers' participation is necessary to capture the benefits that green buildings deliver to the environment, the economy and the community. Their behavioral change in terms of rethinking energy end-use in favor of electricity generated from RERs is important [141, 142]. Therefore, the combined implementation of different intervention policies should be put into practice to reduce carbon footprints for buildings.

The distributed-generation (DG) concept assists to make a transition from traditional to green building. It enables the commercial consumer to generate energy near to/on-site to the consumption site. The availability of sunlight, rapidly increasing competition in the Photovoltaic (PV) market, and the simultaneously increasing efficiency and declining cost of PV panels make it a commonly used on-site generation source [143]. Moreover, PV generation and the load profile of commercial buildings match well and thus allows effective offsetting of peak electricity usage [144-146]. However, a complete off-grid storage system is needed to overcome the solar intermittency problem.

Commercial loads require long-term storage systems, such as batteries and ones based on hydrogen technology. In spite of the lower efficiency of the hydrogen storage system, the use of PV-driven hydrogen generators (electrolyzers) will continue to grow in the future. The hydrogen fuel cell is the key technology for a future hydrogen economy that allows the zero-emission target to be achieved. In the literature, a hybrid power configuration (based on a battery and fuel cells) is preferred over full electrochemical battery power solutions due to its improved performance [147-149].

After deployment of RERs within the storage system, the next step is to effectively manage renewable power production and to create awareness in users towards the technologies. In order to better manage the energy demand and to increase the building's energy efficiency, an intelligent building often employs a building automation system (BAS) to monitor and optimally control various buildings' loads, such as lighting, heating, ventilating and air conditioning (HVAC) systems. Several researchers propose a solution to improve lighting [17, 18], air conditioning, thermal and comfort control [22-24] in existing BAS. However, expanded deployment of variable generation on the bulk power side, distributed energy resources, and new intelligent load devices require new approaches for power management and efficient control strategies [150].

As part of the ZCA building plan, a green building project named Sustainable Initiatives: Sir Samuel Griffith Centre (SSGC), has been designed. The main objective is to exploit the benefits that a green building can offer to achieve a net-zero-emission building plan through effective demand-side management, both as electricity producers and consumers. In this green building design, the abovementioned energy-efficient measures were implemented and new energy-efficient technologies were adopted to reduce energy usage and carbon dioxide (CO_2) emissions. Another purpose of this green building is to function as an energy-aware platform, which is to

be open to future developments, in terms of further adopting new innovative technological solutions and improving building energy management system.

In this chapter, the effectiveness of the energy efficiency measures and technical solutions incorporated in the net-zero-energy building are evaluated. This is achieved through a rigorous analysis of energy use and the performance of devices connected in that building. The results obtained from the monitoring activity from January 2014 to October 2016 are discussed with respect to the performance gap in RERs, devices and control systems. Moreover, we designed a PV system and an improved control strategy based on our recommendations and performed several case studies using the Solar Pro software and MATLAB/Simulink tool. In the future, it will be crucial to analyze the performance of existing green buildings, as consumers need effective communication of practical applications in order to solve the current climate crisis.

The rest of the chapter is organized as follows. Section 3.2 gives a brief introduction of the test green building located at Griffith University, Australia. Later, different factors that affect the net-zero-energy building performance and the outcome obtained from the building's monitoring data are presented in Section 3.3. Recommendations to improve the test green building performance including the latest research-based solutions and better techniques and strategies are outlined in Section 3.4. The scientific analysis of proposed recommendations with real-time and the simulation results are elaborately discussed in Section 3.5. Section 3.6 and 3.7 summarizes the energy analysis of the test building and the cost of technology upgrade respectively. Section 3.8 draws the conclusion for the chapter.

3.2. Test Green Building

This section provides an overview of the test office building SSGC that is an example of genuinely sustainable alternatives used to find practical solutions to environmental issues. It also provides a model that could be incorporated into isolated buildings in remote areas, such as schools in rural communities. The innovative SSGC was officially opened in 2014 and was awarded a 6-star (green-star) rating by the Green Building Council of Australia in 2015. Green Star is a comprehensive, national, voluntary rating system that evaluates the environmental design and construction of buildings. This center (named N-78) is located at Griffith University Nathan Campus, which is in a southern suburb of Brisbane, Australia.

The SSGC is Australia's first teaching and research facility designed to rely entirely on PV modules and hydrogen metal hydride storage technologies for being off-grid. It consists of four levels with the ground and upper floor areas of 7,322 m^2 and 3,740 m^2, respectively. It provides an academic facility with a lecture theatre, and seminar and meeting rooms using 1.1, 1.8 and 5 m^2/person population-density design criteria. In the SSGC, a range of energy efficiency measures is taken to achieve high levels of energy efficiency. For example, lighting control strategies include occupancy control, time scheduling and daylight control. In occupancy control, infra-red motion detectors switch the load by detecting the presence or absence of a person in the space. In the time-scheduling technique, a time clock turns the luminaries on and off at scheduled times. Daylight control is based on photoelectric light sensors that automatically adjust the light flux of luminaries depending on the amount of light available.

An efficient high-voltage alternating-current HVAC system is controlled through thermal and CO_2 emission sensors. The operating

range of the temperature sensors is set according to the green-building design guidelines in order to maintain reasonable comfort levels. External and internal temperature set-points for summer are 24.9°C to 31.9°C and 23.5°C while in winter they are 9.3°C and 21°C, respectively. A flooding set point is also used, which is an automatic program that adjusts the temperature set point when the ambient temperature is extreme and outside the design parameters. For example, if the outside temperature during summer is 38°C (which is 6°C higher than the design conditions), the indoor set-point will be increased by 2°C to ensure a comfortable environment for occupants.

CO_2 sensors are responsible for adjusting the required ventilation through the HVAC system. The installed HVAC system currently provides 7L/person/second of fresh air. The airflow will increase if the CO_2 sensors detect that carbon emissions and gases from volatile organic compounds have increased from a set point. CO_2 control also maintains the CO_2 level between 600ppm to 900ppm in the return air and outside air dampers valve of the air-handling unit (AHU). For energy efficiency, the AHU can initiate an economy cycle when the outside air temperature is between 14°C and 22°C. The economy-cycle control splits the cooling signal into two halves. In the first half, the cooling signal modulates the outside air dampers (open to close) while the second half of the cooling signal modulates the chilled-water valve.

3.2.1 Solar Coverage

PV arrays were installed on the roof of the building and on the northern façade (at different angles for maximum output in different seasons). The building has a total of 1200 panels (970 are installed on the roof and 230 are installed on the northern façade). These panels have a maximum rated power of 375 kW at standard test conditions. Before installation, the average daily energy production of the rooftop and facade panels was projected,

and the results are shown in Fig. 3.1. It is predicted that the rooftop panels constitute 70% to 90% of the total annual energy production. It is also anticipated that the generation capacity of the façade panels will decrease in winters if they installed at the same angle of inclination as the rooftop panels. Based on this anticipation, the rooftop and façade panels are installed at different inclination angles for optimum overall production in all seasons.

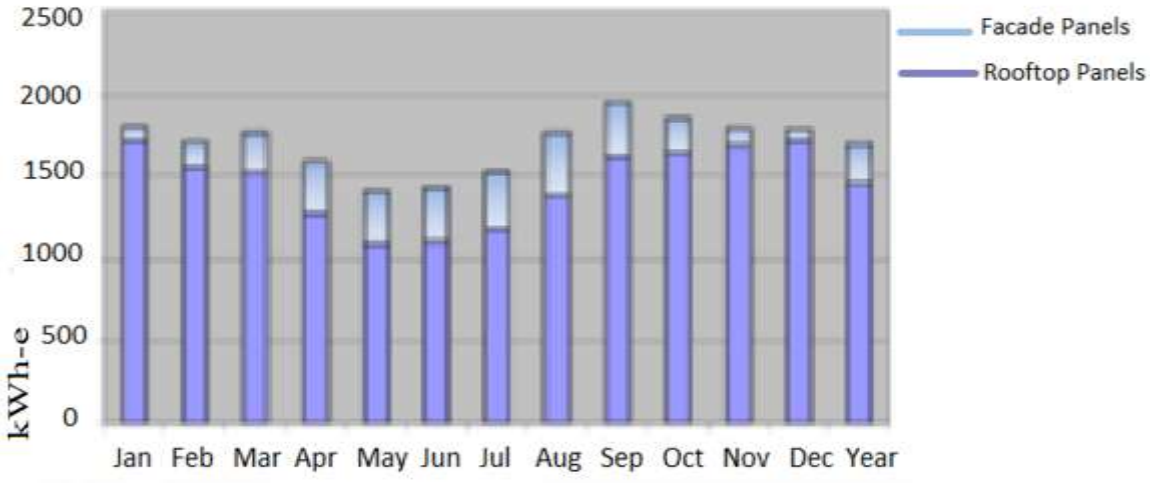

Figure 3.1. Predicted average daily energy production of roof and facade panels

The modules installed on the roof are set at an angle of inclination of 15° to the horizontal for optimum summer production, as shown in Fig. 3.2. Meanwhile, for maximum winter production, the northern facade panels are set at an angle of inclination of 37° to the horizontal (see Fig. 3.3). Together, these panels act to even out production over the year. It is expected that PV panels at these inclination angles provide maximum yearly solar irradiation and optimum production for the SSGC building location of -27.55 latitude & 150.05 longitudes.

Figure 3.2. Stationary PV modules installed on the rooftop

Figure 3.3. Stationary PV modules installed on the facade

3.2.2 Solar Batteries and Hydrogen Fuel Cells

To achieve net-zero energy performance and to reduce the building's load dependency on coal-fired power plants, two different energy storage systems are installed. These are a hybrid power configuration based on electrochemical batteries, and hydrogen metal-hydride storage tanks. The storage system capacity of the lithium-ion battery is 1.3 MWh, where each cell power rating is 1280 Wh with voltage and current ratings of 3.2 V and 400 Ah, respectively. The hydrogen fuel cells consist of two main units, each unit capable of producing 30 kW of power. A hydrogen generator-electrolyzer consumes 36 liters of water to produce 1 kg of hydrogen gas. Approximately 2.7 kg of hydrogen gas is required

to produce 60 kW of power and it takes 6 hours to complete this process.

The hydrogen plant provides chilled and condenser water-cooling systems for the hydrogen-generating electrolyzer equipment. The condenser water-cooling system for the fuel cells includes a heat recovery unit. This unit utilizes the waste heat to heat up the hydrogen metal-hydride storage bottles. A solar hot water system is also utilized to provide hot water to stainless-steel baths housing the hydrogen metal-hydride storage bottles. Figure 3.4 shows the solar power distribution during sunny periods. The first priority is to meet the load demand of the building. The second priority is to charge the lithium-ion batteries, which occurs during solar peak hours. The third operation (after charging the battery) is to produce gaseous hydrogen via the proton-exchange membrane and initiate its storage into hydrogen tanks. If excess power is still available, it is shared with nearby campus buildings.

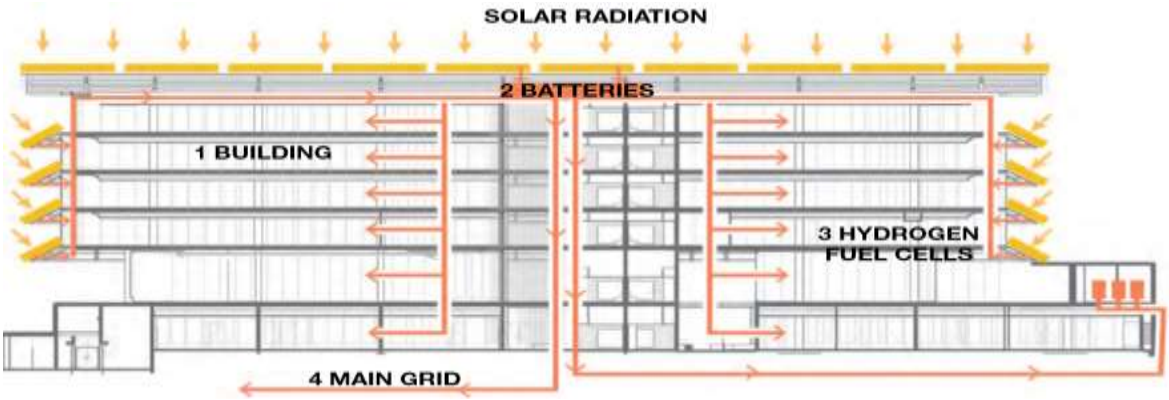

Figure 3.4. Charging batteries and fuel cells with excess solar power in sunny weather

Figure 3.5 shows the cycle of meeting building load demand during cloudy weather conditions or when solar power is off. In this case, the first operation circuit is to supply the immediate demand from a lithium-ion battery power storage tank via a DC/AC converter. The second operation involves power generation using a fuel cell via a DC/DC converter. The hydrogen fuel cells are capable of

providing power over several days in long periods of cloudy conditions or rain.

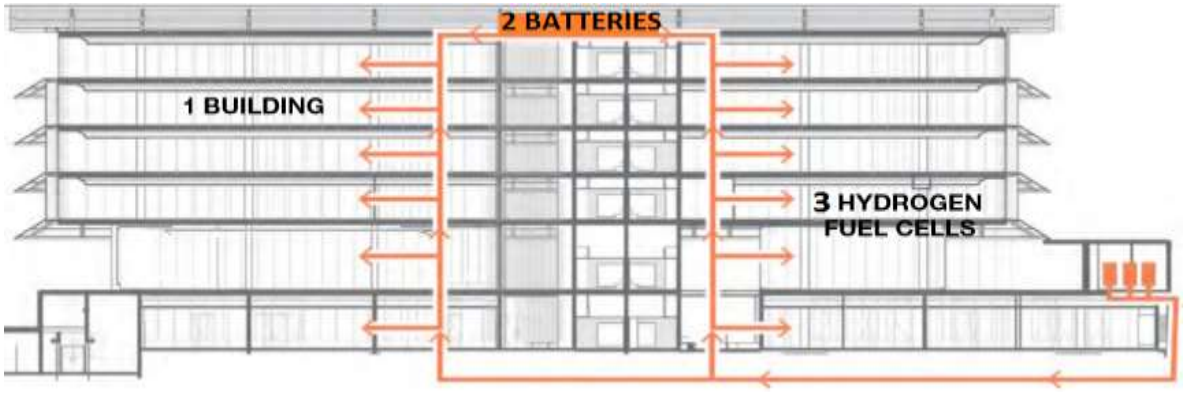

Figure 3.5. Discharging batteries and fuel cells in cloudy weather

3.2.3 Chilled-Water System for Air Conditioning

Chilled water for the building is generated by night and stored in a 750,000 liter insulated storage tank. At night, excess energy is used to chill water for the main air-conditioning system so that it can run on the next day. Figure 3.6 shows the process of water-cooling at night through the chiller and its storage in a 620-kilolitre chilled-water tank. Another air-conditioning unit, separate from the main system, delivers personal levels of temperature and airflow through outlets at each desk or workstation. This reduces the workload of the primary system and provides personal levels of comfort.

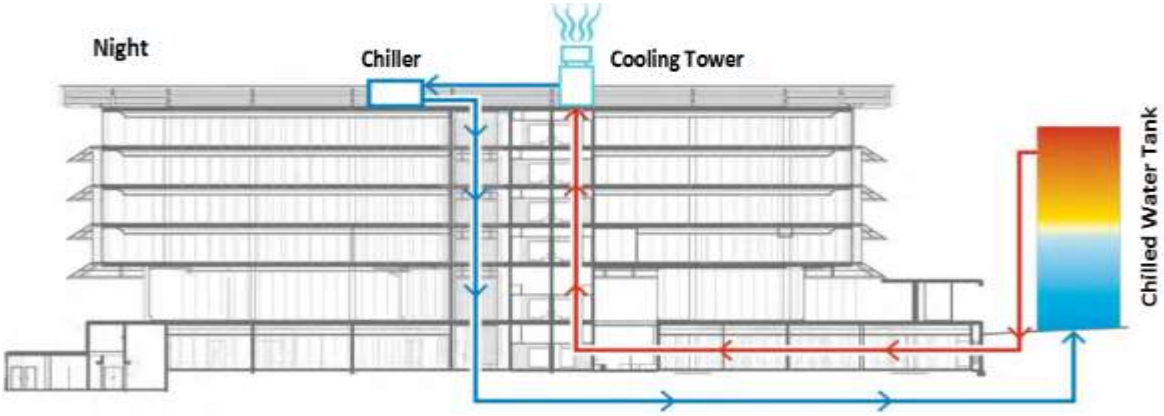

Figure 3.6. Chilled-water tank stores cold water produced at night when most efficient

Figure 3.7 shows the process of chilled-water usage during the day for air conditioning. The supply and return water temperatures for the chilled-water system are 7°C and 13°C respectively. The chiller turns on when there is a rise in entering water temperature and turns off when there is a drop in return water temperature. The chilled-water pump system is controlled by differential pressure switches to maintain the required water flow. The set-point of the cooling tower controls the fan speed to maintain the condenser water temperature entering the chiller.

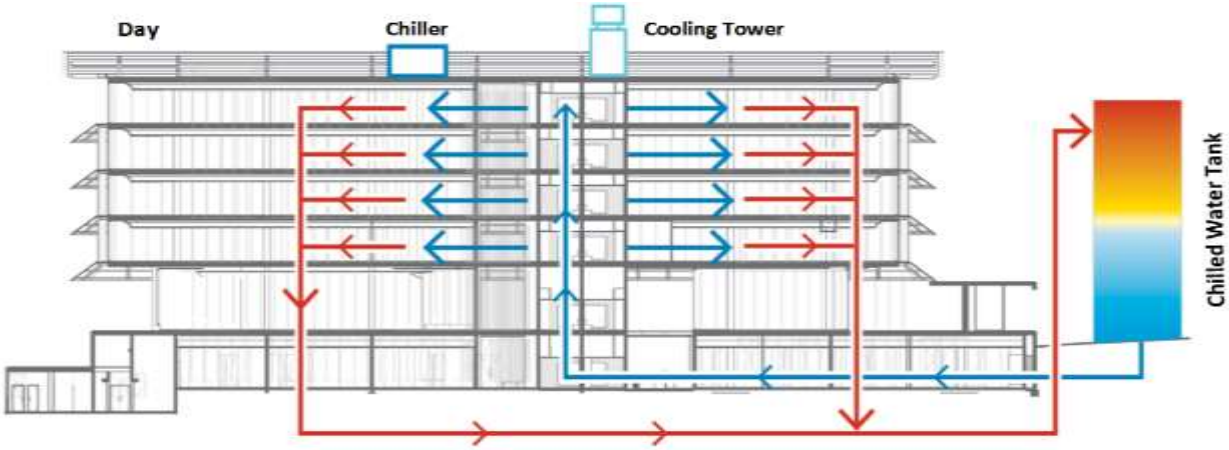

Figure 3.7. Coldwater used during the day for air conditioning

3.2.4 SSGC Main Metering and Sub-Metering Points

One main meter is installed to measure the energy data of the entire building. It gives information about the energy generated from renewable sources, and energy exported and used by the building. At each level of the building, separate distribution boards are installed for lighting, plug-in, mechanical, usable floor area and non-usable floor area loads. The usable floor area is the sum of the floor areas measured at floor level from the general inside face of the walls of all spaces related to the primary function of the building, for example, offices, lecture theatres, laboratories, etc. However, the non-usable floor area is the area occupied by the internal columns and other internal supports, internal walls and permanent partitions, service ducts and the like.

The useable floor area will normally be computed by calculating the fully enclosed covered area and deducting non-usable floor areas such as stairs, corridors, and service areas. These are metered separately. A single-line diagram of the SSGC electrical distribution system is shown in Fig. 3.8. All the sub-metering points are connected to the main switchboard and SSGC microgrid. A fuel-cell plant room is located on level-5 and each fuel cell unit of 30 kW is connected to a separate DC board. Apart from the rooftop, PV modules are installed on levels 1, 2 and 3 of the facade area. Separate meters are installed to measure the electrical parameters of the bidirectional inverters, PV and fuel-cell inverters, and the hydrogen generator-electrolyzer.

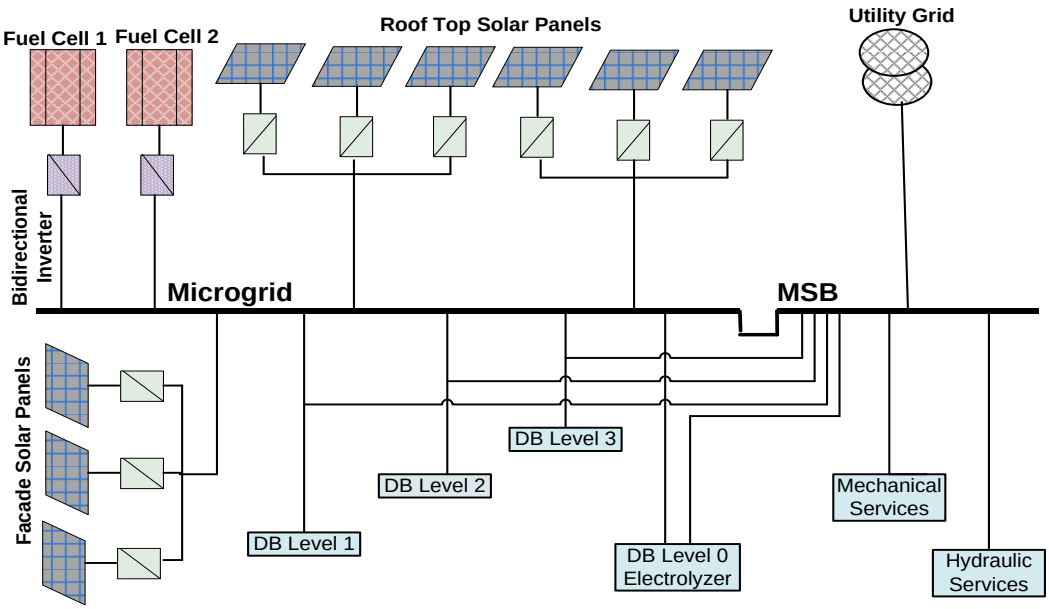

Figure 3.8. Single-line diagram of the SSGC's electrical distribution system

3.2.5 Energy Management

The SSGC building is managed and controlled through a building management system (BMS). All available functions of the BMS are programmed into various systems, such as optimum start/stop, temperature reset, load shed, and special days. The BMS monitors

and records data from the above-mentioned electrical meters connected to the SSGC. The BMS updates the energy data every 15 minutes and the BMS page gives access to the data logged for monitoring purposes.

The key energy meters for data presented in this work include; the main incomer, rooftop solar array, façade solar array, fuel-cell units, and mechanical load. PI System Explorer software and Core Sight software provide access so that data from any energy meter can be monitored. Energy meters provide all the required electrical measurements such as current, voltage and frequency of all phases as well as active, reactive, apparent power and power factors. Solar radiation sensing provides additional information on the installed solar modules and solar data are also monitored through the PI monitoring software. The power output of all PV modules installed at building levels 1, 2 and 3 of the façade area and the rooftop is logged at 5-minute intervals. Daily, weekly, monthly and yearly summaries of load and generation can be obtained through the PI software.

3.3. SSGC Monitoring and Performance Analysis

This section provides an overview of different factors that affect the net-zero-energy building performance. The outcome obtained from the monitoring data of the grid-connected PV system and the installed BMS shows some significant differences from the expected and predicted PV power output and energy-saving results.

3.3.1 Performance Gap due to Low PV Generation

Energy data are monitored and analyzed to determine the factors that cause the low generation from the PV system. Temperature variation and partial shading are the two main reasons for reduced output from the PV unit.

3.3.1.1 Reduced Solar Capacity Caused by Temperature Variation

Although high solar irradiance is generally beneficial to PV electrical generation, it can adversely affect the performance of PV units due to an elevated operating temperature. It is observed from real-time generation data that the solar generation capacity decreases 0.38% with each one-degree rise in temperature from a standard temperature of 25°C. This effect is consistent with the results reported in [151] which shows that solar efficiency can deteriorate by 0.2% to 0.5% per 1°C increase in panel temperature. Overall, this causes a 30% reduction in the generation capacity of the PV modules on the hottest days. Figure 3.9 shows the PV generation capacity on a cooler day (22/01/2016) in summer where the ambient temperature is less than the normal temperature. The average generation on this day is 71 kW with a maximum generation of 260 kW at 12:52 pm.

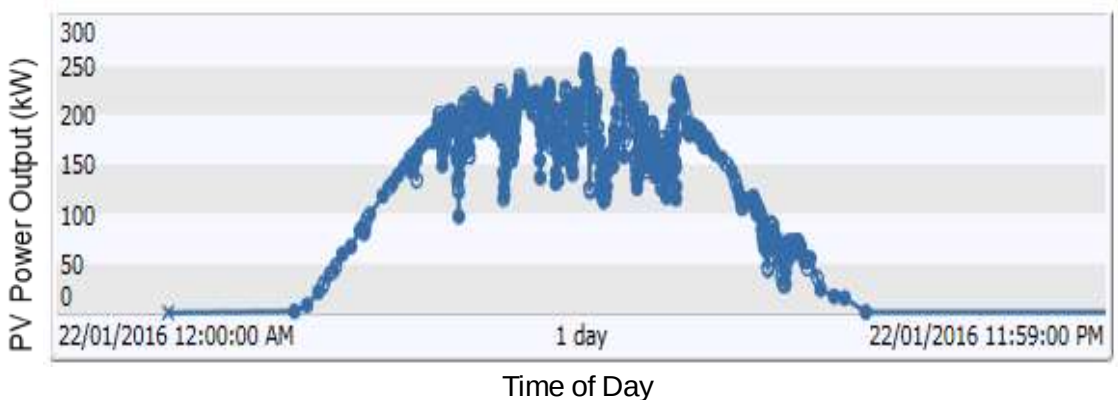

Figure 3.9. PV generation on a cooler day in summer

However, the PV power output dropped significantly in the cloudy hottest summer day (27/01/2015) where the ambient temperature is greater than the standard ambient temperature, as shown in Fig. 3.10. On that day, the average solar generation is only 44 kW. Maximum generation (286 kW) occurs at 9:15 am but the value suddenly falls to 50 kW in 15 minutes, as shown in Fig. 3.11. The short peak occurs on that cloudy day when the weather was sunny for a very short period of time. However, in the rest of the day changes in power output occur due to temperature variations.

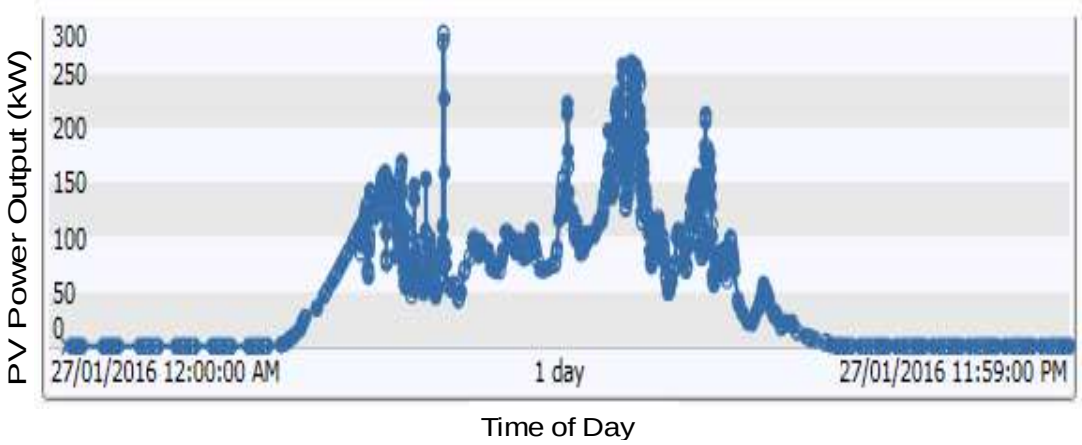

Figure 3.10. Reduction in PV generation on the hottest summer day

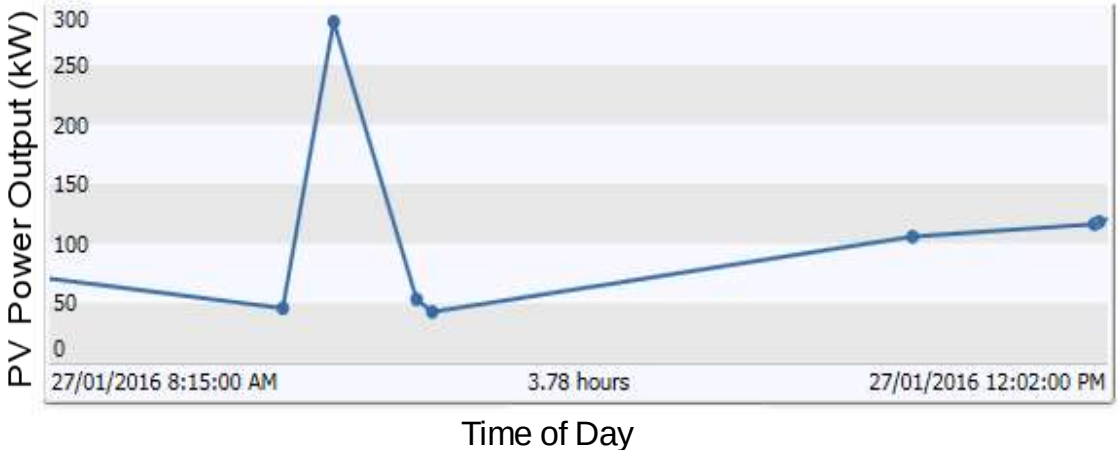

Figure 3.11. Reduction in maximum generation in a short period of time

3.3.1.2 Reduced Solar Capacity due to Partial Shading

The panels installed on the facade at an angle of 37° for optimum solar production in winter cause low power generation in summer due to their angle. In summer, the sun's rotation shades the façade area, which reduces the production capacity by up to 20%. The facade panel's solar generation profile for summer and winter (2015-2016) is shown in Fig. 3.12 and Fig. 3.13, respectively. Table 3.1 shows the PV production data for summer, while Table 3.2 represents the winter solar-generation profile. The average solar generation in summer is only 23 kW, which is approximately half the production in the winter season. This clearly shows that the

solar production of facade panels has fallen significantly during the summer because the panels on the facade become shaded and do not contribute much to PV generation.

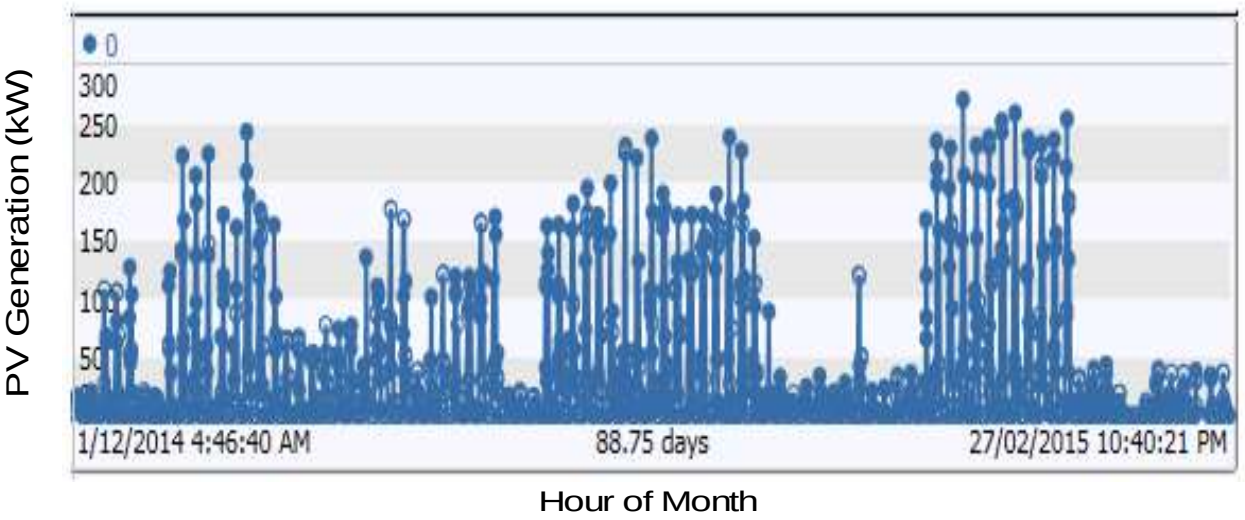

Figure 3.12. PV generation in summer

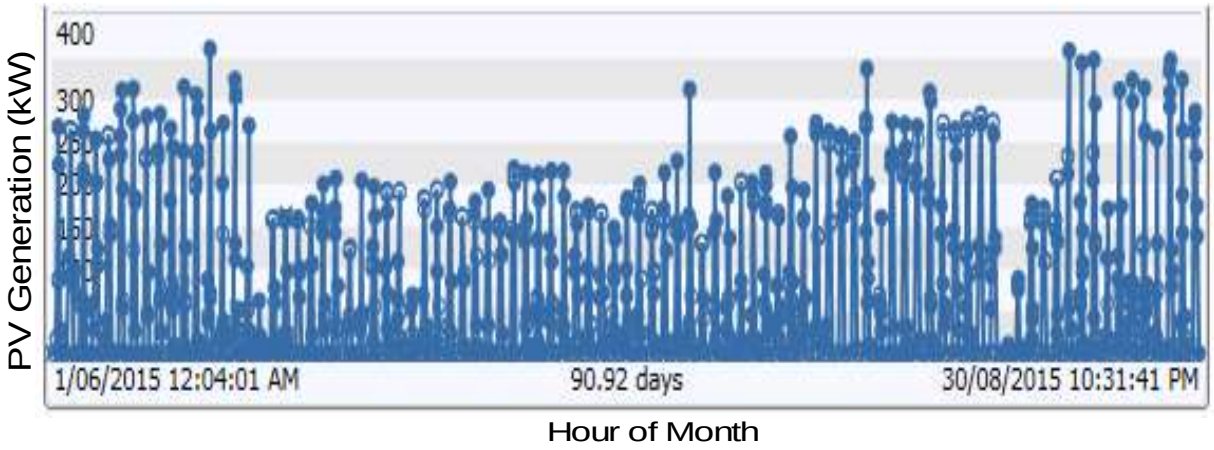

Figure 3.13. PV generation in winter

Table 3.1. Summer Season Generation Data of Facade Panels

Attribute: Power Generation			Season: Summer
Start Time: 1/12/2014			End Time: 28/02/2015
Statistic	Value	Unit	Time Stamp
Accuracy	99.9915	%	1/12/2014 12:00:00 AM
	2018.4140	kW	1/12/2014 12:00:00 AM
Average	22.6788	kW	1/12/2014 12:00:00 AM
Minimum	0	kW	1/12/2014 12:00:00 AM
Maximum	271.2239	kW	7/02/2015 10:47:21 AM

Table 3.2. Winter Season Generation Data of Facade Panels

Attribute: Power Generation			Season: Winter	
Start Time: 1/06/2015			End Time: 31/08/2015	
Statistic	Value	Unit	Time Stamp	
Accuracy	99.9949	%	1/06/2015	12:00:00 AM
Total	3808.8332	kWh	1/06/2015	12:00:00 AM
Average	41.8553	kW	1/06/2015	12:00:00 AM
Minimum	0	kW	1/06/2015	12:00:00 AM
Maximum	359.8386	kW	13/06/2015	12:00:24 AM

3.3.1.3 Overall Difference in Predicted and Generated Power

When a study was conducted to install the solar panels, it was expected that the maximum solar generation would be 375 kW with 1000 W/m^2 radiation capacity at 25°C. The average generation capacity was predicted to be 300 kW as shown in Fig. 3.14.

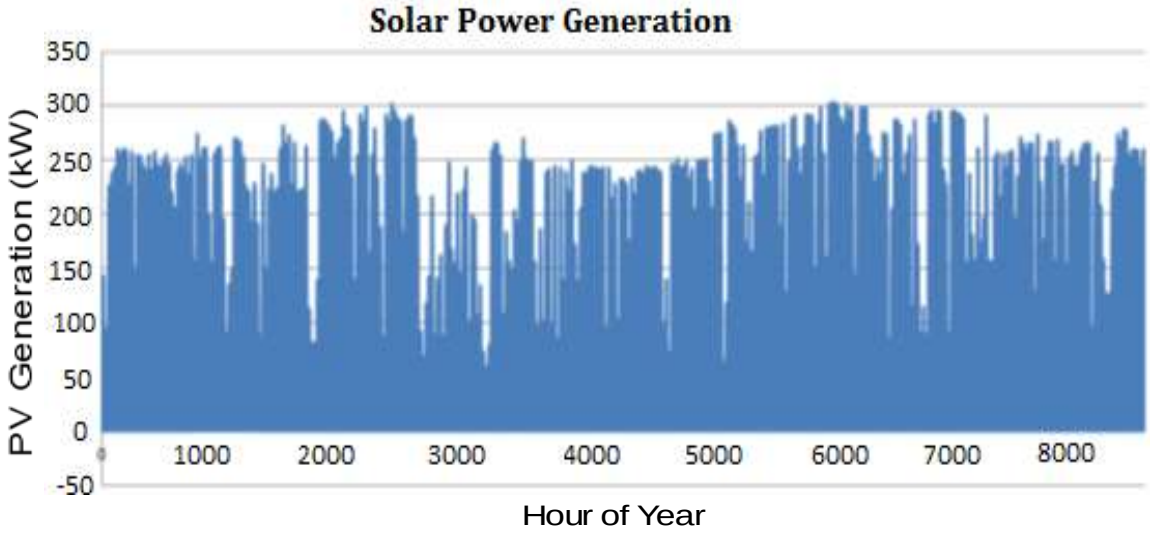

Figure 3.14. Predicted PV generation

However, the average PV generation varies from 220 to 240 kW according to weather conditions as shown in Fig. 3.15. Table 3.3 shows a summary of the annual solar generation. It is clear from the summarized data that the average solar generation is only 44 kW. The maximum solar output is 378 kW that occurred at 11:21 am on 21/04/2015 but for only a short span of time (varying from 30 minutes to 60 minutes. In Tables 3.1 to 3.3 the term accuracy means

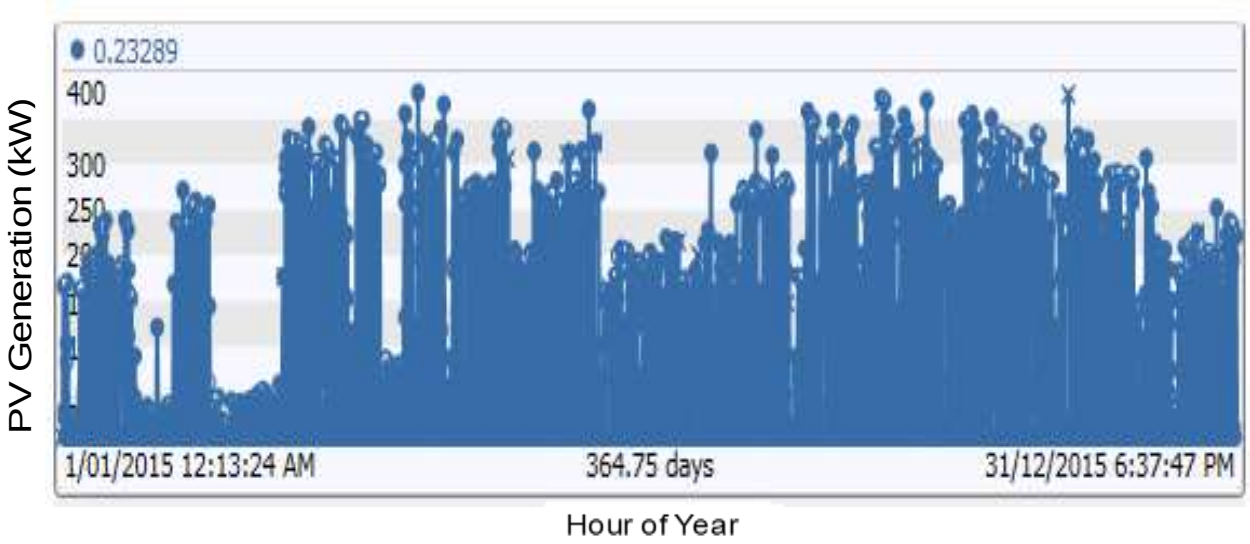

Figure 3.15. Real PV generation output

Table 3.3. Yearly PV Generation Summary

An Attribute: Power Generation			
Start Time: 1/01/2015			End Time: 1/01/2016
Statistic	Value	Unit	Time Stamp
Accuracy	99.9940	%	1/01/2015 12:00:00 AM
Total	16286.3632	kWh	1/01/2015 12:00:00 AM
Average	44.6201	kW	1/01/2015 12:00:00 AM
Minimum	0	kW	1/01/2015 12:00:00 AM
Maximum	378.2972	kW	21/04/2015 11:21:26 AM
Standard Deviation	73.3108	%	1/01/2015 12:00:00 AM
Count	31536000	sec	1/01/2015 12:00:00 AM

the measured solar power generation at a specific timestamp is 99.99 % close to the real value. In other words, the measured values at a specific time are 99.99% accurate. The term total in tables 3.2 and 3.3 refers to the sum of the PV generation in a day.

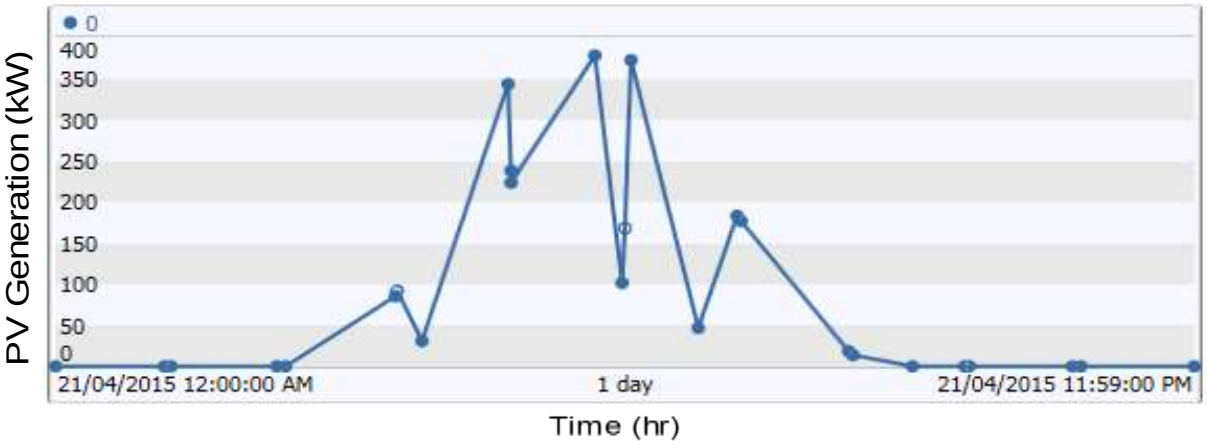

Figure 3.16. PV generation on a sunny day in April

Figure 3.16 provides a more detailed analysis of PV generation on 21st April 2015. The generation curve shows the maximum PV production (378 kW), and that the maximum generation occurs at 11:20 am. However, it falls to 100 kW at 11:54 am. This shows that peak generation occurs for a very short span of time and then it declines with a rate of 9 kW/5 minutes. Both high PV module operating temperature and hot-spot phenomenon contribute to the sharp decline in peak PV generation. The detail about the PV module operating temperature and hot-spot phenomenon is provided in section 3.4.

3.3.2 Performance Gap Due to Inefficient Converters

Renewable-energy-based building or storage systems supply power to satisfy the permanent load demand through DC/AC converters. A charging process of electrochemical batteries and the hydrogen storage process followed by the cycle of power production through fuel cells also require DC/DC converters. In the SSGC building, the efficiency of the installed inverters is 80%. Figure 3.17 shows the charging process of chillers at night (on batteries). The energy flows through PV panels, batteries, and bi-directional inverters. Each time power is converted from DC/AC or AC/DC, 20% of the power is lost because the efficiency of the installed bi-directional inverter is only 80%. The figure below shows the half

process occurs at night time, while at day time the surplus power from PV panels flows to batteries for storage.

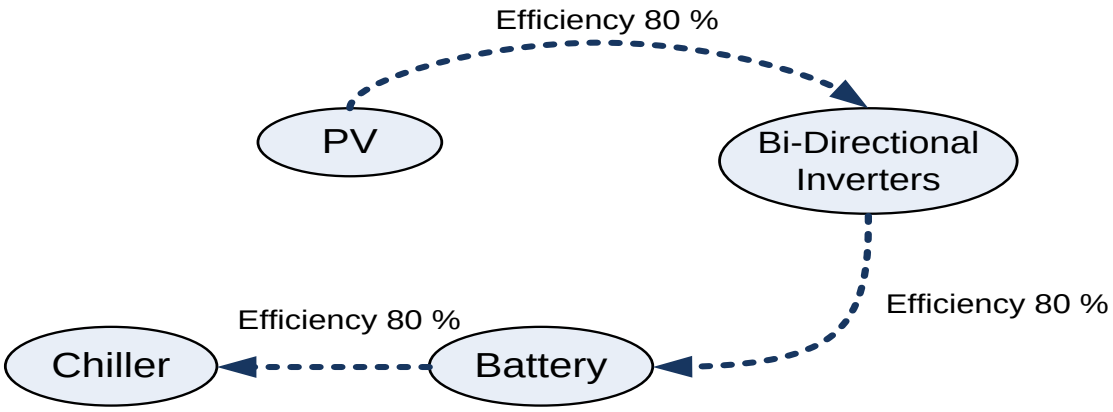

Figure 3.17. Chillers charging process

3.3.3 Inefficient Building Management System Operation

An inefficiently implemented control strategy and faulty sensors cause high-energy consumption and thus reduce the building performance of the SSGC.

3.3.3.1 Designed Control Strategy Problem (No pulse on movement detection)

A highlighted problem in the designed control strategy is that the secondary output of the motion detection sensor goes high (0 to 1) on initial occupancy and remains high until no movement has been detected for 5 minutes, at which point it switches from high to low (1 to 0). A transition is expected from 0 to 1 for every movement detected and latches in for a time period after which it times out and shuts the system down. However, there is no pulse on movement detection as shown in Fig. 3.18.

i. Fault Effect

Energy is wasted because the sensors working with the air conditioning units are not getting re-triggering pulses. At multiple occupancy spaces, air conditioning times out as there is no transition from 0 to 1 for every movement detected. Due to this

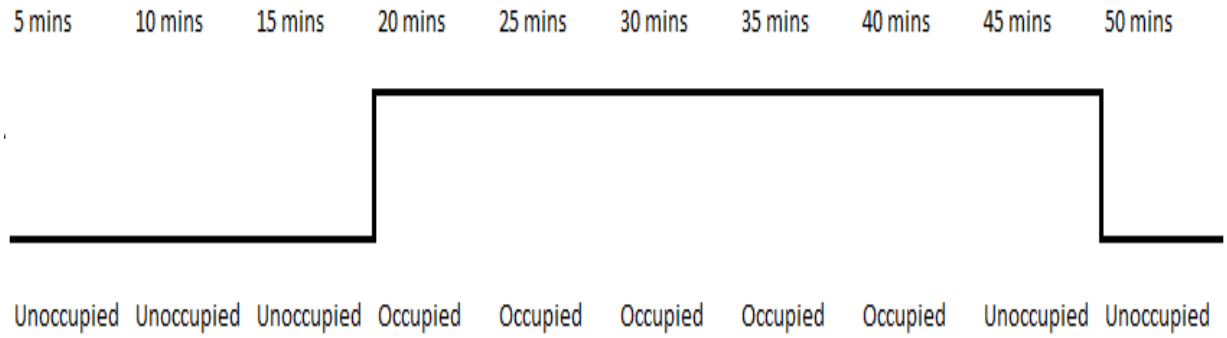

Figure 3.18. Sensor secondary output

software problem, the supplier was bound to remotely force the secondary output from low to high in order to re-trigger the air conditioning to re-start.

3.3.3.2 Some Sensors not Triggering the Controller

It is found that some sensors, for example, installed at level-3 in room numbers 3.28 / 3.29 do not work properly. These sensors did not appear to trigger the digital inputs of the controller to turn on/off the devices based on the motion detection signal.

i. Fault Effect

These sensors are linked with lighting control and result in the light remaining on (and consequently wasting energy).

3.3.3.3 Original Implemented Software

The software was tested during the commissioning phase of construction as having a pulsed input. Figure 3.19 shows the original software that was implemented. This software does work, but it was found that if the motion detector contact failed in the closed position (1 high) it would hold the unit on unless the motion the detector was rectified. Some motion detectors have been noted as faulty on the graphics pages i.e. AHU -1.22.

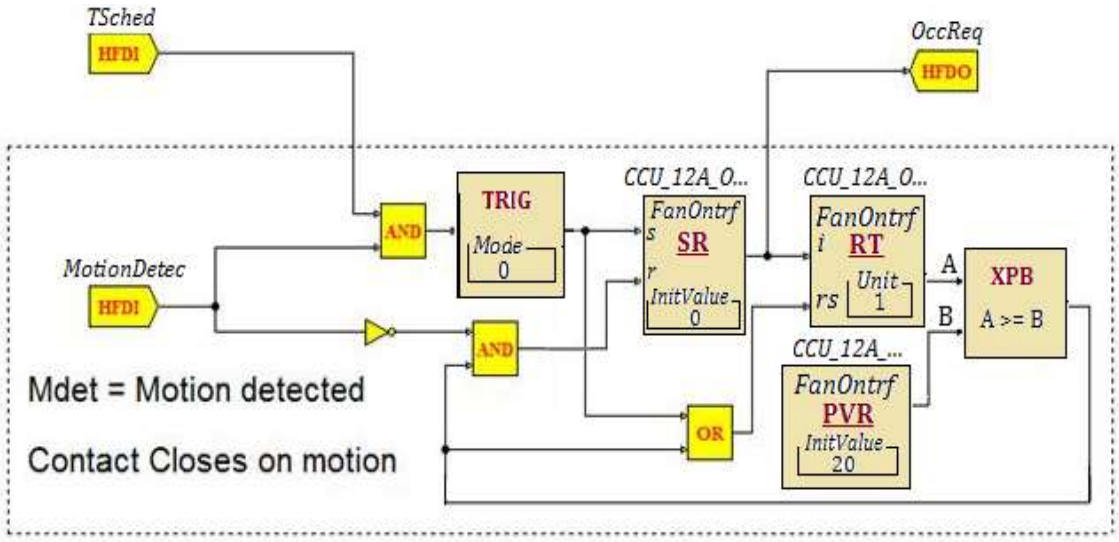

Figure 3.19. Original implemented software

3.4. Recommendations to Improve the SSGC Performance

This section outlines some of the latest research-based solutions that employ better techniques and strategies to improve the net-zero-energy building performance.

3.4.1 The solution to address the Low Performance of PV Modules

The performance of the PV units can be improved by addressing the temperature-variation and partial-shading problems. The solar generation capacity can be further improved by installing a solar tracking system for the PV modules, instead of fixing the panels at a certain angle.

3.4.1.1 Reducing PV Module Operating Temperature

The output power of a PV unit can be enhanced by reducing the module operating temperature through time and temperature-relay actuated dynamic cooling system. The surface temperature of PV modules in Australia is significantly higher than the ambient air temperature in summer. Therefore, a significant cooling effect is required to increase electrical efficiency. Reducing the surface temperature through water cooling techniques at ambient air temperature (35°C to 40°C) is found to increase the energy production capacity of solar panels by approximately 15 to 20%. A

time-based cooling system is preferable over a continuous water cooling system in order to reduce water consumption. In the literature [152], it is found that a time-relay actuated cooling sequence of 5 seconds on and 2 minutes off generates the same energy gain as for continuous water cooling, while requiring only 4% of the water for continuous water consumption.

3.4.1.2 Solar Tracking

Solar production can be increased from the installed panels on the façade by installing a solar tracking system. Research studies show that solar tracking can improve the generated power of a PV module by up to 30 to 40% per annum compared to a fixed module tilted at an optimum angle or by 70% compared to a horizontally fixed module. A two-axis soft robotic actuator (SRA) for solar tracking, specially designed for building-integrated PV applications, is recommended. The low cost and weight of the SRA actuator make it a viable component for dynamic building façades or rooftops. An adaptive solar façade can optimally regulate the energy flow between indoor and outdoor environments. The SRA azimuth angle range could be varied from ± 20° to ± 45°. The energy efficiency of the building and the solar power gain can be improved in both seasons (summer and winter) by installing an SRA solar tracking system [153-155].

3.4.1.3 Hot-Spot Mitigation

A hot spot is the result of a partial shading that lowers the performance of a string of cells over time. The hot-spot phenomenon and how it can be addressed are presented in this part.

i. Partial Shading Problem Formulation

Partial shading produces localized heating in a string of PV cells and causes hot-spot problems. Localized heating not only degrades the string's performance but, over time, it can damage the PV cells [156, 157]. Shading shifts the electrical

characteristics down on a current axis such that the maximum power point current decreases. If the string current becomes higher than the shaded-cell short-circuit current then its voltage becomes reverse bias. In this case, the shaded cell sinks power and generates heat. If the cell sinks significant power over time, the localized temperature increases drastically, forming a hot spot. Although extensive testing has been performed by PV manufacturers to screen out cells that are susceptible to hot-spot problems, it can still occur with partial shading. In addition, the electrical characteristics between cells become mismatched over time and this can start hot-spot problems [158-160].

Hot- spotting is linked to shunt resistance, as higher shunt resistance reduces the chances of occurring hot spots. A traditional solution to this problem is to use a bypass diode over each string in a PV panel. Generally, it is assumed that bypass diodes are sufficient to limit the maximum potential reverse voltage. However, numerous long-term field studies have identified hot-spotting as a significant degradation source over the PV's lifetime, even in systems employing bypass diodes [161-163]. Therefore, more advanced solutions, as mentioned in the next subsection, are required to address this problem.

ii. The solution of Partial Shading Problem

Research studies show that shorter strings result in lower power dissipation and lower temperature in the shaded cells. However, when the string is bypassed all string lengths (12, 24 and 36 shorter to longer), exhibit significant temperature increases and hot-spot susceptibility. These results suggest that open-circuiting, rather than short-circuiting the string, would be a preferable method to eliminate the hot-spotting risk [164, 165]. Recent studies have shown that a feedback-based series-connected Metal-Oxide-Semiconductor Field-Effect Transistor (MOSFET) bypass circuit can reduce over-temperature occurrences due to partial

shadowing. The circuit can sustain a reverse voltage across the shaded cell, thus appreciably reducing the cell temperature. Simulation results indicate a 50% reduction of reverse voltage, corresponding to a temperature decrease of 22°C that leads to a decrease of power dissipation, approximately 62%.

A MOSFET-bypass circuit can be replaced with a diode bypass circuit with negligible additional cost [166]. The automatic switching feature of the MOSFET circuit without control logic and power supply makes it a preferable solution compared to other proposals [167-169]. To implement the recommended strategy, it is necessary to locate the hot-spot points. One idea is to fly drones to locate the hot spots. If this problem is addressed, 30% of the energy can be saved.

3.4.2 Efficient Inverters

There is a need for high-efficiency inverters with ≥ 90% efficiency to save energy. In [170] author proposes a novel single-phase to the three-phase bi-directional inverter with 92.6% efficiency. The proposed design is simulated and its performance is verified with hardware experiments. The latest research [171], proposes a high-efficiency, bi-directional dual active bridge inverter with a novel hybrid modulation design. It has an efficiency of 94.2% and is a promising solution for high-power applications where efficiency and cost are important considerations. High-efficiency inverters based on these innovative designs should be considered for achieving better efficiency. By installing high-efficiency inverters, energy savings can reach 25%.

3.4.3 Efficient BMS Operation

This part highlights an improved control strategy that is designed and implemented to address the problems highlighted in Section 3.3. Improved control strategies lead to efficient BMS

operation that can assist to achieve energy savings and lower power consumption.

3.4.3.1 Better Control of Movement Detection Sensors

The timer code is changed to work with a signal that is 1, so a transition will occur on every movement detected when space is occupied and not just on a rising edge. Figure 3.20 shows the time-control part where software changes are made to address the no pulse on movement detection problem.

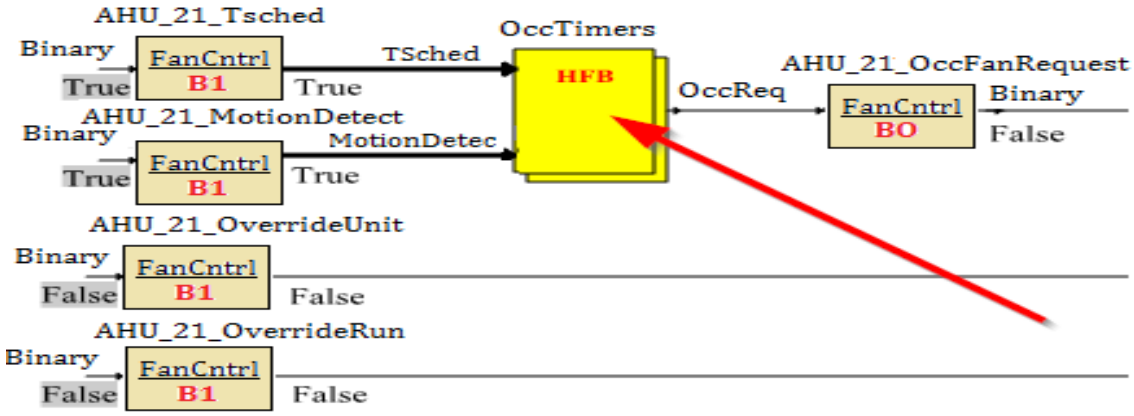

Figure 3.20. Timer control block

3.4.3.2 Improved Software Strategy to Trigger Air-Conditioning Unit

After detecting the fault, an improvement was made to stop a faulty sensor from running the unit 24/7, as shown in Fig. 3.21. This strategy also shuts the unit down when the time schedule becomes unoccupied and saves energy by canceling the run-time timer. This software was developed based on a pulsed input.

i. Strategy Functionality

- There are a time schedule and motion detector associated with this unit. The unit is started when motion is detected and the time schedule is occupied. When no motion is detected for a period of 20 minutes (adjustable) the unit is disabled. In addition, the unit is disabled when the time schedule becomes unoccupied which in turn cancels the timer.

- The motion detector is supplied and configured by others. The motion detector has a dedicated "AC" contact, which closes when motion is detected within the space. A built-in (dip switch setting) timer holds the contact closed until no motion is detected for a period of 5 minutes. The BMS will then proceed to time out its timer.

- If the time schedule is unoccupied and motion is detected for more than 15 minutes, an alarm is raised. This alarm will have text to describe the unit's details.

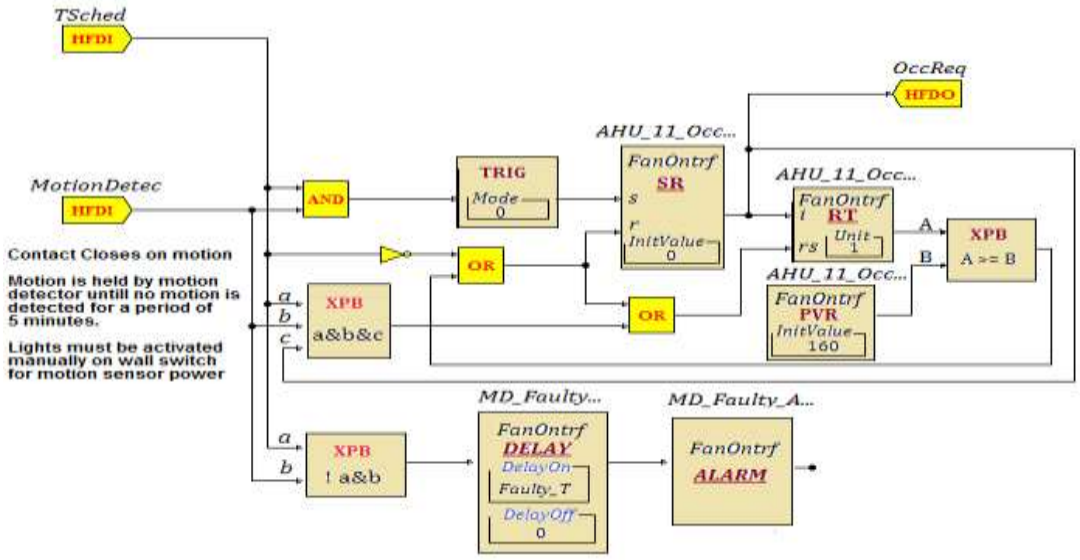

Figure 3.21. Improved software strategy

3.4.3.3 Solution for Sensor Triggering Fault

We observed that some input/output checks are required, and there is a need to change the 'run-on' time of the air conditioning to be 5 minutes after the occupancy sensor transitions from 1 to 0 to solve the sensor triggering a fault. By making these changes in a program, the sensor starts triggering the controller to turn off/on lighting based on movement detection, thus helping to save energy.

3.4.3.4 Energy Saving with Efficient BMS Operation

Figure 3.22 and Figure 3.23 show the level-3 mechanical and lighting load's increased power consumption due to the control-

strategy problem with motion-detection sensors and some faulty sensors controlling the level-3 load. These values were taken on (30/6/2016) when a sensor fault was detected. The mechanical load, average, and maximum power consumption are 2.9 kW and 20 kW, respectively at time instant (t) with daily energy consumption of 17131.23 kWh. Meanwhile, the average and maximum power consumed by the lighting load are 0.7 and 1.98 kW at time instant t, with daily energy consumption of 20414 kWh.

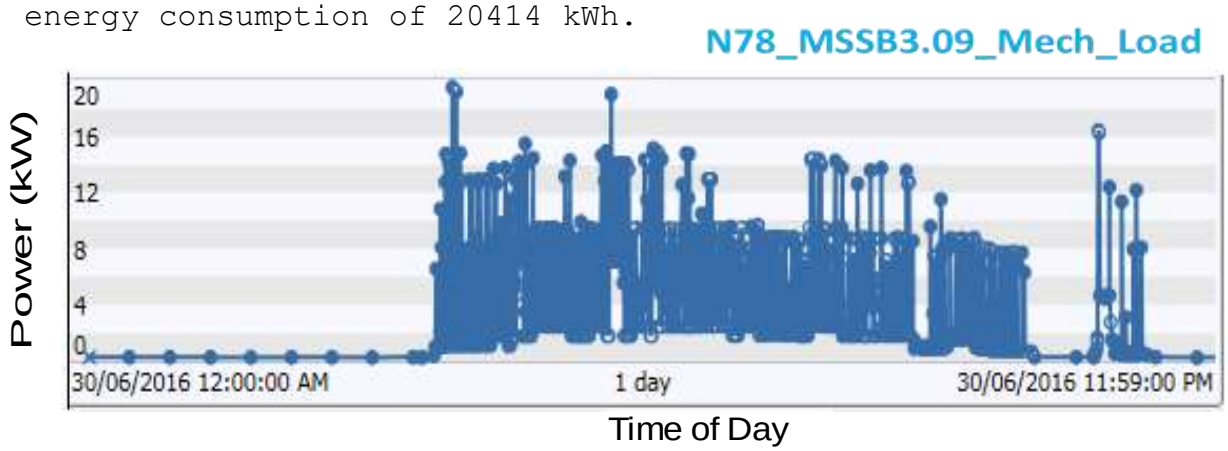

Figure 3.22. Increased mechanical load consumption during sensor faults

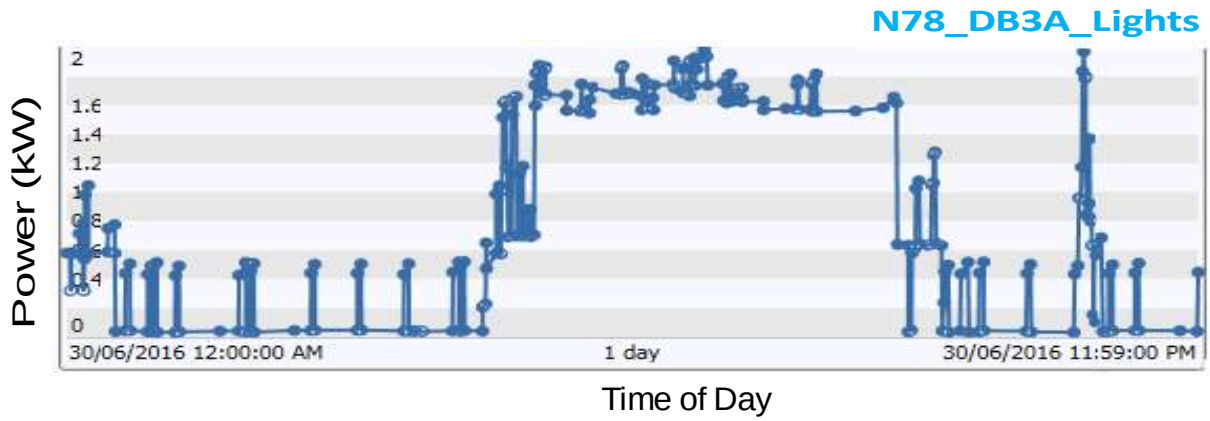

Figure 3.23. Increased lighting power consumption during sensor faults

Figure 3.24 and Figure 3.25 show the reduction in the level-3 mechanical and lighting load power consumption after sensor faults were addressed and a better control strategy was implemented. These values were taken on (26/7/2016); the mechanical load average and maximum power consumption are reduced from 2.9 to 1.92 kW and 20 to 14 kW respectively at time instant t. The daily energy consumption falls from 17131.23 to 16217.47 kWh per day. Meanwhile, the daily energy delivered to the lighting load fell from 20414.13

to 19212.35 kWh per day. The average power consumption of the lighting load reduced from 0.7 to 0.56 at time instant t. Table 3.4 compares the mechanical and lighting load power consumption during and after the sensor faults were addressed.

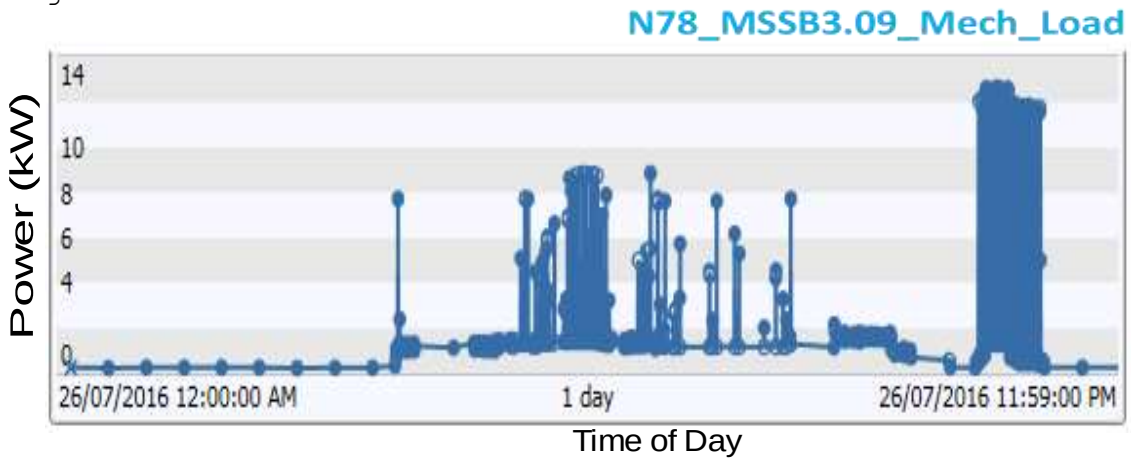

Figure 3.24. Reduced mechanical power consumption after addressing sensor faults

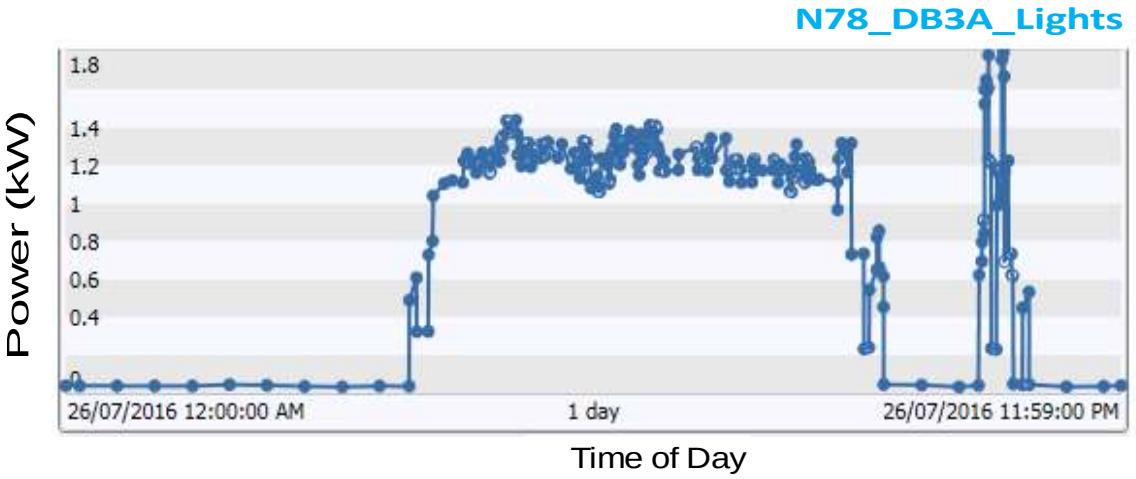

Figure 3.25. Reduced lighting power consumption after addressing sensor faults

Table 3.4. Comparison of Power Consumption during Sensor Faults and when the Fault is Removed

Load Type	Sensor Condition	Power/Energy Consumption over one day			Power/Energy Wastage during Sensor fault over one day		
		Average	Peak	Energy	Average	Peak	Energy
		kW	kW	kWh	%	%	%
Mechanical	Working	1.92	14	16217.47	33	30	5
	Faulty	2.9	20	17131.23			
Lighting	Working	0.56	1.8	19212.35	20	10	5.8
	Faulty	0.7	2.0	20414.02			

3.4.4 The Proposed Transactive Control over Conventional Control

To exploit the full benefits of green buildings, it is necessary to make improvements in the BMS along with energy conservation measures. A lack of an effective BAS can consume large amounts of energy, with 10% to 30% of the energy wasted because of the improper operation [172]. It is possible for buildings to achieve 20%-30% emission savings using an improved energy management system [173]. There is a need to operate the BAS at optimal efficiency with proper trade-offs between cost and comfort, namely transactive control (TC). In this control system, thermostats and energy price signals maintain the comfort level as shown in Fig. 3.26, while in conventional control (CC) the thermostat setting alone controls the equipment [174].

In Australia, electricity consumed by thermostatically controlled equipment varies from 43% (in small office buildings) to 56% (in large-scale modern commercial buildings) [175, 176]. Thus, an existing BAS can be deployed to undertake TC with little or no capital investment, which is ideally suited for thermostatically controlled loads. This control technique can also be applied to sensor-based lighting control systems installed for saving energy in buildings. TC has added several advantages over CC; for example, it makes buildings more demand responsive and this approach can be deployed for both types of price markets (real-time and open). A control system based on both thermal and price signals enables the end-users to directly participate in the open market [177, 178].

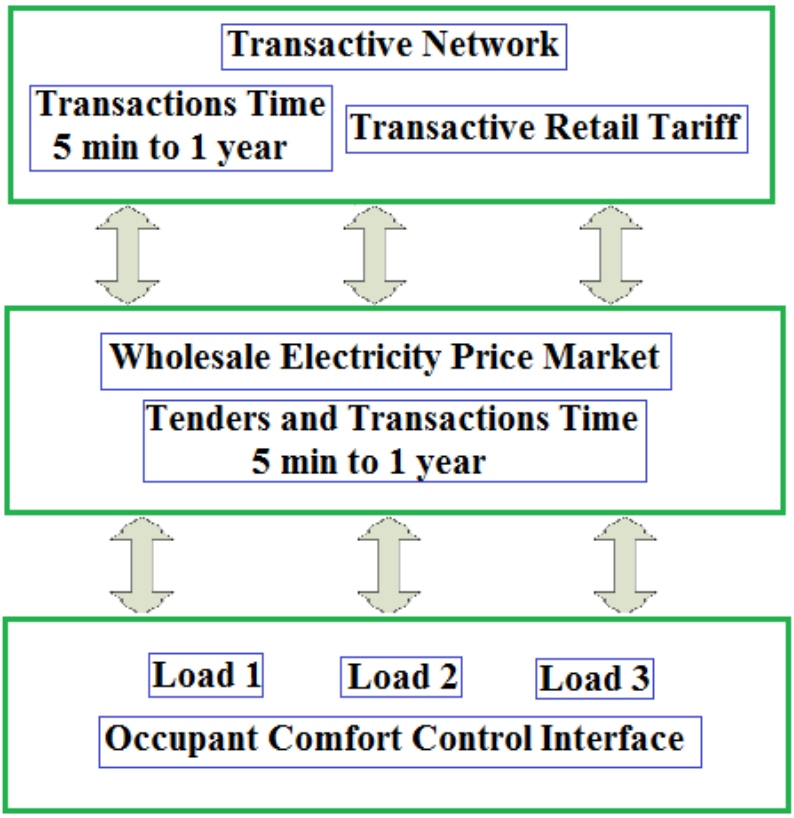

Figure 3.26. Transactive control

3.5. Scientific Analysis of Proposed Recommendations

In this section, we focus on scientific analyses of the proposed recommendations presented in the previous section. The simulation results show the significant improvement in PV electricity generation and energy saving with the TC.

3.5.1 PV System Design and Simulation

We designed and simulated a PV system (equivalent to the PV system in SSGC) to check the improvement in solar electricity generation with high-efficiency inverters and a solar tracking system. Solar Pro software is used to create a 3D model of the SSGC building, shed roof and facade, and horizontal and double-axis tracker PV systems. Table 3.5 provides the parameter values, e.g. architectural features of an SSGC building and specifications of PV panels used for modeling and simulations.

Table 3.5. SSGC Building Architectural Features and Solar Panel Specifications

Specification	Value	Unit
PV Manufacturer	Sun Power	---
Model	SPR-333NE-WHT-D	---
Nominal Power	333	W
Panel Efficiency	20.4	%
Rated Voltage	54.7	V
Rated Current	6.09	A
Open Circuit Voltage	65.3	V
Cells	96	no.
Module Length	1.55	m
Module Height	1.04	m
Building Location	-27.55 Latitude, 153.05 Longitude	degree
Building Height	50	m
Roof Width	150	m
Façade Width	60	m

3.5.1.1 Simulation Cases

In this chapter, the designed PV system models are simulated with six cases. Case 1 represents the PV performance with 0.8 efficiency inverters and without solar tracking for the shed roof. This represents the case of a conventional building-integrated PVs without a solar tracking system. Case 2 replaces the low-efficiency inverter with a high-efficiency (0.954) inverter with a fixed angle. Case 3 is the same as Case 1 but simulations are done for the facade. In Case 4 and 5, the simulation set-up is similar to Case 3 but a horizontal-axis and double- axis tracking system is used, respectively. Case 1 is the base case for Case 2, and Case 3 is the reference case for Case 4 and 5 for performance comparisons. Case 6 repeats Case 3, 4 and 5 for the shed roof. Table 3.6 summarizes the simulation cases for the designed PV system.

Table 3.6. Simulation Cases for the Designed PV System

Case Type	Roof Type	Inverter Efficiency	Tracking System	Tracking Angle
Case 1	shed	0.8	Fixed angle (no tracking)	15°
Case 2	shed	0.954	Fixed angle (no tracking)	15°
Case 3	facade	0.8	Fixed angle (no tracking)	37°
Case 4	facade	0.8	Horizontal axis	Tilt α
Case 5	facade	0.8	Double axis	Tilt α and Azimuth β
Case 6	shed	0.8	Fixed, horizontal axis, double axis	15°, α, β

In Solar Pro, calculations are performed at the module level by taking into account irradiation, temperature data, shading and other loss factors for accurate energy calculation. It allows users to visualize shading and analysis of solar electricity generation on an hourly, monthly or yearly basis. Figure 3.27 shows the 3-D modeling of the SSGC building, shed roof and façade designed using Solar Pro.

3.5.1.2 Results

In Griffith, there are 1200 panels but the obtained results in this section are for 400 modules with 133 kW capacity. All parameters of the PV system in the simulation are taken from the real PV system in the SSGC building. The experimental green building's designer decided to use the PV inverters with 0.8% efficiency considering various other factors such as safety, PV inverter safety, low-noise operation, and price-performance ratio, etc. The efficiency of common inverters available in the market varies from 0.96 to 0.98% [179].

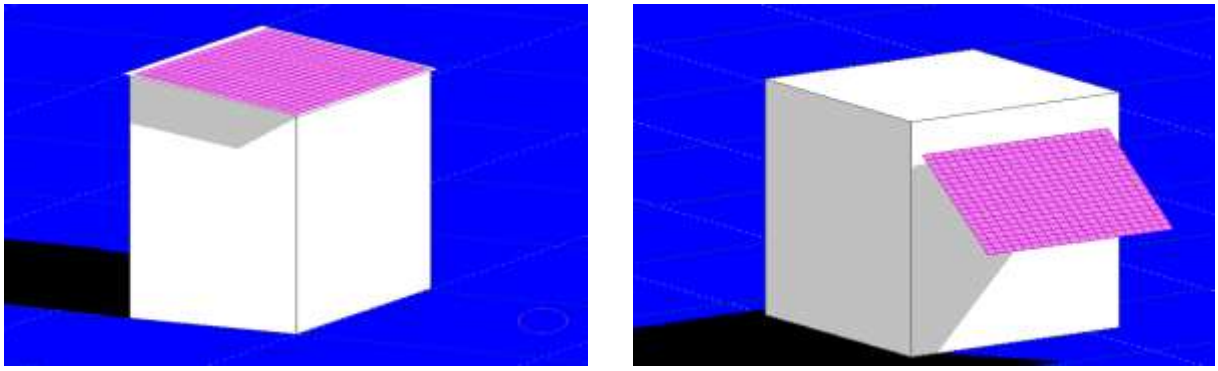

Figure 3.27. Model of shed and facade roof of SSGC building

i. Improvement in PV AC Energy with High-Efficiency Inverters

For the designed PV system with Case 1, the PV AC energy production on a selected day is 603.26 kWh while it increased to 712.50 KWh with the Case 2 set-up. This shows an improvement of 15.34% in PV AC energy generation. Figure 3.28 compares the PV AC energy with low and high-efficiency inverters. Similarly, the specific AC energy increased from 4.53 kWh/kWp to 5.35 kWh/kWp on the same day. Hence, the extraction of power from the PV arrays can be improved by using a high-efficiency inverter.

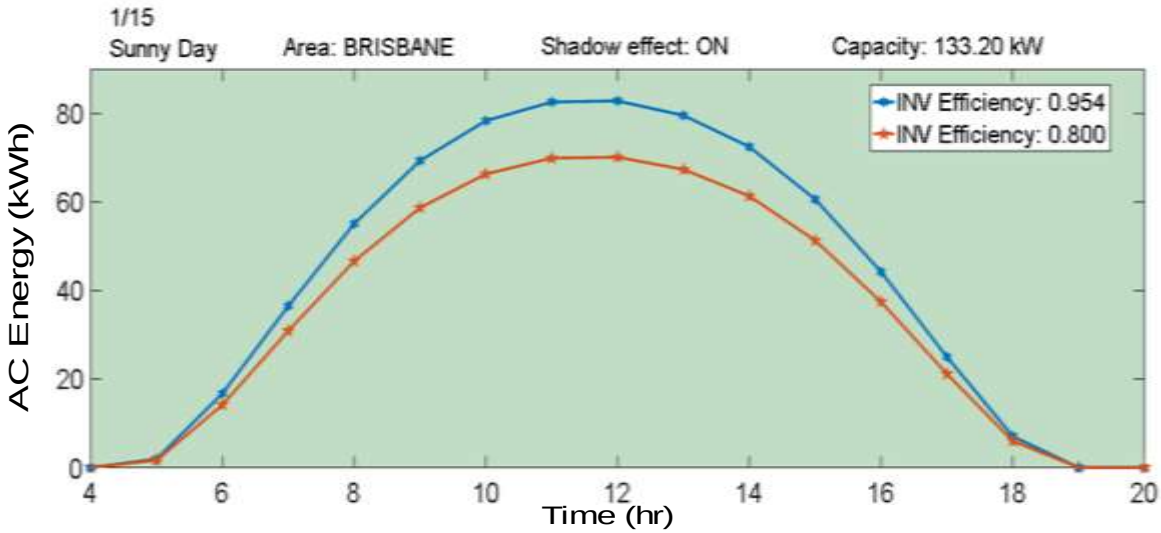

Figure 3.28. Improvement in AC energy with high-efficiency inverter

ii. Improvement in PV Production with Solar Tracking

For Case 3, the daily module AC energy at the reference position tilted 37° w.r.t the wall and oriented to the North was 645.96 kWh. Case 4, which simulates the system with a horizontal-axis tracker

increases the solar electricity generation from 645.96 kWh to 944.20 kWh, a potential gain of 31.1%. For this case, the tilt angle α varies from 71.25° to 22.5° for 5:00 to 18:00 solar hours. For Case 5, AC energy gain is 32% and the azimuth angle β variation is ± 18° to ± 41.37° from 5:00 to 18:00 hours. Figure 3.29 compares the PV AC energy production with and without a solar tracking system for the facade. Tracking for façade Case 6, where we repeat Case 3, 4 and 5 for the shed roof, horizontal- axis and double-axis solar tracking, shows an AC energy gain of 4.5% and 5% respectively compared with no tracking. Moreover, it is cleared from Fig 3.29 that PV generation varies as the sun radiation and angle varies throughout the day. For instance, around 10 am PV generation is maximum because at this time solar irradiance is highest (1000 W/m^2). After that solar insolation will be reduced depending on the angle of the incident of sun rays with the ground which corresponds to the decline in PV generation.

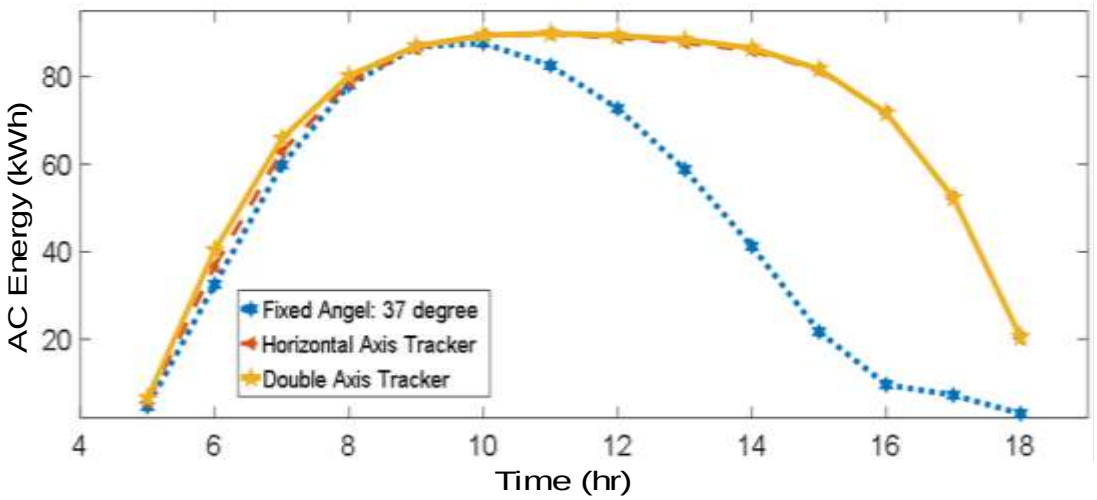

Figure 3.29. Comparison of AC energy without and with solar Tracker

Table 3.7 summarizes the PV performance for the different simulation cases. From our results, we conclude that facade PV panels with a solar tracking system can potentially enhance PV generation by 32 %. This is consistent with findings from [38] and highlights the importance of a tracking system in improving the solar panel's efficiency.

Table 3.7. PV Performance for the Different Simulation Cases

Case Type	Roof Type	Inverter Efficiency	Tracking Angle	PV AC Energy (kWh)	Increase in Energy Production %
Case 1	shed	0.8	15°	603.26	---
Case 2	shed	0.954	15°	712.50	15.34
Case 3	facade	0.8	37°	645.96	----
Case 4	facade	0.8	Tilt α	938.56	31.1
Case 5	facade	0.8	Tilt α and Azimuth β	944.20	32.0
Case 6	shed	0.8	15°	760.62	---
			Tilt α	798.03	4.68
			Tilt α and Azimuth β	804.04	5.4

3.5.2 Bypass Circuit to Reduce Reverse Voltage

In this section, we design and simulate a MOSFET-bypass circuit to address the hot-spotting problem as mentioned in Section 3.1.2. The result shows that the MOSFET-bypass circuit appreciably reduces the reverse voltage and localized heating if compared with the traditional bypass-diode circuit. For simulation, a few cells of the panel were considered to be shaded and irradiated at 300 W/m^2, while fully illuminated cells were irradiated at 1000 W/m^2 at 25°C. Figure 3.30 shows a schematic diagram of the traditional bypass-diode and MOSFET-bypass circuit with full illumination and shaded conditions.

The designed bypass circuit is based on the feedback operation of a series-connected power MOSFET that develops a high voltage drop when a solar cell is shaded. The voltage drop across the power MOSFET is entirely subtracted from the reverse voltage affecting the shaded cell, thus significantly reducing the cell temperature. The development of a reverse voltage across solar panels with the traditional bypass-diode and MOSFET-bypass circuit is in (3.1) and (3.2) respectively.

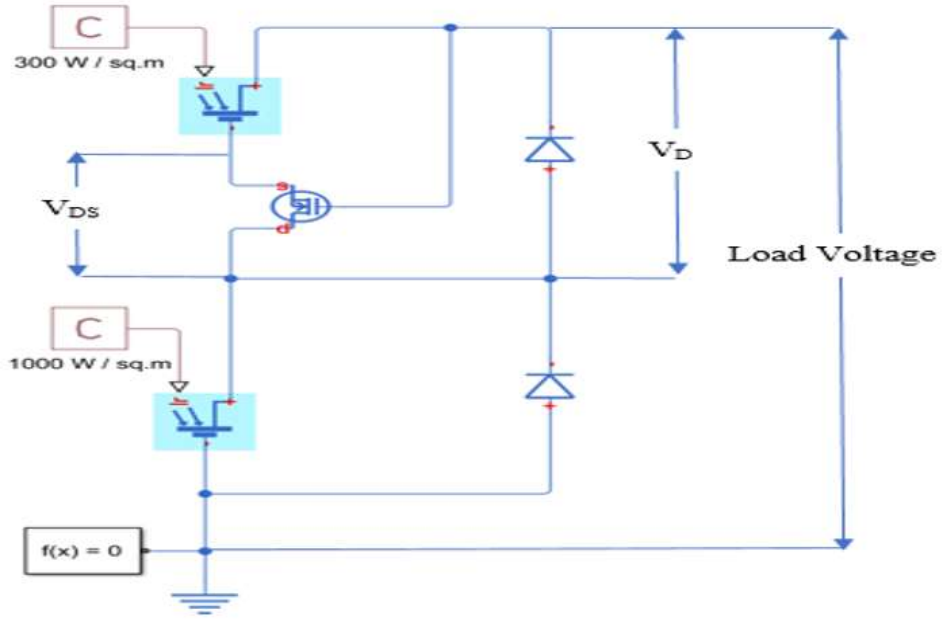

Figure 3.30. Schematic diagram of traditional bypass-diode and MOSFET-bypass circuit with sunny and bypassed conditions

$$V_R = (N-1)V_F + V_D \quad (3.1)$$

$$V_R = (N-1)V_F + V_D - V_{DS} \quad (3.2)$$

where N is the number of shaded cells, V_F is the voltage supplied by a well-illuminated cell, V_D is the diode voltage, V_{DS} is the voltage drop between the drain and source of the MOSFET and V_R is the reverse voltage across a shaded cell. In normal operation, when all the cells are fully illuminated and its output voltage is high, the MOSFET is in its ON state and the string current flows through the panel. However, when the solar panel is shaded, its output voltage is low and the MOSFET tends to reduce its current capability, while the voltage drop between drain and source increases. The presence of the MOSFET allows subtracting the voltage V_{DS} from the maximum reverse voltage V_R developing across shaded solar cells.

3.5.2.1 Results

The traditional bypass-diode and MOSFET-bypass circuit are designed and simulated using the MATLAB/Simulink tool. The result

shows that the MOSFET reduces the string current, which consequently reduces the power dissipation of the shaded cell. Figure 3.31 compares the string current with the traditional bypass-diode and MOSFET-bypass circuit. The string current with the traditional bypass-diode is approximately 1.6A, and it reduces to around 0.6A with a MOSFET-bypass, a 62.5% reduction in string current through shaded cells. The MOSFET bypass circuit causes a 30% reduction in the reverse voltage V_R with a voltage drop V_{DS} of 7.81V across series-connected power MOSFET. The reduction of the reverse voltage and string current implies a corresponding reduction of the power dissipation of the shaded cells, which consequently reduces the cell temperature and mitigates the hot-spotting.

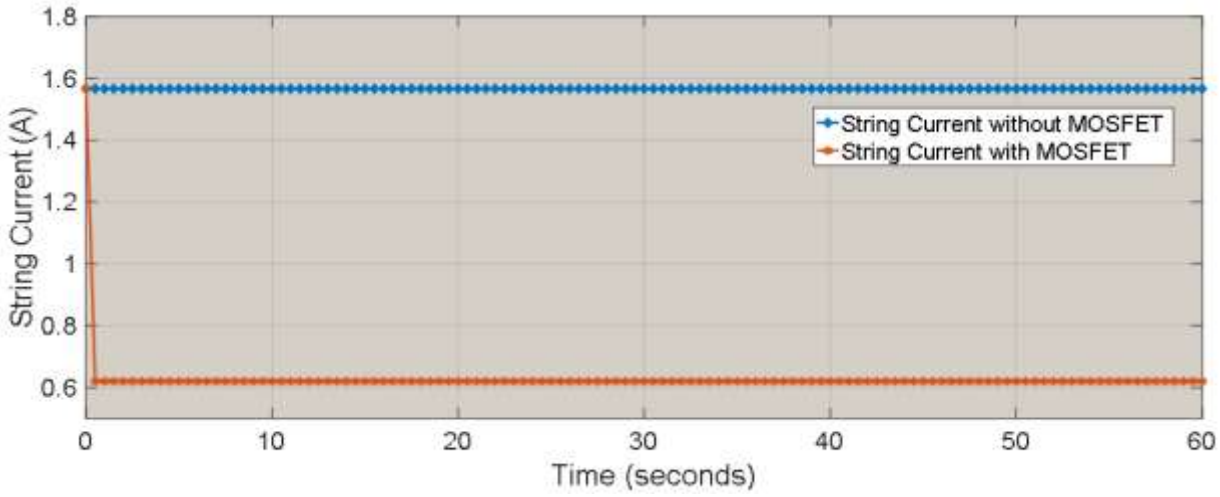

Figure 3.31. String current with and without MOSFET-bypass circuit

3.5.3 Transactive Control of SSGC Building HVAC System

In this section, we focus on control of the SSGC building's HVAC system for demand response to unlock the benefits of TC as mentioned in Section 4.3.3. The TC strategy presented in [180] was applied to the SSGC building's thermostatically controlled HVAC load to make thermostat price responsive. Figure 3.32 shows the SSGC building, level 3, AHU load, with a fixed thermostat setting of 23°C for cooling during occupied hours, referred to as CC. We control this load with both the thermostat setting and an energy

price signal to make it demand-responsive. The designed TC is implemented using the MATLAB/Simulink tool and results show the significant energy saving of using TC rather than CC.

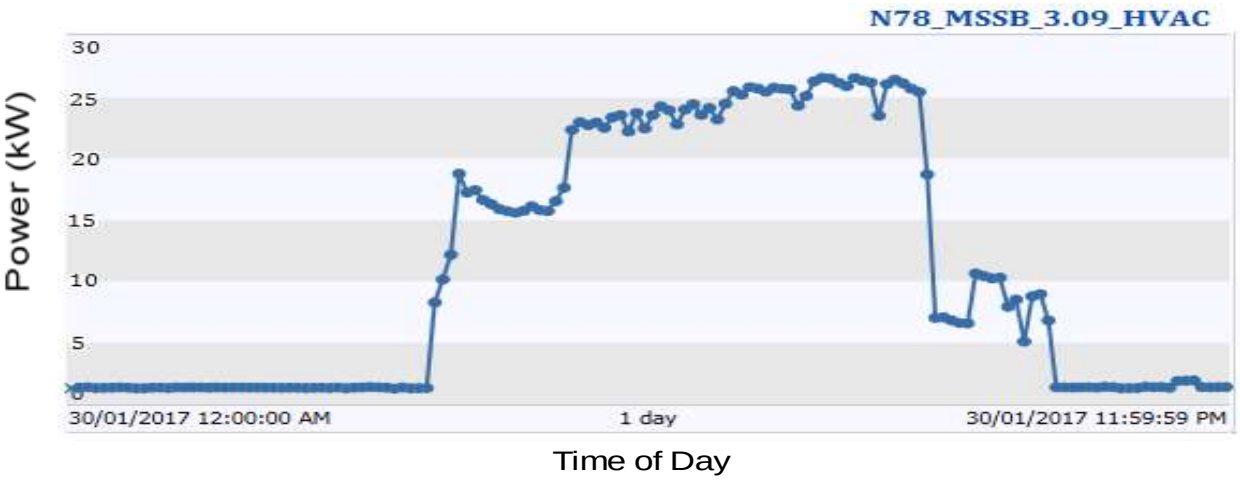

Figure 3.32. HVAC load data with conventional control

To analyze the HVAC electricity consumption saving with zone temperature variation, we model the HVAC consumption given in Fig. 3.32. The fan and chiller consumption are two major contributors to the HVAC energy consumption. Therefore, over a given time horizon the HVAC consumption is a sum of the fan and chiller consumptions and can be written as:

$$HVAC_{pc}(t) = HVAC^{t}_{fpc} + HVAC^{t}_{cpc} \tag{3.3}$$

where $HVAC^{t}_{fpc}$ ($HVAC^{t}_{cpc}$) is fan and chiller power consumption at time instant t in kW. The detail about these components and their functionalities can be found in [181, 182]. The fan and chiller powers can be modeled using a simple control-oriented model drawn from [183, 184] and given as:

$$HVAC_{pc} = \sum_{t=0}^{24}\sum_{i}^{n}\left\{\left(k_f * \left(\frac{q_{zi(t)}}{T_{zi(t)}-T_s}\right)^2\right) + \left(\delta\frac{q_{zi(t)}}{\eta COP} + 1 - \delta\frac{q_t}{\eta COP}\right)\right\} \tag{3.4}$$

where q_{zi} (T_{zi}) is the ith zone load (kW) and temperature (°C), q_t is total building load (kW), T_s is supply air temperature °C, δ ⇒ [0,1] is the damper position, k_f is the fan efficiency and the duct pressure losses parameter is in kWs²/kg², η is chiller efficiency,

COP is the chiller efficiency factor, n is the total number of zones and $HVAC_{pc}$ is the total power consumption of HVAC in kW. The given HVAC model is a good approximation to the measured HVAC consumption at a fixed cooling set-point temperature of 23°C. From this model, the HVAC energy saving can be calculated by varying the zone temperature.

3.5.3.1 Control Logic

The first step in the TC is to calculate the bidding price based on the current indoor temperature and the desired temperature required for comfort. The next step is to get the market-clearing price (MCP) after posting the bid price. Further, the adjusted set-point temperature for the thermostat is calculated based on the market-clearing price. The final step is to reset the thermostat setting to the new adjusted set-point temperature. The bid price and adjusted temperature setting for the thermostat are calculated using (3.5) and (3.6) respectively, and a detailed description of the TC strategy could be found in [180].

$$P_{bid} = \overline{P} + (T_{current} - T_{set}) \frac{2*k*\sigma}{T_{max} - T_{min}} \tag{3.5}$$

$$T_{set,a} = T_{set} + (P_{clear} - \overline{P}) \frac{T_{max} - T_{min}}{2*k*\sigma} \tag{3.6}$$

where $\overline{P}$ is the average price of electricity over the last 24 hours, P_{clear} is the market-clearing price, σ is the standard deviation of the electricity price, T_{max} (T_{min}) is the acceptable temperature range of indoor temperatures, $T_{current}, T_{set}$ $(T_{set,a})$ are current, desired and adjusted the set-point temperature of the zone, k is a parameter that corresponds to the ratio of the customer bid price P_{bid} to the mean price $\overline{P}$. A higher value of k means that P_{bid} is significantly higher than $\overline{P}$ or the customer is willing to pay for less deviation from the current set-point temperature $T_{current}$.

3.5.3.2 Simulation Setup

For simulations, we considered the publicly available real-time pricing (RTP) rate as the market-clearing price P_{clear}, forecast for the next 24-hour period on the Australian Energy Market Operator (AEMO) website. Table 3.8 shows the parameter values used for simulation. The zone bid price P_{bid} is calculated from (3.5), and mainly depends on the mean price of electricity $\overline{P}$ and the allowable temperature range.

3.5.3.3 Results

Figure 3.33 shows the MCP, the mean price and the zone bid-price signals on January 30, 2017. As depicted in Fig. 3.33, the customer bid price P_{bid} is zero when the zone temperature is 23°C or the zone set-point is satisfied.

Table 3.8. Price and Thermal Parameters

Parameter	Value	Unit
P_{clear}	RTP	$/MWh
$\overline{P}$	120	$/MWh
T_{max}	25	°C
T_{min}	22	°C
T_{set}	23	°C
T_s	13-15	°C
T_s	22-25	°C
k	1-10	no.
k_f	1.675	kWs^2/kg^2
η	0.85	%
COP	4.9	dimensionless
Market-Clearing time	30	minutes
Occupied period	07:00 to 18:00	hours

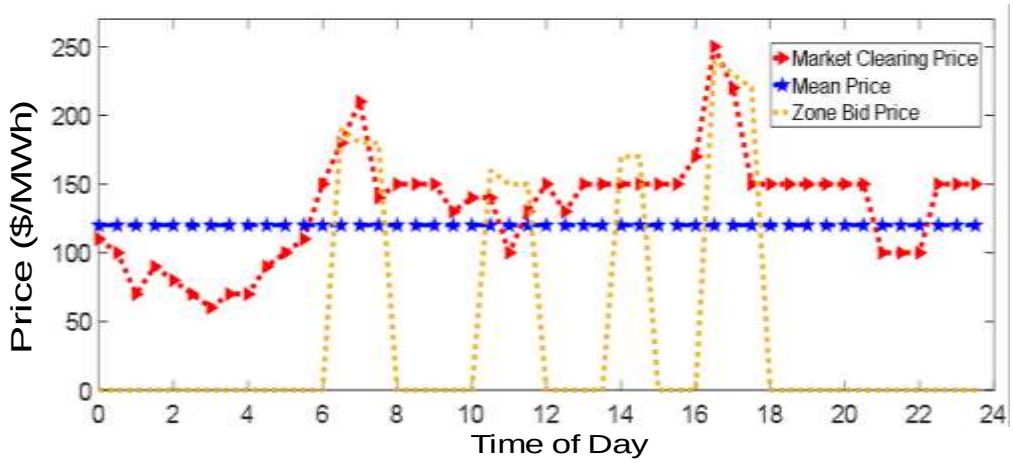

Figure 3.33. Market-clearing, mean and zone bid price

Figure 3.34 shows the impact of the market-clearing price P_{clear} on the zone temperature under TC. The local electricity market clears at the AEMO RTP, and the zone cooling set-point temperature varies accordingly. Moreover, TC maintains the thermal comfort by strictly regulating the zone temperature within the pre-specified temperature limits.

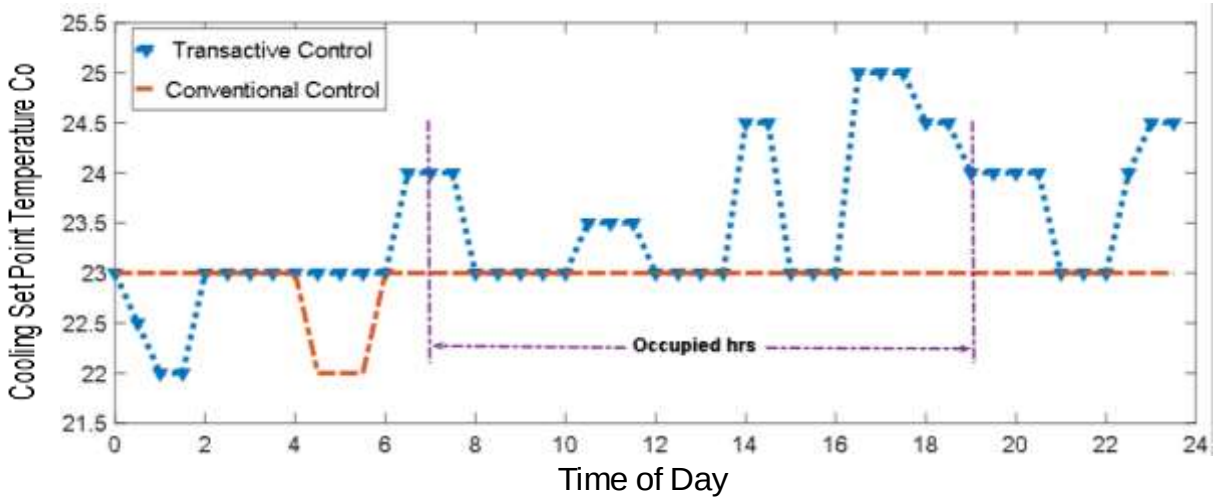

Figure 3.34. Variation in cooling set-point temperature with transactive control

We observe that when the electricity price is high, the indoor temperature increases and the HVAC power demand reduces. This behavior demonstrates that TC is capable of shaping HVAC demand according to a price signal. Table 3.9 shows the HVAC energy and

electricity cost saving with TC compared to CC. The HVAC energy consumption with TC is reduced by 11.34% when compared to its consumption with CC, which corresponds to a 12% cost saving. The results shown in Table 3.9 are based on the zone temperature variation from the desired set point for 5 hours when the consumer bids the price.

Table 3.9. Conventional and Transactive Control Comparison for Energy and Cost-saving

Control Type	Temp Range	Occupancy Time	HVAC Energy Consumption	Energy Cost	Energy Saving	Cost Saving
	°C	hrs.	kWh	$	%	%
Conventional	23	when $P_{bid} \neq 0$	238	42	---	---
Transactive	23-25		211	37	11.34	12.01%

3.6. Energy Analysis of SSGC Building

The SSGC building is designed to be completely off-grid, with PV arrays and a hybrid storage bank consisting of lithium-ion batteries and hydrogen-metal-hydride storage technologies. However, the building receives power from the grid to meet the load demand because the overall energy generation of the SSGC building is less than the energy consumption. This happens due to various factors such as the low power generation of the PV units and fuel cells, and wastage of energy by inefficient operation of several devices. The PV and fuel-cell real output power are less than the estimated power due to temperature variations and power losses caused by inefficient inverters.

Figure 3.35 shows the 30 kW installed fuel-cell inverter weekly power output. The average and maximum outputs of the fuel cell inverters are 0.6 and 2.69 kW at time instant t. Figure 3.36(a) shows the power consumption of the SSGC, on-and-off grid state,

from 18/11/2016 to 25/11/206; here positive power means that the building is getting some power from the grid while negative power indicates that the load is consuming only the power generated by the PV modules. Figure 3.36(b) shows the PV generation over seven days.

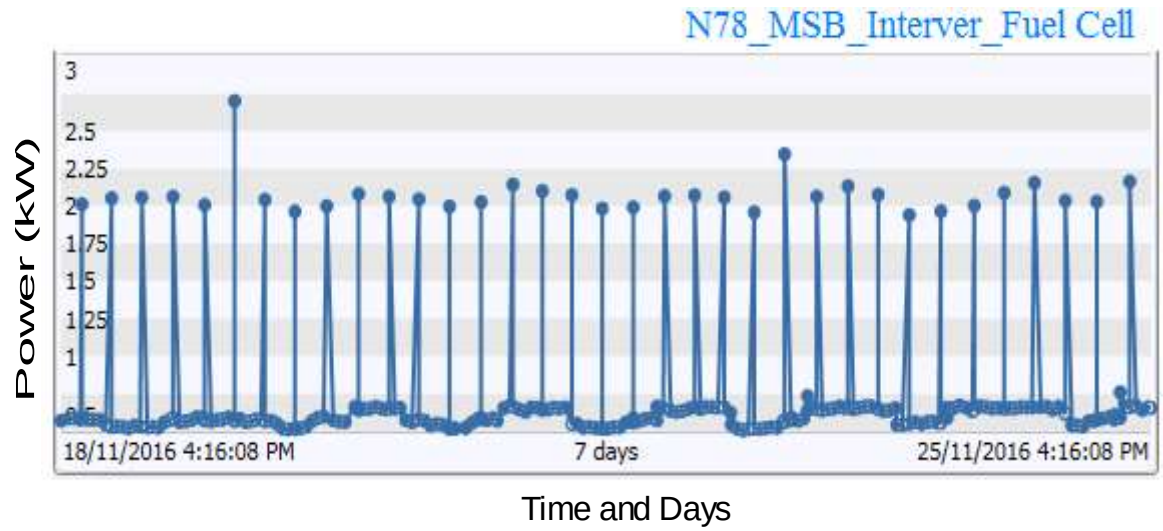

Figure 3.35. Fuel cell inverter output

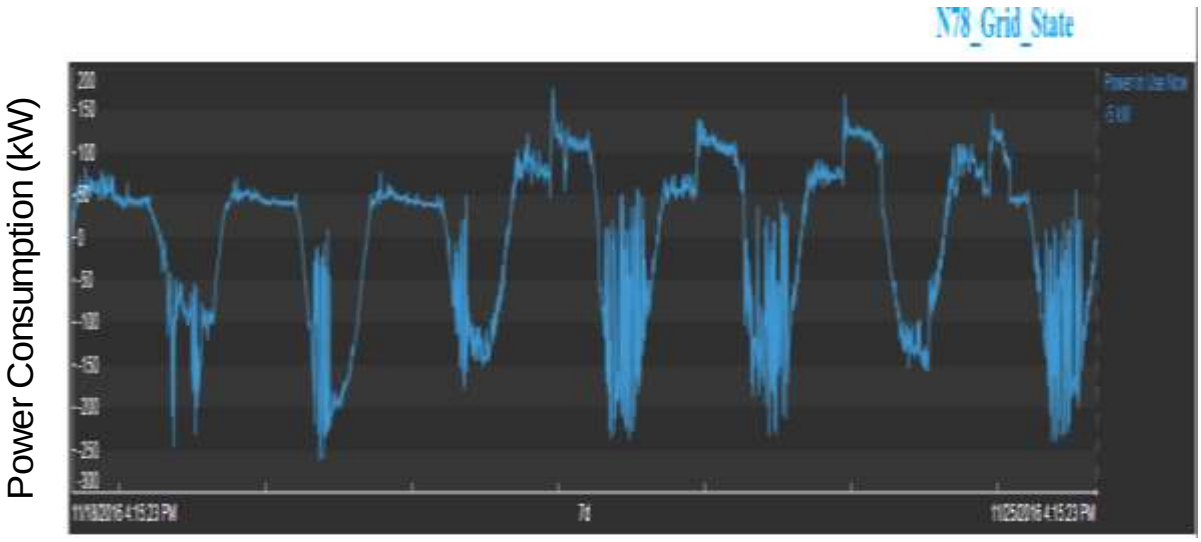

Figure 36(a). SSGC grid on and off state

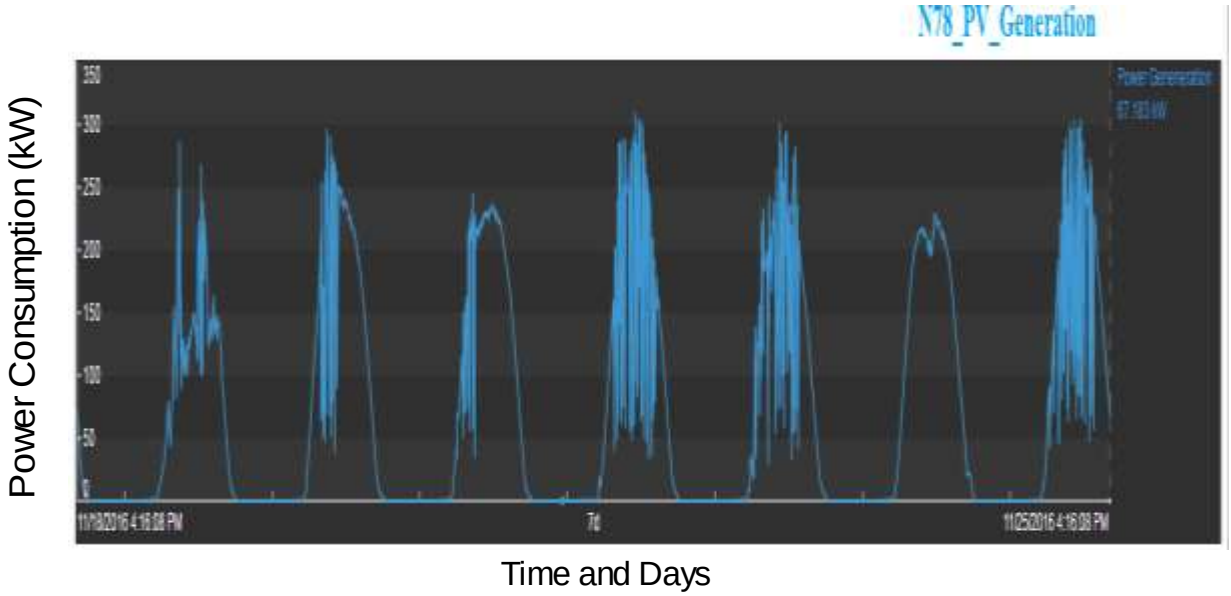

Figure 36(b). Weekly PV array generation

3.7. Cost of Technology Upgrade & Performance Improvement

This section summarizes the technologies adopted in the SSGC with cost and performance descriptions of the proposed technology. The per-unit cost of the recommended technology and the improvement in PV performance after implementation of the suggested solutions are provided in Table 3.10. The 25% saving on PV generation is possible by replacing low-efficiency inverters with high-efficiency inverters as suggested. In the SSGC, the fixed PV panels and the absence of a PV cooling system cause a 50 to 60% degradation in PV performance. The proposed dual-axis solar tracking system and the installation of a cooling system can add a considerable amount of renewable power to the system.

Table 3.10. Proposed Technology Per-unit Cost and Performance

Sr #	Existing Technology	Proposed Technology	Unit Name/Manufacturer	Cost/ unit USD	PV Performance Improvement
1.	Bi-directional inverters with 80 % efficiency	High-efficiency Bi-directional inverters	100 kW hybrid Bi-directional PV storage microgrid inverter with 96.10% efficiency, Sinexcel Electric Ltd.	$ 2000	20 to 25%
2.	Panels at a fixed angle	Dual-axis solar tracking system	9-Inch vertical type dual-axis slewing-drive solar tracker with motor drive, Dezhou Lude Transmission Equipment, Ltd.	$ 1000	30 to 40%
3.	The cooling system is not installed	The relay-based dynamic cooling system	168 kW cooling capacity, solar panel cooling system, Hairf network power Beijing, Ltd.	$ 4000	15 to 20%
4.	Solar bypass diode	Replace diode with MOSFET	IC995 Power transistor MOSFET, GAOYUE Pvt, Ltd.	$ 0.88	20 to 30%

3.8. Chapter Summary

In this chapter, the performance of an innovative 6-star green-star-rated building is evaluated and analyzed in detail. Although the energy-efficient measures and technologies adopted in the SSGC building have contributed significantly to a reduction in energy consumption and carbon emissions, the building's performance is influenced by the low energy production of the PV modules (due to fixed installation, ambient temperature, and shading effects, and inefficient building operation). The inefficient operation of the motion detectors and some faulty sensors results in a loss of communication with the controller, and therefore lighting remains on without occupancy. The measured energy is influenced by this extra power consumption. Consequently, the production and consumption differ significantly from what was expected during the design stage. As a result, the effectiveness of a net-zero-energy

building concept requires an improved design and more efficient control.

There is a need to carefully consider the temperature variations and hot-spot problems that adversely affect the performance of PV units. Measures should be taken at the design stage to address these issues. Secondly, buildings require a more efficient and improved BMS to save energy. The performance of a properly implemented energy management system with skilled operators can vary widely, but energy savings are usually expected to be in the order of 5 to 15%, with some cases resulting in savings of up to 40%. The proposed solution to improve SSGC energy efficiency were implemented using Solar Pro software and MATLAB/Simulink tool. Case studies of improvement in PV production with high-efficiency inverters and solar tracking systems and energy-saving under TC were conducted. The results show that the designed PV system and TC strategy can significantly improve building efficiency. We recommend that the building envelope and layout must be properly considered to ensure the success of adopting innovative technological solutions.

The energy management scheme presented in this chapter is well suited to off-grid commercial buildings with a few numbers of DG units or a single microgrid is involved. However, for geographically distributed microgrids with renewable energy generation facilities, distributed control techniques for energy management is required to manage the available surplus power of geographically distributed prosumers. As a result, in the next chapter, complex interactions between an energy retailer and multiple prosumers are modeled in a distributed fashion with an improved energy-trading scheme.

Chapter 4

Energy Trading in Local Electricity Market with Renewables

Emerging smart grid technologies and increased penetration of renewable energy resources (RERs) direct the power sector to focus on RERs as an alternative to meet both baseload and peak load demands in a cost-efficient way. A key issue in such schemes is the design and analysis of energy-trading techniques involving complex interactions between an aggregator and multiple electricity suppliers (ESs) with RERs fulfilling a certain demand. This is challenging because ESs can be of various categories such as small/medium/large scale, and they are self-interested and generally have different preferences towards trading based on their types and constraints. This chapter introduces a new contract-theoretic framework to tackle this challenge by designing optimal contracts for ESs. To this end, a dynamic pricing scheme is developed that the aggregator can utilize to incentivize the ESs to contribute to both baseload and peak load demands according to their categories. An algorithm is proposed that can be implemented in a distributed manner by trading partners to enable energy trading.

It is shown that the trading strategy under a baseload scenario is feasible, and the aggregator only needs to consider the per unit generation cost of ESs to decide on its strategy. The trading strategy for a peak load scenario, however, is complex and requires consideration of different factors such as variations in the wholesale price and its effect on the selling price of ESs, and the uncertainty of energy generation from RERs. Simulation results demonstrate the effectiveness of the proposed scheme for energy trading in the local electricity market.

4.1. Introduction

With increasing fossil-fuel prices and the environmental pollution caused by these fuels, many countries have started to rely on RERs to meet the growing electricity demand [185, 186]. For example, Australia sets a target of a 20% share of renewable energy in its electricity supply by 2020 [187]. Such a widespread growth of RERs and advancements in smart-grid technology will open new opportunities for electricity trading between aggregators and electricity suppliers (ESs). However, the effectiveness of the trading largely depends on the willingness of ESs to participate. In reality, ESs are selfish in nature and want to maximize their benefits regardless of whether a certain demand is met or not [104]. Meanwhile, an aggregator is also a profit-seeking entity interested to maximize its utility. As such, considering the rationality of the different electricity entities, an incentive scheme is required to motivate them to trade energy.

Existing incentive-driven energy trading schemes are generally classified into three types: 1) price-based, 2) game-theoretic, and 3) contract-theoretic. Pricing is a powerful tool for energy management incorporating an increasing penetration of RERs. It stimulates consumers to behave in an economically optimal way by changing their consumption patterns when electricity prices are

high. In [188] and [189], a zero-pricing and a dynamic period partition time-of-use (TOU) program are proposed respectively, considering current market policies and the surge of renewable-energy development to improve the effectiveness of TOU at the residential level. In [190-192], various load-scheduling and energy storage control strategies are proposed using real-time pricing (RTP) mechanism for a residential site with integrated renewable generation. Although price-based strategies are easy to deploy, their main challenges are to maintain reliability, predictability, and stability of the grid. For instance, it is shown in [193, 194] that large-scale implementation of price-based programs under the RTP schemes creates power grid stability problems.

Game theory, a well-developed mathematical tool that facilitates modeling of rational users [104], has been used to analyze the trading decisions of electricity suppliers and consumers in a smart grid [101, 195-197]. For instance, in [195], a game-theoretic approach is adopted to fairly allocate losses, reduced due to distributed generators participation in an energy management system. The researchers in [196] present a non-cooperative distributed-coordination control approach to coordinate the individual's benefits in a multi-grid environment, and employs differential game theory to achieve the global objectives. However, most of these game-theoretic models are based on the symmetric information model, assuming that players have all the necessary information for electricity trading.

Given this context, researchers focused on the contract-theory approach to incentivize trading participants in the presence of asymmetric information [110]. It is based on the principal-agent theory, in which a principal offers the right contract items to the agents to achieve maximum utility, and the agents truthfully select the contract items according to their type e.g. consumption and generation, to maximize their utilities [198, 199]. Recently,

several studies have used contract theory to model the electricity market mechanism. For instance, in [200], a contract-based scheme is proposed to coordinate many electric vehicles to achieve the charging/discharging request. In [25], a framework is proposed to facilitate electricity trading between aggregators, suppliers, and consumers. In this game, a coalition of suppliers will sell excess power and revenue is divided among partners based on the asymptotic shapely values. The work in [201] presents a peer-to-peer energy-trading scheme that consists of energy-contract offers between fuel-based generators and end-users with inflexible and flexible loads. In [26], a contract-theory based direct energy-trading model is used to address the intermittency of RERs.

Inspired by these existing works, this chapter aims to design a contract-based incentive scheme for various categories of ESs with different types, assuming a heterogeneous setting where aggregators and ESs have different preferences toward the buying/selling price for different trading scenarios. The contributions of this study are summarized as 1) A new contract-theoretic framework is developed that enables different categories of ESs with various types to individually and strategically trade available surplus power with an aggregator in a hierarchical electricity trading system; 2) A novel dynamic pricing mechanism is proposed which assumes that an electricity supplier (ES) selling price varies depending on the current market state, such as fluctuation in the wholesale price and accomplishing the base and peak load demand; 3) A new contract-based distributed algorithm for electricity trading is presented that guarantees the optimal utility of both parties in various trading scenarios; 4) The aggregator maximization problem is formulated as a principal-agent contract-based approach, and the number of constraints of the optimization problem is simplified to develop an equivalent simpler model for the original problem. Further, optimal contracts are theoretically derived for both baseload and peak load scenarios.

This study is mainly motivated by the work in [25, 26, 201], but the developed contract-theoretic scheme is substantially different from these studies. In contrast to [25], the proposed scheme enables ESs to trade their electricity individually and strategically, and the aggregator incentivizes various types of ESs considering their per-unit generation cost. Unlike [201], where a scalable price adjustment process (with fixed increments in buying and selling price) is developed to constitute a network of agreed contracts, a dynamic pricing scheme is proposed in this Chapter where ESs selling price varies depending on the current market state. Compared to the direct electricity-trading scheme in [26], the proposed method incentivizes various types of ESs considering a hierarchical electricity-trading framework with an aggregator as a profit-seeking entity. Although [26] considers different types of suppliers for electricity trading, they have not categorized them and assume a constant selling price for a certain available power which may deteriorate the ESs utility. It is because ESs unit production cost may increase when RERs are not generating much due to their stochastic nature. Table 4.1 summarizes the proposed scheme differences with [26].

Table 4.1. Difference between Proposed and Existing Scheme

Aspect	Previous Scheme [26]	Proposed scheme
Trading mechanism	Direct electricity trading	Hierarchical electricity trading framework
ESs categorization	No categorization	Categorized into three main types and developed trading strategy for each category
Trading scenarios	No classification	Two trading scenarios based on the load demand
Selling price	Constant selling price	Different selling price for different trading scenario
Wholesale price fluctuations impact on the buyer's decision	Not considered	Buyer decides on its strategy taking into account wholesale price fluctuations

The contributions of this study are summarized as:

1) A new contract-theoretic framework is developed that enables different categories of ESs with various types to individually and strategically trade available surplus power with an aggregator in a hierarchical electricity trading system.
2) A novel dynamic pricing mechanism is proposed which assumes that an ES selling price varies depending on the current market state, such as fluctuation in the wholesale price and accomplishing the base and peak load demand.
3) A new contract-based distributed algorithm for electricity trading is presented that guarantees the optimal utility of both parties in various trading scenarios.
4) The aggregator maximization problem is formulated as a principal-agent contract-based approach, and the number of constraints of the optimization problem is simplified to develop an equivalent simpler model for the original problem. Further, optimal contracts are theoretically derived for both baseload and peak load scenarios.

The rest of the Chapter is organized as follows. Section 4.2 presents the system model with details about the aggregator and ESs modeling. Section 4.3 details a theoretical derivation of the contract-based approach for the baseload scenario and an optimal solution of the formulated problem, and Section 4.4 discusses the peak load scenario and the electricity-trading algorithm. Numerical case studies are provided in Section 4.5, followed by the chapter summary in Section 4.6.

4.2. System Model

Figure 4.1 shows the three-level hierarchical system model considered in this study. The power grid is at the top level, and the aggregator is at the second level. The electricity distribution network is at the third level and consists of various categories of ESs and traditional consumers with no generation sources. Traditionally, the aggregator purchases time-varying electricity from the power grid at the wholesale price and sells it to traditional users, where most of the traditional users still enjoy a fixed flat rate, and ESs inject their surplus power into the power grid at a low feed-in-tariff rate. When the wholesale price is less than (greater than or equal to) the flat rate at a given time, it is referred to as baseload (peak load) demand throughout this paper. In a traditional electricity market, for baseload demand, the aggregator generates a profit but suffers a loss when the peak demand scenario occurs.

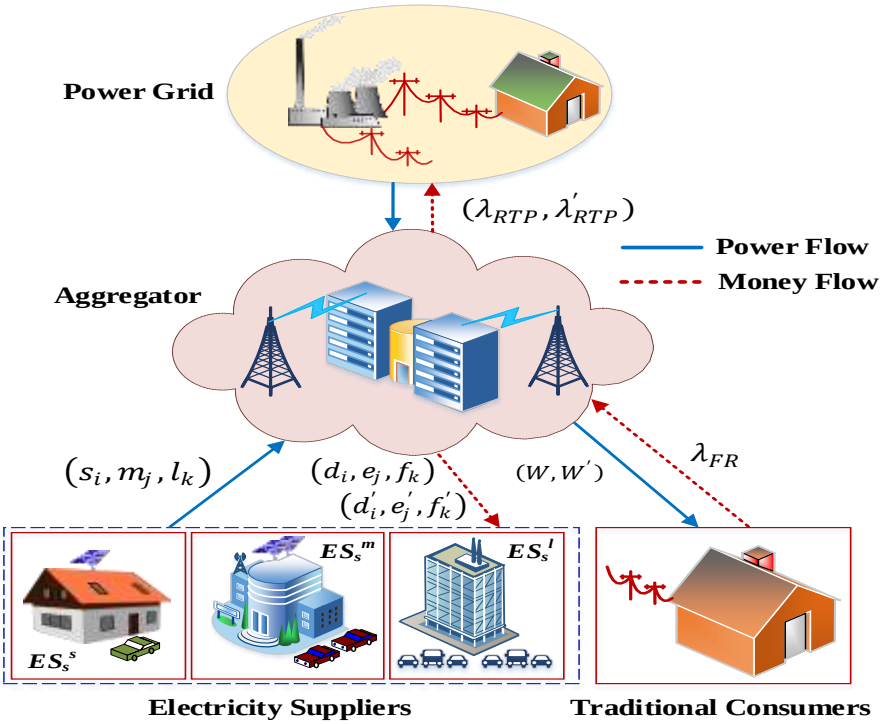

Figure 4.1. Proposed three-layer electricity trading model.

The aggregator can maximize its profit by obtaining cheaper electricity through the proposed contract-based incentive mechanism in both scenarios; however, it needs to consider the current market state and uncertainty of RERs. The aggregator has three significant roles in the developed framework: 1) it acts as an intermediary among different categories of ESs and traditional users. It collects surplus electricity from ESs and sells the collected electricity to traditional users; 2) it interacts with several geographically distributed ESs to satisfy a certain demand; 3) it buys electricity from the power grid when the supply from ESs is less than the consumers' demand.

To reflect the diversity of ESs, they are classified into three main categories based on the installed capacity of RERs. 1) Small-scale electricity suppliers ($\mathrm{ES}s^s$): suppliers who have installed small-capacity wind turbines or solar panels on their rooftops 2) medium-scale electricity suppliers ($\mathrm{ES}s^m$) with medium-capacity renewable-energy systems 3) large-scale electricity suppliers ($\mathrm{ES}s^l$): suppliers who have installed large-capacity wind-turbine or solar systems. We consider a scenario in which one aggregator as a principal offers the right contract items and **S** $\mathrm{ES}s^s$, **M** $\mathrm{ES}s^m$, **L** $\mathrm{ES}s^l$ acting as agents accept the contract according to their type.

4.2.1 Aggregator Model

Suppose that the aggregator pays d, e, f dollars to obtain s, m, l amount of power from $\mathrm{ES}s^s$, $\mathrm{ES}s^m$ and $\mathrm{ES}s^l$ respectively. Let W be the total amount of power the aggregator procures from ESs and $\mathrm{R}(s)$, $\mathrm{R}(m)$, $\mathrm{R}(l)$ be its benefit after obtaining s, m and l units of power. The aggregator's benefit reduces if the required power demand is not fulfilled, for example, if $s+m+l<W$. The aggregator gains maximum benefit when the required power demand is met, i.e., $s+m+l=W$. Thus, with a transaction (d, s), (e, m) and (f, l), the aggregator utility (U_A), which is the benefit minus the cost, is

given by

$$U_A = \big(R(s) + R(m) + R(l)\big) - (d + e + f) \quad (4.1)$$

The first term in (4.1) is the sum of the benefits gained from the various categories of ESs and the second term is the payment made to ESs to obtain the desired amount of power. A self-interested aggregator will determine the quantity of power and the cost to obtain that power from various categories of ESs in order to maximize its utility in a trading process.

4.2.2 Seller Model

The ESs are small/medium/large-scale residential/ commercial/industrial customers with a certain quantity of surplus power for trading in a local electricity market. In this work, we assume that $\mathrm{ES}s^s$, $\mathrm{ES}s^m$ and $\mathrm{ES}s^l$ can provide (2-20 kW), (22-160 kW) and (165-350 kW) of surplus power respectively, based on the installed capacity of their generation facilities. Any supplier who can provide excess power in the range of (2-20 kW) falls in the category of $\mathrm{ES}s^s$. Similarly, customers who can provide surplus power in the range of (165-350 kW) at a given time are in the category of $\mathrm{ES}s^l$. We further characterize the heterogeneity of ESs within their category based on the per-unit generation cost. ESs' per-unit generation cost varies significantly depending on many factors, e.g. investment on RERs installation, their generation reliability, and maintenance costs. We assume that ESs do not sell at a price lower than the per-unit generation cost. Therefore, from now onward, in this Chapter, the per-unit generation cost of ESs is replaced by the term selling price. These cost elements are hidden from the aggregator and are only known to the ESs.

Let the $\mathrm{ES}s^s$, $\mathrm{ES}s^m$ and $\mathrm{ES}s^l$ selling price be $\dot{a}$, $\ddot{a}$, and $\ddot{\ddot{a}}$ respectively. The aggregator payment should be greater than or at least equal to the selling price of the various categories of ESs because they will not sell at a loss. Let there be S type $\mathrm{ES}s^s$, M

type ESs^m and L type ESs^l according to their selling price. Therefore, ESs whose selling price falls into the i^{th}, j^{th}, and k^{th} cost level $\dot{a}_i$, $i \in \mathbf{S} = \{1, \ldots . S\}$, $\ddot{a}_j$, $j \in \mathbf{M} = \{1, \ldots . M\}$, $\ddot{a}_k$, $k \in \mathbf{L} = \{1, \ldots . L\}$ are called i-type ESs^s, j-type ESs^m and k-type ESs^l. For generalization, we make the assumptions given in equation (4.2).

$$\dot{a}_i > \ddot{a}_j > \ddot{a}_k, \quad \forall\, i \in S, j \in M, k \in L \tag{4.2a}$$

$$\dot{a}_1 > \dot{a}_2 \ldots > \dot{a}_S\,, \quad \ddot{a}_1 > \ddot{a}_2 \ldots > \ddot{a}_M\,, \quad \ddot{a}_1 > \ddot{a}_2 .. > \ddot{a}_{\mathrm{L}} \tag{4.2b}$$

$$\dot{a}_i > \lambda_{\mathrm{RTP}}, \quad \forall\, i \in S \tag{4.2c}$$

$$\ddot{a}_j\,, \ddot{a}_k < \lambda_{RTP}, \quad \forall\, j \in M, k \in L \tag{4.2d}$$

where λ_{RTP} is the wholesale price to obtain electricity from the grid. The assumption (4.2a) is based on the installed capacity of the RERs of the ESs. As the RERs' installed capacity increases, the unit production cost decreases because the RERs have a very low maintenance cost, and this ultimately reduces the selling price. The assumption (4.2b) is based on the type of ESs in a category. To further categorize the ESs in a category, we arrange them in ascending order (lower to higher type) based on the selling price and the surplus power procured by an aggregator. (4.2b) suggests that lower-types ESs can provide power at a higher cost so that the aggregator will buy less power from them. In contrast, the aggregator will obtain more power from higher-type ESs because their energy is cheaper. (4.2c) and (4.2d) imply that the ESs^s selling price is higher than the wholesale price, but the ESs^m and ESs^l selling price is lower than the wholesale price respectively.

For trading the selling price of ESs should be $< \lambda_{RTP}$; otherwise, the aggregator has no benefit to trade with ESs. Based on this, following (4.2c), the aggregator does not prefer to trade with ESs^s. Hence, a trading strategy is required for ESs^s that is different from the ESs^m and ESs^l trading scheme to take part in a trading

process. Traditionally, ESs^s inject surplus power to the power grid at the feed-in-tariff rate (λ_T), which is usually very low. Therefore, ESs^s are willing to sell power at a cost lower than $\dot{a}$ but higher than λ_T, in order to participate in a trading process and further enhance their profit. Let $\varphi\dot{a}$ be the price at which ESs^s are ready to sell their surplus power. Where φ is the ratio of the revised selling price and the per-unit production cost of ESs^s. The feasible range of $\varphi\dot{a}$ is $\lambda_T<\varphi\dot{a}<\lambda_{RTP}$ to ensure the rationality of both trading partners.

Suppose that, by selling s, m and l units of power, the ESs^s, ESs^m and ESs^l the benefit is d, e, and f payments respectively from the aggregator. Thus, their utility obtained in the power transaction considering the selling price can be defined as:

$$U(d,s) = d - \varphi\dot{a}s \tag{4.3a}$$

$$U(e,m) = e - \ddot{a}m \tag{4.3b}$$

$$U(f,l) = f - \ddot{a}l \tag{4.3c}$$

As ESs do not want to sell at a loss, we assume that $U(d,s)$, $U(e,m)$, $U(f,l) > 0$ when $d,s>0$; $e,m>0$; $f,l>0$. If a supplier does not take part in the trading, it will get nothing. In this condition the utility is $U(0,0) = 0$.

4.3. Contract-Based Approach for Base Load Scenario

This section derives the aggregator's optimal contracts, i.e., $\eth^*=\{(d_i^*,s_i^*), i\,\epsilon S\}$ for the baseload scenario, where the wholesale price is less than the flat rate. In this scenario, the aggregator generates profit through a traditional trading scheme but can further enhance its profit by adopting the proposed contract incentive mechanism.

To model the interactions of the aggregator and the ESs, we adopt the framework of a contract-based approach. In the considered

scenario, the aggregator wants to purchase a certain amount of power from $\mathrm{ES}s^{s}$, $\mathrm{ES}s^{m}$ and $\mathrm{ES}s^{l}$ in the local electricity market. Although the actual selling price of $\mathrm{ES}s^{s}$, $\mathrm{ES}s^{m}$ and $\mathrm{ES}s^{l}$ is not known to the aggregator, it needs to determine the quantity of power each type of ES can provide and the cost to obtain that power so that its utility is maximized.

Suppose that the aggregator trading scheme for the i-type $\mathrm{ES}s^{s}$ is given in the form of (d_i, s_i), where d_i is the agreed payment and s_i is the amount of power the aggregator would obtain from the i-type $\mathrm{ES}s^{s}$. Therefore, the set inclosing the aggregator schemes for all S $\mathrm{ES}s^{s}$ constructs a contracts ð ={(d_i, s_i), $i \epsilon S$} with (d_i, s_i) being called a contract item. Similarly, (e_j, m_j), (f_k, l_k) are contract items for j-type $\mathrm{ES}s^{m}$ and k-type $\mathrm{ES}s^{l}$ respectively.

For a contract theoretic approach, it is crucial that the solution is incentive compatible and individually rational.

Definition 1: A trading strategy (d_i, s_i), (e_j, m_j), (f_k, l_k) is said to be individually rational (IR), if for i-type $\mathrm{ES}s^{s}$, j-type $\mathrm{ES}s^{m}$ and k-type $\mathrm{ES}s^{l}$, we have:

$$U_i(d_i, s_i) = d_i - \varphi\dot{a}s_i \geq 0 \tag{4.4a}$$

$$U_j(e_j, m_j) = e_j - \ddot{a}m_j \geq 0 \tag{4.4b}$$

$$U_k(f_k, l_k) = f_k - \ddot{a}l_k \geq 0 \tag{4.4c}$$

Here, $U_i(\cdot)$, $U_j(\cdot)$, $U_k(\cdot)$ is the utility function for i-type $\mathrm{ES}s^{s}$, for j-type $\mathrm{ES}s^{m}$ and k-type $\mathrm{ES}s^{l}$. The IR constraint confirms that $\mathrm{ES}s^{s}$, $\mathrm{ES}s^{m}$ and $\mathrm{ES}s^{l}$ will have a positive utility if they follow this scheme, hence motivating ESs to actively participate in the trading process.

Definition 2: A trading strategy (d_i, s_i), (e_j, m_j), (f_k, l_k) is said to be incentive-compatible (IC) within a category if, for the i-type ESs^s, j-type ESs^m and k-type ESs^l, we have:

$$U_i(d_i, s_i) \geq U_i(d_{i'}, s_{i'}) \qquad i \neq i',\ i,\ i' \epsilon S \tag{4.5a}$$

$$U_j(e_j, m_j) \geq U_i(e_{j'}, m_{j'}) \qquad j \neq j',\ j,\ j' \epsilon M \tag{4.5b}$$

$$U_k(f_k, l_k) \geq U_k(f_{k'}, l_{k'}) \qquad k \neq k',\ k,\ k' \epsilon L \tag{4.5c}$$

Equation (4.5a) ensure that an i-type ESs^s selects a contract item designed according to its selling price. If a lower i-type ESs^s selects a contract item designed for a higher i-type ESs^s then the high demand for power may degrade its utility. Similarly, if a higher i-type ESs^s selects a contract item designed for a lower i-type ESs^s then, due to the lower power demand, payment cannot compensate for the total production cost. Thus, with IC constraints, i-type ESs^s, j-type ESs^m and k-type ESs^l gain no profit by hiding the true cost and falsely select the contract item of others' type, because only their type of contract within a category brings maximal utility. Likewise, a trading strategy should meet the IC constraint according to the ESs' category.

Definition 3: A trading strategy, i.e., (d_i, s_i) is said to be incentive-compatible (IC) according to its category, if for the i-type ESs^s, we have:

$$U_i(d_i, s_i) \geq U_i(e_j, m_j) \quad \forall\, i \epsilon S,\ j \epsilon M,\ i \neq j \tag{4.6a}$$

$$U_i(d_i, s_i) \geq U_i(f_k, l_k) \quad \forall\, k \epsilon L,\ i \epsilon S,\ i \neq \mathrm{k} \tag{4.6b}$$

Equation (4.6) confirms that ESs^s choose the contract item designed according to their category of supply capacity. If an i-type ESs^s selects the contract item designed for a j-type ESs^m or k-type ESs^l then its utility is degraded, as the aggregator demands a higher amount of power than is available, and the opposite is true

for j-type ESs^m or k-type ESs^l. Similar equations hold for j-type ESs^m and k-type ESs^l IC constraints according to their category and are given in (4.7) and (4.8) respectively.

$$U_j(e_j, m_j) \geq U_j(d_i, s_i) \quad \forall\, j \in M,\ i \in S,\ j \neq i \tag{4.7a}$$

$$U_j(e_j, m_j) \geq U_j(f_k, l_k) \quad \forall\, j \in M,\ k \in L,\ j \neq \mathrm{k} \tag{4.7b}$$

$$U_k(f_k, l_k) \geq U_k(d_i, s_i) \quad \forall\, k \in L,\ i \in S,\ k \neq i \tag{4.8a}$$

$$U_k(f_k, l_k) \geq U_k(e_j, m_j) \quad \forall\, k \in L,\ j \in M,\ k \neq j \tag{4.8b}$$

A well-designed contract should also consider the supply capacity of ESs according to their category and type, i.e.,

$$s_{i,min} \leq \ s_i \leq s_{i,max} \qquad \forall\ i \in S \tag{4.9a}$$

$$m_{j,min} \leq \ m_j \leq m_{j,max} \qquad \forall\ j \in M \tag{4.9b}$$

$$l_{k,min} \ \leq l_k \leq l_{k,max} \qquad \forall\ k \in L \tag{4.9c}$$

$$s.t. \qquad m_{j,min} > s_{i,max} \qquad j = 1,\ i = S$$
$$l_{k,min} > m_{j,max} \qquad k = 1,\ j = M$$

where $s_{i,min}$, $s_{i,max}$, $m_{j,min}$, $m_{j,max}$, $l_{k,min}$, $l_{k,max}$ are the minimum and maximum supply capacity of ESs^s, ESs^m and ESs^l respectively. Several ESs of various categories will fulfill the aggregator demand, therefore we can write

$$W = \sum_{i=1}^{S} n_i s_i + \sum_{j=1}^{M} n_j m_j + \sum_{k=1}^{L} n_k r_k \tag{4.10}$$

where n_i, n_j, n_k is the number of i-type ESs^s, j-type ESs^m and k-type ESs^l respectively, and W is the total hourly power demand. Even though obtaining the number of each type of ES is a challenging task, in the literature, a multi-armed bandit model is available to build a learning algorithm, in order to find the number of each type of ES. In a multi-armed bandit model, each contract item is regarded as an arm, and the learning algorithm is a procedure of

the exploration (type) versus exploitation (profit) trade-off. Interested readers are referred to [200, 202, 203] for more detail about the learning algorithms and the bandit model.

4.3.1 Optimal Contract Calculation

The aggregator's best trading strategies i.e., optimal contracts towards all S-type ESs^s, M-type ESs^m, L-type ESs^l can be obtained by solving the following maximization problem.

$$\max U_A = \sum_{i=1}^{\mathrm{S}} n_i(R(s_i) - d_i) + \sum_{j=1}^{\mathrm{M}} n_j(R(m_j) - e_j) + \sum_{k=1}^{\mathrm{L}} n_k(R(l_k) - f_k) \quad (4.11)$$

$$\text{s.t. } (4.4)(4.5)(4.6)(4.7)(4.8)(4.9) \text{ and } (4.10) \quad (4.11a)$$

From equation (4.11) it can be deduced that the optimal contract-designing problem is a complex problem with $\mathrm{S}^2 + \mathrm{M}^2 + \mathrm{L}^2$, IR and IC constraints, which results in computational complexity. Here, it is required to derive necessary and sufficient conditions for simplifying the problem. Likewise, in [26, 106], the optimal solution elements, i.e., the payments $\{d_i, e_j, f_k\}$ and the amount of electricity traded $\{s_i, m_j, l_k\}$, are monotonically increasing in i-type, j-type, and k-type ESs respectively. Hence, following Lemma 1 & 2 in [106] and Lemma 1 in [26], the number of IR and IC constraints can be reduced as follows:

$$d_1 \geq \varphi \dot{a}_1 s_1, \quad e_1 \geq \ddot{a}_1 m_1, \quad f_1 \geq \ddot{a}_1 l_1 \quad (4.12)$$

$$s_S > s_{S-1} \ldots\ldots > s_1 > 0 \quad (4.13a)$$

$$m_M > m_{M-1} \ldots\ldots > m_1 > 0 \quad (4.13b)$$

$$l_L > l_{L-1} \ldots\ldots > l_1 > 0 \quad (4.13c)$$

Equation (4.12) implies that if the IR constraint holds for the lowest-type ES, whose energy is most expensive in a category, and then the IR constraint for all other types is automatically satisfied. Following the assumption (4.2b) $\ddot{a}_1 > \ddot{a}_2 \ldots\ldots > \ddot{a}_{\mathrm{L}}$ (4.13) implies that the aggregator procures more power from the ESs whose

energy is cheaper, which means that ESs with a cheaper energy option can gain more profit. With equation (4.12) and (4.13) suppositions, the number of IR and IC constraints is reduced and equation (4.11) can be written as:

$$\max U_A = \sum_{i=1}^{S} n_i(R(s_i) - d_i) + \sum_{j=1}^{M} n_j(R(m_j) - e_j) + \sum_{k=1}^{L} n_k(R(l_k) - f_k) \quad (4.14)$$

$$s.t. \ (4.9)\ (4.10)\ (4.12) \text{ and } (4.13) \quad (4.14a)$$

Theorem 1. The proposed energy trading strategy of the aggregator that maximizes its utility is the optimal energy trading strategy.

Proof: To determine the optimal contract items that maximize the aggregator utility, we assume that the power demands from $ES s^s$, $ES s^m$ and $ES s^l$ are known and satisfy equation (4.13). That is, the optimal price and the given contracted power amount are positively correlated with one another. Therefore, as the amount of contracted power increases, the optimal trading increases as well. Now, considering the linearity of the contract function in equation (4.14), the optimal contract items $d_i^*(s_i)$, $e_j^*(m_j)$ and $f_k^*(l_k)$ can be derived using Theorem 1 in [26] as follows:

$$d_i^*(s_i) = \varphi \dot{a}_i s_i \quad \text{if } i = 1 \quad (4.15a)$$

$$d_i^*(s_i) = d_{i-1}^* + \varphi \dot{a}_i (s_i - s_{i-1}) \quad \text{if } i = [2, \dots S] \quad (4.15b)$$

$$e_j^*(m_j) = \ddot{a}_j m_j \quad \text{if } j = 1 \quad (4.16a)$$

$$e_j^*(m_j) = e_{j-1}^* + \ddot{a}_j (m_j - m_{j-1}) \quad \text{if } j = [2, \dots M] \quad (4.16b)$$

$$f_k^*(l_k) = \ddot{a}_k l_k \quad \text{if } k = 1 \quad (4.17a)$$

$$f_k^*(l_k) = f_{k-1}^* + \ddot{a}_k (l_k - l_{k-1}) \quad \text{if } k = [2, \dots L] \quad (4.17b)$$

By substituting the values of $d_i^*(s_i)$, $e_j^*(m_j)$ and $f_k^*(l_k)$ in (4.14), the optimal amount of electricity, i.e., s_i^*, m_j^*, l_k^* that the aggregator buys from different ESs can be obtained as

$$s_i^* = d_i/\varphi\dot{a}_i \quad \text{if } i = 1 \tag{4.18a}$$

$$s_i^* = n_i d_i + n_{i-1} d_{i-1}/(n_i + n_{i-1})\,\varphi\dot{a}_i + s_{i-1}^* \quad \text{if } i = [2, \dots S] \tag{4.18b}$$

$$m_j^* = m_j/\ddot{a}_j \quad \text{if } j = 1 \tag{4.19a}$$

$$m_j^* = n_j e_j + n_{j-1} e_{j-1}/\left(n_j + n_{j-1}\right)\ddot{a}_j + m_{j-1}^* \quad \text{if } j = [2, \dots M] \tag{4.19b}$$

$$l_k^* = l_k/\ddot{a}_k \quad \text{if } k = 1 \tag{4.20a}$$

$$l_k^* = n_k f_k + n_{k-1} f_{k-1}/(n_k + n_{k-1})\,\ddot{a}_k + l_{k-1}^* \quad \text{if } k = [2, \dots L] \tag{4.20b}$$

Since the optimal solution is derived based on equation (4.12) and (4.13), which took individual rationality and incentive compatibility into consideration, the following corollary can be stated: Corollary 1. The proposed energy trading contract is both individually rational and incentive compatible.

4.4. Contract-Based Approach for Peak Load Scenario

This section derives the optimal contracts, i.e., $\eth^* = \left\{(f_k^{'*}, l_k^*, \mathrm{r}_k), i \in L\right\}$ for the peak load scenario for time slots when the wholesale price is greater than or equal to the flat rate. To design an optimal contract strategy for this scenario, the aggregator needs to consider various factors such as the intermittency problem of RERs and the wholesale price spikes effect on the ESs' selling price.

4.4.1 Seller and Buyer Modeling

Peak load demand refers to a period of time when the electricity demand peaks at its highest level and causes wholesale price spikes. At these times, the wholesale price may exceed the fixed flat rate [204] and the aggregator suffers a loss through the traditional trading scheme. It can generate profit by obtaining cheaper

electricity from ESs; however, the aggregator benefit of trading with ESs in this scenario depends on the consistency of RERs' generation and the selling price of ESs. Due to the intermittent and uncontrollable characteristics of the output of RERs, potential ESs may not be able to provide the contracted power during the peak demand period, and thus the aggregator utility deteriorates. For that reason, the aggregator introduces the concept of a reliability level to capture the power supply uncertainty of ESs. This reliability level is expressed using a random variable ɾ, and it expresses the probability to meet the contracted energy by ESs within the contracted periods. The ESs' reliability levels are assumed to be within the range of [0, 1] for simplicity, and it is drawn identically and independently. The reliability level ɾ = 0, when the power provided by ESs by the end of the contracted time is zero. Likewise, the reliability level ɾ = 1, when the power provided by ESs by the end of the contracted time becomes equal or more than the contracted quantity. As to the power that ESs cannot provide, there is one way to complement it: the aggregator buys deficit power from the power grid but imposes penalty charges to ESs for the cost of the complement power. Considering the huge penalty charges in the case of power shortages, ESs will set a higher selling price for the same amount of power compared to the baseload scenario.

4.4.2 Contract-Based Approach Formulation

Let $\lambda_{RTP}^{\acute{}}$ be the price to obtain electricity from the power grid when peak demand occurs. In this work, we assume that $\lambda_{RTP}^{\acute{}} > \lambda_{RTP} > \dot{a}$, $\ddot{a}$, $\ddot{\ddot{a}}$. Let r_i be the reliability level of ESs^s and $\acute{d}$ the payment to obtain s amount of power in a peak demand scenario. If ESs^s are unable to provide the contracted amount of electricity at times of wholesale price spikes then they suffer penalty charges for the supply shortage. Penalty charges are assumed to be equal to $\lambda_{RTP}^{\acute{}}$. As $\lambda_{RTP}^{\acute{}} >> \dot{a}$; therefore, in order to encourage ESs^s to make contracts for the peak demand scenario with a probability of high penalty

charges in case of supply shortages, the aggregator pays more than the baseload scenario to obtain the same amount of power, therefore, we assume $\acute{d}>d$. Moreover, in reality $\acute{\lambda}_{RTP}$ is public information, which is known to both the aggregator and ESs. Thus, ESs are unwilling to sell their electricity at the same rate in both scenarios. Therefore, in this study, $\acute{d}$ is set to be positively correlated to $\acute{\lambda}_{RTP}$ to maximize the ESs utility.

For the peak demand scenario, the aggregator will design the contract item $(\acute{d}_i, s_i, \mathrm{r}_i)$ for i-type $\mathrm{ES}s^s$, where $\acute{d}_i$ is the payment to obtain the s_i amount of electricity from $\mathrm{ES}s^s$ when peak demand occurs. The cost to supply the contracted amount s_i is $s_i\varphi\dot{a}\mathrm{r}_i$ and the power deficit cost is $s_i(1-\mathrm{r}_i)\acute{\lambda}_{RTP}$. The total cost will be $s_i\varphi\dot{a}\mathrm{r}_i+s_i(1-\mathrm{r}_i)\acute{\lambda}_{RTP}$.

In this case, the $\mathrm{ES}s^s$ utility function, which is benefit minus cost, is given as

$$\acute{U}_s(\acute{d},s,\mathrm{r}) = \acute{d}_i - \left(\varphi\dot{a}_i s_i \mathrm{r}_i + (1-\mathrm{r}_i)s_i\acute{\lambda}_{RTP}\right) \tag{4.21}$$

Similarly, the $\mathrm{ES}s^m$ and $\mathrm{ES}s^l$ utility function for this case can be obtained by replacing the baseload payments $(e_j,\ f_k)$ by the peak demand scenario payments $(\acute{e}_j,\ \acute{f}_k)$ respectively.

$$\acute{U}_m(\acute{e},m,\mathrm{r}) = \acute{e}_j - \left(\ddot{a}_j m_j \mathrm{r}_j + \left(1-\mathrm{r}_j\right)m_j\acute{\lambda}_{RTP}\right) \tag{4.22a}$$

$$\acute{U}_l(\acute{f},l,\mathrm{r}) = \acute{f}_k - \left(\ddot{a}_k l_k \mathrm{r}_k + (1-\mathrm{r}_k)l_k\acute{\lambda}_{RTP}\right) \tag{4.22b}$$

The first term in equation (4.21) and (4.22) is the benefit that ESs obtain by selling $s,\ m,\ l$ amounts of electricity. The second term is the cost to produce the $s,\ m,\ l$ amounts of power and the third term is the cost to complement the deficit power. The third term is zero when $\mathrm{r}=1$, which indicates the condition when ESs maximize their utility by providing the contracted amount of power. However, the ESs' utility decreases as r decreases because the cost to complement the power increases. In equation (4.21) and (4.22), $\acute{d}_i,\ \acute{e}_j,\ \acute{f}_k$ can be calculated for two conditions.

4.4.2.1 $\acute{\lambda_{RTP}} = \lambda_{FR}$

When the difference between $\acute{\lambda_{RTP}}$ and λ_{FR} is zero, it represents the breakeven condition for the aggregator in a traditional electricity market, as the buying and selling price is the same. In this case, the aggregator trades with ESs to make a profit and ESs are willing to sell their surplus power at a higher rate than for the baseload scenario. Let $\acute{a_\iota}$, $\acute{\ddot{a}}_j$, $\acute{\ddot{a}}_k$ be the payment made by the aggregator to obtain s, m, l amounts of power from $\mathrm{ES}s^s$, $\mathrm{ES}s^m$ and $\mathrm{ES}s^l$ respectively in this condition. Thus, the ESs' utilities obtained in the transaction can be defined as:

$$\acute{d_i} = \acute{a_\iota} s_i \mathrm{r}_i + (1 - \mathrm{r}_i) s_i \acute{\lambda}_{RTP} \qquad \forall \{i = 1 \ldots . S\} \tag{4.23}$$

$$\acute{e_j} = \acute{\ddot{a}}_j m_j \mathrm{r}_j + (1 - \mathrm{r}_j) m_j \acute{\lambda}_{RTP} \qquad \forall \{j = 1 \ldots . M\} \tag{4.24}$$

$$\acute{f_k} = \acute{\ddot{a}}_k l_k \mathrm{r}_k + (1 - \mathrm{r}_k) l_k \acute{\lambda}_{RTP} \qquad \forall \{k = 1 \ldots . L\} \tag{4.25}$$

Where

$$\acute{a_\iota} = \varphi \dot{a_i} + 0.015, \quad \acute{\ddot{a}}_j = \ddot{a}_j + 0.015, \quad \acute{\ddot{a}}_k = \ddot{a}_k + 0.015 \tag{4.26}$$

$$s.t. \qquad \varphi \acute{a_\iota}, \ \acute{\ddot{a}}_j, \ \acute{\ddot{a}}_k < \lambda_{\mathrm{FR}} \tag{4.26a}$$

Equation (4.26) suggests that in this condition the per-unit payment to ESs is 0.015 $/kWh higher than the baseload scenario for the same amount of power as that procured by the aggregator.

4.4.2.2 $\acute{\lambda_{RTP}} > \lambda_{FR}$

This condition represents the case where the aggregator suffers a loss through a traditional trading scheme, as the buying price is higher than the selling price. In this case, the aggregator's objective is to avoid loss through trading with ESs. The aggregator loss is positively correlated to the ($\acute{\lambda_{\mathrm{RTP}}} - \lambda_{FR}$) price difference that directly depends on $\acute{\lambda_{\mathrm{RTP}}}$ because λ_{FR} is constant. This is intuitive since, ESs, being rational in nature, would also

correspond their selling price to $\lambda_{\mathrm{RTP}}^{\acute{}}$. Let the aggregator payments is $\bar{\acute{a}}_\iota$, $\bar{\ddot{a}}_j$, $\overline{\ddot{\acute{a}}_k}$ to procure s, m, l amounts of power from ESs^s, ESs^m, ESs^l respectively in this condition. Thus, the ESs' utility functions are given as:

$$\acute{d}_i = \bar{\acute{a}}_i s_i \mathrm{r}_i + (1-\mathrm{r}_i) s_i \acute{\lambda}_{RTP} \qquad \forall \{i = 1 \ldots\ldots S\} \tag{4.27}$$

$$\acute{e}_j = \bar{\ddot{a}}_j m_j \mathrm{r}_j + (1-\mathrm{r}_j) m_j \acute{\lambda}_{RTP} \qquad \forall \{j = 1 \ldots\ldots M\} \tag{4.28}$$

$$\acute{f}_k = \overline{\ddot{\acute{a}}_k} l_k \mathrm{r}_k + (1-\mathrm{r}_k) l_k \acute{\lambda}_{RTP} \qquad \forall \{k = 1 \ldots\ldots L\} \tag{4.29}$$

Where

$$\bar{\acute{a}}_\iota = \varphi \acute{a}_i + (\lambda_{\mathrm{RTP}}^{\acute{}} - \lambda_{FR}) * 0.2, \quad \bar{\ddot{a}}_j = \ddot{a}_j + (\lambda_{\mathrm{RTP}}^{\acute{}} - \lambda_{FR}) * 0.2, \quad \overline{\ddot{\acute{a}}_k} = \ddot{a}_k + (\lambda_{\mathrm{RTP}}^{\acute{}} - \lambda_{FR}) * 0.2 \tag{4.30}$$

$$s.t. \qquad \varphi \bar{\acute{a}}_\iota,\ \bar{\ddot{a}}_j,\ \overline{\ddot{\acute{a}}_k} < \lambda_{\mathrm{FR}} \tag{4.30a}$$

$$\varphi \bar{\acute{a}}_\iota,\ \bar{\ddot{a}}_j,\ \overline{\ddot{\acute{a}}_k} > \varphi \acute{a}_\iota,\ \acute{\ddot{a}}_j,\ \ddot{\acute{a}}_k \tag{4.30b}$$

The following can be inferred from equation (4.30); 1) in this condition the 0.1 $/kWh price difference of $\lambda_{\mathrm{RTP}}^{\acute{}}$ and λ_{FR} corresponds to the 0.02 $/kWh increment in per-unit payment to ESs compared to the baseload scenario for the same amount of power obtained by the aggregator; 2) every time there is an increment of 0.1 $/kWh in the $\lambda_{\mathrm{RTP}}^{\acute{}}$ and λ_{FR} price difference due to an increase in the wholesale price ($\lambda_{\mathrm{RTP}}^{\acute{}}$) leads to an increment of 0.02 $/kWh in the per-unit payment to ESs. This is to ensure that as $\lambda_{\mathrm{RTP}}^{\acute{}}$ increases the ESs' benefit also grows. However, the ESs' revenue increases with an increase of $\lambda_{\mathrm{RTP}}^{\acute{}}$, until the per-unit payment is less than the flat rate. This is because a per-unit payment equal to the flat rate is the saturation point and beyond that the aggregator utility becomes negative, thus (4.26a)(4.30a) and (4.30b) assure the aggregator utility under different scenarios. In addition, equation (4.26) and (4.30) are designed carefully considering the various cost constraints mentioned in (4.2) to ensure fair-trading between the aggregator and the ESs.

4.4.3 Optimal Contract Calculation

Similar to the baseload scenario, in order to derive the aggregator's optimal trading strategies for the peak load scenario, we need to define the following constraints: IR, IC, ESs' supply capacity and total power demand. The ESs' supply capacity and the IC constraints are the same as for the baseload scenario as defined in equation (4.9) and (4.13) respectively, whereas the aggregator's total peak power demand is given as

$$W' = \sum_{i=1}^{S} \acute{n}_i s_i + \sum_{j=1}^{M} \acute{n}_j m_j + \sum_{k=1}^{L} \acute{n}_k r_k \quad (4.31)$$

where $\acute{W}$ is the total hourly peak power demand of the aggregator and $\acute{n}_i$, $\acute{n}_j$, $\acute{n}_k$ is the number of i-type $\mathrm{ES}s^s$, j-type $\mathrm{ES}s^m$ and k-type $\mathrm{ES}s^l$ respectively contributing to fulfilling the peak load demand. Since the peak demand ($\acute{W}$) is greater than the baseload demand (W), we assume that $\acute{n}_i$, $\acute{n}_j$, $\acute{n}_k > n_i$, n_j, n_k correspondingly.

The IR constraint under condition 1 and condition 2 in the simplified form are given below following (4.12).

$$\acute{d}_1 \geq \varphi \acute{a}_1 s_1, \quad \acute{e}_1 \geq \acute{\ddot{a}}_1 m_1, \quad \acute{f}_1 \geq \acute{\ddot{a}}_k l_1 \quad (4.32)$$

$$\acute{d}_1 \geq \varphi \overline{\acute{a}_1} s_1, \quad \acute{e}_1 \geq \overline{\acute{a}_1} m_1, \quad \acute{f}_1 \geq \overline{\acute{\ddot{a}}_1} l_1 \quad (4.33)$$

Equation (4.32) and (4.33) imply that if the IR constraint of the supplier whose energy is most expensive in a category is satisfied then the IR constraint for all other ESs will automatically exist since we made the assumption ($\acute{a}_1 > \acute{a}_2 > \ldots \acute{a}_M$), ($\overline{\acute{a}_1}, \overline{\acute{a}_2} \ldots \overline{\acute{a}_L}$) following (4.2b). The aggregator's optimal contracts for the peak load scenario considering all types of ESs can be obtained by solving the following optimization problem:

$$\max(\acute{U}_A) = \sum_{i=1}^{S} n_i \left(R(s_i) - \left(\acute{d}_i\right)\right) + \sum_{j=1}^{M} n_j (R(m_j) - (\acute{e}_j)) + \sum_{k=1}^{L} n_k (R(l_k) - (\acute{f}_k)) \quad (4.34)$$

$s.t.$ (9)(13)(31)and (32) for condition 1 (4.34a)

(9) (13) (31) and (33) for condition 2

The solution of (4.34), i.e. $(\acute{d_\iota}^*, s_i^*, \mathrm{r}_i)$, $(\acute{e_j}^*, m_j^*, \mathrm{r}_j)$, $(\acute{f_k}^*, l_k^*, \mathrm{r}_k)$, $\forall\ i \in$ S, $j \in$ M, $k \in$ L, can be easily obtained by following subsection 4.3.1, where $\varphi\dot{a}_i$, $\ddot{a}_j$, $\dddot{a}_k$ are replaced by $\acute{a}_\iota$, $\acute{\ddot{a}}_j$, $\acute{\dddot{a}}_k$ for condition 1 and replaced by $\bar{a}_\iota$, $\bar{\ddot{a}}_j$, $\overline{\dddot{a}_k}$ for condition 2.

4.4.4 Electricity Trading Algorithm

This section presents a procedure for the aggregator to procure power from ESs and an algorithm for electricity trading between an aggregator and ESs that can be implemented by both parties in a distributed manner.

Following the optimal contracts, i.e., $\{d_i^*, s_i^*\}$, $(\acute{d_\iota}^*, s_i^*, \mathrm{r}_i)$ etc., from the previous sections, the aggregator achieves a higher utility from higher types of ESs than from lower types in a category, i.e. $U_k^L > U_k^{L-1}$, $U_j^M > U_j^{M-1}$, $U_i^S > U_i^{S-1}$. Moreover, the aggregator utility from the lowest type of ES in a large-scale category is higher than from the highest type of ES from a medium-scale category. Similar conditions apply to medium and small-scale category ESs, therefore we can write $U_k^1 > U_j^M$ & $U_j^1 > U_i^S$. Subject to: The difference between the requested amount of power and the surplus power from any ES is within a -2.5% variation.

In a developed electricity-trading scheme, each type of ES provides a certain excess power at a specific rate. If the difference between the surplus power and the requested amount of power is more than -2.5% then the ES either rejects the contract or will provide that requested power at a higher rate. This is because an ES opportunity cost increases if it may not be able to capitalize on unsold power, therefore it would like to sell as much as it could have [205]. In this situation, it is more economical for the aggregator to buy power from an ES whose surplus power is within the -2.5% variation of the requested quantity. This way, the

proposed scheme enables all types of ESs within a category to take part in a trading process, depending on the demand in an hour. The systematic algorithm is provided in Algorithm 1.

Algorithm 1. Contract-Based Electricity Trading Algorithm

1: Initialize: W, $\acute{W}$, λ_{RTP}, $\lambda_{\acute{RTP}}$, λ_{FR}, ESs' reliability level Γ_i, Γ_j, Γ_k, ESs' supply capacity, number of ESs, i.e., n_i, $\acute{n}_i$.

2: Compute IC constraint using (4.13) for steps 3, 4 and 5.

3: **If** $\lambda_{RTP}<\lambda_{FR}$
Compute IR constraint of the lowest type of ES that satisfies (4.12). Solve the problem (4.14) to derive optimal contracts (d_i^*, s_i^*), (e_j^*, m_j^*), (f_k^*, l_k^*) as described in subsection 4.3.1.

4: **else** $\lambda_{\acute{RTP}}=\lambda_{FR}$
Calculate IR constraint of the lowest type of ES that satisfies (4.32). Solve the problem (4.34) for condition 1 to derive optimal contracts $(\acute{d_i}^*, s_i^*, \Gamma_i)$, $(\acute{e_j}^*, m_j^*, \Gamma_j)$, $(\acute{f_k}^*, l_k^*, \Gamma_k)$ as defined in 4.4.3.

5: **else if** $\lambda_{\acute{RTP}} >\lambda_{FR}$
Compute IR constraint of the lowest type of ES that satisfies (4.33). Solve maximization problem (4.34) for condition 2 to derive optimal contracts as described in subsection 4.4.3.
endif

6: Aggregator sends the contracts i.e., (d_i^*, s_i^*), $(\acute{d_i}^*, s_i^*, \Gamma_i)$, $i \in S$, to ESs and purchases electricity from them.

7: ESs accept the contracts and the aggregator procures power from them following subsection 4.4.4.

4.5. Numerical Analysis

In this section, the performance of the proposed contract-based approach is presented and is evaluated for both baseload and peak load demand scenarios considering one aggregator and 48 ESs from which there are 10, 16 and 22, i-type ESs^s, j-type ESs^m and k-type

ESs^l respectively. ESs^s selling prices ($\varphi\dot{a}_i$) are chosen randomly from a range of [0.38 to 0.65] $/kWh from highest to lowest type in a small-scale category, and the value of φ is 0.67. Likewise, ESs^m and ESs^l selling prices ($\ddot{a}_j, \ddot{a}_k$) vary from [0.34 to 0.64] and [0.11 to 0.32] $/kWh in accordance with highest to lowest type in a medium and large-scale category respectively. The demand of the aggregator is chosen randomly from a range of [500-7000] kWh. The unit price to buy electricity from the wholesale market is 0.67 $/kWh for the baseload scenario and for the peak load scenario the price varies from 0.68 to 5.4 $/kWh. The aggregator sells the electricity to retail customers at a fixed flat rate of 1.1 $/kWh. The feed-in-tariff rate is 0.11 $/kWh and its value is taken from [206]. All cost values are chosen following the assumptions in (4.2). Simulations are performed for seven different hours from 10 am to 4 pm. The aggregator demands and ESs' surplus powers are updated each hour. Table 4.2 lists the various simulation cases to evaluate the performance of the designed contract-based incentive scheme.

Table 4.2. Simulation Cases to Evaluate the Developed Incentive Schemes

Trading Scheme	Reliability Level	Case Type	Wholesale price	Condition	Performance Evaluation
Traditional	1.0	Base Case	0.67	$\lambda_{RTP}<\lambda_{FR}$	Aggregator profit
Contract-Based	1.0	Case I	0.67		Aggregator/ESs profit
		Case II	1.1	$\lambda_{RTP}=\lambda_{FR}$	Aggregator/ESs utility
		Case III	2.0	$\lambda_{RTP}>\lambda_{FR}$	Aggregator profit/loss
		Case IV	1.2 to 4.6		Total payment to ESs
		Case V	1.8		ESs participation
		Case VI	1.2 to 5.4		ESs optimal revenue
	1.0 to 0.6	Case VII	1.2 to 4.6		Reliability impact on trading partners utility

4.5.1 Aggregator Profit under Base Case and Case I

This case study compares the aggregator profit under the traditional and contract-based trading scheme, and the results are shown in Fig. 4.2. It is observed that given the same power demand at different hours, the contract-based electricity-trading scheme outperforms the traditional scheme in terms of aggregator profit.

In the traditional scheme, an aggregator obtains electricity from the power grid at a wholesale price; however, the contract-based scheme allows the aggregator to obtain more profit by purchasing cost-effective electricity from ESs. The reason is that, in the contract approach, each contract is designed for the corresponding ESs' type, and the maximum profit is generated by following the IR and IC constraints (4.12) and (4.13) respectively. Nonetheless, in a traditional scheme, the aggregator purchases the bulk amount of electricity at the wholesale price, sells it to retail consumers at a fixed flat rate, and thus cannot improve its profit.

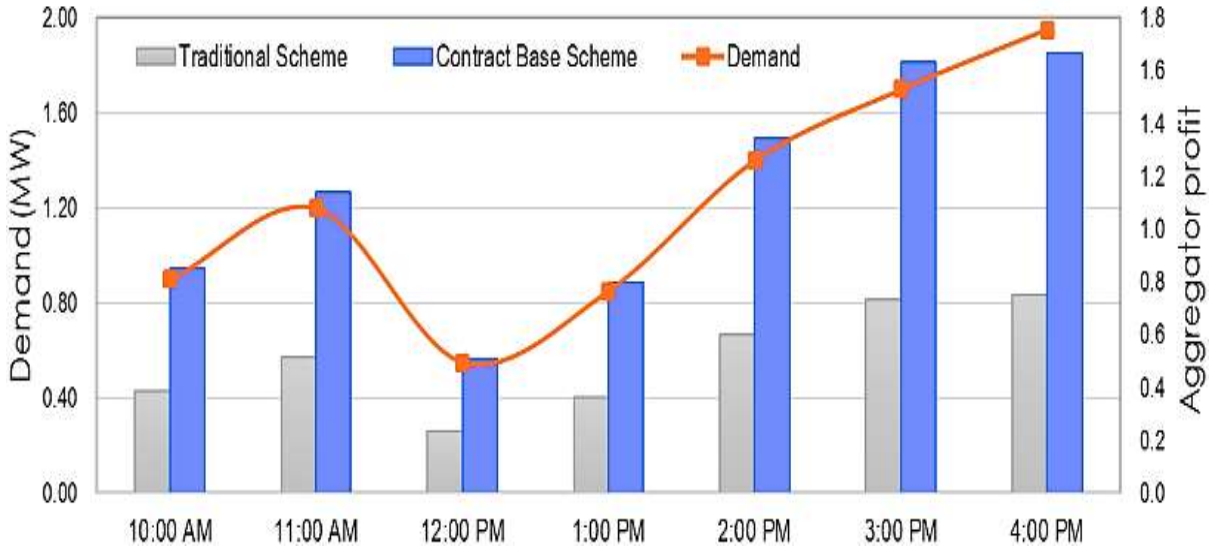

Figure 4.2. Profit generated by aggregator with different schemes under Case I.

4.5.2 Aggregator Utility for Base Case and Case II

The objective of this study is to compare the performance of two schemes when wholesale price becomes equal to a flat rate. The

simulation results are shown in Fig. 4.3 demonstrates that for the same power demand, as in Case I, the profit with the traditional trading scheme under this case is zero. This is because the retail revenue from customers is equal to the purchasing cost. However, the aggregator generates profit by trading with ESs through the contract-based trading scheme at the breakeven point. For instance, at 4 pm with 1.96 MW demand, the aggregator profit is 1.67 $/kWh and the ESs' revenue is 0.30 $/kWh following the subsection 4.4.2 condition (1) trading strategy. Given the same setting as in Fig 4.2, Fig 4.3 reveals that the aggregator profit at 4 pm is reduced from 1.67 to 1.62 $/kWh because it is paying more to get the same amount of power in Case II.

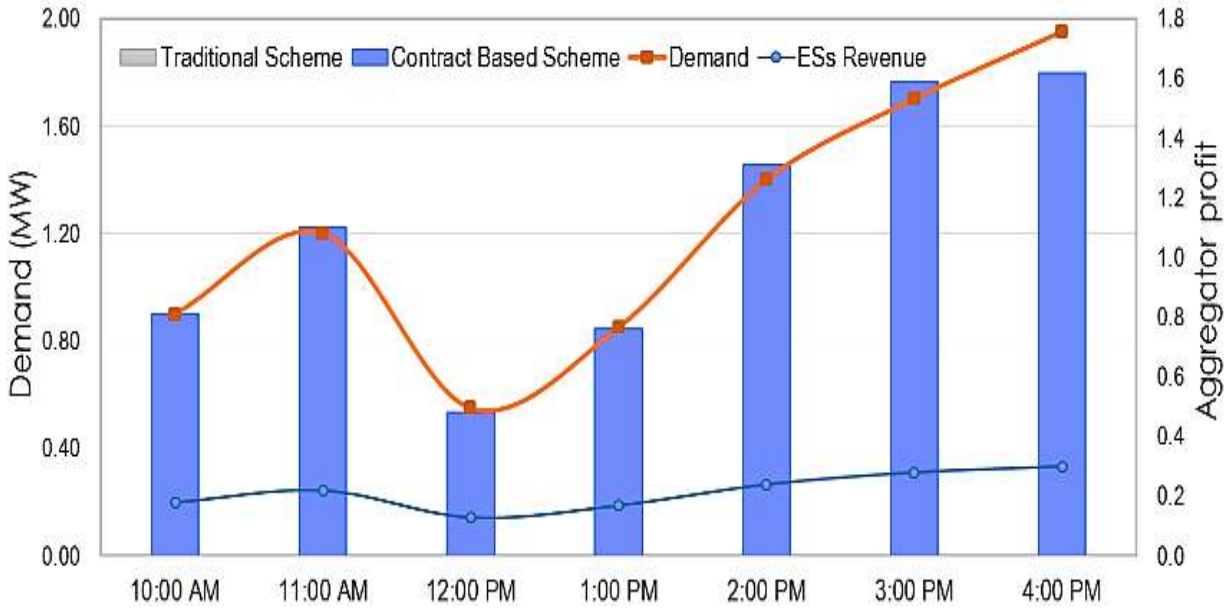

Figure 4.3. Aggregator and ESs utility with different schemes for Case II.

4.5.3 Comparison of Aggregator Profit for Base Case and Case III

The simulations, in this case, compare the performance of two schemes when wholesale price surpasses the fixed flat rate. This happens when the power demand increases in extreme weather conditions and wholesale price climbs, which causes a financial loss of aggregator under the traditional trading scheme. However, aggregator gains profit by adopting the contract-based trading

scheme as shown in Fig 4.4. The result reveals that the aggregator generates revenue by employing the designed strategy mentioned in subsection 4.4.2 condition (2). For example, at 3 pm with 6 MW demand, the aggregator's loss with the traditional scheme is -4.20 $/kWh and its profit with the contract-based scheme is 4.50 $/kWh with ESs' revenue of 2.10 $/kWh. It is clear that the ESs' revenue is positively correlated with energy demand and a rise in wholesale price, and is higher than the previous case. This is because ESs correspond their selling price with the wholesale price.

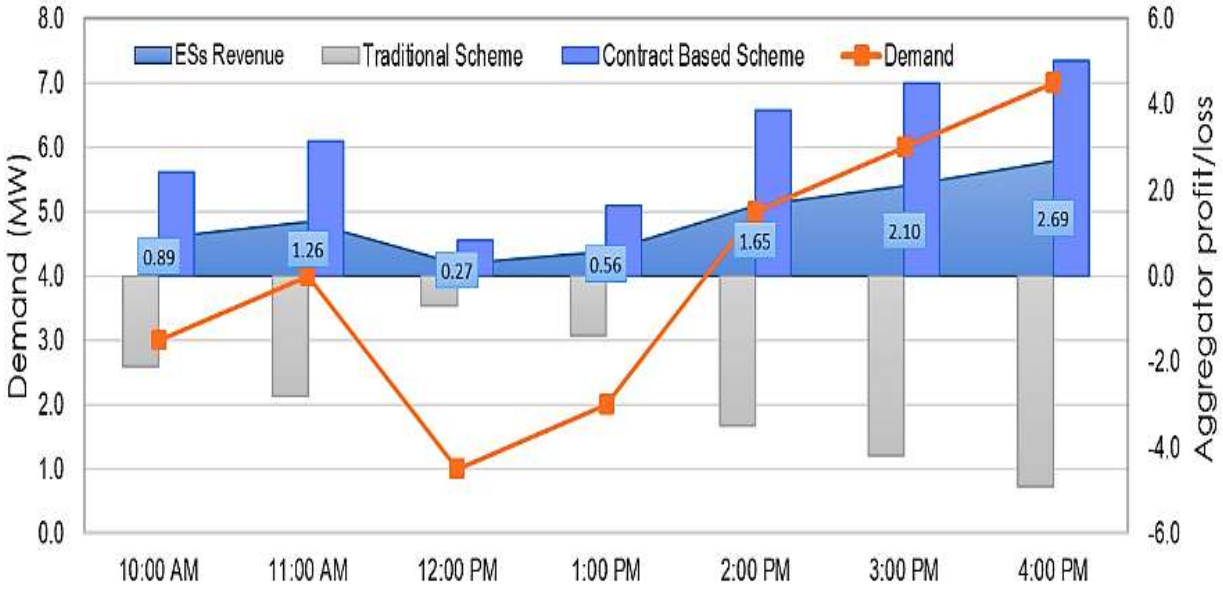

Figure 4.4. Aggregator and ESs revenue with different schemes under Case III.

4.5.4 ESs' Payment versus Wholesale Price Spikes (Case IV)

In this case, we perform simulations to examine the wholesale price spikes and ESs reliability level effect on the payment they received. Figure 4.5 reveals that the payments received by ESs from the aggregator to meet a specific power demand increase as the wholesale price increases. It is intuitive that, as the wholesale price grows, ESs have a strong incentive to increase their selling price. The payments received by ESs, i.e., for 1-2 and 4-7 MW demand are in the scenario where the ESs are paying no penalty charges because they are providing all the contracted amount of electricity

with r=1. However, as the reliability level goes down, the ESs' profit significantly reduces, i.e., for 2-4 MW demand because the penalty charges for deficit power is higher than their selling price. Thus, to ensure that ESs benefit in a trading process with a probability of penalty charges, ESs set a higher selling price than in the base case for the same demand as the wholesale price increases following (4.30). This way, the proposed strategy aligns the ESs' benefit with wholesale price spikes.

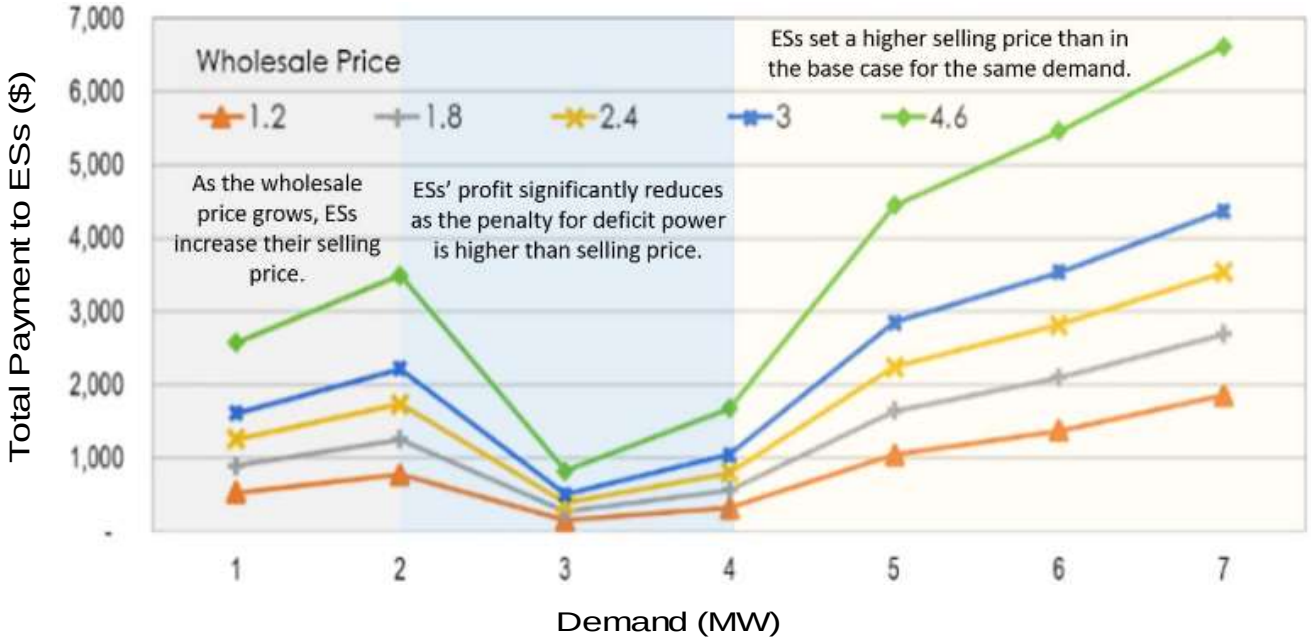

Figure 4.5. ESs payment at various wholesale prices.

4.5.5 Power Obtained from Different Categories of ESs (Case V)

This study aims to illustrate how much electricity the aggregator procures in the optimal contracts from various types of ESs in various categories. It is clearly seen from Fig 4.6 that the aggregator obtains most of the required power from ESs^{l} followed by ESs^{m} and $\mathrm{ESs}^{\mathrm{s}}$. Further, within a category, the aggregator trades more electricity with higher types of ESs than with lower types following subsection 4.4.4. The main reason is that the aggregator will obtain more power from ESs whose energy is cheaper to derive more profits. It also reveals that, as electricity demand increases,

more lower types of ESs are included in the contract to meet that demand. In addition, ESs^{s} can participate in a trading process despite their high per-unit production cost as discussed in subsection 4.2.2. Moreover, the difference between the profits gained by the aggregator through trading at a given demand is affected by the amount of electricity obtained from various types of ESs and the corresponding payments.

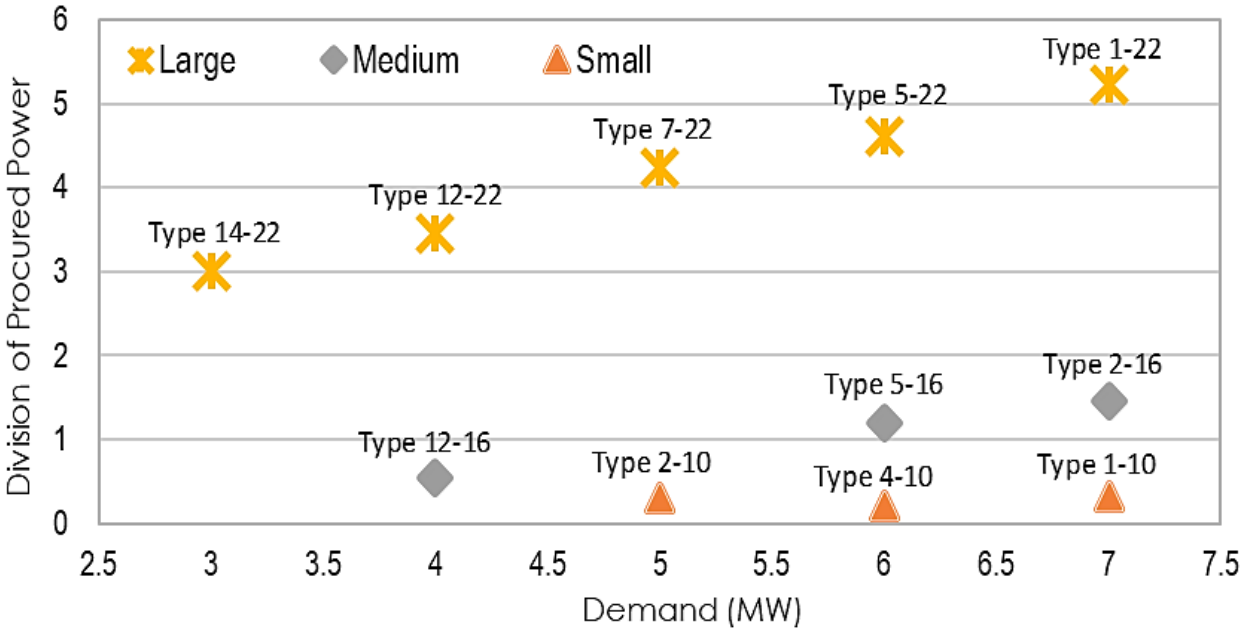

Figure 4.6. Power procured from ESs based on their category and types.

4.5.6 Optimal Revenue of ESs (Case VI)

In this case, we study the existence of optimal revenue for a given demand and how it affected by the variations in the wholesale price. Figure 4.7 demonstrates that, in each case where a certain demand is given, an optimal revenue does exist at which the ESs utility reaches a maximum and stays constant. The main reason is that the aggregator will pay more to ESs to meet a certain demand as the wholesale price increases until the per-unit payment to ESs is less than the flat rate following the 4.4.2 payment constraint (4.30a). This is because the aggregator's utility becomes negative when the per-unit payment to ESs is more than the flat rate. Fig

4.7 highlights that ESs' revenue increases as the wholesale price grows from 1.2 to 4.2 $/kWh; after that, it remains constant with further increases in the wholesale price. This way the designed scheme ensures the benefit of both trading partners and a win-win result arises.

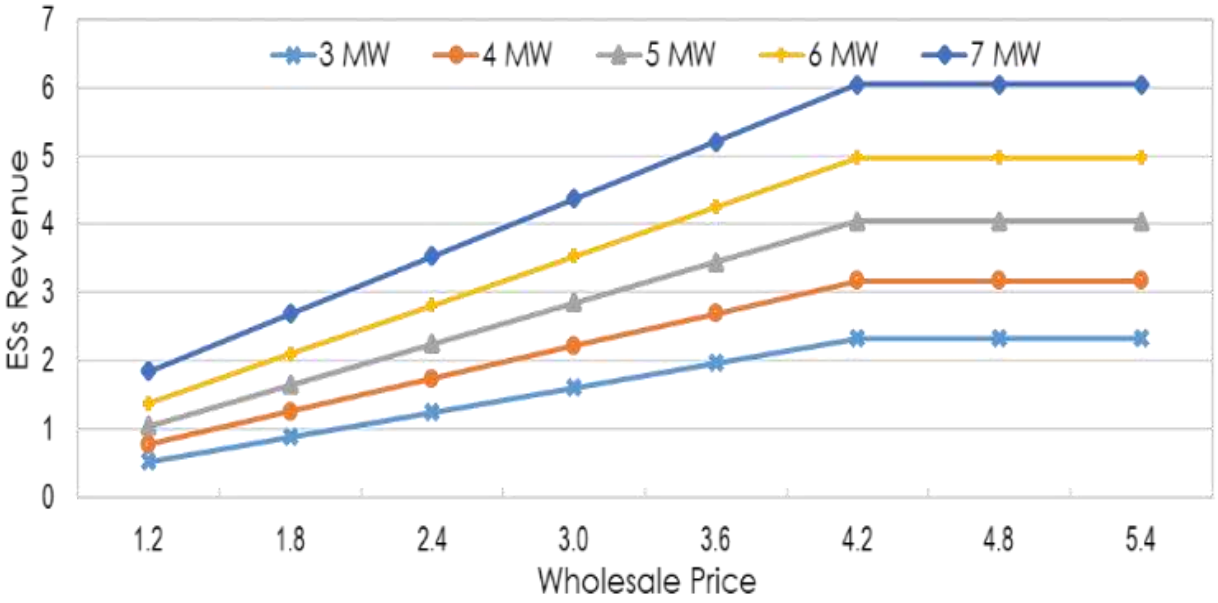

Figure 4.7. ESs optimal revenue at various wholesale price spikes.

4.5.7 Trading Partners Utility versus Reliability (Case VII)

In Case VII, the aggregator and the ESs' utilities are evaluated at three different reliability levels with variations in the wholesale price, as shown in Fig 4.8. It can be deduced that two factors reduce the aggregator utility: 1) increments in the wholesale price 2) low-reliability level of ESs. This is because, as the wholesale price increases, the ESs' selling price rises, and the aggregator has to pay more to procure power. Moreover, as a low-reliability level is negatively correlated with the deficit power, the aggregator's total payment to purchase a certain amount of demand grows because it purchases the deficit power from the wholesale market at a high price. Furthermore, from the ESs' perspective, the penalty charges to balance the deficit power at

low-reliability levels significantly reduce the ESs' revenue, and this impact is more prevalent at a high wholesale price. For instance, at wholesale price 3, ESs and aggregator utility decrease from 12.9 to 10.1 and 11.7 to 8.37, respectively, with a change in the reliability level from 0.8 to 0.6.

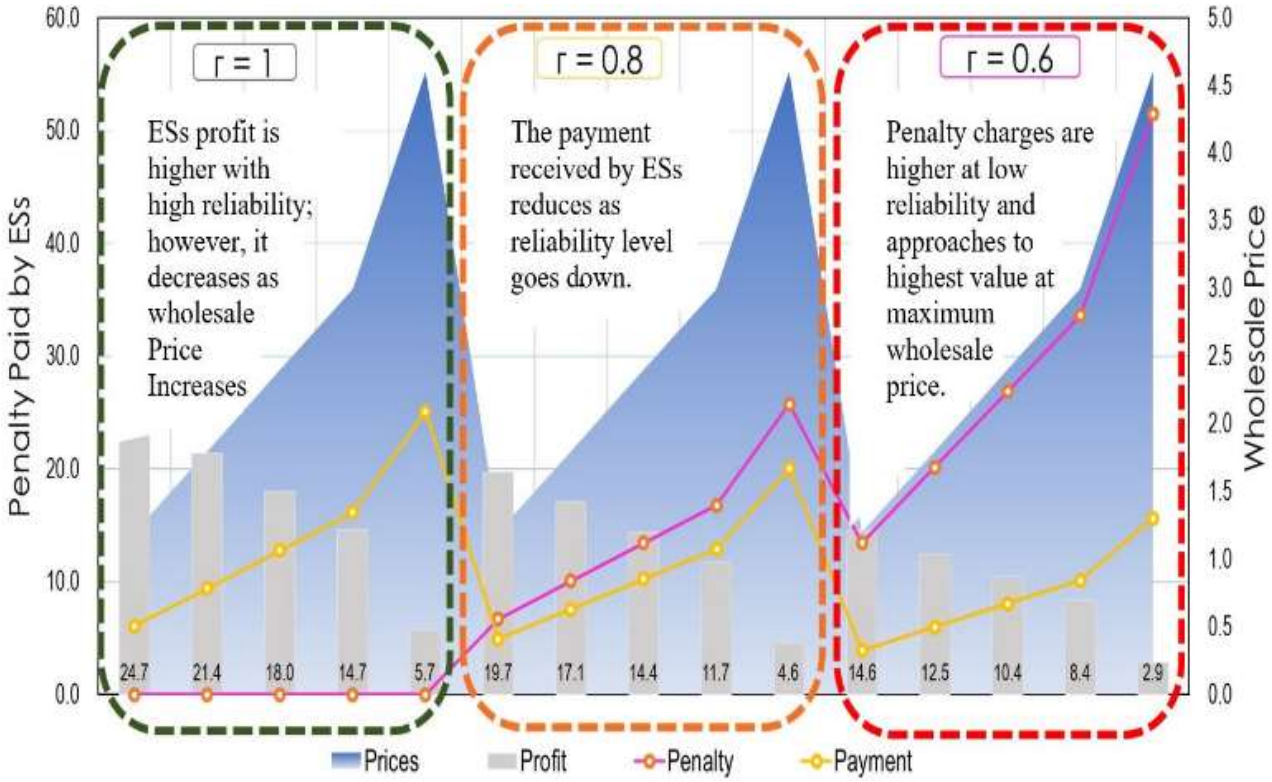

Figure 4.8. Aggregator and ESs revenue at different reliability levels.

4.6. Chapter Summary

In this chapter, a novel framework is developed for studying the complex interactions between an aggregator and different categories of ESs of various types to trade their surplus power to the aggregator strategically in the smart grid. The interaction between aggregator and ESs is formulated as an optimal-contract design problem, and optimal contracts are theoretically derived for both baseload and peak load scenarios. By adopting the proposed scheme, the aggregator can maximize its profits while stimulating ESs to satisfy the load demand with positive utility. Comprehensive simulation results show the effectiveness of the proposed contract-based incentive mechanism over a conventional trading scheme.

The results indicate that with the proposed scheme the aggregator can procure the same amount of energy with only 22.55% and 16.41% of the payment in baseload and peak load scenario respectively with the traditional scheme. Meanwhile, the developed strategy brings significant profit increment of 38.14%, 51.37%, and 72.22% for 1.2, 1.8 and 2.4 $/kWh wholesale price respectively compared to a conventional scheme. The designed incentive mechanism is characterized for regular distributions, as the aggregator only needs to publish an optimal unit price to ESs for implementation. Moreover, it is easily deployable on a large scale in smart-grid operations of the future because of its compatibility with the current electricity-tariff structure.

It is important to note that this successful energy trading solely depends on the spontaneous participation of electricity suppliers in an energy-trading scheme motivated by proper incentive mechanisms. Certainly, this spontaneous participation of consumers in the smart grid not only has energy management benefits but also can be used for energy imbalance management in case of a supply shortage due to the stochastic nature of DREGs and/or when there is peak demand stress on the grid. Hence, in the following chapter, a consumer-centric energy imbalance management scheme is investigated that can effectively reduce peak demand and energy consumption when there is a shortage of supply in a smart grid power system.

Chapter 5
Optimal Price Based Control of HVAC Systems

Price-based demand response (PBDR) is a powerful technique that can be used to handle the aggregated peak demand, energy consumption and cost by controlling heating, ventilation, and air-conditioning (HVAC) thermostat settings based on time-varying price signals. Optimizing the scheduling of HVAC systems in multizone buildings is a challenging task, as occupants in various zones have different thermal preferences dependent on time-varying indoor and outdoor environmental conditions and price signals. This paper proposes an intelligent and new PBDR control strategy for multizone office buildings fed from renewable energy resources (RERs) and/or utility grid to optimize the HVAC operation considering the varying thermal preferences of occupants in various zones as a response of real-time pricing (RTP) signals.

Occupants' varying thermal preferences represented as a coefficient of a bidding price (chosen by the occupants) in response to price signals are modeled using an artificial neural network (ANN) and integrated into the optimal HVAC scheduling. A

control mechanism is developed to determine the varying HVAC thermostat settings in various zones based on the ANN prediction model results. The effect of the proposed strategy on aggregator utility with wider implementation of the developed mechanism is also considered. In addition, a detailed mathematical model of a commercial building is presented to evaluate the thermal response of a multizone office building to the operation of an HVAC system.

The developed thermal model considers all architectural and geographical effects to provide an accurate calculation of the HVAC load demand for analyses. The optimization problem for the proposed PBDR control strategy is formulated using a building's thermal model and an occupant's thermal preferences model, and simulation results are obtained using MATLAB/Simulink tool. The results indicate that the proposed strategy with realistic parameter settings shows a reduction in peak demand varying from 7.19% to 26.8%, contingent on the occupant's comfort preferences in the coefficient of the bidding price compared to conventional control (CC). This shows that the proposed approach successfully optimizes the HVAC operation in a multizone office building while maintaining the preferred thermal conditions in various zones. Moreover, this technique can help in balancing the energy supply and demand due to the stochastic nature of RERs by cutting electricity consumption.

5.1. Introduction

Commercial buildings' electricity consumption is about 26% of the aggregated consumption in Sydney, Australia. The commercial sector's contribution to the peak (26%) is higher than its contribution to total energy usage (19.3%) [207, 208]. The average annual growth in peak summer demand is approximately 3.8% a year, almost twice the rate of growth in total electricity consumption [209]. HVAC systems are responsible for nearly half (45%) of the commercial peak demand. Cooling, as the largest single load in

Australia, accounts for more than 30% of the commercial peak demand [210]. Although the industrial sector dominates the total load demand, the joint commercial and residential HVAC operation are more dependent on temperature variations, while its contribution to the peak load increases from 17% to 20% over the peak hours on the hottest/most humid summer days [211]. The growing peak-hour demand puts considerable stress on power-supply companies to construct additional power plants and to maintain regulation services.

However, much of this expanded capacity to accommodate the maximum possible peak demand lies idle other than for short periods. For instance, Australia's largest distributor of electricity has estimated that $11 billion in network infrastructure is used for the equivalent of four or five days a year [40]. Similarly, another distribution network has estimated that around 20% of network capacity is used for the equivalent of 23 hours per year [41]. Thus, to reduce the peak load of HVAC systems, TransGrid, Energy Australia and the New South Wales Planning Department jointly manage the Demand Management and Planning Project (DMPP). One of the activities of the DMPP is the widespread implementation of an innovative HVAC program that can reduce electrical demand during peak hours by replacing conventional HVAC systems with innovative HVAC technologies. The project team estimated the potential for a 300kVA reduction in peak demand at a cost of support of AU$ 242/kVA [211]. Although this program received an AU$ 1 million grant for implementation, the program failed due to timing and facilitation constraints.

Another approach to relieving the growing demand stress on traditional power grid is to install distributed renewable energy generators (DREGs) at commercial buildings. However, the stochastic input from RERs can bring difficulty in balancing the electricity demand and supply [212]. Considering these challenges, the effective way to reduce the peak demand/electricity

consumption of HVAC systems is the control of HVAC thermostat settings in accordance with variations in electricity rates for demand response (DR).

The control of the thermostat for DR, in general, can be categorized as 1) transaction-based and 2) price-based. Transactive control (TC) utilizes a market-based control technology to make thermostatically controlled loads more demand responsive. The TC adjusts the thermostat setting based on the market-clearing price (MCP). However, in the PBDR program users change their energy usage pattern in response to changes in electricity pricing. Time-of-use (TOU), real-time pricing (RTP) and critical peak pricing are different pricing mechanisms used for the DR program [106, 213].

Several designs of transactive controllers for residential as well as commercial building HVAC systems are available in the literature. For example, in [128, 214] Olympic Peninsula and American Electric Power projects investigate TC for residential HVAC systems. The researchers in [215] design the RTP in a transactive environment to define the final thermostat set-point of a residential HVAC based on the bidding price. In [180] similar design concepts are applied to those in [128, 214] to control the thermostat in commercial building HVAC systems. The work in [180] adjusted the zone temperature set-point based on the MCP. The adjusted set-point might be lower or higher than the desired set-point, so it might not strictly respect a customer's comfort preferences. In addition, TC implementation required extension of existing standards, and development of new interface standards, and many more studies are required to overcome the TC challenges [216, 217]. In contrast to [180], the current work proposes an easily implementable PBDR controller to change the thermostat setting by considering customer preferences in both thermal comfort and price selection.

In the literature, considerable work [218-222] has been done to design the DR algorithms for scheduling residential HVAC loads to obtain energy cost savings and/or energy efficiency. In [218] a fuzzy-logic based and in [219] model predictive control (MPC) system is developed to control residential HVAC units to reduce the peak power demand. An adaptive supervisory on/off algorithm is presented in [220] to increase the efficiency of a centralized HVAC system. This work studied the influence of gas consumption on control signals and internal temperature. However, these controllers do not consider a thermal comfort model for DR and are non-responsive to price signals. In recent years, many research studies introduce HVAC load control strategies based on thermal comfort modeling and price signaling. For instance, in [221] a smart thermostat is developed where the desired comfortable levels set by consumers determine the on/off state of the air-conditioner; however, the smart thermostat is unable to respond to price signals. The work in [222] proposes an automatic thermostat set-point control strategy in a residential home, which response to the price variation in a TOU tariff, and examines the influence of the peak period length, home size and set-point offset on peak energy savings without considering the thermal comfort.

The proposed PBDR control strategy is most closely related to recent DR strategies that respond to varying price signals while meeting user thermal comfort requirements. In [223] a control algorithm is proposed that regulates the running state of HVAC units in a community microgrid according to the RTP with bounded temperature constraints for cost savings. In [224] and [225] controllers are designed using various mathematical approaches to model a residential HVAC system. The developed controllers are able to reduce the peak consumption for HVAC of homes in response to RTP while taking into account thermal comfort requirements. In these strategies to consider the cost/comfort trade-off for consumers, when the energy price exceeds the maximum purchasing price of a customer, the thermostat setting will be increased by

2 to 3 °C, which may cause discomfort to many users. The mechanism designed in [226] and [227] controls the residential HVAC thermostat setting within a pre-determined thermal comfort interval in response to changing prices; in a single thermal zone. However, commercial buildings have multiple zones with a thermally interconnected dynamical system and therefore require careful attention to optimize the DR of HVAC systems. Considering this, unlike the above literature, the current work proposes a PBDR controller for a commercial building's HVAC operation, which involves a large number of occupants with varying thermal comfort preferences and with control of multiple zones.

Another research community works to optimize the DR of the HVAC systems in multizone buildings. A pre-cooling strategy is considered in [228-230] to utilize commercial buildings' thermal storage potential for demand shifting during peak hours. In [231] a control strategy has been proposed for aggregation and coordination of industrial and commercial loads for DR using RTP. In [232] a predictive model of HVAC air-circulation fan power consumption is developed to use the commercial HVAC system for fast DR. Reference [233] investigates event-driven DR strategies to reduce commercial HVAC energy consumption. A commercial HVAC unit is controlled in [234] for multiple-occupant spaces for optimal peak load reduction while maintaining human comfort using a predicted mean vote (PMV) model. In [27] predictive control and in [28] fuzzy control is proposed to minimize the energy consumption of HVAC systems where the occupants' comfort is based on the acceptable range of the PMV index. The PMV model relied on a group level presentation of thermal comfort and was unable to reflect variations in behavior related to the thermal environment. The research studies [235, 236] show that at a certain temperature some occupants feel cooler and more uncomfortable than others due to the difference in physiological and psychological responses based on gender and adaptive behavior. This implies that occupants have different thermal comfort preferences that need to

be considered when designing an HVAC control strategy. Considering this, participatory approaches were used in [237] and [238] to allow occupants to adjust their thermostat set-points according to their preference to integrate an individual occupant's preference into HVAC control. However, these strategies [27, 28, 234-238] are non-responsive to time-varying electricity prices for HVAC control. Unlike these studies, in this work, a practical and new dynamic PBDR control strategy is proposed to optimize the commercial building HVAC systems energy consumption, while considering the varying thermal comfort preferences of occupants in various zones in response to RTP signals.

Moreover, to analyze HVAC energy usage, the importance of accurate modeling of the HVAC system is undeniable. In the field of HVAC system modeling, the most complicated part is the development of an accurate model for a commercial building. This is because the components that need to be modeled for buildings are not limited to a building's construction. Internal building loads that include the number of people within the space, their activities and the heat gain from lighting must also be modeled [239]. The authors in [240] study the transmission of heat and moisture through the walls, roofs, and ceilings to estimate the indoor air temperature and humidity. However, they do not consider the transmission of heat and moisture through ventilation and internal loads. In [241] the research is focused on reducing the order of dynamic models of temperature and humidity in commercial multi-zone buildings for model-based HVAC control. References [227] and [241] use MPC that requires many assumptions to facilitate HVAC energy usage calculations. The study in [242] and [243] only correlates the occupancy and air-infiltration rate with commercial building electricity consumption respectively. In this Chapter, a precise thermal and power model is developed for HVAC components by considering all the above-mentioned factors that influence the HVAC energy consumption.

Compared with previous studies, the key contributions are:

- A commercial building HVAC system that is a complex, thermally interconnected dynamical system is considered, in contrast to residential buildings where researchers consider only one zone, which is cooled and heated up by the HVAC system. In this study, five zones with varying thermal comfort preferences are controlled.
- Occupants' varying thermal preferences in the coefficient of the bidding price are modeled by employing an ANN, which is trained using a machine-learning algorithm, and these preferences are directly integrated into the objective function in the optimal HVAC scheduling problem.
- A new PBDR control mechanism is proposed to control the HVAC thermostat setting in various zones to cater to the varying thermal preferences of occupants in response to RTP signals while maintaining the indoor environmental conditions of human occupancy in occupant-controlled multizone office buildings.
- Comprehensive simulation case studies are performed to show the effectiveness and applicability of the proposed PBDR controller.

The rest of the Chapter is planned as follows. Section 5.2 presents the HVAC system modeling, while Section 5.3 formulates the control problem and describes the pricing data. Section 5.4 presents the proposed PBDR control methodology. Section 5.5 is devoted to the experimental setup, while Section 5.6 provides simulation results and a discussion on thermal comfort. Section 5.7 describes the chapter summary.

5.2. System Modeling

The structure of the proposed PBDR control methodology and a typical configuration of a commercial building HVAC system with

multiple zones are shown in Fig. 5.1(a) and Fig. 5.2(b) respectively. The study considered multiple occupants in a multizone building getting power from RERs and/or power grid. Each zone is equipped with an HVAC controller, which has load control capabilities. The HVAC controllers are connected over a local area network to a central control agent (CCA) that receives the occupant's comfort preferences in the coefficient of bidding price to control the thermostat setting in each zone. This study assumed that the CCA is owned, operated and maintained by the building manager. The main equipment of the HVAC system is air-handling units (AHU) and variable-air-volume (VAV) boxes responsible for producing and distributing cool/warm air for all zones.

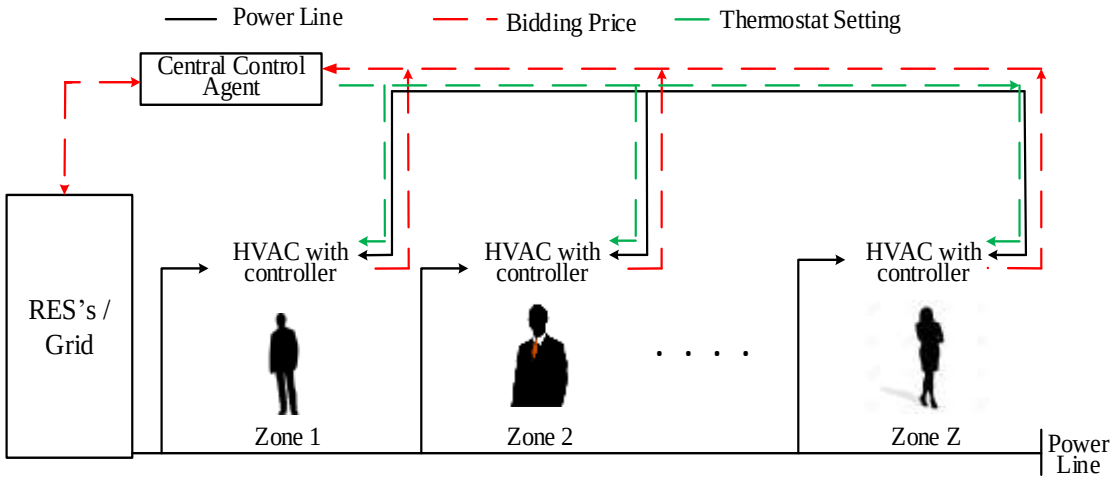

Figure 5.1(a). System model depicting the flow of signals

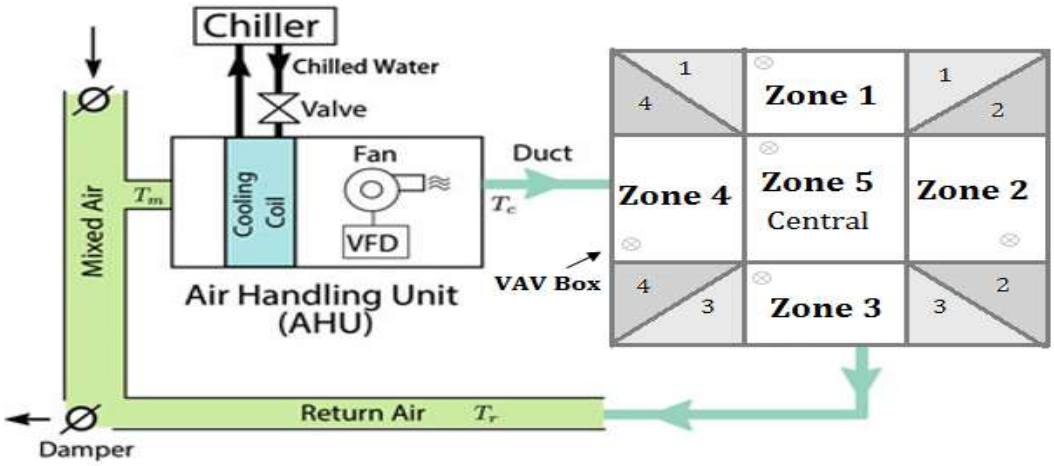

Figure 5.1(b). Typical commercial building HVAC system configuration

A detailed description of the air distribution system can be found in [181, 182]. The air moves through VAV boxes before reaching a given space, while the zone cool air mass flow rate delivered to space is controlled by changing the damper position at each VAV box. A thermal zone is a space that is cooled/heated by one VAV box. In this work, a single centralized chiller is considered, which works for one AHU for providing cool/warm air to multiple zones, and a VAV box is associated with each temperature zone.

5.2.1 Supply Fan Model

The fan power consumption principally depends on the air mass flow rate and the pressure difference between the inlet and outlet. Earlier simulation work [184] found that the AHU supply fan power versus fan mass flow rate fits a quadratic model. In addition, the pressure drop is approximately linear with the total mass flow rate. With this form of fit and simplification, the fan power is modeled as a quadratic function of the total mass flow [183, 244]:

$$P_t^f = k_f(m(t))^2 \tag{5.1}$$

where P_t^f is the power consumed by the fan in kW to supply the required airflow rate to all zones, k_f (kW.s^2/kg^2) is the parameter that considers both the duct pressure losses and fan efficiency. The total supply airflow rate $m(t)$ is the sum of the airflow rate into each zone $m_z(t)$ in kg/sec and is given as

$$m(t) = \sum_{z=1}^{Z} m_z(t) \tag{5.2}$$

where z is the zone index, z= [1,…Z]. A zone airflow rate is dependent on the zone load, zone temperature, and supply air temperature. It can be expressed in mathematical form as [184]

$$\sum m_z(t) = \sum \frac{q_{z(t)}}{1.2(T_{z(t)} - T_s)} \tag{5.3}$$

where $q_{z(t)}$ is the zone load in kW, $T_{z(t)}, T_s$ are the zone and supply air temperatures in °C, and 1.2 is a conversion factor.

5.2.2 Chiller Model

In the literature, comprehensive and complex chiller models are available [245, 246] but these models are not control-oriented. This paper considers a simple control-oriented chiller model [183, 184]:

$$P_t^c = \varphi \frac{\sum q_z(t)}{\eta COP} + (1-\varphi)\frac{q_t}{\eta COP} \tag{5.4}$$

where P_t^c is the total power consumed by the chiller in kW that is used to generate the chilled water consumed by the cooling coil for all zones, q_t is the total load of the building in kW, $\varphi \Rightarrow [0,1]$ is the damper position, η is the chiller efficiency factor and COP is the chiller coefficient of performance. q_t and COP can be calculated as [184].

$$q_t = \sum m_z(t)\left(T_{o(t)} - T_s\right) \tag{5.5}$$

$$COP = 7.93\theta^3 - 21.12b\theta^2 + 16.49\,\theta + 2.22 + 0.1(T_w - 6) \tag{5.6}$$

where $T_{o(t)}$, T_w are the outside air and chilled water temperatures in °C, and θ is the cooling coil and design load ratio.

5.2.3 HVAC Power Consumption

The aggregated power usage of the HVAC system is the sum of the fan and chiller power consumptions and is given as

$$P_t = P_t^f + P_t^c \tag{5.7}$$

Putting the values of (5.2), (5.3) into (5.1), and (5.5) into (5.4), (5.7) over the given time horizon for Z zones can be re-written as:

$$P_t = \sum_t^w \sum_z^Z \{(k_f * \left(\frac{q_{z(t)}}{1.2(T_{z(t)} - T_s)}\right)^2) + (\varphi \frac{q_{z(t)}}{COP} + (1-\varphi)\frac{m_{z(t)}(T_{o\,(t)} - T_s)}{COP})\} \quad (5.8)$$

where P_t is the total power consumed by the HVAC load in kW and t is the time index, t = [1….W]. It can be noted from (5.8) that the fan and chiller power consumptions depend on the zone load. Therefore, to provide reliable and accurate DR, a precise calculation of the zone load is required.

5.2.4 Zone Cooling and Heating Load

The key design component for most HVAC systems is an accurate assessment of the cooling load (CL) and heating load (HL) requirements because these loads can significantly affect the comfort and the productivity of the occupants, the operating cost and the energy consumption. The peak HL in winter months occurs before sunrise and there is no considerable change in the outside environment during the winter season. In contrast, in summer, solar radiation causes a significant variation in outdoor environmental conditions throughout the day, and all indoor heating components add to the CL. Therefore, CL calculations are fundamentally more complex and require consideration of unsteady-state processes [247, 248]. Moreover, the CL's contribution to the commercial peak load is the largest. For these reasons, this paper considers zones with cooling requirements only and presents detailed mathematical modeling of the CL calculation based on the cooling load temperature difference (CLTD) method with solar CL factors suggested by the American Society of Heating, Refrigeration and Air-Conditioning Engineers (ASHRAE). This method considers all factors that influence the HVAC electricity consumption such as building size, outdoor environmental conditions, indoor activities, and thermal load, etc.

5.2.5 Cooling Load Calculation

The building CL is the sum of the external and internal CL of each zone $q_c^z(t)$ and it includes both sensible and latent CL components. The sensible load refers to the dry-bulb temperature, while the latent load refers to the wet-bulb temperature of the zone. The CL heat balance model is based on dynamic conditions, which consider the heat stored in the building envelope and interior materials.

5.2.5.1 External Cooling Load Calculation

The heat transferred through the building's roof, walls and glass are called the external CL. The basic conduction equations for heat gain/conductive load from roof, wall, and glass are given as

$$q_r(t) = \cup_r * A_r * CLTD_r^c \quad (t) \tag{5.9}$$

$$q_w(t) = \cup_w * A_w * CLTD_w^c \quad (t) \tag{5.10}$$

$$q_g^c(t) = \cup_g * A_g * CLTD_g^c \quad (t) \tag{5.11}$$

The solar load through glass is the sum of a conductive and a solar transmission load that occurs when solar radiation is absorbed, stored and scattered in the atmosphere. The sum of the CL through glass can be calculated as

$$q_g(t) = q_g^c(t) + q_g^s \quad (t) \tag{5.12}$$

Where $q_r(t)$, $q_w(t)$, $q_g(t)$ are the hourly heat gains by conduction through roof, wall, and glass in watts, $\cup_r$, $\cup_w$, $\cup_g$ are the thermal transmittances for roof, wall, and glass in W/m^2.C , A_r, A_w, A_g are the areas of roof, wall, and glass in m^2, $q_g^c(t)$, q_g^s (t) are the conductive and solar transmission components of the glass load in watts.

The solar transmission load through glass is given as

$$q_g^s = A_g * S_c * S_{cl} \tag{5.13}$$

Where S_c is the shading coefficient, S_{cl} is the solar CL factor, $CLTD_r^c(t)$, $CLTD_w^c(t)$, $CLTD_g^c(t)$, are the hourly-corrected CLTD values for roof, wall, and glass in °C. In [249] hourly CLTD values for roof $(CLTD_r)$, wall $(CLTD_w)$ and glass $(CLTD_g)$ are provided for one typical set of conditions. Therefore, it is required to calculate the CLTD correction factors for roof, wall, and glass according to Sydney weather conditions. The CLTD correction factors can be calculated as:

$$CLTD_r^c = [CLTD_r + (T_{in}^D - T_{in}^R) + ((T_o^{DB} - {DR}/{2}) - T_o^M)] \quad (5.14)$$

$$CLTD_w^c = [CLTD_w + (T_{in}^D - T_{in}^R) + (T_o^{DB} - {DR}/{2}) - T_o^M)] \quad (5.15)$$

$$CLTD_g^c = [CLTD_g + (T_{in}^D - T_{in}^R) + (T_o^{DB} - {DR}/{2}) - T_o^M)] \quad (5.16)$$

where T_{in}^D, T_{in}^R are the indoor design and indoor room temperatures, T_o^{DB}, T_o^M are the outdoor dry bulb and mean daily temperatures and DR is the daily temperature range in °C. Climatic design conditions for Sydney are taken from [248] and these are based on long-term (20-25 years) hourly observations.

5.2.5.2 Internal Cooling Load Calculation

The heat generated by occupants, equipment, and lights in a zone is called the internal load. The various internal loads (e.g. occupants and appliances) consist of sensible and latent heat transfers, but the lighting load is sensible. The conversion of the sensible heat gain to space CL is affected by the thermal storage characteristics of that space. However, the latent heat gains are considered to be instantaneous.

i. Heat Gain from People and Appliances

The CL due to occupancy and appliances is the sum of sensible and latent CL components. The sensible and latent CL from people and appliances is calculated as:

$$q_p^s(t) = N * q_h^s * CLF_p \quad (5.17)$$

$$q_p^{lt} = N * q_h^l \quad (5.18)$$

$$q_a^s(t) = q_a^{in} * U_f * R_f * CLF_a \quad (5.19)$$

$$q_a^{lt} = q_a^{in} * \cup_f \quad (5.20)$$

(5.17) and (5.18) are used to calculate the dynamic occupancy patterns in a zone. Where N is the number of people in a zone, q_h^s, q_h^l are the sensible and latent heat gains due to individuals' activities in watts, CLF_p, CLF_a are the people and appliances CL factors by an hour of occupancy, q_a^{in} is the rated energy input from appliances in watts, U_f, R_f are the usage and radiation factors of appliances, CLF_p, CLF_a capture the time lags of the CLs affected by the building's thermal mass.

The total CL due to occupancy and appliances is given as:

$$q_p(t) = q_p^s + q_p^{lt} \quad (5.21)$$

$$q_a(t) = q_a^s + q_a^{lt} \quad (5.22)$$

where q_p^s, q_p^{lt}, q_a^s q_a^{lt} are the sensible and latent cooling loads (CLs) from people and appliances in watts.

ii. Lighting Heat Transfer

The sensible CL from lighting is given by

$$q_l = W * L_{uf} + SB_{af} * CLF_l \quad (5.23)$$

where W is the lighting load in watts, L_{uf} is the lighting use factor, SB_{af} is the special ballast allowance factor and CLF_l is the CL factor of light, by an hour of occupancy.

iii. Heat Transfer through Infiltration Air

The infiltration air CL has both sensible and latent load components and can be calculated as

$$U_{L1} = U_1 + U_{C2};\ \ U_{L2} = U_{C1};\ \ U_{dc} = 0 \tag{5.24}$$

$$U_{L1} = U_1 + U_{C2};\ \ U_{L2} = U_{C1};\ \ U_{dc} = 0 \tag{5.25}$$

The total infiltration air CL is given by

$$q_{ia}(t) = A_f(t) * (h_{o,t} - h_{i,t}) \tag{5.26}$$

where $A_f(t)$ is the infiltration airflow rate in m^3/min, T_o, T_i °C, W_o, W_i gm/gm, h_o, h_i J/gm are the outside and inside dry bulb temperatures, humidity ratio, and air enthalpy respectively, q_a^s, q_{ia}^{lt} are the sensible and latent CL in watts due to infiltration air. The values of the shading coefficient, solar CL, lighting, and people CL factors, the rates of sensible and latent heat gain from occupancy, and the infiltration airflow rate are taken from [249].

5.2.5.3 Zone Load Calculation

The zone CL is the sum of all external and internal CL components and is given by

$$q_z(t) = q_r(t) + q_w(t) + q_g(t) + q_p(t) + q_a(t) + q_l(t) + q_{ia}(t) \tag{5.27}$$

where $q_r(t), q_w(t)$, $q_g(t)$ are the total CLs for roof, wall, and glass, $q_p(t)$, $q_a(t)$, $q_l(t)$, $q_{ia}(t)$ are the total CLs due to occupancy, appliances, lights and infiltration air, q_z is the aggregate CL of the zth zone in kW.

5.3. Control Problem and Pricing Data

In this section, a general control problem is formulated using the model developed in Section II, and detail about pricing information is given.

5.3.1 Problem Formulation

The proposed model has two objectives: (1) minimizing the peak load demand and the aggregated power usage (P_t) of the HVAC system, and (2) minimizing the difference between the controllable/modified temperature set-point and the desired reference temperature of the zone. The objective function of the proposed model can be is re-written as:

$$min_{q_z[.],T_{z,ref}[.]} = \sum_t^W \sum_z^Z \{(k_f * (m_z(t))^2) + (\varphi \frac{q_{z(t)}}{COP} + (1-\varphi)\frac{q_t}{COP})\} + \sum_t^W \sum_z^Z (T_{z,sp}^t - T_{z,ref(t)}) \quad (5.28)$$

Subject to the following constraints due to control requirements:

$$m_{z,min} \leq m_z(t) \leq m_{z,max} \quad (5.28a)$$

$$T_{z,sp}^t, T_{z,ref(t)} \in [T_{z,max}, T_{z,min}] \quad (5.28b)$$

$$q_{z,min} \leq \frac{q_t}{1.2\,(T_{z(t)} - T_s)} \leq q_{z,max} \quad (5.28c)$$

where $m_{z,min}$, $m_{z,max}$, $q_{z,min}$, $q_{z,max}$ and $T_{z,min}$, $T_{z,max}$ are lower and upper bounds of the zth zone's, supply airflow rate, zone load, and zone temperature respectively. In (5.28) $T_{z,sp}^t$, $T_{z,ref(t)}$ represent the modified temperature set-point to save energy and the reference temperature of a zone at time t. The first term in the objective function (5.28) computes the aggregated HVAC energy consumption over W time intervals. The energy consumption is a function of the cooling load $q_z(t)$ as defined in (5.8), usually in kW per hour. The first term of the objective function in (5.28) is obtained by

putting the values of (5.3) and (5.5) in (5.8). The objective function (5.28) is solved by using a multi-objective optimization tool available in MATLAB. Since the time interval is assumed to be 30 minutes in this study, the hourly usage on a 30 min basis is divided by 2 in the objective function. The temperature deviations between modified thermostat set-points and the reference temperature set-point in a zone are handled by the second term in the objective function. The controller aims to keep the modified/inside temperature close to a reference temperature set-point by minimizing the deviation between the two in various zones.

In CC, commercial HVAC units' operation is based on a reference temperature set-point that does not change frequently throughout the considered time period, and thus the HVAC operates regardless of price fluctuations. The reference temperature is chosen by a building manager/aggregator taking into account a group level presentation of thermal comfort in a multizone office building. The major drawback of CC is that with a fixed reference temperature set-point both the aggregator and consumers are unable to utilize the advantages of dynamic electricity pricing, while the above model overcomes this drawback by operating the HVAC unit at variable thermostat set-points in response to the price fluctuations in various zones. The deployment of variable thermostat settings in various zones achieves financial benefits while keeping the indoor environment within the occupants' thermal comfort limit. Therefore, the current work proposes a DR strategy for determining cost-efficient variable thermostat set-points for a PBDR controller within a temperature range specified in constraint (5.28b). The variable thermostat settings in various zones are determined as a function of the occupants' chosen bidding price at each time t as a response to price fluctuations. The proposed PBDR control strategy is discussed in Section 4.

5.3.2 Pricing Data

Pricing data is obtained from the Australian Energy Market Operator (AEMO). Wholesale electricity prices are decided by AEMO depending on the supply and demand at a 5-minute interval and the average over every 30 minutes. On the AEMO website, the day-ahead wholesale electricity priced on a 5-minute and 30-minute basis is available. The pricing system in Australia adopts an RTP structure in the wholesale market and a TOU tariff in the retail market for customers with smart meters. However, TOU tariffs do not reflect the actual variations of the wholesale price at the time of consumption. To coin the real-time wholesale price structure for the retail market the authors in [250] design the real-time retail price. They have shown that the retail price follows the pattern of the wholesale price. Based on this, the half-hour ahead forecasts wholesale energy settlement price is considered as the real-time retail price of electricity in this work. Half-hour ahead electricity prices are chosen because Australia's National Electricity Market operates as a continuous-trading market for each half-hour interval [251].

In addition, the retail electricity price on a 30-minute basis is preferred over 5-minute and hourly-based pricing for the following reasons. Significant accessible computing resources and software would be required to implement 5-minute settlement intervals. New spike loads away from the expected peak hours occur when hourly pricing is implemented; therefore, this new aggregated load affects the utility. The effective spread of demand after the typical peak occurs with 30-minute based retail prices of electricity [252]. Figure 5.2 shows the 30-minute based day-ahead time-varying electricity price in AU$ obtained from the AEMO electricity market [253]. The chosen electricity price is on a typical hot summer day of 6 November 2018. The electricity value

on that particular day is chosen carefully considering historical electricity prices. It represents those hot summer days where the peak electricity price substantially increases from the average price of electricity.

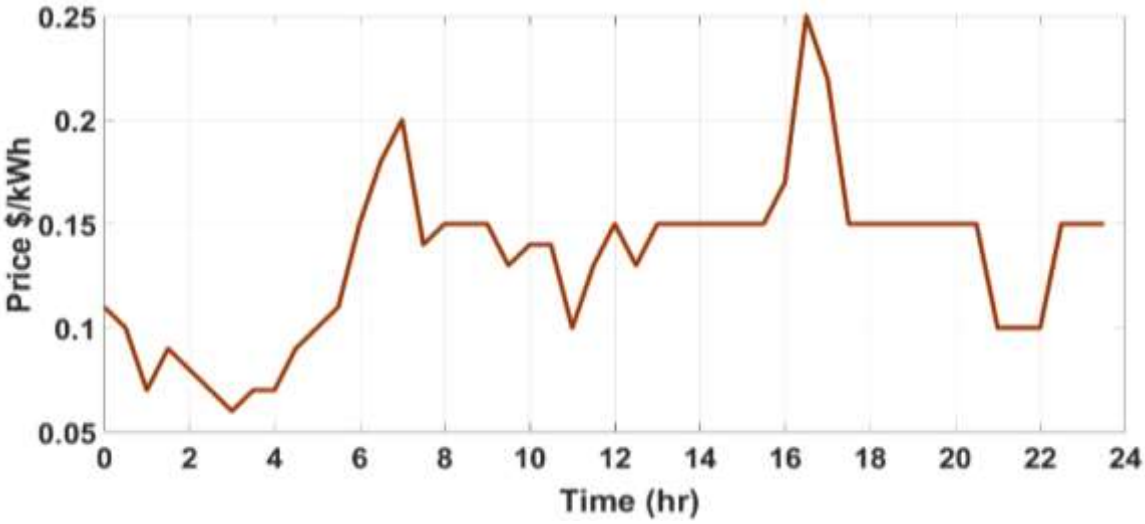

Figure 5.2. Day-ahead retail electricity price on a hot summer day

5.4. Price-Based Demand Response Control Strategy

The proposed PBDR controller is responsible for controlling the thermostat setting in $z \in Z$ zones in a multizone office building. It is assumed that each zone has multiple rooms with a number of occupants as shown in Fig. 5.1(a) and they have varying thermal comfort requirements in each zone. In this study, occupants in Z zones reflect their thermal preferences in a coefficient of bidding price ($P^t_{bc,\ z}$). This is a price of electricity that occupants of various zones offer considering variations in retail price (P^t_R) at each 30-minutes timestamp t. Occupants in Z zones can select a reference temperature ($T_{z,\ ref}$), minimum ($T_{z,\ \min}$) and maximum temperature ($T_{z,\ \max}$) and set-point interval (a^t_z) to further express their thermal comfort preferences. $T_{z,ref}$ is the desired temperature at which most of the occupants in a zone feel comfortable, and that may be the same or different in each zone. $T_{z,\min}$ and $T_{z,\max}$ represent the allowable temperature range in response to the

variation of P_R^t. If the occupants of a certain zone feel cooler at time t, they bid considerably lower than the retail price, which indicates that the occupants want to increase the thermostat set-point from the reference temperature. In contrast, a bidding price higher than the retail price reflects the feeling of warmth, and thus a decrease in the thermostat set-point is required from the reference temperature. Meanwhile, a bidding price equal to the retail price signifies that the occupants want to maintain the thermostat at the reference temperature set-point.

The proposed PBDR controller calculates the price difference (ΔP^t) between P_R^t and $P_{bc,z}^t$ in Z zones on a 30-minute basis for a total simulation time t ϵ W. The controller will take control action when P_R^t is higher or lower than $P_{cb,z}^t$ by increasing or decreasing the temperature in each zone based on the price difference (ΔP^t). If P_R^t is equal to $P_{cb,z}^t$, the thermostat from the PBDR controller maintains the $T_{z,ref}$ set by the occupants in a zone. The controller changes the set-point of the thermostat within a range of $T_{z,min}$ to $T_{z,\max}$ in a zone in response to P_R^t. When $P_{bc,z}^t$ is significantly lower than P_R^t at time step t then the thermostat can be set to $T_{z,\min}$and when it is substantially higher than P_R^t then the thermostat setting can be as high as $T_{z,\max}$. The temperature change (ΔT^t) from the previous setting at each time depends on the set-point interval a_z^t. Previous controllers [20][22] either compare the current retail price with the last day's average price of electricity or a constant threshold price to change the thermostat setting. However, using an average price or a constant threshold price is not suitable for high fluctuations in the retail price in the real-time market. This may cause the controller to not increase the thermostat setting when the load should be curtailed. In addition, a constant threshold price is unable to consider the varying thermal comfort preferences of occupants in a multizone office building.

In contrast, the current work compares the retail price with the dynamic bidding price $P_{cb,z}^{t}$ that occupants change at each time step in various zones. This way the proposed strategy is able to cater to the occupants' varying choice of $P_{bc,z}^{t}$ with respect to time-varying P_{R}^{t}. Furthermore, in previous studies [19][20][26], the coefficient for comfort is unitless and thus it is difficult for occupants to show their comfort preferences in response to price signals, while the proposed strategy allows them to choose the comfort coefficient of their preference.

Occupants in a multizone building will choose $P_{cb,z}^{t}$ at each time step to change the thermostat setting according to their requirements. The feasible range of $P_{cb,z}^{t}$ is given as

$$P_{R(min)}^{t} \leq P_{cq,z}^{t} \leq P_{R(max)}^{t} \tag{5.29}$$

where $P_{R(min)}^{t}$, $P_{R(max)}^{t}$ are the minimum and maximum values of the 30-minute ahead forecast retail electricity price. Equation (5.29) implies that $P_{cb,z}^{t}$ should be greater than the minimum value of the 30-minute ahead forecast retail electricity price $P_{R(min)}^{t}$, and it can be as high as the maximum value of the retail price $P_{R(max)}^{t}$ according to customers' comfort preference at time t. According to (5.29) occupants cannot bid less than $P_{R(min)}^{t}$ to participate in the DR program.

Since the occupants' choice of bidding price at each time step t in a zone follows the variations of P_{R}^{t} which corresponds to their thermal comfort preferences obtained by the desired thermal comfort is evaluated based on the price difference between P_{R}^{t} and $P_{cq,z}^{t}$. The price difference ΔP^{t} is the subtraction of the electricity retail price P_{R}^{t} from the bidding price $P_{cq,z}^{t}$ and it is calculated at each timestamp t in various zones when the new retail price is updated in every 30 minutes as

$$\Delta P^{t} = P_{R}^{t} - P_{cq,z}^{t} \tag{5.30}$$

When P_R^t is higher (lower) than $P_{cq,z}^t$, ΔP^t are a positive (negative) number and the PBDR controller starts to work. Otherwise, ΔP^t is zero and the controller stops working immediately and maintains or returns to $T_{z,ref}$.

The magnitude of the price difference is used to evaluate the different occupants' thermal comfort preferences, and based on this they are categorized into three main types:

1) high comfort; 2) moderate comfort; 3) low comfort

High comfort occupants' bidding price $P_{cb,z}^t$ is equal/close to P_R^t for most of the occupied hours, which leads to a zero /lower positive price difference ($\underline{\Delta P^t}$). Thus, a zero/ low magnitude of the positive price difference $\underline{\Delta P^t}$ indicates higher requirements on thermal comfort and consequently, the designed strategy maintains the thermostat at the reference temperature/allows temperature variations close to the reference temperature set-point respectively. For other hours, the bidding price $P_{cb,z}^t$ can be higher than P_R^t , which results in a negative price difference ($-\Delta P^t$) and thus thermostat set-point is decreased from the reference temperature.

In contrast, low comfort occupants' bidding price $P_{cb,z}^t$ is significantly lower than P_R^t for most of the occupied hours, which results in a higher positive price difference ($\overline{\Delta P}^t$). The high magnitude of the positive price difference $\overline{\Delta P}^t$ represents a lower thermal comfort requirement (and hence a higher temperature set-point). For the remaining hours, the bidding price can be equal/close to P_R^t to maintain the thermostat at/near the reference temperature set-point. Meanwhile, modest comfort occupants' bidding prices reasonably vary from P_R^t for most of the occupied hours for a moderate temperature variation from the reference temperature set-point. Moreover, in a high/moderate comfort zone $T_{z,max}$ is lower than for a low comfort zone and this suggests that,

in these zones at times of high retail price, the maximum temperature variation is lower than the low comfort zone.

The magnitude of the price difference can be negative, zero and low at times of a low retail price in various zones, however, it increases correspondingly in each zone as the retail price increases and yields a higher positive price difference $\overline{\Delta P}^{t}$. The upper and lower bound of the price difference in each zone is different and can be calculated using (5.31) and (5.32) respectively.

$$\overline{U}_{t,z} = P^{t}_{R(max)} - P^{t}_{cq,z(max)} > 0 \quad (5.31)$$

$$\underline{U}_{t,z} = P^{t}_{R} - P^{t}_{cq,z} \leq 0 \quad (5.32)$$

where $\overline{U}_{t,z}$, $\underline{U}_{t,z}$ are upper and lower bounds of the price difference and $P^{t}_{R(max)}$, $P^{t}_{cq,z(max)}$ are the maximum values of the retail and bidding prices in a zone during occupancy hours. Equation (5.31) implies that, at a time of maximum retail price, the occupants bid the maximum price $P^{t}_{cq,z(max)}$ so that the temperature variation does not exceed the maximum temperature limit $T_{z,max}$ set by the occupants in a zone. This suggests that at the upper bound of the price difference $\overline{U}_{t,z}$, the thermostat is set at $T_{z,max}$ in a zone. Since a high comfort occupant's maximum temperature limit $T_{z,max}$ is lower than for low comfort occupants, they bid considerably higher than other occupants at times of maximum retail price, and thus the value of the upper bound $\overline{U}_{t,z}$ is lower in the high comfort zone than in the low comfort zone.

The lower bound of the price difference $\underline{U}_{t,z}$ represents the minimum price difference between the retail and bidding prices at time step t when the retail price is low. The value of the lower bound $\underline{U}_{t,z}$ can be negative or zero in high and moderate comfort zones but it is zero in low comfort zones to approach the minimum temperature limit $T_{z,min}$ that is less than/equal to the reference temperature

$T_{z,ref}$ in high and moderate comfort zones but equal to $T_{z,ref}$ in low comfort zones.

Since the control action of the PBDR strategy is based on the price difference ΔP^t to change the set-point temperature, it is required to calculate the thermostat setting as a function of ΔP^t. To model the relation between the changes in price with the temperature a prediction model with an ANN is used. Initially, the bidding is carried out and the market is cleared at the agreed price. This clearing value is one of the parameters used to predict the change in temperature with the bidding price. The inputs to the ANN are the outside temperature, preferred indoor temperature, the bidding price, retail price, and the agreed price. The output of the network is a relation between the bidding price, retail price, and indoor temperature. Therefore, for n days the number of inputs to the ANN function is 5 × n × 24, which represents the inputs to the training algorithm, and the output is a 1 × n × 24 matrix as shown in Fig. 5.3.

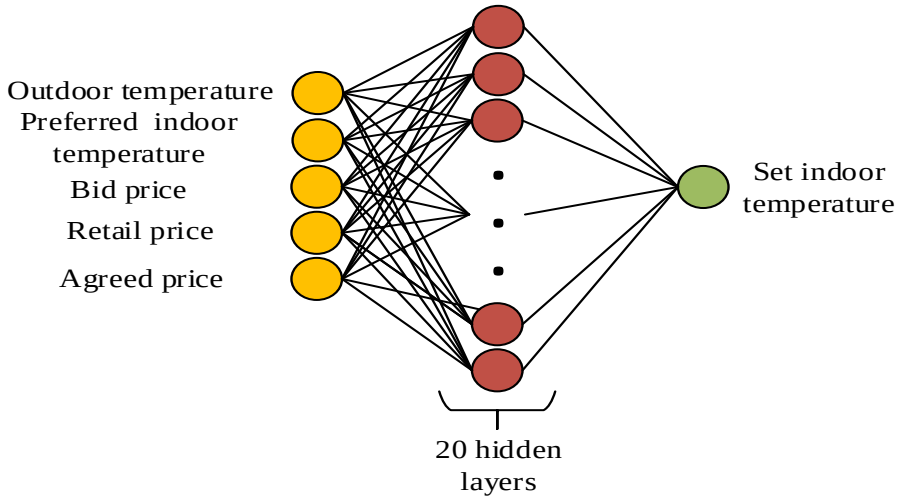

Figure 5.3. The neural network training model

The model was trained with 20 hidden layers and the mean square error was the stopping condition. The training was performed with data for a year, with a resolution of 1 hour, i.e. the data set had a length of 8760. The neural-network model accurately reflected the relationship between the bidding price, retail price and the

thermal behavior of the user at the given weather profiles. Figure 5.4 shows the training, validation and test phases of the machine-learning algorithm, which indicates that the training produces a good fit.

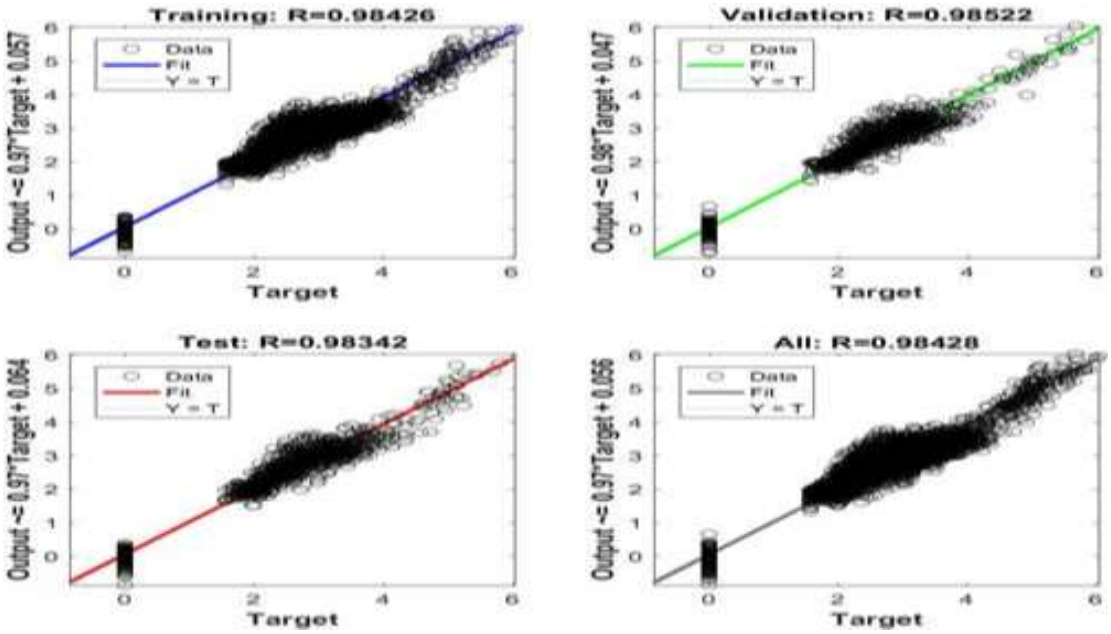

Figure 5.4. Prediction model results based on artificial neural network

A linear regression model is used to represent the ANN prediction model, resulting in the mathematical form

$$\Delta T^t = a\,\Delta P^t + b \tag{5.33}$$

where a and b are linear regression coefficients. Equation (5.33) converts the price difference ΔP^t to the temperature change ΔT^t that the thermostat accepts. The ANN prediction model results in the form of (5.33), implying that 1 ΔP^t, which is equivalent to 0.01 AU$/kWh, results in an increment of 0.25 °C in the thermostat setting to decrease the HVAC load. In other words, four times the price difference ($4\Delta P^t$) is used to increase the thermostat setting by 1°C for energy saving at peak hours. In previous work, when the retail price is much higher than the threshold price, the temperature sharply increases by 2 to 3°C. The sharp rise in temperature is undesirable for the following reasons: 1) it may affect human health through thermal shock; 2) it gives a large

mechanical burden to the heat pump; 3) some customers feel discomfort in a high-temperature difference from the initial set-point when the retail price is higher for an extended period. In this study, considering these drawbacks and the varying thermal preferences of occupants, the temperature change is discretized to a set-point interval a_z^t, which varies from 0.25 to 1°C maximum according to the occupants' choice at each time t. Further the number of price differences (h_z) in each zone for a given time is given by (5.34) and depends on the temperature range and occupants' chosen set-point interval a_z^t.

$$h_z = \frac{T_{z,max} - T_{z,ref}}{a_z^t} + 1 \tag{5.34}$$

The number of price differences h_z is negatively correlated with the set-point interval, being higher in a low set-point interval zone and decreasing with a high set-point interval. This is because with a low set-point interval there are more temperature variations within an occupants' chosen temperature range $[T_{z,max} - T_{z,min}]$ in a zone.

The new set-point temperature T_{sp}^t with a temperature change ΔT^t from the reference temperature at a bidding price $P_{cb,z}^t$ higher, lower or equal to the retail price P_R^t is determined as

$$T_{z,sp}^t\ [C^o] = T_{z,ref} + \Delta T^t \qquad if \quad P_R^t > P_{cb,z}^t = + \Delta P^t \tag{5.35a}$$

$$T_{z,sp}^t\ [C^o] = T_{z,ref} - \Delta T^t \qquad if \quad P_R^t < P_{cb,z}^t = - \Delta P^t \tag{5.35b}$$

$$T_{z,sp}^t\ [C^o] = T_{z,ref} \qquad if \quad P_R^t = P_{cb,z}^t = 0\ \Delta P^t \tag{5.35c}$$

The above equations calculate the new set-point temperature for the thermostat settings according to the temperature change ΔT^t that depends on the price difference ΔP^t. The thermostat set-points are calculated in advance using a 24-hrs ahead forecast half-hourly RTP signal. Equation (5.35a) operates the HVAC system at a

higher temperature than the reference temperature when the electricity retail price is higher, and consequently, the HVAC consumption is reduced. Equation (5.35b) ensures that the HVAC is set to a lower set-point than the reference temperature to make the indoor environment more comfortable for high comfort occupants, when the price of electricity reduces, while equation (5.35c) maintains the indoor temperature at the reference temperature set-point. The new set-point temperature T_{sp}^{t} the range is given as

$$T_{z,min} \leq T_{sp}^{t} \leq T_{z,max} \tag{5.36}$$

Equation (5.36) suggests that the new set-point temperature T_{sp}^{t} should be between the minimum and maximum temperature limits of the zone set by the occupants. The T_{sp}^{t} constraint ensures that the thermal comfort remains within the ASHRAE comfort standard for a trade-off between comfort and energy saving.

Since the objective is to minimize the aggregated HVAC consumption during off-peak and peak times, while maintaining various zones' temperature close to the reference temperature set-point, for optimal scheduling of the HVAC system, it is necessary to calculate the HVAC electricity consumption as a function of the thermostat set-point in a zone. The HVAC model developed in Section 5.2 for a multizone office building is used to calculate the electricity consumption when the indoor temperature is maintained equal to $T_{z,ref}$. Previous thermostat controllers [33][34][35] do not have an HVAC model and thus these controllers cannot calculate how much electricity was consumed by HVAC nor evaluate whether the load was curtailed during off-peak/peak periods compared to normal operation. However, the proposed PBDR controller uses precise HVAC modeling for an accurate DR. The mathematical modeling presented in Section 5.2 is used to develop the HVAC load function for the

PBDR controller. Equation (5.28) calculates the HVAC electricity consumption as a function of the thermostat set-point in a zone.

A multizone building is initially simulated with $T_{z,ref}$ and the simulation results are calculated for each time step t. The change in electricity consumption is then evaluated for the increase and decrease by a_z^t steps from $T_{z,ref}$. The HVAC electricity consumption changes are calculated by subtracting the electricity consumption at the modified set-point from the consumption at the reference temperature set-point for each step. The temperature change ΔT^t that subtracts the indoor temperature from the set-point temperature is denoted by ΔT^t. A linear regression model is used to predict HVAC consumption as a function of ΔT^t during each 30-minute time step as follows:

$$P_h^t = 0.07925\Delta T^t - 0.00291 \quad [kWh/30\ minutes] \tag{5.37}$$

The systematic control strategy is provided in Algorithm 1.

Algorithm 1. PBDR control strategy procedure

for every time t,

1: Take 30-minutes ahead forecast retail electricity price P_R^t.

2: Take input from various zones' occupants

$$P_{cq,z}^t,\ T_{z,min},\ T_{z,max},\ T_{z,ref},\ a_z^t$$

3: Compare P_R^t and $P_{cq,z}^t$ to calculate the price difference ΔP^t in the various zones using (5.29) at each time step t.

4: Evaluate the various zones' occupants' thermal comfort preferences based on the magnitude of the price difference.

5: The upper and lower bounds of the price difference $\overline{U}_{t,z}$, $\underline{U}_{t,z}$ are calculated using (5.31) and (5.32) to examine the price difference range in various zones.

6: Calculate the temperature change ΔT^t as a function of the price difference ΔP^t using (5.33).

7: The number of price differences h_z is calculated using (5.34) that depends on the temperature range and the set-point interval a_z^t in various zones.

8: Calculate the new thermostat set-point T_{sp}^t with a temperature change ΔT^t from the reference temperature $T_{z,ref}$ using (5.35a) ,(5.35b) and (5.35c) depending on the magnitude and polarity of the price difference ΔP^t.

9: Calculate the electricity consumption as a function of temperature change ΔT^t using (5.37).

5.4.1 Additional Functionality of Proposed Controller

The designed PBDR control strategy allows the occupants to bid an electricity price within a range of a minimum $P_{R(min)}^t$ to maximum $P_{R(min)}^t$ retail price based on their preference. However, the occupant's choice of a low bidding price may affect the aggregator profit with wider implementation of the proposed controller. The aggregator uses the RTP structure to purchase electricity from the wholesale market and then sell it to consumers for profit. However, with price fluctuation, a low choice of bidding price $P_{cq,z}^t$ equal to $P_{R(min)}^t$ by multiple consumers for an extended period of time may exceed the aggregator's purchasing cost over a given time horizon and cause a financial loss for it. In this case, the aggregator can impose a restriction on the consumers to choose a low bidding price $P_{cq,z}^t$ greater than the threshold price $(P_{th,z}^t)$ to take part in a DR program. This restriction facilitates the wider implementation of the proposed controller by allowing higher payment for the aggregator to avoid loss when required. This additional functionality paves the way for wider implementation of the proposed controllers. In this study, the threshold price $P_{th,z}^t$ is calculated based on the historical average prices of RTP for a

week. We consider the previous seven days 30-minutes based forecast RTP and calculate the average price. This average price is considered as a threshold price to protect the aggregator utility with wider implementation of the proposed controller.

The threshold price $P_{th,z}^{t}$ can be calculated as

$$P_{th,z}^{t} = \sum_{n=n1}^{n2} \sum_{t=t1}^{t2} \frac{P_{n.t}^{RTP}}{n} \quad (5.38)$$

where t_1, t_2 are the working hours and n_1, n_2 are the number of days selected to calculate the average price of electricity.

5.5. Experimental Setup

In this study, a real office building of Macquarie University located at 50° south latitude in Sydney, Australia is considered. The climate zone of the above-mentioned building is warm temperate. The building's architectural features and thermal parameters are shown in Table 5.1. Thermal parameters are taken from [32] according to the building materials of construction and the Chiller COP is calculated using (6).

Table 5.1. Architectural Features and Thermal Parameters of Building

Building Component/Parameter	Value	Unit
Orientation	S 55°, E 158°	
Zones	5	no.
Rooms	20	no.
People/room	2	no.
Floor Area	595	m^2
Roof, Wall, Window Area/room	30, 20, 5	m^2
Lighting requirement/room	1500	Watts
Occupancy/Lighting Load time	08:00-18:00	hrs.
Time index w	24	hrs
Roof Thermal Transmittance U_r	0.312	$W/m^2.C$
Wall Thermal Transmittance U_w	1.134	$W/m^2.C$
Glass Thermal Transmittance U_g	3.120	$W/m^2.C$
Shading coefficient S_c	0.72	unitless
Coefficient of Performance COP	4.90	unitless
Chiller Efficiency η	86	%

The building envelope consists of five zones (4 exterior and 1 interior) having 20 rooms of equal area. Zones 1, 2, 3 and 4 are in the north (3 office rooms), east (4 office rooms), south (3 office rooms) and west (4 office rooms) directions respectively, while zone 5 is in the center (6 rooms) with no exterior walls as shown in Fig. 5.1(b). Zone 5 consists of four office rooms, one kitchen and a common room with a computer and printing facility. The areas of floor, roof, wall, and window are 6400, 320, 216 and 54 ft^2 respectively. In this work, 8:00 to 18:00 hrs occupancy is assumed for people, with lighting remaining on during this time. Each office room has two persons and two computers, with a lighting requirement of 1500 watts per room. The kitchen has two ovens, a coffee maker, and a dishwasher. The common room includes appliances such as a computer, printer, etc.

The proposed PBDR strategy was tested for the thermal load profile of the test building. The CL requirements for the five zones were calculated using the mathematical modeling developed in Section 5.2, and the HVAC demand is calculated by considering the full and dynamic occupancy pattern in zones. Full occupancy implies that a certain number of occupants are utilizing the workplace at all times during occupancy hours. However, dynamic occupancy implies that occupants are not present at the working place at all times as they may move outside for lunch, a meeting or for any other activity. Thus, sensible and latent heat gains and people CL factors that depend on the number of people in a zone at one time are reduced which consequently reduces the load on the HVAC system. The HVAC demand is highest in case of full occupancy and it reduces as a zones' load is decreased by varying the people load at various time steps as shown in Fig. 5.5.

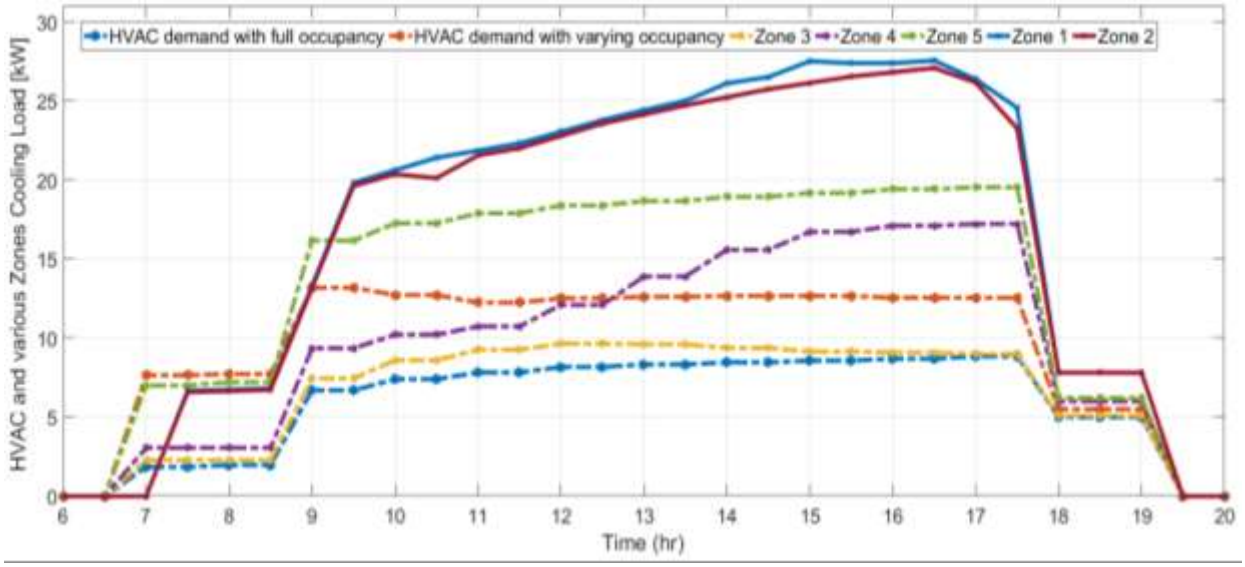

Figure 5.5. Various zones' cooling load and HVAC consumption

Zones 1 to 4 face in a different direction and therefore experience variations in solar radiation at various periods of time. This aspect is more prominent in zone 2 and zone 4 cooling load calculation. Both zones have the same number of rooms with equal loads but different load patterns because of the varying solar radiation load factor according to the zone direction. As zone 2 is in the east direction, so solar radiation is higher than zone 4 for hrs 8 to 12 of occupancy. In contrast, zone 4 solar load is higher than zone 2 for hrs 14 to 18 of occupancy. The cooling load in all zones increases at 8h when people start coming to work and is maintained at high levels until 18h with some fluctuations during occupancy hours. After 18h the load reduces to a low level because people leave the building.

For simulation, zones are categories according to the occupant's thermal comfort preferences as shown in Table 5.2. Since zone 1 and 2 have similar cooling load patterns with high comfort requirements, we assume that both zones have a similar preference in choosing a bidding price, temperature range, and set-point interval. Therefore, we only conduct simulation results for zone 1, assuming that zone 3 has similar results.

Table 5.2. Zones Categorization

Zone No.	Comfort Preferences
Zone 1 and Zone 3	high comfort requirement
Zone 2	medium comfort requirement
Zone 4 and Zone 5	low comfort requirement

Table 5.3 demonstrates the simulation cases for the formulated building model with energy and cost-saving results. The CC represents the HVAC energy consumption at a 23°C fixed cooling set-point temperature with a full occupancy pattern in all zones. The PBDR control strategy demonstrates the proposed algorithm results applied with a time-varying retail price. For the PBDR strategy, the experiment was performed for time-varying bidding prices, temperature ranges and set-point intervals chosen by customers in various zones according to their comfort preferences.

5.6. Results and Discussion

In this section, simulation results are discussed to evaluate the performance of the proposed PBDR controller with variable parameters. HVAC energy consumption and cost-saving results in various zones based on the bidding price are provided. In addition, thermal comfort satisfaction based on the ASHRAE comfort standard [38] with temperature variation in various zones is evaluated.

5.6.1 Occupants' Bidding Price and Thermal Preferences with High Set-Point Interval

To demonstrate the effectiveness of the proposed strategy, firstly, occupants' thermal comfort preferences in the coefficient of the bidding price, and thus the temperature variation based on that bidding price are evaluated with a high set-point interval of 1°C as shown in Figs. 5.6 and 5.7 respectively. The high set-point interval 1°C is chosen to compare the performance with CC, where the thermostat setting is increased/decreased by 1°C based on the outdoor temperature and weather conditions. Figure 5.6 compares

the thermal comfort preferences of occupants in various zones in the coefficient of the bidding price. It shows the 10-h profile of the 0.5-h average retail price, the bidding price and the price difference of the retail and bidding price in various zones.

Figs. 5.6(a)(b) uncover that zone 1 and 2 occupants with high and moderate comfort preferences respectively bid a price higher than the retail price at the start of working hours (i.e., t= 8 to 9h) to maximize their comfort, and for the rest of the working hours, their bidding price is close to the retail price to maintain the desired comfort. This effect is more evident at times of low retail price (i.e., t = 9.5 – 16h) and during that time the price difference is zero in zone 1. Meanwhile, zone 2 reasonably varies the bidding price from the retail price for a low positive price difference. However, when the electricity price significantly increases (i.e., t > 16h), zones 1 and 2 bid the maximum price (i.e., 0.18 and 0.14 $/kWh) to remain within their desired comfort zone, which is 22 to 25°C and 22 to 26°C respectively as shown in Figs. 5.7(a)(b). Even though occupants bid the maximum price at times of highest retail price, it is not very close to the retail price, which results in a noticeable price difference in both zones, and it is higher in zone 2.

Likewise, Figs. 5.6(c)(d) show the bidding price based on the retail price in zones 4 and 5 respectively. These zones with a low comfort requirement bid quite low in response to the retail price for most of the working hours, which results in a high positive price difference. Though both of the zones have a low comfort requirement, the main difference is that the zone 5 maximum bidding price (maximum temperature limit) is lower (higher) than zone 4. This implies that at times of high retail price zone 5 occupants have high a positive price difference compared to zone 4 (i.e., t 16 to 18 h). Overall, different zones' bidding price comparison reveals that as occupants' comfort requirement reduces they allow frequent changes in temperature setting by considerably varying

the bid price from the retail price, which results in a high positive price difference, specifically at times of a high retail price.

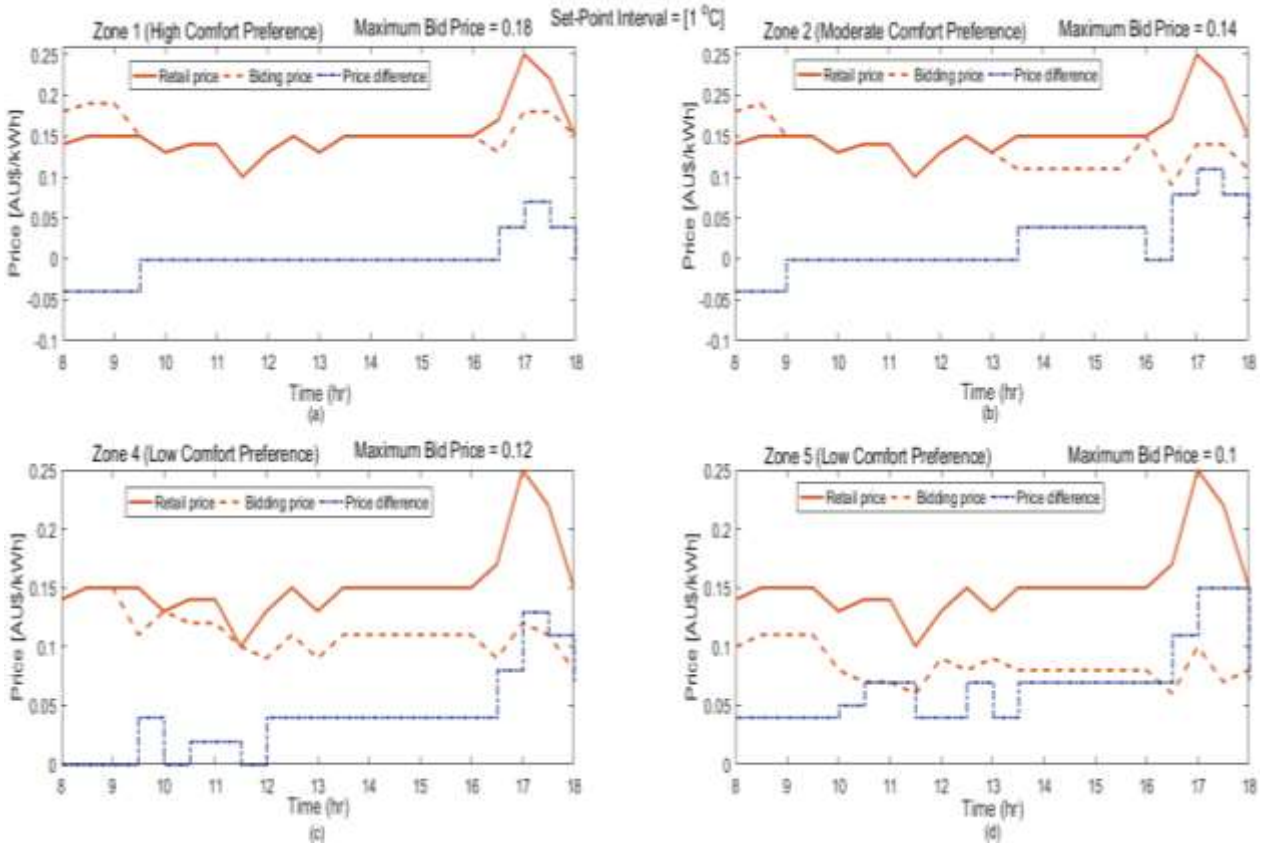

Figure 5.6. Bidding Price and price difference in various zones at a set-point interval of 1°C

Figure 5.7 compares the temperature variation in various zones in response to price differences as shown in Fig. 5.6. It shows the 10-h profile of the 0.5-h average retail price and temperature variation in various zones. The temperature variation is the temperature difference between the reference temperature and the modified temperature in response to the bidding price. For example, a 3°C variation means that the modified temperature is 3°C higher than the reference temperature. However, the temperature does not abruptly vary from the reference temperature in the one-time step because of the set-point interval of 1°C chosen by the occupants of all zones. The set-point interval of 1°C indicates that at each time step the temperature variation from the previous set-point is limited to 1°C.

Figs. 5.7(a)(b) reveal that in zones 1 and 2 the thermostat set-point is reduced from the reference temperature by -1°C for t= 8 to 9h and the modified set-point is calculated using (5.35b). This is because, in these zones for the mentioned price, occupants' bidding price is higher than the retail price as shown in Figs. 5.6(a)(b), which results in a negative price difference using (5.30), and consequently the temperature is reduced. These occupants prefer to decrease the cooling set-point at the start of the working hours to maintain the thermal zone at a comfortable level for the time ahead when the temperature may increase considerably in response to a high retail price. In zones 1 and 2, the temperature variation is 0 to 1°C at times of low retail price, however, it increases up to 2 and 3°C respectively based on the price difference when the retail price significantly increases (i.e., t= 17h).

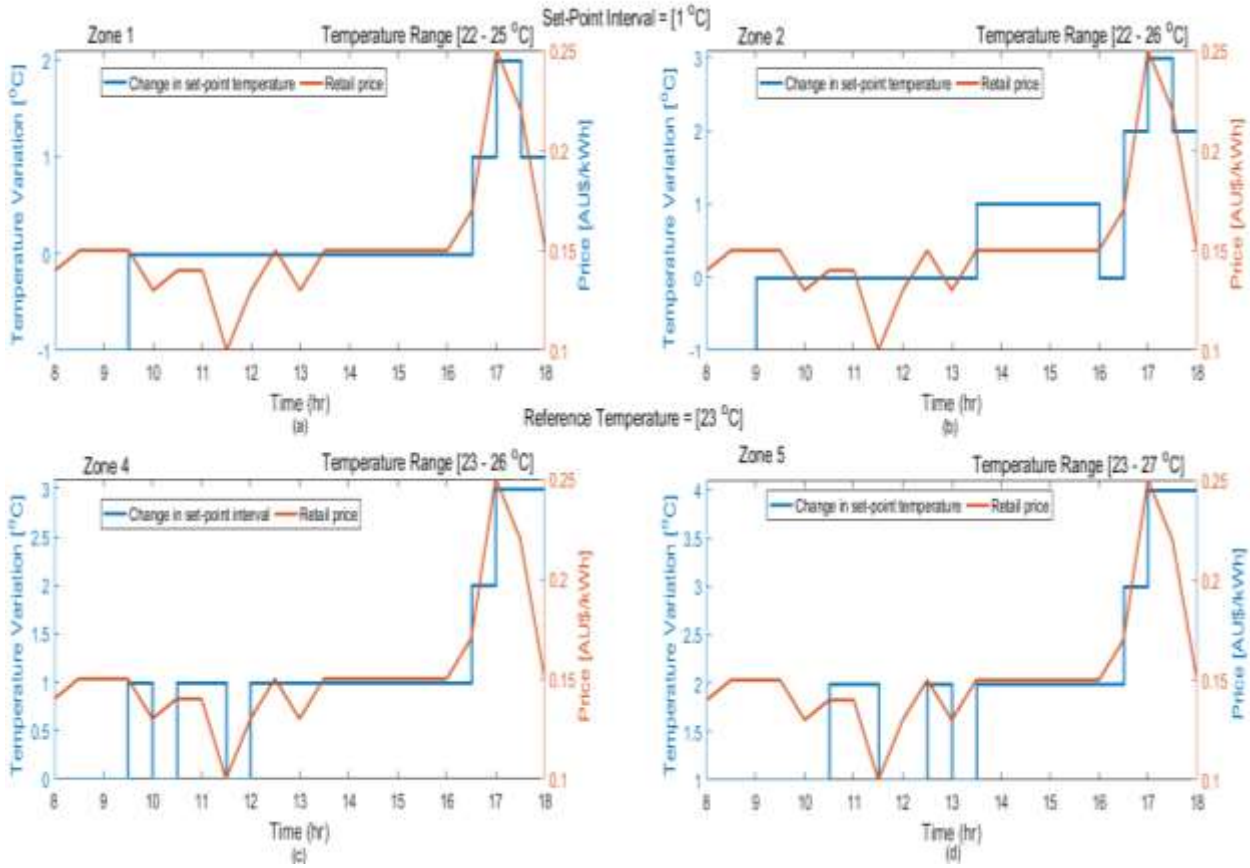

Figure 5.7. Temperature variation in various zones as a function of bidding price at a set-point interval of 1°C

In zones 4 and 5, based on the price difference, the zone temperature fluctuates throughout the time period, however, temperature variations are more frequent and higher in zone 5 because of the high positive price difference compared to zone 4 as shown in Figs. 5.7(c)(d). This suggests that zone 5 occupants' maximum temperature limit is higher than in zone 4 for time steps when the retail price climbs for a trade-off between comfort and cost-saving.

5.6.2 Occupants' Bidding Price and Thermal Preferences with Lower Set-Point Interval

Here, the simulation results are obtained with similar parameter settings as in the previous case but with the low set-point interval of 0.25°C. These results provide insight into the set-point interval's effect on the bidding price and consequently the temperature variation in various zones. Figure 5.8, in comparison with Fig. 5.7, reveals that the temperature changes more frequently in various zones with a set-point interval of 0.25°C during simulation hours. This is because the occupants in various zones do not prefer high-temperature changes for energy saving in response to the retail price; therefore, they prefer to maintain a constant thermostat setting until the price remains within a certain limit as shown in Fig. 5.8. However, with a low set-point interval the occupants have an opportunity to change their comfort preferences following the retail price with low-temperature changes that have a minimal impact on human comfort.

The high and low set-point interval effect on the bidding price and thus on temperature variations is more evident in zone 1, which has a high comfort preference as shown in Figs. 5.6(a) and 5.8(a). That comparison reveals that in zone 1 the bidding price is higher with a set-point interval of 1°C than with 0.25°C (i.e., t = 9 to 16h) to avoid high-temperature changes from the reference set-point. A similar effect can be observed in other zones, for

instance, in zone 5 for t= 13.5 to 16.5h the thermostat setting remains constant with a set-point interval of 1°C, however, it constantly changes with a 0.25°C set-point interval for the same time. The results shown in Figs. 5.8(c)(d) indicates that the design algorithm overcomes the group level presentation of an occupant's thermal comfort in a multizone building and changes the thermostat setting in various zones in the coefficient of the bidding price. In addition, the proposed strategy takes into account the preferred set-point interval of the occupants in each zone to cater to the varying preferences about temperature changes.

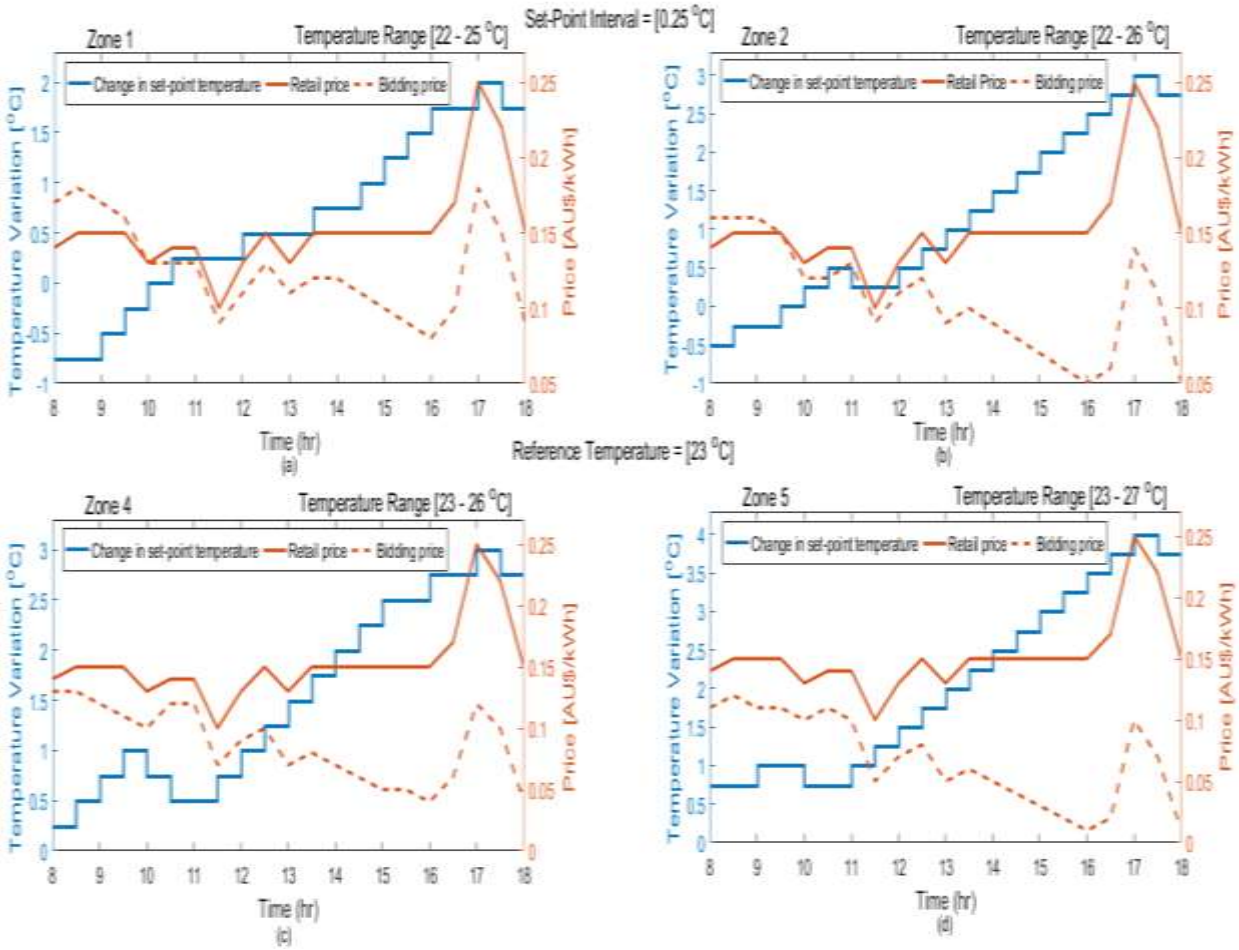

Figure 5.8. Bidding price and temperature variation in various zones at a set-point interval of 0.25°C

5.6.3 Comparison of Bidding Price and Price Difference in two Zones at various Set-Point Intervals

In this part, the relationship between the total bidding price, the price difference, and the set-point interval are examined. The occupants' total bidding price and the price difference during the simulation hours at various set-point intervals are calculated in two chosen zones. Zones 1 and 5 are selected because they represent two extremes, high and low comfort preference zones respectively. Figure 5.9 compares the aggregated bidding price and the price difference in zones 1 and 5 at three different set-point intervals 0.25, 0.5 and 1°C, and further, it shows a comparison between the aggregated electricity cost with CC and bidding price. The results reported here indicate that the occupants' aggregated bidding price is positively correlated with the set-point interval, and it is significantly higher in high comfort zones compared to low comfort zones. For instance, the aggregated bidding price increases from 2.65 to 3.17 and 1.42 to 1.76 AU$/kWh in zones 1 and 5 respectively, with changes in the set-point interval from 0.25 to 1°C. This shows a 16.4 and 19.1% reduction in electricity cost per kWh with changes in the set-point interval from 1 to 0.25°C for zones 1 and 5 respectively.

From these results, it can be further inferred that, with the proposed strategy, high and low comfort occupants can save 0.94 to 17.1% and 45.0 to 55.6% on the electricity cost per kWh with set-point intervals of 1 to 0.25°C respectively compared to CC. On the other hand, the price difference is negatively correlated with the set-point interval because a higher bidding price in a zone leads to a lower positive price difference. For instance, the price difference in zone 5 decreases from 1.78 to 1.69 AU$/kWh with a change in the set-point interval from 0.25 to 0.5°C.

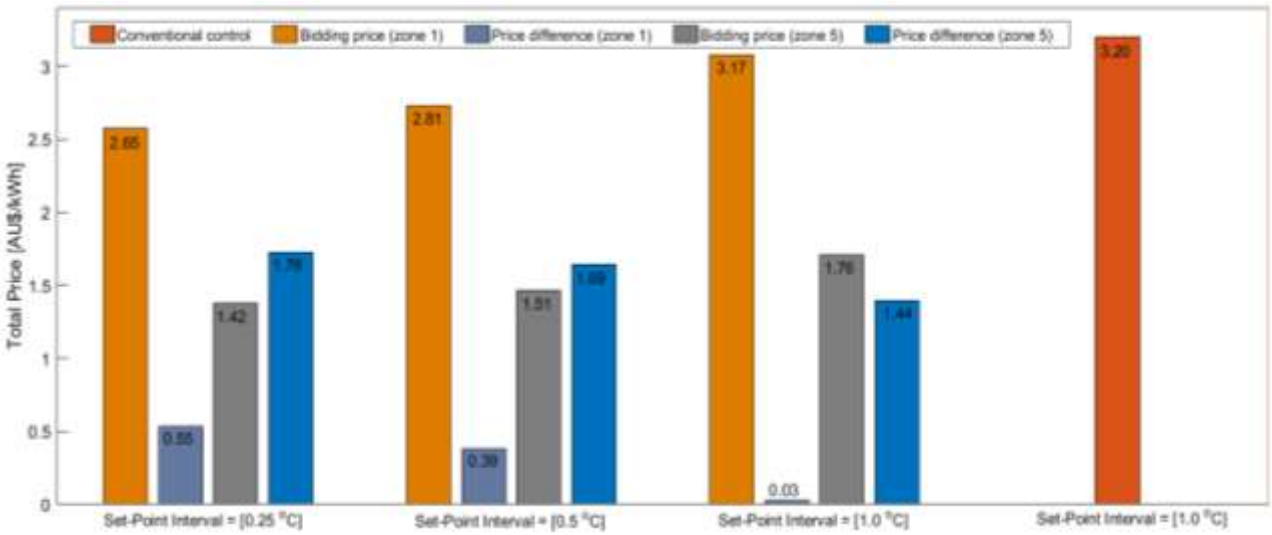

Figure 5.9. Aggregated bidding price and price difference at various set-point intervals

5.6.4 Effect of various Set-Point Intervals on HVAC Consumption in various Zones

Figure 5.10 shows the effect of temperature variations in various zones on the HVAC energy consumption evaluated at two set-point intervals, and further compares the HVAC demand with conventional and PBDR control strategies. In CC, the HVAC is operated to maintain a reference temperature (23°C) in a multizone building for t= 8 to 18h regardless of the retail price. In contrast, the PBDR control strategy causes a regular change in the HVAC thermostat setting in various zones based on the electricity price. The simulation results show that the HVAC load in various zones is curtailed compared to CC, with temperature variations for energy and cost-saving. The HVAC demand at a constant reference temperature and at variable temperature set-points are subtracted for 8h ≤ t ≤ 18h to calculate the energy saving in various zones.

It is clear from Fig. 5.10 that the HVAC demand with CC is higher in all zones than the PBDR control strategy except for t= 8 to 9h in zones 1 and 2, where the occupants bid higher than the retail price to decrease the cooling set-point from the reference temperature. The case study results reveal that at both set-point

intervals the energy consumption in low comfort zones (i.e., zones 4 and 5) is significantly lower than in the moderate and high comfort zones following high-temperature variations in these zones. However, at a lower set-point interval the HVAC operation constantly changes and causes an additional reduction in HVAC consumption, specifically in peak hours (i.e., 15h ≤ t ≤ 17.5h) compared to the case with a higher set-point interval. This indicates that with similar parameter settings the designed controller with a low set-point interval causes more reduction in HVAC demand than with a higher set-point interval.

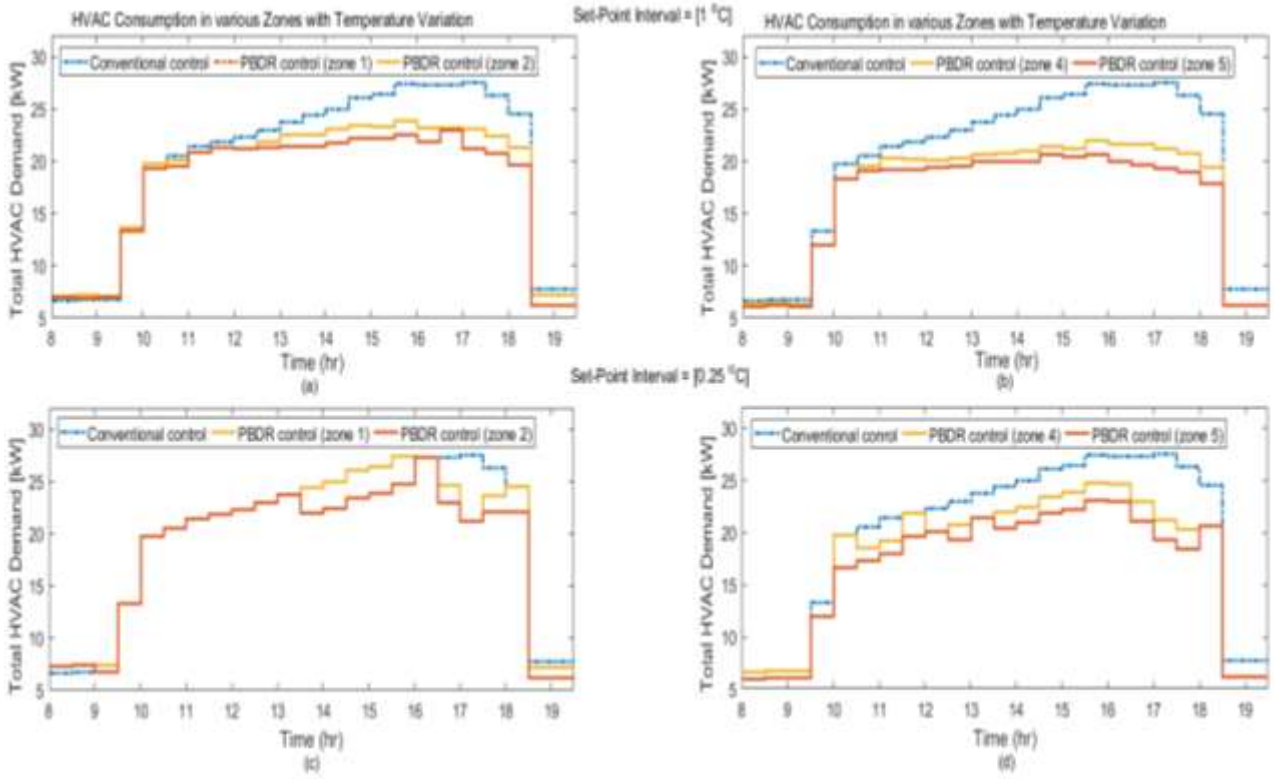

Figure 5.10. Significant reduction in HVAC energy consumption with PBDR controller in various zones at two set-point intervals

5.6.5 Comparison of HVAC Energy and Cost Saving in various Zones

Table 5.3 provides a comparison of the percentage of HVAC energy and cost savings under conventional and PBDR control. The saving results at a higher set-point interval with the PBDR strategy is compared with CC; further, the higher and lower set-point interval

results with the PBDR controller are evaluated. The proposed controller allocates the variable temperature set-points in various zones for each half-hour of the day that is used as thermostat set-points to control the HVAC load with the retail price. The results reported in Table 5.3 suggest that the designed algorithm operates effectively to reduce the aggregated peak demand, off-peak demand, and electricity cost during off-peak and peak times, considering the comfort requirement of various types of occupants. For instance, zone 1 occupants with high comfort requirements can reduce the HVAC demand by 2.15 and 7.19% during off-peak and peak times respectively, compared to CC with a set-point interval of 1^{o}C. This energy-saving corresponds to 3.36 and 8.90% curtailments in electricity cost with indoor temperature variations for only a tiny fraction of the given time. These occupants' energy and cost savings are 14.34 and 14.55% respectively during peak times with a 0.25^{o}C set-point interval that is 43.0% higher than for a 1^{o}C set-point interval.

These saving results indicate that the proposed strategy with low-temperature changes is very effective to save energy and cost with minimal effect on human health. It is clear from Table 5.3 that the aggregated demand of the HVAC system is significantly lower with the proposed strategy than with CC. For example, the aggregated demand with CC is 449.04 kWh during occupancy hours that is reduced to 412.8 and 362.9 kWh in high to low comfort zones (i.e., zones 1 and 5) respectively with the designed controller operating at high set-point intervals. This corresponds to 8.06 to 19.17% curtailment in the HVAC demand during the simulation hours compared to CC.

Similarly, peak saving results are achieved in various zones with the developed strategy. For instance, the peak demand reduces from 162.66 kWh to 139.33, 131.74, 128.49 and 118.99 kWh in zones 1, 2, 4 and 5 respectively with a 0.25°C set-point interval, corresponding to 14.55, 19.45, 21.21 and 27.24% reductions in the electricity bill compared to CC. These results indicate that the PBDR controller is very effective in reducing the electricity cost, specifically during peak hours when the energy price is higher.

Table 5.3. Comparison of Aggregated Daily Energy and Cost Saving for Base Case and Case 1

HVAC Control	Zone	Temp Range	Set-Point Interval	HVAC Demand Off-Peak Hours	HVAC Demand Peak Hours	Energy Cost Off-Peak Hours	Energy Cost Peak Hours	Energy Saving Off-Peak Hours	Energy Saving Peak Hours	Cost Saving Off-Peak Hours	Cost Saving Peak Hours
	No.	°C	°C	kWh	kWh	AU$	AU$	%	%	%	%
Conventional		23	1.0	449.04	162.66	69.61	29.55	---	---	---	---
PBDR Controller	Zone 1	22-25	1.0	439.35	150.95	67.27	26.92	2.15	7.19	3.36	8.90
			0.25	412.8	139.33	63.45	25.25	8.06	14.34	8.84	14.55
	Zone 2	22-26	1.0	417.30	139.59	63.82	25.07	7.06	14.18	8.31	15.16
			0.25	395.92	131.74	60.65	23.80	11.80	19.09	12.87	19.45
	Zone 4	23-26	1.0	400.20	137.74	61.27	24.66	10.87	15.32	11.98	16.54
			0.25	381.7	128.49	58.61	23.28	14.98	21.07	15.80	21.21
	Zone 5	23-27	1.0	373.82	127.17	57.2	22.72	16.75	21.81	17.82	23.11
			0.25	362.9	118.99	55.49	21.50	19.17	26.84	20.27	27.24

5.7. Thermal Comfort

The proposed PBDR controller, along with energy and cost savings, can potentially introduce thermal discomfort due to the constant change of the thermostat set-points in various zones based on the retail price. Thus, it is essential to evaluate the performance of the proposed strategy with respect to acceptable thermal environmental conditions for human occupancy. For this ASHRAE standard 55 [254], that establishes the range of indoor environmental conditions to achieve acceptable thermal comfort for occupants, is followed. As per the ASHRAE standard, to maintain thermal comfort the humidity ratio should be ≤ 12 moisture/kilogram of dry air and the dew point temperature < 18°C.

Figure 5.11 shows the comfort zone of the test building in summer drawn on a psychometric chart with a metabolic rate of 1.2 met and clothing insolation of 0.6 clo according to the considered building-working environment. The green line indicates the upper limit of the dew point temperature, while the orange line represents the maximum allowable humidity ratio. The comfort zone shows the indoor temperature variation in various zones in response to the retail price. Figure 5.11 results indicate that the indoor temperature variations are within the comfort zone. This implies that under PBDR control occupants can enjoy significant cost saving with temperature variations in various zones within the ASHRAE comfort zone.

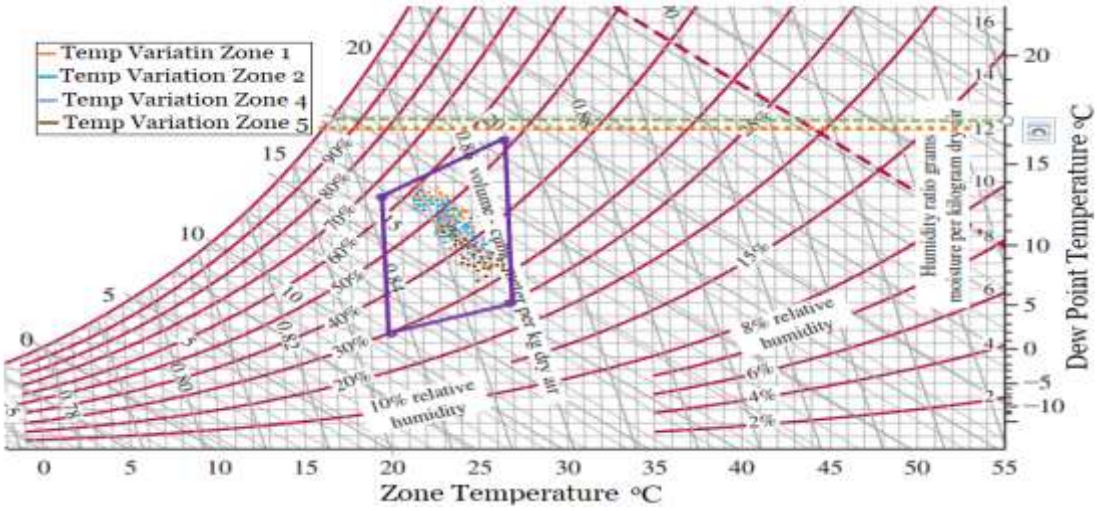

Figure 5.11. Comfort zone for a commercial building in the summer season

Figure 5.12 provides the percentage of time when the zone temperature is more than the reference temperature at two set-point intervals for the simulation hours. The case study results report that, for customers with high comfort preferences, the indoor temperature stays at 23°C for 71.4% of the occupancy hours. For these customers, temperature excursions of -1, +1 and +2°C from the reference temperature (23°C) occur in 14.2, 9.50 and 4.76% of the occupied hours respectively with a set-point interval of 1°C.

Similarly, in zones 4 and 5, +2 and +3°C excursions occur around 57.4 and 52.38% of the occupied time respectively. Meanwhile, zone 2, with a moderate comfort requirement, is +1 and +2°C away from the reference temperature for 33.3% and 9.50% of the occupancy hours respectively. Similar temperature variation patterns with more fluctuations occur at a set-point interval of 0.25°C. For instance, occupants with a low comfort requirement in zone 5 maintain the thermostat setting between 23-24°C and 24-25°C for 28.57% and 19.05% of the occupancy time, while a 4°C excursion occurs only for 4.76% of the occupied hours. It should be noted that the customer preferences for the comfort required are stringently maintained by the proposed strategy. The thermal comfort, therefore, is not overly disturbed through the implementation of the proposed PBDR strategy.

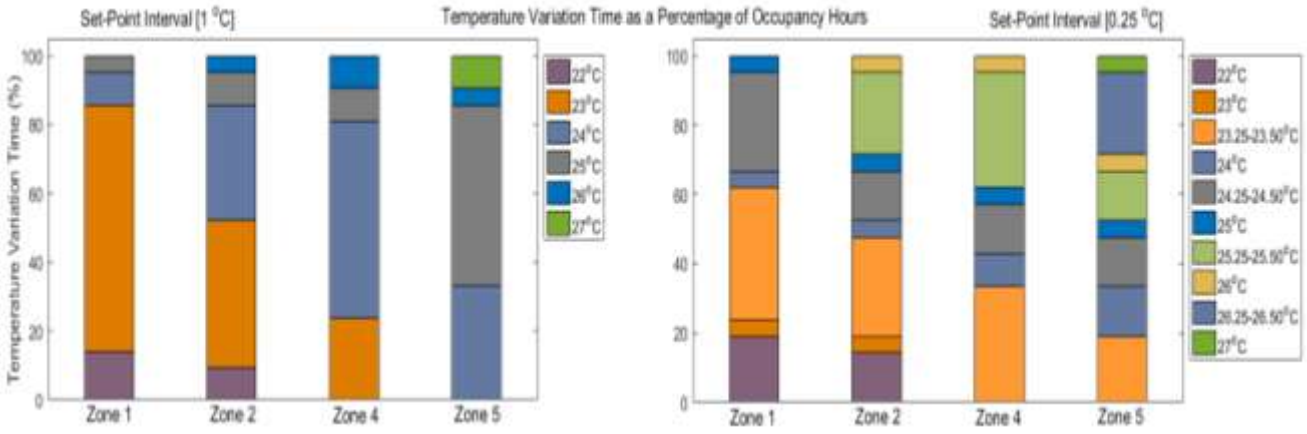

Figure 5.12. Percentage of time when the indoor temperature is below/above the reference temperature

5.8. Chapter Summary

In this Chapter, an easily deployable and improved PBDR control strategy in a real-time environment is proposed for a commercial building HVAC system. The experimental results indicate that the proposed technique brings significant peak load curtailments of 7.19 to 21.7% and 14.34 to 26.84% for high to low comfort occupants at 1 and 0.25°C set-point intervals respectively. This implies an 8.91 to 21.21% and 14.55 to 27.24% saving on a peak electricity

bill correspondingly. In addition, the indoor air temperature is mostly maintained inside the thermal comfort zone. For customers with lower comfort preferences of about 4.76% to 9.50% of the total hours of occupancy, the temperature becomes +3 and +4 °C higher than the reference temperature. This implies that, when the thermostat is varied during periods of high electricity price, the developed strategy does not cause a noteworthy change in the thermal discomfort.

The obtained results through extensive simulation studies under various conditions demonstrate the effectiveness and applicability of the proposed strategy. In contrast to conventional strategies, where a group level presentation of occupants' thermal comfort in a multizone building is implemented, the developed PBDR controller successfully reflects the varying thermal preferences of the occupants for optimal scheduling of the HVAC operation. For utilities and RERs integrated building operators, a real-time wholesale price based tariff is effective to reduce the peak load, the overall electricity consumption, and energy imbalance management. This may assist utilities in avoiding the cost of constructing additional power plants and transmission lines, with associated maintenance. The PBDR control procedure allows consumers to successfully take advantage of dynamic pricing and enjoy substantial cost savings in electricity usage. Alternatively, this plan can contribute greatly in facilitating an effective DR framework, enabling the utility provider to adopt effective demand management policies using RTP.

Chapter 6

Conclusion and Future Work

This thesis seeks to bring the possible advantages of an optimal demand-side management system by modeling the energy usage behavior of self-interested distributed entities in a smart grid. This research has studied the propriety distributed energy resources (DERs) and consumers in a smart grid and has proposed novel energy management schemes for optimal utilization of renewable energy resources (RERs) and improving the building's energy efficiency. General concluding remarks of this dissertation and research directions for the future are provided below.

6.1. Thesis Conclusions

This thesis has discussed the prospects and challenges of modeling the energy usage behavior of distributed entities in a smart grid. In order to accomplish this, novel demand-side management (DSM) strategies are proposed for local power management and control with renewables. The main purpose of the case studies

presented in this dissertation is to assess the performance of the developed algorithms and control strategies. However, an extensive literature survey is carried out before applying the proposed techniques in simulation results. The survey is composed of the state-of-the-art of the prospects and feasibilities of smart grid and microgrid, DERs applications in microgrids and DSM techniques. This comprehensive and structured literature review is presented in **Chapter 2**.

New cost-effective coordinated measures, technologies and control techniques for improving the smart buildings' energy performance are presented in **Chapter 3**. Real-time data monitoring and analysis results show that the performance of the smart building is influenced by the number of factors including low PV production, inefficient building operation and traditional control of building's responsive loads. As a result, advanced technologies (e.g. efficient invertors, dual-axis tracking system, and MOSFETs) and control strategies (e.g. transactive control and an efficient controller) are proposed for improving the PV production and saving energy and cost by controlling thermostatic loads respectively. Scientific analysis under real PV system parameters and commercial load are carried out to demonstrate the effectiveness of the proposed technologies and techniques. It is evident from the critical analyses of the case studies that the proposed approaches ensure stable islanded operation of smart buildings in terms of asset utilization, efficient energy management, and cost-effectiveness.

Research challenges associated with making energy consumers an integral part of energy management schemes in a smart grid while respecting their privacy are considered in **Chapter 4**. A mathematical model based on a non-cooperative contract-theoretic approach is developed to capture the complex interactions between an aggregator and geographically distributed electricity

suppliers. Further, a novel dynamic pricing mechanism is designed that an aggregator utilizes to incentivize the electricity suppliers considering various variable factors. Furthermore, a distributed algorithm is presented to characterize the regular distributions of the developed strategy for implementation. The performance of the proposed approach is validated by performing several case studies such as a change in reliability level, wholesale price fluctuations, effects of penalty charges, and aggregator revenue under different trading scenarios.

A simulation benchmark model for a thermally interconnected dynamical commercial heating, ventilation, and air-conditioning (HVAC) system is developed in **Chapter 5**. A novel comfort aware energy imbalance management scheme is presented in the designed system. The potential impacts of time-varying electricity prices on the consumer's thermal requirements are studied. The effects of occupant's choice of bidding price and set-point interval on the HVAC consumption are analyzed. A new price-based demand response controller is designed to control the HVAC thermostat setting in a multi-zone office building. An optimum HVAC scheduling algorithm is proposed for energy and cost savings in response to price signals while providing the desired quality of service. Finally, several case studies such as variable commercial loading in various zones, high and low set-point interval's effect on HVAC consumption, and bidding price variation with pricing are carried out to quantify the performance of the proposed approach.
Overall, the following conclusions can be drawn from this research work:

- Real case studies of smart buildings are crucial to expanding renewable energy deployments by using flexible loads in a business community.

- Large-scale deployment of renewable resources with the aid of the smart grid provides an opportunity for robust DSM through energy efficiency, demand response (DR) and other energy productivity measures.
- Demand management with renewable energy has the potential to utilize the consumers' capacity as a flexible load with the integration of renewable energy in order to develop a cost-efficient demand-side flexibility system. In a developed system energy consumers are capable to optimize and control renewable energy, storage system, energy efficiency, and demand-controls.
- Coordinated load control strategies not only effective in providing load balancing services to the smart grid but also has the advantage of the reduction in peak load demand, avoidance of overvoltage events, and overcoming RERs uncertainty at the distribution level.
- In an energy-constrained electricity market, the involvement of consumers in energy management schemes can significantly improve the power network stability, and considerably enhance the social benefit for the whole power system.
- The excess energy of geographically DERs can be traded with an aggregator. This can benefit all parties such as producers, consumers, and utilities.
- The strategic use of RERs with storage technologies can ensure grid stability by avoiding low-value grid export.
- Dynamic pricing as a DSM tool can facilitate peak-load curtailment to avoid large capital investments.
- There is an opportunity for decentralized energy systems in the future for the commercial sector with the integration of renewable energy, load management, and consumer participation.

6.2. Future Research Directions

Most of the work presented in this thesis has the potential for future work, for extending effective demand management schemes in a smart grid to more dynamic scenarios with more complex environments. Moreover, with the increasing RERs and electric vehicles (EVs) penetration, particularly in the Australian Distribution Network, there are several challenges that require further research and developments. The future research directions of this dissertation are summarized below.

- Coordinated measures, new technologies, and transactive control can significantly improve the energy efficiency of smart buildings, as explained in **Chapter 3**. However, RERs efficiency can be further improved by using Nanotechnology-based products for renewable energy. For instance, solar cells' efficiency can be improved by using Nano-structured solar cells. Thus research on Nano-materials for improving storage technologies, conversion systems and renewable resources efficiency is an interesting future direction. Another future direction can be to include multiple players (e.g. autonomous commercial buildings, aggregators, EVs charging stations) in energy management systems where coordination among multiple players is required. In addition, the future aim of this study could be to investigate the cost of PV panels, cooling systems, and solar tracking systems.
- The energy trading scheme with renewables has been discussed in this thesis. This work can be extended to study the more practical scenario where multiple sets of small/medium/large scale producers exist and they compete with each other to sell their electricity. One potential challenge that needs to be addressed to incorporate this scenario is to prioritize the same category and type of

producers to procure energy in the electricity trading market under the circumstances of asymmetric information. Another interesting extension of this work would be to investigate the benefits of the power grid, e.g., the stability of the grid and the reduction in overvoltage events through local power management schemes. Moreover, the local electricity market is quite affected by the other types of energy, such as natural gas, heat/cold supplement, etc. The impact of multi-energy supplement and storage technologies can be included for a more rigorous analysis. The analysis may evaluate the sellers' profit by taking into account multi-energy generation and storage units operational parameters and related costs. In addition, one future direction of this study could be to investigate how state-of-charge of storage units is effected through RERS uncertainty.

- In the context of the comfort-aware energy-imbalance management scheme in a smart grid, as explained in **Chapter 5** of this dissertation, very important future work is to increase the scalability of the proposed approach by including a higher number of HVAC units. Another future direction could be recording the number of occupants in real-time for instantaneous load calculation if a large number of occupants shared one room/commonplace while considering the dynamic comfort preferences in a zone. Moreover, the load recovery effect, which generally appears after limiting the power of HVACs during a DR event period, can be examined for a fairer comparison with existing techniques. Furthermore, a range of electricity tariff systems such as critical peak pricing, extreme day pricing, and critical peak rebates can be included for economic analysis of the demand-management scheme to see the effectiveness of the proposed approach under various scenarios.

- In the developed energy management schemes, the electricity demand is assumed to be known, but the predictions of demand are not that accurate nowadays, especially, when the demand is obtained from the consumers. The uncertainty is still a big problem, therefore, the current work can be extended by considering the uncertainty of demand

Appendix A

Reuse Permissions of the Published Papers for Chapters 3, 4, and 5

Title: Performance analysis of an experimental smart building: Expectations and outcomes

Author: U. Amin,M.J. Hossain,J. Lu,E. Fernandez

Publication: Energy

Publisher: Elsevier

Date: 15 September 2017

Title: Optimal Utilization of Renewable Power Production by Sharing Power among Commercial Buildings: Case Study of Griffith University

Conference Proceedings: 2018 Australasian Universities Power Engineering Conference (AUPEC)

Author: U. Amin

Publisher: IEEE

Date: Nov. 2018

Copyright © 2018, IEEE

Logged in as:
Uzma Amin
Macquarie University
LOGOUT

Thesis / Dissertation Reuse

The IEEE does not require individuals working on a thesis to obtain a formal reuse license, however, you may print out this statement to be used as a permission grant:

Requirements to be followed when using any portion (e.g., figure, graph, table, or textual material) of an IEEE copyrighted paper in a thesis:

1) In the case of textual material (e.g., using short quotes or referring to the work within these papers) users must give full credit to the original source (author, paper, publication) followed by the IEEE copyright line © 2011 IEEE.
2) In the case of illustrations or tabular material, we require that the copyright line © [Year of original publication] IEEE appear prominently with each reprinted figure and/or table.
3) If a substantial portion of the original paper is to be used, and if you are not the senior author, also obtain the senior author's approval.

Requirements to be followed when using an entire IEEE copyrighted paper in a thesis:

1) The following IEEE copyright/ credit notice should be placed prominently in the references: © [year of original publication] IEEE. Reprinted, with permission, from [author names, paper title, IEEE publication title, and month/year of publication]
2) Only the accepted version of an IEEE copyrighted paper can be used when posting the paper or your thesis on-line.
3) In placing the thesis on the author's university website, please display the following message in a prominent place on the website: In reference to IEEE copyrighted material which is used with permission in this thesis, the IEEE does not endorse any of [university/educational entity's name goes here]'s products or services. Internal or personal use of this material is permitted. If interested in reprinting/republishing IEEE copyrighted material for advertising or promotional purposes or for creating new collective works for resale or redistribution, please go to http://www.ieee.org/publications_standards/publications/rights/rights_link.html to learn how to obtain a License from RightsLink.

If applicable, University Microfilms and/or ProQuest Library, or the Archives of Canada may supply single copies of the dissertation.

BACK CLOSE WINDOW

Bibliography

[1] X. Fang, S. Misra, G. Xue, and D. Yang, "Smart Grid — The New and Improved Power Grid: A Survey," IEEE Communications Surveys & Tutorials, vol. 14, pp. 944-980, 2012.

[2] C. Wei, "A Conceptual Framework for Smart Grid," in *2010 Asia-Pacific Power and Energy Engineering Conference*, 2010, pp. 1-4.

[3] J. Lazar and M. McKenzie, "Smart Grids Standards Road Map," Department of Resources, Energy and Tourism, 2012.

[4] International Energy Agency, "Technology Roadmap Smart Grids," 2011. Available: https://www.iea.org/publications/freepublications/publication/smartgrids_roadmap.pdf.

[5] U. S Department of Energy, "The Smart Grid: An Introduction," Communication, vol. 99, p. p. 48, 2010.

[6] Union of Concerned Scientists, (2017, 1 August). Benefits of Renewable Energy Use. Available: https://www.ucsusa.org/clean-energy/renewable-energy/public-benefits-of-renewable-power.

[7] "Energy Aggrement of 29 June 2018," The Danish Government, Social Democracy, The Danish People's Party, The Red-green Alliance, The Alternative, The Social Liberal Party 2018.

[8] REN21, "Renewables 2018-Global Status Report," Paris France, p. 326, 2018.

[9] A. Bari, J. Jiang, W. Saad, and A. Jaekel, "Challenges in the Smart Grid Applications: An Overview," International Journal of Distributed Sensor Networks, vol. 10, p. 974682, February 2014.

[10] Energy Networks Australia and CSIRO, "Electricity Network Transformation Roadmap," 2017.

[11] "Renewable Energy and Load Management," Institute for Sustainable Futures University of Technology Sydney and Australian alliance for Energy Producivity2007.

[12] IEC, "Grid Integration of Large-Capacity Renewable Energy Sources and use of Large-Capacity Electrical Energy Storage," Report, vol. 39, 2009.

[13] "Smart Grids in Distribution Networks: Roadmap Developement and Implementation," International Energy Agency, France2015.

[14] (2019). Green Star: Why Choose Green Star? Available: https://new.gbca.org.au/green-star/.

[15] H. Zhou, T. Bhattacharya, D. Tran, T. S. T. Siew, and A. M. Khambadkone, "Composite Energy Storage System Involving Battery and Ultracapacitor With Dynamic Energy Management in Microgrid Applications," *IEEE Transactions on Power Electronics*, vol. 26, pp. 923-930, 2011.

[16] G. O. Suvire, M. G. Molina, and P. E. Mercado, "Improving the Integration of Wind Power Generation Into AC Microgrids Using Flywheel Energy Storage," *IEEE Transactions on Smart Grid,* vol. 3, pp. 1945-1954, 2012.

[17] A. Pellegrino, V. R. M. L. Verso, L. Blaso, A. Acquaviva, E. Patti, and A. Osello, "Lighting Control and Monitoring for Energy Efficiency: A Case Study Focused on the Interoperability of Building Management Systems," *IEEE Transactions on Industry Applications*, vol. 52, pp. 2627-2637, 2016.

[18] C. Basu, J. J. Caubel, K. Kim, E. Cheng, A. Dhinakaran, A. M. Agogino, et al., "Sensor-Based Predictive Modeling for Smart Lighting in Grid-Integrated Buildings," *IEEE Sensors Journal*, vol. 14, pp. 4216-4229, 2014.

[19] G. Q. Chaudhary, M. Ali, M. M. Mukhtar, U. Khalid, U. Awan, and A. Adeel-ur-Rehamn, "Design optimization and experimental investigation of solar assisted 1 Ton (3.516 KW) vapor absorption air conditioning system," in *2015 Power Generation System and Renewable Energy Technologies (PGSRET)*, 2015, pp. 1-6.

[20] H. Hao, A. Kowli, Y. Lin, P. Barooah, and S. Meyn, "Ancillary service for the grid via control of commercial building HVAC systems," in *2013 American Control Conference*, 2013, pp. 467-472.

[21] M. Maasoumy, C. Rosenberg, A. Sangiovanni-Vincentelli, and D. S. Callaway, "Model predictive control approach to online computation of demand-side flexibility of commercial buildings HVAC systems for Supply Following," in *2014 American Control Conference*, 2014, pp. 1082-1089.

[22] G. Mantovani and L. Ferrarini, "Temperature Control of a Commercial Building With Model Predictive Control Techniques," *IEEE Transactions on Industrial Electronics*, vol. 62, pp. 2651-2660, 2015.

[23] L. Wang, Z. Wang, and R. Yang, "Intelligent Multiagent Control System for Energy and Comfort Management in Smart and Sustainable Buildings," *IEEE Transactions on Smart Grid*, vol. 3, pp. 605-617, 2012.

[24] A. Kumar and G. P. Hancke, "An Energy-Efficient Smart Comfort Sensing System Based on the IEEE 1451 Standard for Green Buildings," *IEEE Sensors Journal*, vol. 14, pp. 4245-4252, 2014.

[25] Z. Li, L. Chen, and G. Nan, "Small-Scale Renewable Energy Source Trading: A Contract Theory Approach," *IEEE Transactions on Industrial Informatics*, vol. 14, pp. 1491-1500, 2018.

[26] B. Zhang, C. Jiang, J. Yu, and Z. Han, "A Contract Game for Direct Energy Trading in Smart Grid," *IEEE Transactions on Smart Grid*, vol. 9, pp. 2873-2884, 2018.

[27] P. M. Ferreira, A. E. Ruano, S. Silva, and E. Z. E. Conceição, "Neural networks based predictive control for thermal comfort and energy savings in public buildings," *Energy and Buildings*, vol. 55, pp. 238-251, December 2012.

[28] L. Ciabattoni, G. Cimini, F. Ferracuti, M. Grisostomi, G. Ippoliti, and M. Pirro, "Indoor thermal comfort control through fuzzy logic PMV optimization," in *2015 International Joint Conference on Neural Networks (IJCNN)*, 2015, pp. 1-6.

[29] State and Local Climate and Energy Program, February, 2015. Available: http://www.epa.gov/statelocalclimate/state/topics/renewable.html.

[30] C.-C. Teng, J.-S. Horng, M.-L. Hu, L.-H. Chien, and Y.-C. Shen, "Developing energy conservation and carbon reduction indicators for the hotel industry in Taiwan," *International Journal of Hospitality Management*, vol. 31, pp. 199-208, March 2012.

[31] X. Dequaire, F. Pacheco Torgal, M. Mistretta, A. Kaklauskas, C. G. Granqvist, and L. F. Cabeza, "A Multiple-Case Study of Passive House Retrofits of School Buildings in Austria," in Nearly Zero Energy Building Refurbishment: A Multidisciplinary Approach, London: Springer London, 2013, pp. 253-278.

[32] H. Bernardo, C. H. Antunes, A. Gaspar, L. D. Pereira, and M. G. da Silva, "An approach for energy performance and indoor climate assessment in a Portuguese school building," *Sustainable Cities and Society*, vol. 30, pp. 184-194, April 2017.

[33] V. Oree, A. Khoodaruth, and H. Teemul, "A case study for the evaluation of realistic energy retrofit strategies for public office buildings in the Southern Hemisphere," *Building Simulation*, vol. 9, pp. 113-125, April 01 2016.

[34] E. Asadi, M. G. da Silva, C. H. Antunes, C. H. Antunes, and L. Dias, "A multi-objective optimization model for building retrofit strategies using TRNSYS simulations, GenOpt and MATLAB," *Building and Environment*, vol. 56, p. 8, 2012.

[35] K. Sun and T. Hong, "A simulation approach to estimate energy savings potential of occupant behavior measures," *Energy and Buildings*, vol. 136, pp. 43-62, February 2017.

[36] A. Baniassadi and D. J. Sailor, "Synergies and trade-offs between energy efficiency and resiliency to extreme heat – A case study," *Building and Environment*, vol. 132, pp. 263-272, March 2018.

[37] J. M Pearce, D. Denkenberger, and H. Zielonka, "Accelerating applied sustainability by utilizing return on investment for energy conservation measures," *International Journal of Energy, Environment and Economics*, vol. 17, p. 11, 2009.

[38] M.-H. Chang, P. Sandborn, M. Pecht, W. K. C. Yung, and W. Wang, "A return on investment analysis of applying health monitoring to LED lighting systems," *Microelectronics Reliability*, vol. 55, pp. 527-537, February 2015.

[39] M. Ferreira, M. Almeida, A. Rodrigues, and S. M. Silva, "Comparing cost-optimal and net-zero energy targets in building retrofit," *Building Research & Information*, vol. 44, pp. 188-201, February 2016.

[40] "Ausgrid, Supply and Demand: our five year network plan," 2011-12.

[41] "ENA Submission to Senate Committee Inquiry on Electricity Prices," Energy Network Association 2012.

[42] W. Wang, Y. Xu, and M. Khanna, "A survey on the communication architectures in smart grid," *Computer Networks*, vol. 55, pp. 3604-3629, October 2011.

[43] U. S. Department of Energy, "Communications Requirements of Smart Grid Technologies," October 2010. Available: https://www.energy.gov/sites/prod/files/gcprod/documents/Smart_Grid_Communications_Requirements_Report_10-05-2010.pdf.

[44] F. Rahimi and A. Ipakchi, "Demand Response as a Market Resource Under the Smart Grid Paradigm," IEEE Transactions on Smart Grid, vol. 1, pp. 82-88, 2010.

[45] Canadian Electricity Association, "The smart grid: a pragmatic approach," 2010. Available: https://electricity.ca/wp-content/uploads/2017/05/SmartGridpaperEN.pdf.

[46] "Enabling Tomorrow s Electricity System. Report of the Ontario Smart Grid Forum," Ontario Smart Grid Forum 2010. Available: http://www.iemo.com/imoweb/pubs/smart_grid/Smart_Grid_Forum-Report.pdf.

[47] C. Greer, D. A. Wollman, D. E. Prochaska, P. A. Boynton, and J. A. Mazer, "NIST Framework and Roadmap for Smart Grid Interoperability Standards, Release 3.0," 2014.

[48] "Federal Energy Regulatory Commission, Smart Grid Policy," 16 July 2009. Available: https://www.ferc.gov/whats-new/comm-meet/2009/071609/E-3.pdf.

[49] V. Giordano, F. Gangale, G. Fulli, M. Sanchez Jimenez, L. Papaioannou, A. Colta, et al., "Smart Grid Projects in Europe - Lessons Learned and Current Developments," *European Commission-JRC Reference Report* 2011.

[50] S. Chowdhury, S. P. Chowdhury, and P. Crossley, Microgrids and Active Distribution Networks. London, United Kingdom: The Institute of Engineering and Technology, 2009.

[51] (2015). Why is Renewable Energy Important. Available: https://www.renewableenergyworld.com/index/tech/why-renewable-energy.html.

[52] (2015). Energy Forum and Types of Renewable Energy Available: https://www.renewableenergyworld.com/index/tech.html.

[53] "UK Renewable Energy Roadmap," Department of Energy and Climate Change 2012. Available: https://assets.publishing.service.gov.uk/government/uploads/system/uploads/attachment_data/file/48128/2167-uk-renewable-energy-roadmap.pdf.

[54] Z. Shuiying, L. Chi, and Q. Liqiong, "Solar Industry Development and Policy Support in China," *Energy Procedia*, vol. 5, pp. 768-773, January 2011.

[55] Z. Jiang and R. A. Dougal, "Hierarchical microgrid paradigm for integration of distributed energy resources," in *2008 IEEE Power and Energy Society General Meeting - Conversion and Delivery of Electrical Energy in the 21st Century*, 2008, pp. 1-8.

[56] N. Mahmud, A. Zahedi, and M. S. Rahman, Control of Renewable Energy Systems. Singapore: Springer 2018.

[57] P. T. Manditereza and R. Bansal, "Renewable distributed generation: The hidden challenges – A review from the protection perspective," *Renewable and Sustainable Energy Reviews*, vol. 58, pp. 1457-1465, May 2016.

[58] A. O. Otuoze, M. W. Mustafa, and R. M. Larik, "Smart grids security challenges: Classification by sources of threats," *Journal of Electrical Systems and Information Technology*, vol. 5, pp. 468-483, December 2018.

[59] Y. Agarwal, T. Weng, and R. K. Gupta, "Understanding the role of buildings in a smart microgrid," in 2011 Design, Automation & Test in Europe, 2011, pp. 1-6.

[60] R. Zamora and A. K. Srivastava, "Controls for microgrids with storage: Review, challenges, and research needs," *Renewable and Sustainable Energy Reviews*, vol. 14, pp. 2009-2018, September 2010.

[61] D. E. Olivares, C. A. Cañizares, and M. Kazerani, "A centralized optimal energy management system for microgrids," in *2011 IEEE Power and Energy Society General Meeting*, 2011, pp. 1-6.

[62] H. Asano and S. Bando, "Load fluctuation analysis of commercial and residential customers for operation planning of a hybrid photovoltaic and cogeneration system," in *2006 IEEE Power Engineering Society General Meeting*, 2006, p. 6 pp.

[63] A. M. Giacomoni, S. Y. Goldsmith, S. M. Amin, and B. F. Wollenberg, "Analysis, modeling, and simulation of autonomous microgrids with a high penetration of renewables," in *2012 IEEE Power and Energy Society General Meeting*, 2012, pp. 1-6.

[64] A. K. Abdelsalam, A. M. Massoud, S. Ahmed, and P. N. Enjeti, "High-Performance Adaptive Perturb and Observe MPPT Technique for Photovoltaic-Based Microgrids," *IEEE Transactions on Power Electronics*, vol. 26, pp. 1010-1021, 2011.

[65] A. Chatterjee and A. Keyhani, "Neural Network Estimation of Microgrid Maximum Solar Power," *IEEE Transactions on Smart Grid*, vol. 3, pp. 1860-1866, 2012.

[66] D. Quiggin, S. Cornell, M. Tierney, and R. Buswell, "A simulation and optimisation study: Towards a decentralised microgrid, using real world fluctuation data," Energy, vol. 41, pp. 549-559, May 2012.

[67] Unleashing the Power of Energy Storage. Available: http://energystorage.org/energy-storage.

[68] X. Tan, Q. Li, and H. Wang, "Advances and trends of energy storage technology in Microgrid," **International Journal of Electrical Power & Energy Systems**, vol. 44, pp. 179-191, January 2013.

[69] Z. Xu, X. Guan, Q. Jia, J. Wu, D. Wang, and S. Chen, "Performance Analysis and Comparison on Energy Storage Devices for Smart Building Energy Management," *IEEE Transactions on Smart Grid*, vol. 3, pp. 2136-2147, 2012.

[70] B. H. Chowdhury, H. T. Ma, and N. Ardeshna, "The challenge of operating wind power plants within a microgrid framework," in *2010 Power and Energy Conference At Illinois (PECI)*, 2010, pp. 93-98.

[71] J. M. Guerrero, M. Chandorkar, T. Lee, and P. C. Loh, "Advanced Control Architectures for Intelligent Microgrids—Part I: Decentralized and Hierarchical Control," *IEEE Transactions on Industrial Electronics*, vol. 60, pp. 1254-1262, 2013.

[72] H. Mahmood and J. Jiang, "Modeling and Control System Design of a Grid Connected VSC Considering the Effect of the Interface Transformer Type," *IEEE Transactions on Smart Grid*, vol. 3, pp. 122-134, 2012.

[73] X. Fan and G. Gong, "Security challenges in smart-grid metering and control systems," *Technology Innovation Management Review*, 2013.

[74] M. Daoud and X. Fernando, "On the Communication Requirements for the Smart Grid," *Energy and Power Engineering*, vol. 3, pp. 53-60, 2011.

[75] A. R. Metke and R. L. Ekl, "Security Technology for Smart Grid Networks," *IEEE Transactions on Smart Grid*, vol. 1, pp. 99-107, 2010.

[76] C. Efthymiou and G. Kalogridis, "Smart Grid Privacy via Anonymization of Smart Metering Data," in *2010 First IEEE International Conference on Smart Grid Communications*, 2010, pp. 238-243.

[77] A. Rial and G. Danezis, "Privacy-preserving smart metering," Chicago, USA, 2011.

[78] F. Li, B. Luo, and P. Liu, "Secure Information Aggregation for Smart Grids Using Homomorphic Encryption," in *2010 First IEEE International Conference on Smart Grid Communications*, 2010, pp. 327-332.

[79] H. Son, T. Y. Kang, H. Kim, and J. H. Roh, "A Secure Framework for Protecting Customer Collaboration in Intelligent Power Grids," *IEEE Transactions on Smart Grid*, vol. 2, pp. 759-769, 2011.

[80] A. Llaria, O. Curea, J. Jiménez, and H. Camblong, "Survey on microgrids: Unplanned islanding and related inverter control techniques," *Renewable Energy*, vol. 36, pp. 2052-2061, August 2011.

[81] (2017). Demand Response and Demand Side Management What's the Difference? Available: http://www.energyadvantage.com/blog/demand-response-demand-side-management-whats-difference/.

[82] C. W. Gellings, "The concept of demand-side management for electric utilities," *Proceedings of the IEEE*, vol. 73, pp. 1468-1470, 1985.

[83] W. Prindle and M. Koszalka, Smart Grid: Integrating Renewable, Distributed and Efficient Energy: Academia Press, 2011.

[84] (2015). What is Demand-side Management (DSM)? Available: https://www.ema.gov.sg/Demand_Side_Management.aspx.

[85] W. E. Liu, K. Liu, and D. Pearson, "Consumer-centric smart grid," in ISGT 2011, 2011, pp. 1-6.

[86] What is energy efficiency? Available: https://www.ovoenergy.com/guides/energy-guides/what-is-energy-efficiency.html.

[87] (2019). Energy productivity and energy efficiency. Available: https://www.energy.gov.au/government-priorities/energy-productivity-and-energy-efficiency.

[88] Zero Emissions Beyond, "Zero Carbon Australia Building Plan," Melbourn: Scribe 2013. Available: *https://bze.org.au/wp-content/uploads/buildings-plan-bze-report-2013.pdf*.

[89] Beyond Zero Emissions, "Zero Carbon Australia Stationary Energy Plan," A Research Collaboration, The University of Melbourne and Energy Research Institute, 2010. Available: http://media.bze.org.au/ZCA2020_Stationary_Energy_Report_v1.pdf.

[90] L. Zheng and J. Lai, "Environmental and economic evaluations of building energy retrofits: Case study of a commercial building," *Building and Environment*, vol. 145, pp. 14-23, November 2018.

[91] S. Chen, J. Guan, M. D. Levine, L. Haiying, and P. Yowargana, "Evaluation on Retrofit of One Existing Residential Building in North China: Energy Saving, Environmental and Economic Benefits," *Procedia Engineering*, vol. 121, pp. 3-10, January 2015.

[92] F. E. Boafo, J.-G. Ahn, S.-M. Kim, J.-H. Kim, and J.-T. Kim, "Fenestration refurbishment of an educational building: Experimental and numerical evaluation of daylight, thermal and building energy performance," *Journal of Building Engineering*, vol. 25, p. 100803, September 2019.

[93] B. Nicolae and B. George-Vlad, "Life cycle analysis in refurbishment of the buildings as intervention practices in energy saving," *Energy and Buildings*, vol. 86, pp. 74-85, January 2015.

[94] D. Jareemit and B. Limmeechokchai, "Influence of Changing Behavior and High Efficient Appliances on Household Energy Consumption in Thailand," *Energy Procedia*, vol. 138, pp. 241-246, October 2017.

[95] K. Mizobuchi and K. Takeuchi, "Replacement or additional purchase: The impact of energy-efficient appliances on household electricity saving under public pressures," *Energy Policy*, vol. 93, pp. 137-148, June 2016.

[96] A. Garg, J. Maheshwari, P. R. Shukla, and R. Rawal, "Energy appliance transformation in commercial buildings in India under alternate policy scenarios," *Energy*, vol. 140, pp. 952-965, December 2017.

[97] C. Boomsma, R. V. Jones, S. Pahl, and A. Fuertes, "Do psychological factors relate to energy saving behaviours in inefficient and damp homes? A study among English social housing residents," *Energy Research & Social Science*, vol. 47, pp. 146-155, Janaury 2019.

[98] I. E. Agency, "Transition to Sustainable Buildings: strategies and opportunities to 2050," Paris 2013. Available: https://www.iea.org/publications/freepublications/publication/Building2013_free.pdf.

[99] S. Pless and P. Torcellini, "Net-Zero Energy Buildings : A Classification System Based on Renewable Energy Supply Options," 2010.

[100] M. Pilz and L. Al-Fagih, "Game-Theoretic Approaches to Energy Trading: A Survey," CoRR, vol. abs/1702.02915, February 2017.

[101] F. Wei, J. Q. Liu, Z. H. Yang, and F. Ni, "A game theoretic approach for distributed energy trading in district energy networks," in *2017 IEEE Conference on Energy Internet and Energy System Integration (EI2)*, 2017, pp. 1-6.

[102] (2018, 15 February). Why is energy trading important Available: https://hackernoon.com/why-is-energy-trading-important-73b62469c3d7.

[103] C. Lin, D. Deng, C. Kuo, and Y. Liang, "Optimal Charging Control of Energy Storage and Electric Vehicle of an Individual in the Internet of Energy With Energy Trading," *IEEE Transactions on Industrial Informatics*, vol. 14, pp. 2570-2578, 2018.

[104] S. Maharjan, Q. Zhu, Y. Zhang, S. Gjessing, and T. Basar, "Dependable Demand Response Management in the Smart Grid: A Stackelberg Game Approach," *IEEE Transactions on Smart Grid*, vol. 4, pp. 120-132, 2013.

[105] W. Saad, Z. Han, H. V. Poor, and T. Basar, "Game-Theoretic Methods for the Smart Grid: An Overview of Microgrid Systems, Demand-Side Management, and Smart Grid Communications," *IEEE Signal Processing Magazine*, vol. 29, pp. 86-105, 2012.

[106] K. Zhang, Y. Mao, S. Leng, S. Maharjan, Y. Zhang, A. Vinel, et al., "Incentive-Driven Energy Trading in the Smart Grid," *IEEE Access*, vol. 4, pp. 1243-1257, 2016.

[107] L. Duan, L. Gao, and J. Huang, "Cooperative Spectrum Sharing: A Contract-Based Approach," *IEEE Transactions on Mobile Computing*, vol. 13, pp. 174-187, 2014.

[108] L. Gao, X. Wang, Y. Xu, and Q. Zhang, "Spectrum Trading in Cognitive Radio Networks: A Contract-Theoretic Modeling Approach," *IEEE Journal on Selected Areas in Communications*, vol. 29, pp. 843-855, 2011.

[109] D. M. Kalathil and R. Jain, "Spectrum Sharing through Contracts for Cognitive Radios," *IEEE Transactions on Mobile Computing*, vol. 12, pp. 1999-2011, 2013.

[110] P. Bolton and M. Dewatripont, Contract Theory: The MIT Press, 2004.

[111] "Benefits of demand response in electricity markets and recommendations for achieving them," U.S. Department of Energy, February 2006.

[112] "Assessment of Demand Response and Advanced Metering," Federal Energy Regulatory Commission, November 2018.

[113] R. Deng, Z. Yang, M. Chow, and J. Chen, "A Survey on Demand Response in Smart Grids: Mathematical Models and Approaches," *IEEE Transactions on Industrial Informatics*, vol. 11, pp. 570-582, 2015.

[114] X. Zhang, G. Hug, J. Z. Kolter, and I. Harjunkoski, "Model predictive control of industrial loads and energy storage for demand response," in *2016 IEEE Power and Energy Society General Meeting (PESGM)*, 2016, pp. 1-5.

[115] M. M. Rahman, A. Alfaki, G. M. Shafiullah, M. A. Shoeb, and T. Jamal, "Demand response opportunities in residential sector incorporated with smart load monitoring system," in *2016 IEEE Innovative Smart Grid Technologies - Asia (ISGT-Asia)*, 2016, pp. 1183-1188.

[116] P. Yang, P. Chavali, and A. Nehorai, "Parallel autonomous optimization of demand response with renewable distributed generators," in *2012 IEEE Third International Conference on Smart Grid Communications (SmartGridComm)*, 2012, pp. 55-60.

[117] L. Park, Y. Jang, H. Bae, J. Lee, C. Yun Park, and S. CHo, "Automated energy scheduling algorithms for residential demand response systems," *Energies*, vol. 10: 1326, 2017.

[118] M. Chertkov and V. Chernyak, "Ensemble of Thermostatically Controlled Loads: Statistical Physics Approach," *Scientific Reports*, vol. 7, p. 8673, August 2017.

[119] J. Claridge, ""Innovative HVAC Program Repoert", Demand Side Management & Planning Project," New South Wales Department of Planning, TransGrid and Energy Australia, 2006.

[120] J. Shen, C. Jiang, and B. Li, "Controllable Load Management Approaches in Smart Grids," *Energies*, vol. 8, pp. 11187-11202, 2015.

[121] V. Trovato, Doctor of Philosophy, Electrical and Electronics Engineering, Imperial College London, London, 2015.

[122] M. Babar Rasheed, "User Comfort Aware Energy Management System for Smart Homes," Doctor of Philosophy, Computer Engineering, The Comsats Institue of Information and Technology, Lahore, 2017.

[123] J. Torriti, "Price-based demand side management: Assessing the impacts of time-of-use tariffs on residential electricity demand and peak shifting in Northern Italy," Energy, vol. 44, pp. 576-583, August 2012.

[124] M. Roozbehani, M. Dahleh, and S. Mitter, "On the stability of wholesale electricity markets under real-time pricing," in 49th IEEE Conference on Decision and Control (CDC), 2010, pp. 1911-1918.

[125] K. M. Tsui and S. C. Chan, "Demand Response Optimization for Smart Home Scheduling Under Real-Time Pricing," *IEEE Transactions on Smart Grid*, vol. 3, pp. 1812-1821, 2012.

[126] S. Behboodi, D. P. Chassin, N. Djilali, and C. Crawford, "Transactive control of fast-acting demand response based on thermostatic loads in real-time retail electricity markets," *Applied Energy*, vol. 210, pp. 1310-1320, January 2018.

[127] D. J. Hammerstrom, R. Ambrosio, J. Brous, T. A. Carlon, and D. P. Chassin, "Pacific Northwest GridWise™ Testbed Demonstration Projects Part I. Olympic Peninsula Project," Pacific Northwest National Laboratory, Richland, Washington, U.SOctober 2007.

[128] S. Widergren, A. Somani, K. Subbarao, C. Marinovici, J. Fuller, J. Hammerstrom, et al., "AEP Ohio gridSMART Demonstration Project Real-Time Pricing Demonstration Analysis," Pacific Northwest National Laboratory, United States of America, February 2014.

[129] D. P. Chassin, J. Stoustrup, P. Agathoklis, and N. Djilali, "A new thermostat for real-time price demand response: Cost, comfort and energy impacts of discrete-time control without deadband," *Applied Energy*, vol. 155, pp. 816-825, October 2015.

[130] "Australian Energy Update 2018," Australian Governemnt: Department of the Environment and Energy, August 2018. Available: https://www.energy.gov.au/sites/default/files/australian_energy_update_2018.pdf.

[131] M. Wright, "Australian Sustainable Energy Zero Carbon Australia Stationary Energy Plan," The University of Melbourne Energy Research Institute 2010.

[132] Tyndall, "The Radical Emission Reduction Conference," Centre for Climate Change Research, 19 July 2013.

[133] Spratt and David, "Most of Australia' Can Expect More Than 50 Degrees by End of Century," News. Crikey, July 2011.

[134] "New Report Examines Risks of 4 Degree Hotter World by End of Century," World Bank, 18 November 2012.

[135] "Net Zero Energy Building Plan," Melbourne Energy Institute 2013.

[136] Green Building Council Australia, "Why Choose Green Star?," Green Building Council Australia, 20 March 2012. Available: https://www.gbca.org.au/uploads/91/2139/GBCA012%20Green%20Benefits130510.pdf.

[137] "NABERS and Green Star Rating,"Commonwealth Department of Climate Change and Energy Efficiency, 16 March 2012.

[138] B. Elliston, M. Diesendorf, and I. MacGill., "Simulations of Scenarios with 100% Renewable Electricity in the Australian National Electricity Market.," in In Proceedings of the AuSES SOLAR 2011 Conference, Sydney, Australia, 2011.

[139] "100 Per Cent Renewables Study - Draft Modelling Outcomes.","Australian Energy Market Operator (AEMO), July 2013.

[140] S. Pless and P. Torcellini, "Net-Zero Energy Buildings: A Classification System Based on Renewable Energy Supply Options ", Colorado, June 2010. Available: https://www.nrel.gov/docs/fy10osti/44586.pdf.

[141] S. Li, "Social Incentive Policies to Engage Commercial Building Occupants in Demand Response," in *2014 IEEE International Conference on Automation Science and Engineering (CASE)*, 2014.

[142] R. J. M, x, and sok, "Combining smart energy meters with social media: Increasing energy awareness using data visualization and persuasive technologies," in *Collaboration Technologies and Systems (CTS), 2014 International Conference*, 2014, pp. 27-32.

[143] E. Kabalci, E. Hossain, and R. Bayindir, "Microgrid test-bed design with renewable energy sources," in *Power Electronics and Motion Control Conference and Exposition (PEMC)*, 2014 16th International, 2014, pp. 907-911.

[144] D. Liyanage and S. Rajakaruna, "Performance evaluation and cost-benefit analysis of a large solar PV installation at a mine site in Western Australia," in *2011 IEEE PES Innovative Smart Grid Technologies*, 2011, pp. 1-8.

[145] A. E. M. Operator, "Rooftop PV Information Paper-National Electricity Forecasting 2012," AEMO 2012. Available: https://www.aemo.com.au/media/files/other/forecasting/rooftop_pv_information_paper_20_june_2012.pdf.

[146] J. Poortmans, E. Voroshaszi, W. Deceuninck, and J. Szlufcik, "Higher performance and improved reliability: Key to making photovoltaics the mainstream sustainable electricity generation source of the 21st Century," in *2015 IEEE International Reliability Physics Symposium*, 2015.

[147] F. Ciancetta, A. Ometto, A. Rotondale, G. D. Ovidio, C. Masciovecchio, and A. Dannier, "Energy storage system comparison for mini electrical bus," in *2016 International Symposium on Power Electronics, Electrical Drives*, Automation and Motion (SPEEDAM), 2016, pp. 1115-1119.

[148] M. Gruss and Z. Hradilek, "Research of hydrogen storage system using LabVIEW software," in *Electric Power Engineering (EPE)*, 2015 16th International Scientific Conference on, 2015, pp. 473-477.

[149] J. Vaculik, Z. Hradilek, P. Moldrik, and D. Minarik, "Calculation of efficiency of hydrogen storage system at the fuel cells laboratory," in *Electric Power Engineering (EPE)*, Proccedings of the 2014 15th International Scientific Conference on, 2014, pp. 381-384.

[150] "GridWise Transactive Energy Framework Version 1.0," The GridWise Architecture Council, January 2015. Available: https://www.gridwiseac.org/pdfs/te_framework_report_pnnl-22946.pdf.

[151] T. N. Anderson, M. Duke, G.L. Morrison, and J. K. Carson, "Performance of a Building Integrated Photovoltaic/Thermal (BIPVT) Solar Collector," *Solar Energy*, vol. 83, p. 10, 2009.

[152] D. Lowrie, P. Rodgers, V. Eveloy, and A. R. Baba, "Enhancement of flat-type solar photovoltaics power generation in harsh environmental conditions," in *2014 Semiconductor Thermal Measurement and Management Symposium (SEMI-THERM)*, 2014, pp. 139-145.

[153] D. Rossi, Z. Nagy, and A. Schlueter, "Adaptive distributed robotics for environmental performance, occupant comfort and architectural expression," *Int'l J Arch Comp*, vol. 10, pp. 341-360, 2012.

[154] P. Jayathissa, Z. Nagy, N. Offedu, and A. Schlueter, "Numerical simulation of energy performance, and construction of the adaptive solar facade," *Advanced Building Skins*, 2015.

[155] B. Svetozarevic, Z. Nagy, J. Hofer, D. Jacob, M. Begle, E. Chatzi, et al., "SoRo-Track: A two-axis soft robotic platform for solar tracking and building-integrated photovoltaic applications," *in 2016 IEEE International Conference on Robotics and Automation (ICRA)*, 2016, pp. 4945-4950.

[156] Y. El Basri, L. S. M. Bressan, H. Alawadhi, and C. Alonso, "A proposed graphical electrical signatures supervision method to study PV module failures," *Solar Energy*, pp. 247–256, 2015.

[157] D. DeGraaff, R. Lacerda, and Z. Campeau, "Degradation Mechanisms in Si Module Technologies Observed in the Field; Their Analysis and Statistics," presented at the *NREL 2011 Photovoltaic Module Reliability Workshop Golden*, Colorado, 2011.

[158] R. Moreton, E. Lorenzo, and L. Narvarte, "Experimental observations on hot-spots and derived acceptance/rejection criteria," *Solar Energy*, pp. 28-40, 2015.

[159] S. Daliento, F. Di Napoli, P. Guerriero, and V. d'Alessandro, "A modified bypass circuit for improved hot spot reliability of solar panels subject to partial shading," *Solar Energy*, vol. 134, pp. 211-218, 2016.

[160] P. Manganiello, M. Balato, and M. Vitelli, "A Survey on Mismatching and Aging of PV Modules: The Closed Loop," *IEEE Transactions on Industrial Informatics*, vol. 62, pp. 7276-7286, November 2015.

[161] S. Kaplanis and E. Kaplani, "Energy performance and degradation over 20 years performance of BP c-Si PV modules," *Simulation Modelling Practice Theory*, vol. 19, pp. 1201-1211, 2011.

[162] H. Yang, W. Xu, H. Wang, and M. Narayanan, "Investigation of reverse current for crystalline silicon solar cells—New concept for a test standard about the reverse current," in *Photovoltaic Specialists Conference (PVSC)*, 2010 35th IEEE, 2010, pp. 002806-002810.

[163] C. E. Chamberlin, M. A. Rocheleau, M. W. Marshall, A. M. Reis, N. T. Coleman, and P. A. Lehman, "Comparison of PV module performance before and after 11 and 20 years of field exposure," in *Photovoltaic Specialists Conference (PVSC)*, 2011 37th IEEE, 2011, pp. 000101-000105.

[164] Q. Zhang and L. Qun, "Temperature and reverse voltage across a partially shaded Si PV cell under hot spot test condition," *in Photovoltaic Specialists Conference (PVSC)*, 2012 38th IEEE, 2012, pp. 001344-001347.

[165] K. A. Kim and P. T. Krein, "Photovoltaic hot spot analysis for cells with various reverse-bias characteristics through electrical and thermal simulation," in *Control and Modeling for Power Electronics (COMPEL), 2013 IEEE 14th Workshop*, 2013, pp. 1-8.

[166] P. Guerriero, F. D. Napoli, M. Coppola, and S. Daliento, "A new bypass circuit for hot spot mitigation," in *2016 International Symposium on Power Electronics, Electrical Drives*, Automation and Motion (SPEEDAM), 2016, pp. 1067-1072.

[167] K. A. Kim and P. T. Krein, "Reexamination of Photovoltaic Hot Spotting to Show Inadequacy of the Bypass Diode," *IEEE Journal of Photovoltaics*, vol. 5, pp. 1435-1441, 2015.

[168] M. Coppola, F. D. Napoli, P. Guerriero, D. Iannuzzi, S. Daliento, and A. D. Pizzo, "An FPGA-Based Advanced Control Strategy of a GridTied PV CHB Inverter," *IEEE Transactions on Power Electronics*, vol. 31, pp. 806-816, 2016.

[169] P. Guerriero, F. Di Napoli, V. d'Alessandro, and S. Daliento, "Accurate maximum power tracking in photovoltaic systems affected by partial shading," *International Journal of Photoenergy*, 2015.

[170] H. Qian, "A High-Efficiency Grid-Tie Battery Energy Storage System " Doctor of Philosophy Electrical Engineering Virginia Polytechnic Institute and State University, Blacksburg, Virginia 2011.

[171] Y. W. Cho, W. J. Cha, J. M. Kwon, and B. H. Kwon, "High-Efficiency Bidirectional DAB Inverter Using a Novel Hybrid Modulation for Stand-Alone Power Generating System With Low Input Voltage," *IEEE Transactions on Power Electronics*, vol. 31, pp. 4138-4147, 2016.

[172] S. Somasundaram, S. Katipamula, R. Pratt, E. Mayhorn, B. Akyol, A. Somani, et al., "Transaction-Based Building Controls Framework, Volume 1: Reference Guide," Pacific Northwest National LaboratoryDecember 2014.

[173] "Low Energy High Rise (LEHR) Report", University of Sydney, March 2009. Available: https://thewarrencentre.org.au/wp-content/uploads/2011/11/LEHR-Research-Survery-Report-Ver-5.2.pdf.

[174] Katipamula, Srinivas, RG Lutes, H Ngo, and R. Underhill, "Transactional Network Platform: Applications," Pacific Northwest National Laboratory, Richland, WA.2013.

[175] "Baseline Energy Consumption and Greenhouse Gas Emissions in Commercial Buildings in Australia," Dept. of Climate Change and Energy Efficiency, 2012.

[176] Joel Anderson, Duane A. Robinson, and Z. Ma, "Energy analysis of net zero energy buildings: a case study," CLIMA 2016: Proceedings of the 12th REHVA World Congress, p. 10, 2016.

[177] "HU. Junjie, Y. Guangya, KOK. Koen, XUE. Yusheng and B. Henrik, "Transactive control: a framework for operating power systems characterized by high penetration of distributed energy resources," *Journal of Modern Power Systems and Clean Energy*, vol. 5, pp. 451-464, May 2017.

[178] S. Katipamula, "Smart buildings can help smart grid: Transactive controls," in 2012 IEEE PES Innovative Smart Grid Technologies (ISGT), 2012, pp. 1-1.

[179] S. Jason. (2019, 10 December 2019). Clean Energy Reviews. Available: https://static1.squarespace.com/static/5354537ce4b0e65f5c20d562/t/5d74dea3d2ff7501b49446ba/1567940263465/Fronius Primo Solar Inverter Specification data sheet EN.pdf.

[180] D. P. C. S.Katipamula, D.D.Hatley, "Transactive Controls: Market Based Gridwise Controls for Building System," Pacific Northwest Nat. Lab., Rich-land, WA, USA 2006.

[181] R. Mcdowall, Fundamentals of HVAC Systems: Elsevier, 2006.

[182] Y. Ma and F. Borrelli, "Fast stochastic predictive control for building temperature regulation," in *2012 American Control Conference (ACC)*, 2012, pp. 3075-3080.

[183] N. Radhakrishnan, S. Yang, R. Su, and K. Poolla, "Token based scheduling of HVAC Services in commercial buildings," in *2015 American Control Conference (ACC)*, 2015, pp. 262-269.

[184] N. Nassif, S. Kajl, and R. Sabourin, "Evolutionary algorithms for multi-objective optimization in HVAC system control strategy," in *Fuzzy Information, 2004. Processing NAFIPS '04. IEEE Annual Meeting* ,2004, pp. 51-56 Vol. 1.

[185] A. Syed, J. Melanie, S. Thorpe, and K. Penney, "Australian Energy: National and State Projections to 2029-30," Australian Bureau of Agricultural and Resource Economics, March 2010. Available: http://citeseerx.ist.psu.edu/viewdoc/download?doi=10.1.1.178.2209&rep=rep1&type=pdf.

[186] D. Hurlbut, "State clean energy practices: Renewable portfolio standards," National Renewable Energy Laboratory, Golden, USA 2008.

[187] Department of the Environmental Analysis, "Australia's 2030 climate change target," Australian Government Department of the Environment and Energy 2015. Available: https://www.environment.gov.au/system/files/resources/c42c11a8-4df7-4d4f-bf92-4f14735c9baa/files/factsheet-australias-2030-climate-change-target.pdf.

[188] L. Zhao, Z. Yang, and W. Lee, "The Impact of Time-of-Use (TOU) Rate Structure on Consumption Patterns of the Residential Customers," *IEEE Transactions on Industry Applications*, vol. 53, pp. 5130-5138, 2017.

[189] M. Ding, X. Wang, J. Wang, Z. Yang, H. Zhong, and J. Yang, "A dynamic period partition method for time-of-use pricing with high-penetration renewable energy," in *2017 IEEE Conference on Energy Internet and Energy System Integration (EI2)*, 2017, pp. 1-6.

[190] T. Li and M. Dong, "Real-Time Residential-Side Joint Energy Storage Management and Load Scheduling With Renewable Integration," *IEEE Transactions on Smart Grid*, vol. 9, pp. 283-298, 2018.

[191] D. Liu, Y. Xu, Q. Wei, and X. Liu, "Residential energy scheduling for variable weather solar energy based on adaptive dynamic programming," *IEEE/CAA Journal of Automatica Sinica*, vol. 5, pp. 36-46, 2018.

[192] D. Krishnamurthy, C. Uckun, Z. Zhou, P. R. Thimmapuram, and A. Botterud, "Energy Storage Arbitrage Under Day-Ahead and Real-Time Price Uncertainty," *IEEE Transactions on Power Systems*, vol. 33, pp. 84-93, 2018.

[193] "Data Collection for Demand-Side Management for Quantifying its Influence on Reliability: RESULTS AND RECOMMENDATIONS " North American Electric Reliability Corporation, December 2007.

[194] M. Roozbehani, M. A. Dahleh, and S. K. Mitter, "Volatility of Power Grids Under Real-Time Pricing," *IEEE Transactions on Power Systems*, vol. 27, pp. 1926-1940, 2012.

[195] K. Wang, Z. Ouyang, R. Krishnan, L. Shu, and L. He, "A Game Theory-Based Energy Management System Using Price Elasticity for Smart Grids," *IEEE Transactions on Industrial Informatics*, vol. 11, pp. 1607-1616, 2015.

[196] W. Liu, W. Gu, J. Wang, W. Yu, and X. Xi, "Game Theoretic Non-Cooperative Distributed Coordination Control for Multi-Microgrids," *IEEE Transactions on Smart Grid*, vol. 9, pp. 6986-6997, 2018.

[197] P. Samadi, V. W. S. Wong, and R. Schober, "Load Scheduling and Power Trading in Systems With High Penetration of Renewable Energy Resources," *IEEE Transactions on Smart Grid*, vol. 7, pp. 1802-1812, 2016.

[198] S. Steven, "Risk Sharing and Incentives in the Principal and Agent Relationship," *The Bell Journal of Economics*, vol. 10, 1979.

[199] E. I. Hoppe and P. W. Schmitz, "Contracting under Incomplete Information and Social Preferences: An Experimental Study," *The Review of Economic Studies*, vol. 80, pp. 1516-1544, 2013.

[200] Y. Gao, Y. Chen, C. Wang, and K. J. R. Liu, "A contract-based approach for ancillary services in V2G networks: Optimality and learning," in *2013 Proceedings IEEE INFOCOM*, 2013, pp. 1151-1159.

[201] T. Morstyn, A. Teytelboym, and M. D. Mcculloch, "Bilateral Contract Networks for Peer-to-Peer Energy Trading," *IEEE Transactions on Smart Grid*, vol. 10, pp. 2026-2035, 2019.

[202] P. AUER, N. CESA-BIANCHI, and P. FISCHER, "Finite-time analysis of the multiarmed bandit problem," *Machine Learning*, vol. 47, p. 22, 2002.

[203] S. Sheng and M. Liu, "Profit Incentive in Trading Nonexclusive Access on a Secondary Spectrum Market Through Contract Design," *IEEE/ACM Transactions on Networking*, vol. 22, pp. 1190-1203, 2014.

[204] H. Zhong, L. Xie, and Q. Xia, "Coupon Incentive-Based Demand Response: Theory and Case Study," *IEEE Transactions on Power Systems*, vol. 28, pp. 1266-1276, 2013.

[205] P. G. D. Silva, D. Ilić, and S. Karnouskos, "The Impact of Smart Grid Prosumer Grouping on Forecasting Accuracy and Its Benefits for Local Electricity Market Trading," *IEEE Transactions on Smart Grid*, vol. 5, pp. 402-410, 2014.

[206] (2018). Electricity and Gas Tariff. Available: https://www.esc.vic.gov.au/electricity-and-gas/electricity-and-gas-tariffs-and-benchmarks/minimum-feed-tariff, accessed on 5 Nov, 2018.

[207] Australian Sustainable Built Environment Council (ASBEC), "The Second Plank: Building a Low Carbon Economy with Energy Efficient Buildings," 2008. Available: https://www.asbec.asn.au/files/ASBEC%20CCTG%20Second%20Plank%20Report%202.0_0.pdf.

[208] "Commercial Building Disclosure: A National Energy Efficiency Program " Australian Government Department of the Environment and Energy 2011.

[209] "Country Energy's Electricity Network Revised Regulatory Proposal 2009-2014," Essential Energy, 16 January 2009. Available: https://www.aer.gov.au/system/files/Country%20Energy%20Revised%20Proposal%2016%20January%202009.pdf.

[210] "Guide to Best Practice Maintenance & Operation of HVAC Systems for Energy Efficiency," Council of Australian Governments (COAG) National Strategy on Energy Efficiency, January 2012.

[211] J. Claridge, "Innovative HVAC Program Report: Demand Management and Planning Project," NSW Department of Planning, TransGrid and Energy Australia, 2006.

[212] W. Chiu, H. Sun, and H. V. Poor, "Energy Imbalance Management Using a Robust Pricing Scheme," *IEEE Transactions on Smart Grid*, vol. 4, pp. 896-904, 2013.

[213] H. Hao, C. D. Corbin, K. Kalsi, and R. G. Pratt, "Transactive Control of Commercial Buildings for Demand Response," *IEEE Transactions on Power Systems*, vol. 32, pp. 774-783, 2017.

[214] R. A. D.hammerstrom, J.Brous, "Pacific Northwest Gridwise Testbed Demonstration Projects," Pacific Northwest Nat. Lab., Rich-land, WA, USA 2007.

[215] E. Fernandez, P. Jamborsalamati, M. J. Hossain, and U. Amin, "A communication-enhanced price-based control scheme for HVAC systems," in *2017 IEEE Innovative Smart Grid Technologies - Asia (ISGT-Asia)*, 2017, pp. 1-6.

[216] S. Katipamula, "Transactive Controls in Buildings: Challenges and Opportunities," *DOE Electricity Advisory Committee Meeting*, 2016.

[217] F. Rahimi, A. Ipakchi, and F. Fletcher, "The Changing Electrical Landscape: End-to-End Power System Operation Under the Transactive Energy Paradigm," *IEEE Power and Energy Magazine*, vol. 14, pp. 52-62, 2016.

[218] A. R. Al-Ali, N. A. Tubaiz, A. Al-Radaideh, J. A. Al-Dmour, and L. Murugan, "Smart grid controller for optimizing HVAC energy consumption," *in 2012 International Conference on Computer Systems and Industrial Informatics*, 2012, pp. 1-4.

[219] K. X. Perez, M. Baldea, and T. F. Edgar, "Integrated smart appliance scheduling and HVAC control for peak residential load management," in *2016 American Control Conference (ACC)*, 2016, pp. 1458-1463.

[220] A. Tyukov, M. Shcherbakov, A. Sokolov, A. Brebels, and M. Al-Gunaid, "Supervisory model predictive on/off control of HVAC systems," in *2017 8th International Conference on Information, Intelligence, Systems & Applications (IISA)*, 2017, pp. 1-7.

[221] Y. Li, J. D. L. Ree, and Y. Gong, "The Smart Thermostat of HVAC Systems Based on PMV-PPD Model for Energy Efficiency and Demand Response," in *2018 2nd IEEE Conference on Energy Internet and Energy System Integration (EI2)*, 2018, pp. 1-6.

[222] W. Surles and G. P. Henze, "Evaluation of automatic priced based thermostat control for peak energy reduction under residential time-of-use utility tariffs," *Energy and Buildings*, vol. 49, pp. 99-108, June 2012.

[223] J. Cao, B. Yang, K. Ma, C. Chen, and X. Guan, "Residential HVAC load control strategy based on game theory," in *2017 Chinese Automation Congress (CAC)*, 2017, pp. 5933-5938.

[224] J. H. Yoon, R. Baldick, and A. Novoselac, "Dynamic Demand Response Controller Based on Real-Time Retail Price for Residential Buildings," *IEEE Transactions on Smart Grid*, vol. 5, pp. 121-129, 2014.

[225] M. Alhaider and F. Lingling, "Mixed integer programming for HVACs operation," in *2015 IEEE Power & Energy Society General Meeting*, 2015, pp. 1-5.

[226] M. Avci, M. Erkoc, and S. S. Asfour, "Residential HVAC load control strategy in real-time electricity pricing environment," in *2012 IEEE Energytech*, 2012, pp. 1-6.

[227] M. Avci, M. Erkoc, A. Rahmani, and S. Asfour, "Model predictive HVAC load control in buildings using real-time electricity pricing," *Energy and Buildings*, vol. 60, pp. 199-209, May 2013.

[228] G. S. Pavlak, G. P. Henze, and V. J. Cushing, "Optimizing commercial building participation in energy and ancillary service markets," *Energy and Buildings*, vol. 81, pp. 115-126, October 2014.

[229] E. M. Greensfelder, G. P. Henze, and C. Felsmann, "An investigation of optimal control of passive building thermal storage with real time pricing," *Journal of Building Performance Simulation*, vol. 4, pp. 91-104, June 2011.

[230] S. Bhattacharya, K. Kar, and J. H. Chow, "Economic Operation of Thermostatic Loads under Time Varying Prices: An Optimal Control Approach," *IEEE Transactions on Sustainable Energy*, pp. 1-1, 2018.

[231] A. Abdulaal and S. Asfour, "A linear optimization based controller method for real-time load shifting in industrial and commercial buildings," *Energy and Buildings*, vol. 110, pp. 269-283, January 2016.

[232] G. Goddard, J. Klose, and S. Backhaus, "Model Development and Identification for Fast Demand Response in Commercial HVAC Systems," *IEEE Transactions on Smart Grid*, vol. 5, pp. 2084-2092, 2014.

[233] D. Christantoni, S. Oxizidis, D. Flynn, and D. P. Finn, "Implementation of demand response strategies in a multi-purpose commercial building using a whole-building simulation model approach," *Energy and Buildings*, vol. 131, pp. 76-86, November 2016.

[234] E. Biyik, S. Genc, and J. D. Brooks, "Model predictive building thermostatic controls of small-to-medium commercial buildings for optimal peak load reduction incorporating dynamic human comfort models: Algorithm and implementation," in 2014 IEEE Conference on Control Applications (CCA), 2014, pp. 2009-2015.

[235] A. Yasuoka, H. Kubo, K. Tsuzuki, and N. Isoda, "Gender Differences in Thermal Comfort and Responses to Skin Cooling by Air Conditioners in the Japanese Summer," *Journal of the Human-Environment System*, vol. 18(1):011-020, October 2015.

[236] Z. Gou, W. Gamage, S. Siu-Yu Lau, and S. Sing-Yeung Lau, "An investigation of thermal comfort and adaptive behaviors in naturally ventilated residential buildings in tropical climates: a pilot study," *Buildings*, vol. 8, 3 January 2018.

[237] V. L. Erickson and A. E. Cerpa, "Thermovote: Participatory Sensing for Efficient Building HVAC Conditioning," presented at the *Proceedings of the Fourth ACM Workshop on Embedded Sensing Systems for Energy-Efficiency in Buildings*, Toronto, Canada 2012.

[238] A. Ghahramani, F. Jazizadeh, and B. Becerik-Gerber, "A knowledge based approach for selecting energy-aware and comfort-driven HVAC temperature set points," *Energy and Buildings*, vol. 85, pp. 536-548, December 2014.

[239] R. Z. Homod, "Review on the HVAC System Modeling Types and the Shortcomings of Their Application," *Journal of Energy*, vol. 2013, Article ID 768632, p. 10, 2013.

[240] X. Lü, "Modelling of heat and moisture transfer in buildings: I. Model program," *Energy and Buildings*, vol. 34, pp. 1033-1043, November 2002.

[241] S. Goyal and P. Barooah, "A method for model-reduction of non-linear thermal dynamics of multi-zone buildings," *Energy and Buildings*, vol. 47, pp. 332-340, April 2012.

[242] Y.-S. Kim and J. Srebric, "Impact of occupancy rates on the building electricity consumption in commercial buildings," *Energy and Buildings*, vol. 138, pp. 591-600, March 2017.

[243] S. Goubran, D. Qi, W. F. Saleh, and L. Wang, "Comparing methods of modeling air infiltration through building entrances and their impact on building energy simulations," *Energy and Buildings*, vol. 138, pp. 579-590, March 2017.

[244] A. Kelman and F. Borrelli, "Bilinear Model Predictive Control of a HVAC System Using Sequential Quadratic Programming," IFAC Proceedings, vol. 44, pp. 9869-9874, January 2011.

[245] Y.-W. Wang, W.-J. Cai, Y.-C. Soh, S.-J. Li, L. Lu, and L. Xie, "A simplified modeling of cooling coils for control and optimization of HVAC systems," *Energy Conversion and Management*, vol. 45, pp. 2915-2930, November 2004.

[246] L. Lu, W. Cai, L. Xie, S. Li, and Y. C. Soh, "HVAC system optimization—in-building section," *Energy and Buildings*, vol. 37, pp. 11-22, January 2005.

[247] A. Bhatia, "Cooling Load Calculations and Principles," Stony Point, New York: Continuing Education and Development, Inc.

[248] ASHRAE Handbook Fundamentals, SI Edition ed.: Supported by ASHRAE Research, 2005.

[249] ASHRAE Handbook Fundamentals, SI Edition ed.: Supported by ASHRAE Research, 1997.

[250] E. Fernandez, M. J. Hossain, and M. S. H. Nizami, "Game-theoretic approach to demand-side energy management for a smart neighbourhood in Sydney incorporating renewable resources," *Applied Energy*, vol. 232, pp. 245-257, December 2018.

[251] T. M. Christensen, A. S. Hurn, and K. A. Lindsay, "Forecasting spikes in electricity prices," *International Journal of Forecasting*, vol. 28, pp. 400-411, April 2012.

[252] "Applications for authorisation-National Electricity Code," 10 December 1997, p. 60. Available: https://www.pc.gov.au/research/supporting/electricity-code/electricitycode.pdf

[253] Day-Ahead, Electricity Price & Demand Available: https://www.aemo.com.au/Electricity/National-Electricity-Market-NEM/Data-dashboard.

[254] American Society of Heating, Refrigerating and Air Conditioning ENgineers (ASHRAE), "Thermal Environmental Conditions for Human Occupancy," *ANSI/ASHRAE Standard 55-2010.*